



E-ISSN 2667-5846

EXPERIMED

Volume **13** Issue **2** August 2023

experimed.istanbul.edu.tr



ISTANBUL
UNIVERSITY
PRESS

EXPERIMED

INDEXING AND ABSTRACTING

ULAKBIM TR Index

Chemical Abstracts Service (CAS)

EBSCO - Central & Eastern European Academic Source

SOBIAD

EXPERIMED

OWNER

Prof. Dr. Günnur DENİZ

Department of Immunology, Istanbul University, Aziz Sancar Institute of Experimental Medicine, Istanbul, Türkiye

RESPONSIBLE MANAGER

Prof. Dr. Bedia ÇAKMAKOĞLU

Department of Molecular Medicine, Istanbul University, Aziz Sancar Institute of Experimental Medicine, Istanbul, Türkiye

CORRESPONDENCE ADDRESS

Istanbul University, Aziz Sancar Institute of Experimental Medicine,
Vakıf Gureba Avenue, 34093, Çapa, Fatih, Istanbul, Türkiye
Phone: +90 (212) 414 22 29
E-mail: experimed@istanbul.edu.tr

PUBLISHER

Istanbul Üniversitesi Yayınevi / Istanbul University Press
Istanbul University Central Campus,
34452 Beyazıt, Fatih / Istanbul, Türkiye
Phone: +90 (212) 440 00 00

Authors bear responsibility for the content of their published articles.

The publication language of the journal is English.

This is a scholarly, international, peer-reviewed and open-access journal published triannually in April, August and December.

Publication Type: Periodical

EXPERIMED

EDITORIAL MANAGEMENT BOARD

Editor-in-Chief

Prof. Dr. Bedia ÇAKMAKOĞLU

Department of Molecular Medicine, Istanbul University, Aziz Sancar Institute of Experimental Medicine, Istanbul, Türkiye – bedia@istanbul.edu.tr

Co-Editors-in-Chief

Assoc. Prof. Umut Can KÜÇÜKSEZER

Department of Immunology, Istanbul University, Aziz Sancar Institute of Experimental Medicine, Istanbul, Türkiye – uksezer@istanbul.edu.tr

Assoc. Prof. Vuslat YILMAZ

Department of Neuroscience, Istanbul University, Aziz Sancar Institute of Experimental Medicine, Istanbul, Türkiye – vuslat.yilmaz@istanbul.edu.tr

Managing Editor

Prof. Dr. Sema Sırma EKMEKÇİ

Department of Genetics, Istanbul University, Aziz Sancar Institute of Experimental Medicine, Istanbul, Türkiye – sirmasem@istanbul.edu.tr

Editorial Management Board Members

Dr. Canan Aysel ULUSOY

Department of Neuroscience, Istanbul University, Aziz Sancar Institute of Experimental Medicine, Istanbul, Türkiye – canan.ulusoy@istanbul.edu.tr

MSc. Barış ERTUĞRUL

Department of Molecular Medicine, Istanbul University, Aziz Sancar Institute of Experimental Medicine, Istanbul, Türkiye – baris.ertugrul@istanbul.edu.tr

Section Editors

Prof. Dr. Elif ÖZKÖK

Department of Neuroscience, Istanbul University, Aziz Sancar Institute of Experimental Medicine, Istanbul, Türkiye – eozkok@istanbul.edu.tr

Assoc. Prof. Sinem BİRELLER

Department of Biochemistry, Faculty of Pharmacy, Acıbadem Mehmet Ali Aydınlar University, Istanbul, Türkiye – sinem.bireller@acibadem.edu.tr

Assoc. Prof. Ferda PAÇAL

Department of Lab Animal Science, Istanbul University, Aziz Sancar Institute of Experimental Medicine, Istanbul, Türkiye – ferda.pacal@istanbul.edu.tr

Assoc. Prof. Ali Cihan TAŞKIN

Department of Lab Animal Science, Istanbul University, Aziz Sancar Institute of Experimental Medicine, Istanbul, Türkiye – ataskin@istanbul.edu.tr

Language Editors

Elizabeth Mary EARL

Department of Foreign Languages, Istanbul University, Istanbul, Türkiye – elizabeth.earl@istanbul.edu.tr

Rachel Elana KRIS

Department of Foreign Languages, Istanbul University, Istanbul, Türkiye – rachel.kriss@istanbul.edu.tr

Statistics Editor

Sevda ÖZEL YILDIZ

Department of Biostatistic, Istanbul Medical Faculty, Istanbul University, Istanbul, Türkiye – sevda@istanbul.edu.tr

EXPERIMED

EDITORIAL BOARD

Aziz SANCAR (Honorary Member)

Department of Biochemistry and Biophysics, University of North Carolina School of Medicine, Chapel Hill, North Carolina, USA – aziz_sancar@med.unc.edu

Abid HUSSAINI

Department of Pathology and Cell Biology, Columbia University, Taub Institute, New York, USA – abid.hussaini@columbia.edu

Ahmet GÜL

Department of Internal Medicine, Istanbul University School of Medicine, Istanbul, Türkiye – agul@istanbul.edu.tr

Ali Önder YILDIRIM

Department of Lung Biology and Diseases, Helmholtz Zentrum München, München, Germany – oender.yildirim@helmholtz-muenchen.de

Batu ERMAN

Department of Molecular Biology, Genetics and Bioengineering, Sabanci University, Istanbul, Türkiye – batu.erman@boun.edu.tr

Çağla EROĞLU

Department of Cell Biology, Duke University, North Carolina, USA – cagla.eroglu@duke.edu

Ebba LOHMANN

Department of Neurodegenerative Diseases, Tübingen University, Tübingen, Germany – ebba.lohmann@uni-tuebingen.de

Elif APOHAN

Department of Biology, İnönü University, Malatya, Türkiye – elif.apohan@inonu.edu.tr

Erdem TÜZÜN

Department of Neuroscience, Istanbul University, Aziz Sancar Institute of Experimental Medicine, Istanbul, Türkiye – erdem.tuzun@istanbul.edu.tr

Gökçe TORUNER

Department of Hematology, MD Anderson Cancer Center, Houston, Texas, USA – gatoruner@mdanderson.org

Günnur DENİZ

Department of Immunology, Istanbul University, Aziz Sancar Institute of Experimental Medicine, Istanbul, Türkiye – gdeniz@istanbul.edu.tr

Gürol TUNÇMAN

Department of Genetics and Complex Diseases, Harvard University, Massachusetts, USA – gtuncman@hsph.harvard.edu

Hannes STOCKINGER

Molecular Immunology Unit, Vienna School of Medicine, Pathophysiology Center, Vienna, Austria – hannes.stockinger@medunivien.ac.at

Rukset ATTAR

Department of Obstetrics and Gynecology, Yeditepe University, Istanbul, Türkiye – rattar@yeditepe.edu.tr

İhsan GÜRSEL

Department of Molecular Biology and Genetics, Bilkent University, Ankara, Türkiye – ihsangursel@bilkent.edu.tr

Melih ACAR

Texas University Pediatric Research Institute, Dallas, Texas, USA – melihacar@gmail.com

Numan ÖZGEN

Department of Pathology and Immunology, Baylor University School of Medicine, Texas, USA – numan.oezguen@bcm.edu

Serhat PABUÇÇUOĞLU

Department of Reproduction & Artificial Insemination, Istanbul University-Cerrahpaşa School of Veterinary, Istanbul, Türkiye – serpab@iuc.edu.tr

Sühendan EKMEKÇİOĞLU

MD Anderson Cancer Center, Texas University, Houston, Texas, USA – sekmekcioglu@mdanderson.org

Yusuf BARAN

Department of Molecular Biology and Genetics, İzmir Institute of Technology, İzmir, Türkiye – yusufbaran@iyte.edu.tr

EXPERIMED

CONTENTS

ORIGINAL ARTICLES

- 73 **Effect of Chronic Unpredictable Mild Stress on Hippocampus and Serum Markers in Rats**
Mehmet Deniz Yener, Tuncay Colak, Sema Kurnaz Ozbek, Sureyya Ceylan, Esra Acar, Hale Maral Kir
- 80 **Gingipain Injection Affects Intestinal Oxidant-Antioxidant Status and Alkaline Phosphatase in Overfed Zebrafish**
Gizem Gunduz, Merih Beler, Ismail Unal, Derya Cansiz, Ebru Emekli-Alturfan, Kemal Naci Kose
- 86 **Evaluation of DNA Microarray in Biomarker Detection in Cell-free DNA from Colorectal Cancer Cell Lines: A Proof-of-Concept Study**
Hasan Huseyin Kazan, Ceyhan Piril Karahan, Ekin Celik, Ahmet Caglar Ozketen, Duygu Birgucu Cagil, Mehmet Ali Ergun
- 93 **Cyclosporine Treatment Increases the ACE/ACE2 Ratio in Adipose Tissue and Aorta**
Samed Emre Darilmaz, Ilknur Bingul, Merva Soluk-Tekkesin, Nergis Demir, Seldag Bekpinar
- 97 **Characterization of Rubidium-Based Nanoparticles by Green Synthesis and Their Effect on Colorectal Cancer Cells**
Dilsad Ozerkan, Ishak Afsin Kariper
- 103 **Comparison of Gene Expression Levels in the p53 Pathway in Blood and Bone Marrow of Healthy Individuals**
Aynur Daglar Aday, Gozde Oztan, Ilknur Suer
- 109 **Investigation of the Toxicologic and Biochemical Effects of Silk Fibroin/Gold Nanoparticles-Based Nanofiber Using Zebrafish Embryos**
Ozan Ozcan, Ismail Unal, Elif Tufan, Ebru Emekli-Alturfan, Tugba Tunali-Akbay
- 115 ***In vitro* Antileishmanial Activity of *Lavandula angustifolia* Essential Oil on *Leishmania infantum* Parasites**
Zeynep Islek, Fikrettin Sahin
- 121 **Cryptotanshinone Protects Against Acute Pulmonary Edema**
Umit Yilmaz, Mehmet Demir
- 127 **Comparative Toxicity Responses of Thirdhand Smoke Derived from Conventional Cigarette and Heated Tobacco Products in Human Bronchial Epithelial Cells**
Rengin Reis, Kubra Kolci
- 133 **Pressure Ulcers in Palliative Care Unit Patients**
Mahmut Said Degerli
- 142 **Investigation of the Effect of Serum IL-1 β Levels on Atherosclerosis: A Turkish Population-Based Study**
Dilveen Dlawer Omer, Fatma Tuba Akdeniz, Seda Gulec Yilmaz, Zerrin Barut, Deryanaz Billur, Ayca Turer Cabbar, Turgay Isbir
- 148 **The Potential Role of Hematological and Biochemical Parameters in Pregnant Women with Viral Infection**
Nadire Elif Ergun, Saime Surmen, Saide Erturk, Derya Buyukkayhan, Mustafa Gani Surmen
- 156 **The Effect of Otitis Media with Effusion on Language and Cognitive Skills in School Age Children**
Merve Savas

EXPERIMED

Experimed is proud to published the second issue of 2023 with fourteen valuable original research articles related to 20 different universities with several faculties and departments and multidisciplinary areas from Turkiye.

I am very appreciative of;

Researchers who have published their original scientific outcomes in Experimed,

Editorial Board Team who has conduct with great labour in all stages,

Dear Institute Director Prof. Dr. Günnur Deniz who has expressed her supportive gratitude for Experimed to University's management platform,

As a member of the Istanbul University Press team, Eda Kolukisa Doğru, Merve Ağırğün and Ertuğrul Yaşar worked hard to ensure timely publication.

We are very pleased that our growing influence in the literature with this amazing Experimed Team gives us more courage to shed more light on science with new publications.

Prof. Dr. Bedia Çakmaköğlü

Effect of Chronic Unpredictable Mild Stress on Hippocampus and Serum Markers in Rats

Mehmet Deniz Yener¹ , Tuncay Colak¹ , Sema Kurnaz Ozbek² , Sureyya Ceylan² ,
Esra Acar³ , Hale Maral Kir⁴ 

¹Department of Anatomy, Faculty of Medicine, Kocaeli University, Kocaeli, Turkiye

²Department of Histology, Faculty of Medicine, Kocaeli University, Kocaeli, Turkiye

³Department of Biochemistry, Faculty of Pharmacy, Kocaeli Health and Technology University, Kocaeli, Turkiye

⁴Department of Biochemistry, Faculty of Medicine, Kocaeli University, Kocaeli, Turkiye

ORCID ID: M.D.Y. 0000-0002-4379-5793; T.C. 0000-0002-9483-3243; S.K.O. 0000-0002-2608-1975; S.C. 0000-0002-7889-2040;
E.A. 0000-0002-0814-0820; H.M.K. 0000-0003-2473-8272

Cite this article as: Yener MD, Colak T, Kurnaz Ozbek S, Ceylan S, Acar E, Kir HM. Effect of chronic unpredictable mild stress on hippocampus and serum markers in rats. *Experimed* 2023; 13(2): 73-79.

ABSTRACT

Objective: Unpredictable stress is a common factor that we encounter in our daily lives. In this context, we wanted to investigate the morphological effects of a chronic unpredictable mild stress (CUMS) model on rat hippocampus and serum levels of brain derived neurotrophic factor (BDNF) and glial fibrillary acidic protein (GFAP).

Materials and Methods: This study was carried out on 16 Wistar albino rats which were divided into control and experiment groups. The CUMS model protocol was applied, and the morphological structures of the hippocampus were examined. The serum GFAP/BDNF levels were measured by ELISA method.

Results: The mean BDNF level was 1.65 ± 0.17 ng/mL in the control group and 2.25 ± 0.29 ng/mL in the CUMS group. The mean GFAP level was 3.04 ± 0.45 ng/mL in the control group and 2.96 ± 0.58 ng/mL in the CUMS group. When the polymorph cell layer (PCL) in gyrus dentatus was examined; the mean number of cells in the control group was 20 ± 1.38 for the left PCL and 17 ± 1.35 for the right PCL. In the stress group; the mean number of cells in the polymorph cell layer of gyrus dentatus was 27 ± 2.08 cells for the left side and 23 ± 2.01 for the right side.

Conclusions: As a result, morphological changes were observed in the gyrus dentatus region which has an important role in memory formation. The cells in the polymorph cell layer of gyrus dentatus underwent changes under stress.

Keywords: Chronic stress, hippocampus, brain derived neurotrophic factor (BDNF), glial fibrillary acidic protein (GFAP)

INTRODUCTION

Homeostasis is the conservation of the organism's cellular balance against environmental factors (1). Stress is considered as a factor that disrupts homeostasis (2). In stressful situations, there are changes in the levels of many biomediators and at the same time, stress factors cause changes in various reflex communication pathways. These changes can cause morphological alterations in tissues that are highly sensitive to external factors such as the brain. The imbalance of these changes causes pathologies in living organisms (3).

The hippocampus area is related to the cognitive process of the brain such as memory and sense of direction in mammals (4). Gyrus dentatus is a morphological and functional neuroanatomic region of the hippocampus that consists of three basic morphological layers curled into each other in rats. These layers are molecular, pyramidal and polymorphic cell layers. Degeneration of the cells in these layers plays a part in the etiopathology of many neurological diseases (5).

Chronic stress conditions cause adaptations to regain homeostasis in the organism. These adaptations are biological steps that regulate the response to stress (6).

Corresponding Author: Mehmet Deniz Yener **E-mail:** m.denizyener@hotmail.com

Submitted: 13.03.2023 **Revision Requested:** 27.04.2023 **Last Revision Received:** 13.06.2023 **Accepted:** 14.06.2023 **Published Online:** 07.08.2023



Content of this journal is licensed under a Creative Commons Attribution-NonCommercial 4.0 International License.

Intermediary biological factors released from these pathways enable the rearrangement of many biological structures and adaptation of the physiological structure of the organism to the stress condition (2). If stress factors are at a level that disrupts cellular homeostasis and the adaptation process is insufficient, tissue and organ pathologies emerge. In particular, chronic stress may have irreversible consequences for the structural and functional integrity of the cell.

Neurons are in constant interaction with the microenvironment and are very sensitive to external stimuli. If the level of stress in which an organism interacts increases, disturbances in cellular biological pathways may occur (7). The adaptation mechanisms of the organism undergo reorganization to balance this situation (8). Neurons are surrounded by astrocytes and play an active role in many metabolic activities. Disturbances that may occur in astrocytes are directly related to neuron survival. Glial fibrillary acidic protein (GFAP) is an intermediary filament produced by the astrocyte cell throughout the central nervous system (CNS). In addition, an increased GFAP level is used as a marker for reactive astrogliosis pathology in animal models (9).

Neurotrophin is a fundamental signaling molecule in the CNS responsible for neuron growth, axon elongation, and the existence of a synapse during the developmental period. Also, the brain-derived neurotrophic factor (BDNF) protein is the most extensive growth factor in the CNS which is essential for neuronal survival (10). Along with CNS effects; BDNF, a neurotrophic peptide, also has peripheral effects and these effects are related to regulating the peripheral energy metabolism. This reasonably effective neurotrophic factor is being studied as a possible marker for the nervous system in mammals (11).

In this context, it was intended to investigate the morphological effects of chronic mild stress on hippocampal tissue and serum BDNF/GFAP levels in rats.

MATERIALS AND METHODS

Animals and Standard Procedures

In the study, four-months-old 190-200 gr female *Wistar albino* rats (n=16) were used. We divided the rats into two groups in standard cages two weeks before the initiation of the study process and provided standard room conditions. Menstrual cycles of rodents were considered and analyzed. During anesthesia; a combination of ketamine hydrochloride (90 mg/kg; Ketalar, Parke-Davis) and xylazine hydrochloride (12mg / kg, 2%; Rompun, Bayer) was administered intraperitoneally to the rodents. Euthanasia performed by cervical dislocation under anesthesia. Afterwards, intracardiac blood collection was performed. The principles of "Guidelines for the Care and Use of Laboratory Animals" were applied.

Stress Model and Groups

The chronic unpredictable mild stress (CUMS) method was chosen as a stress protocol because it prevents rodents from

learning stress factors and is a reliable method that has been used in many studies. In this study, the CUMS protocol which was previously defined by Willner P. (12) was used as a stress model. A total of eight different stressors were identified (Table 1) and the order of the stressors were previously determined. At the end of the experiment, anhedonia behaviors which are considered as an indicator of the depression status of the animals were closely monitored and measured.

Table 1. Stressors applied in CUMS model.

1. Cage inclination, 45°C / 24 hours	5. Changing day-night cycle
2. Hanging from the tail, 1 minute	6. Cage shaking, 10 minutes
3. Buoyancy in cold water 4°C / 5 minutes	7. Cage wetting 200 mL / 24 hours
3. Buoyancy in hot water 45°C / 5 minutes	8. Exchanging sawdust between cages

In this study, two groups were formed as the experimental group and control group. Then we applied the stressors to the experimental group for 28 days. The order of the application protocol was randomly determined before the start of the experiments.

Sucrose Consumption Test

During the 4th week of the experiment, a sucrose preference test was conducted to measure anhedonic behaviors in stressed animals. For the test, two water bottles were placed in each cage and applied for six days. One bottle contained 200mL of 20% sucrose solution, and the other contained 200mL of tap water. The rats were allowed to drink from both bottles during the first five days for habituation. The water bottles were changed every 12 hours. Sucrose consumption was calculated as the ratio of sucrose consumption to total consumption: $\text{Sucrose consumption} = (\text{sucrose consumption} \times 100) / \text{total consumption}$.

Histological Preparation and Procedure

Brain tissues were fixed in 10% buffered formaldehyde for a week. Histological preparations were performed as previously described (13). Brain tissues were dehydrated through upgrading levels of ethanol solutions and cleared in xylene then embedded in paraffin. Before proceeding to the histological serial sectioning stage, the coordinates of the desired cross-sectional area were determined according to the region of bregma (Bregma -3.00 mm) using the brain atlas (*Paxinos, Watson*) of the hippocampus region of the animals whose brain tissues were completely removed. Sections of the brain tissues were stained with hematoxylin and eosin to determine the hippocampus microstructure. The end boundary of the pyramidal cell layer in the CA3 region within

the hippocampus tissue was determined as the counting area and a border perpendicular to the tissue axis was drawn at this point. Cell count was performed in the region between this axis and the granular cell layer of the hippocampus.

ELISA Method and Biochemical Procedures

Blood samples (3mL) were obtained from the left ventricle. Blood specimens were allowed to clot for two hours at room temperature and centrifuged for 15 minutes at 1000 g force at 4-8°C. The supernatants were collected and diluted 1/10 before the assay. Serum samples were stored at -40°C. The serum BDNF and GFAP levels were determined with Enzyme Linked Immunosorbent Assay (ELISA; Elabscience USA) kits were used and measured with the Alisei Quality System Seac Radim Company analyzer (Italy/Rome)-ELISA reader on the basis of the manufacturer's instructions (BDNF, Catalog number E-ELR1235; GFAP, Catalog number E-ELR1428). The results were multiplied by the dilution coefficient and their concentrations were calculated according to the kit standards.

Data Analysis and Statistics

A Kolmogorov-Smirnov analysis was performed for the normal distribution suitability test in the statistical evaluation of the study results. An independent t-test was applied for the values that corresponded to normal distribution. The Mann Whitney U test was used for the parameters that did not comply with normal distribution. The p values of 0.05 or less were considered statistically significant. The statistical analysis SPSS 22.0 (IBM, Packet program) was used. The GraphPad Prism8 package program was used for graphics design.

RESULTS

During the study, animal weights were monitored, and the mean weights at the beginning of the study were 193 gr for the control group and 198 gr for the stress group. Body mass increase was less in rats under chronic stress protocol when compared to the control group. Even so there was no significant difference between the mean weights of the groups. The temporal change graph of the mean values of animal weights according to the groups is given in Figure 1.

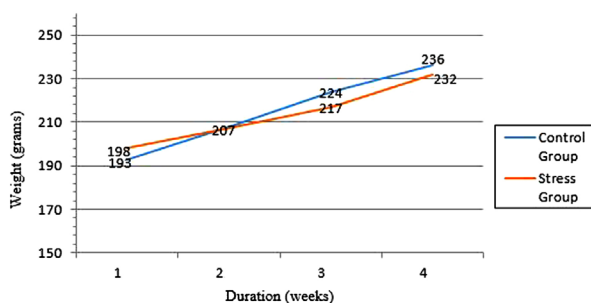


Figure 1. Variations in the average weight of animals according to the groups and time.

The sucrose consumption test, which is an important parameter in stress model validation, was applied to the rodents. In the study, there was a significant decrease in sucrose consumption when the rats underwent the CUMS procedure as compared to the control group ($p < 0.05$).

We performed a histological evaluation of the hippocampus tissue separately for the right and left sides. We measured the hippocampus thickness for both groups on the vertical axis 'coronal section' and compared them statistically. The molecular, pyramidal and polymorphic area thicknesses with complete hippocampus tissue thicknesses and subdomains were also evaluated among the groups. The mean thickness of the left hippocampus was $1,581 \pm 61.01 \mu\text{m}$ for the control group. In the stress group rats, the mean left hippocampus thickness was $1,486 \pm 48.94 \mu\text{m}$. The mean thickness of the right hippocampus was $1,544 \pm 36.75 \mu\text{m}$ for the control group. In the stress group rats, the mean right hippocampus thickness was $1,478 \pm 91.82 \mu\text{m}$. Figure 2 shows the right and left hippocampal thicknesses according to the groups.

When the hippocampus thicknesses of the rats in the experimental and control groups were compared statistically, no significant difference was found in terms of their thickness ($p > 0.05$). Between the groups; no significant difference was found between molecular, pyramidal and polymorphic area thicknesses ($p < 0.05$). When the polymorphic cell layer (PCL) in the gyrus dentatus was examined, the average number of cells was 20 ± 1.38 cells/field for the left PCL and 17 ± 1.35 cells/field for the right PCL in the control group. In the stress group, the average number of cells in the polymorphic cell layer of the gyrus dentatus was 27 ± 2.08 cells/field for the left side and 23 ± 2.01 cells/field for the right side. The cell count in the polymorph cell layer of gyrus dentatus of the hippocampus is given in Figure 3.

When the gyrus dentatus regions were examined, there was a statistically significant difference among the groups cell count in the PCL ($p < 0.05$). When the stress group and control group were compared for the left hippocampus, there was a significant increase in the cell count in the relevant area of the stress group compared to the control ($p = 0.021$). A statistically significant increase in the cell count in the dentate gyrus of the rodent brain in the stress group was found as compared to the control for the right hippocampus ($p = 0.026$). When both experimental groups were compared statistically, there were no significant differences between cell counts in the gyrus dentatus regions of the right and left hemispheres ($p > 0.05$).

The obtained histological images were examined morphologically in both groups. It was observed that the cells in the polymorph cell layer of the animals belonging to the stress group were morphologically spindled. Furthermore, there was a statistically significant increase in the polymorph cell count in the stress group ($p < 0.05$). In the PCLs of the rodents belonging to the stress group, the cells increased with a spindle morphological structure. The histological images of the stress and control groups are shown in Figure 4.

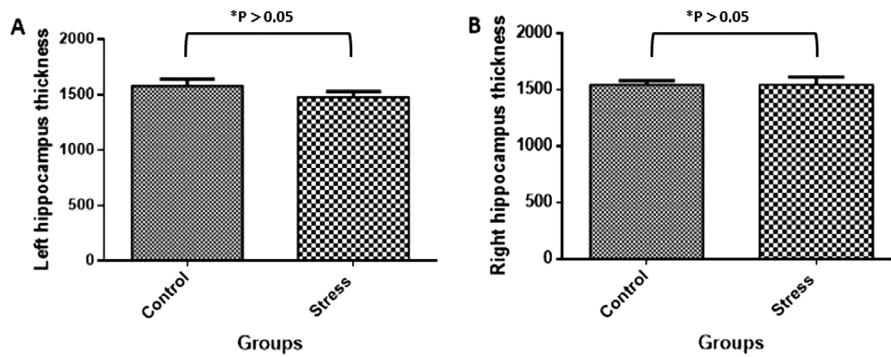


Figure 2. Right and left hippocampus thicknesses for groups. A. Inter-group hippocampal thickness for left hippocampus coronal section, B. Inter-group hippocampal thickness for right hippocampus coronal section.

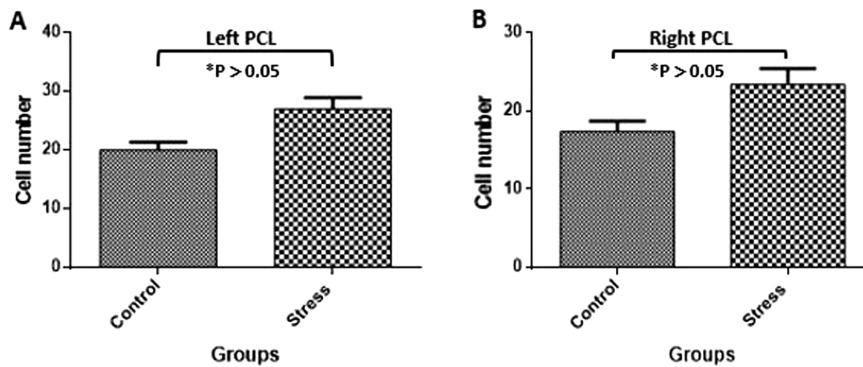


Figure 3. Cell count in the polymorph cell layer, gyrus dentatus. A. Inter-group cell count for the left PCL in gyrus dentatus, B. Inter-group cell count for the right PCL in gyrus dentatus.

We performed the BDNF and GFAP measurements via the ELISA method in serum obtained after intracardiac blood collection. The mean BDNF level was 1.65 ng/mL in the control group and 2.25 ng/mL in the CUMS group. The mean GFAP level was 3.04 ng/mL in the control group and 2.96 ng/mL in the CUMS group. There was no statistically significant difference among the groups in terms of the BDNF and GFAP serum levels ($p > 0.05$, Figure 5).

DISCUSSION

Stress has a significant impact on the brain, and it can cause changes in brain function and structure. The response of stress hormones affects various brain regions, particularly the hippocampus, which is crucial for memory formation. The hypothalamic-pituitary-adrenal (HPA) axis is the primary biological pathway for regulating the effects of stress on the organism. Stress hormones which a steroid structure secreted through this system makes radical changes in the metabolism (3). A thorough understanding of the mechanism of the action of stress can be an effective way to treat diseases such as neuron degeneration.

It is known that stress affects neurobiological pathways and in this way affects neurons, astrocytes and microglia (14). During this process; neurons, astrocytes and glial cells are affected by the HPA axis by means of immunological pathways, and neurotrophic factors. One of the most characterized neurotrophic factors is BDNF, which modulates brain health and neuronal survival (11). The activity dependent expression of BDNF is a crucial mechanism for synaptic plasticity that improves a mammals' learning ability (15). This study investigated whether there was a correlation between BDNF, which has important effects on the biological pathways of CNS and the morphology of the hippocampus under stress. In this study, no difference was found between the experimental group of rats BDNF serum levels which had been applied with the CUMS. The GFAP is a structural filament protein that is mainly expressed in astrocytes (9). The astrocytic cytoskeleton filament protein GFAP plays a role in many processes in the CNS. It has important effects, especially on neuronal survival. Astrocytes have critical roles in maintaining neuronal metabolism, regulating neuroimmunological reactions and maintaining the blood-brain barrier. GFAP, an astrocyte marker,

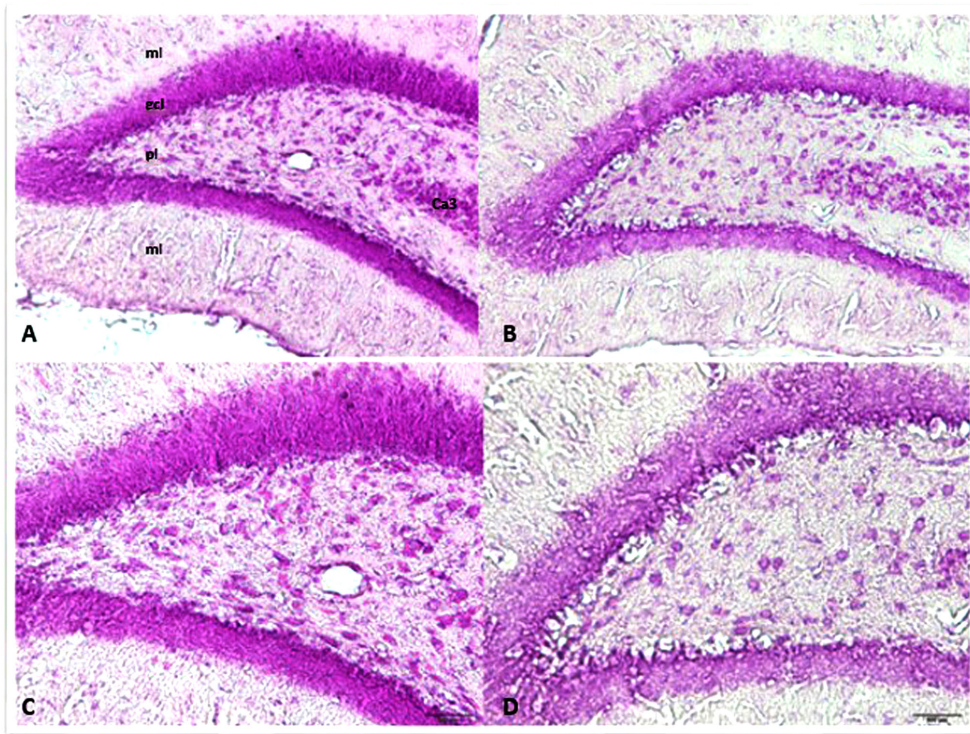


Figure 4. Microscopic images of gyrus dentatus and subunits of CUMS and control group. A. CUMS group gyrus dentatus, 200X; B. Control group gyrus dentatus, 200X; C. CUMS group gyrus dentatus, 400X; D. Control group gyrus dentatus, 400X; pl: Polymorph layer; gcl: Granular cell layer; ml: Molecular layer; Ca3: Cornu ammonis3.

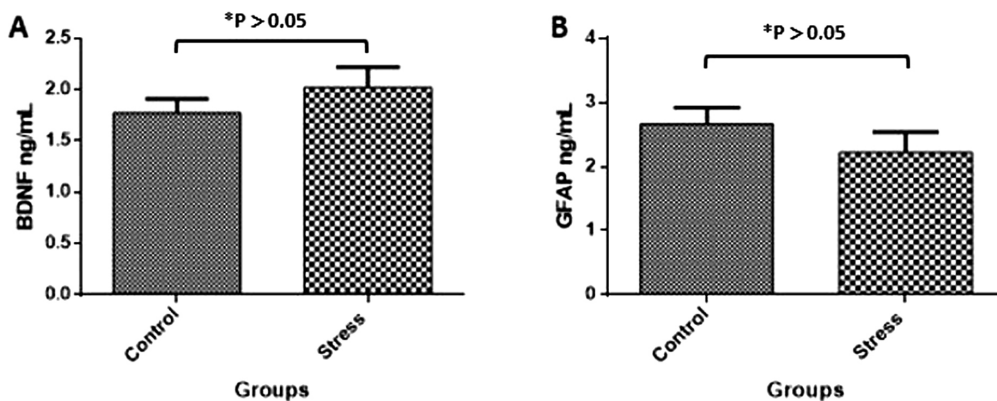


Figure 5. Serum BDNF and GFAP levels for CUMS and control groups. A. Intergroup comparisons of serum BDNF levels, B. Intergroup comparisons of serum GFAP levels.

increases expression in a brain injury or CNS degenerations (16). In this context; we examined the GFAP serum levels as a biomarker for astrocytes, an important component of CNS, as well as hippocampus morphology. There were no significant differences in the GFAP serum levels among the groups.

Excessive stress is a phenomenon that damages the brain tissue. The hippocampus is damaged both cognitively and

morphologically under this condition (6). It is even reported that there is a decrease in hippocampal volume with chronic depression. This volumetric reduction was reported to be due to the pyramidal cell depletion in the cornu ammonis region (17). The organism activates an adaptation mechanism in response to stress. However, the hippocampus also degenerates during chronic stress conditions that disrupt hemostasis (10). The most devastating outcomes occur during chronic severe

stress situations where the adaptation mechanism of the cell is inadequate. Cellular degeneration is inevitable in prolonged periods of intense stress (18). However, it should be noted that mild stress provides cellular stimulation and keeps the organism alert (19). It is reported that neurogenesis decreases during chronic severe stress conditions and increases in acute stress conditions in the hippocampus area. *In vivo* studies showed that the hippocampus also increased neurogenesis in single dose corticosterone administration. Other studies showed that stress hormones cause an increase in fibroblast growth factor (FGF2) receptors in rats hippocampal cells (20). In this study, no difference was found between the hippocampus thickness of rats. The biological pathways underlying the different response mechanisms of animals to stress is thought to contribute to the development of treatment options for stress-dependent diseases. In this context; we applied a mild stress model that is frequently faced in daily life and used an unpredictable experimental model. We prevented the animals from getting accustomed to stress and adapting to it. We examined the morphological changes and cell count changes in the polymorph cell layer in the hilum of the dentate gyrus area under chronic unpredictable mild stress. This study observed a cellular increase in morphologically spindled cells in the region of the PCL. We determined that there was a statistically significant increase in the cell count in the PCL. The close relationship between changes in this area and memory is emphasized in the literature. Degenerations in this part of the gyrus dentatus are closely associated with memory disorders (21).

In another *in vivo* study; when the hippocampal neurogenesis of rodents was inhibited under stress conditions, temporal prolongation in the decrease of stress hormones to normal serum levels was observed. In other words, inhibited neurogenesis was associated with elevated stress-induced high glucocorticoid levels for longer periods. Hippocampal neurogenesis was suggested to buffer the stress responses and depressive behaviors in mammals (22). It is suggested that hippocampal neurogenesis has a buffer function against stress conditions, in mice (19). In this study, we determined cellular changes between the groups 'stress/control' in the PCL of gyrus dentatus against mild stress. The cellular increase in the stress group is considered to be part of an adaptation mechanism to stress, which is also mentioned in the literature. Possible cellular increases in the polymorph cell layer under chronic unpredictable stress may bring about new cellular connections. In this case, it is thought that new cells originating from the progenitor area may cause memory disorders. Newly formed cells can create new synapses independent of the information flow and create new pathways in memory formation in this area. This process is formed as a result of the organism's struggle with stress and can create disruptions in memory condensation (21). This could provide a neurobiological approach to explaining post-stress memory disorders and contribute to improving treatment options.

CONCLUSION

This study aimed to determine how CUMS morphologically affects the hippocampus of rodents. In addition, we evaluated the serum values of BDNF and GFAP which are accepted as biological markers for neurons and astrocytes with morphological changes. When we compared the stress and control groups, we observed changes in the hippocampus of animals under stress conditions. These changes were observed in the gyrus dentatus region which has an important role for memory formation. The cells in the PCL of gyrus dentatus underwent changes under stress. In the results obtained, there was an increase in the cell count in the PCL of gyrus dentatus in the stress group. In addition, the cellular morphologies changed and became spindle shaped. However, the study did not find any significant difference when CUMS and the control groups were compared in terms of hippocampus thickness. In addition, there was no significant difference in the BDNF and GFAP serum markers levels between the groups.

Ethics Committee Approval: Ethical approval of the study was obtained from Animal Experiments Local Ethics Committee, Kocaeli University (2015/44).

Authors' Contributions: Conception/Design of Study - M.D.Y., T.C.; Data Acquisition – M.D.Y., S.K.O., E.A.; Performing experiments – M.D.Y., S.K.O., E.A.; Data Analysis/Interpretation – M.D.Y., T.C.; Statistical Analyses – M.D.Y., S.K.O., E.A.; Drafting Manuscript – M.D.Y., T.C.; Critical Revision of Manuscript – M.D.Y., T.C., S.K.O., S.C., E.A., H.M.K.; Final Approval and Accountability - M.D.Y., T.C.

Conflicts of Interests: The authors declare that they have no competing interests.

Financial Disclosure: This study supported by Scientific Research Projects Coordination Unit, Kocaeli University (2016/032).

REFERENCES

1. Selye H. Homeostasis and heterostasis. *Perspect Biol Med* 1973; 16(3): 441–5.
2. Davies KJA. Adaptive homeostasis. *Mol Aspects Med* 2016; 49: 1–7.
3. Lucassen PJ, Pruessner J, Sousa N, Almeida OFX, Van Dam AM, Rajkowska G, et al. Neuropathology of stress. *Acta Neuropathol* 2014; 127(1): 109–35.
4. O'Keefe J. A review of the hippocampal place cells. *Prog Neurobiol* 1979; 13(4): 419–39.
5. Jaroudi W, Garami J, Garrido S, Hornberger M, Keri S, Moustafa AA. Factors underlying cognitive decline in old age and Alzheimer's disease: The role of the hippocampus. *Rev Neurosci* 2017; 28(7): 705–14.
6. Czéh B, Michaelis T, Watanabe T, Frahm J, de Biurrun G, van Kampen M, et al. Stress-induced changes in cerebral metabolites, hippocampal volume, and cell proliferation are prevented by antidepressant treatment with tianeptine. *Proc Natl Acad Sci U S A* 2001; 98(22): 12796–801.
7. Pfisterer U, Khodosevich K. Neuronal survival in the brain: neuron type-specific mechanisms. *Cell Death Dis* 2017; 8(3): e2643.

8. Willner P. The chronic mild stress (CMS) model of depression: History, evaluation and usage. *Neurobiol Stress* 2016; 6: 78–93.
9. Kamphuis W, Mamber C, Moeton M, Kooijman L, Sluijs JA, Jansen AHP, et al. GFAP isoforms in adult mouse brain with a focus on neurogenic astrocytes and reactive astrogliosis in mouse models of Alzheimer disease. *PLoS One* 2012; 7(8): e42823.
10. Quesseveur G, David DJ, Gaillard MC, Pla P, Wu MV, Nguyen HT, et al. BDNF overexpression in mouse hippocampal astrocytes promotes local neurogenesis and elicits anxiolytic-like activities. *Transl Psychiatry* 2013; 3(4): e253.
11. Kojima M, Mizui T. Chapter Two - BDNF propeptide: A novel modulator of synaptic plasticity. In: Litwack G, editor. *Vitamins and Hormones*. Academic Press 2017; vol. 104, p. 19–28.
12. Willner P, Towell A, Sampson D, Sophokleous S, Muscat R. Reduction of sucrose preference by chronic unpredictable mild stress, and its restoration by a tricyclic antidepressant. *Psychopharmacology (Berl)* 1987; 93(3): 358–64.
13. Qin C, Bai Y, Zeng Z, Wang L, Luo Z, Wang S, et al. The cutting and floating method for paraffin-embedded tissue for sectioning. *J Vis Exp* 2018; (139): 58288.
14. Vallières L, Campbell IL, Gage FH, Sawchenko PE. Reduced hippocampal neurogenesis in adult transgenic mice with chronic astrocytic production of interleukin-6. *J Neurosci* 2002; 22(2): 486–92.
15. Park H, Poo M ming. Neurotrophin regulation of neural circuit development and function. *Nat Rev Neurosci* 2013; 14(1): 7–23.
16. Middeldorp J, Hol EM. GFAP in health and disease. *Prog Neurobiol* 2011; 93(3): 421–43.
17. Qiao H, Li MX, Xu C, Chen HB, An SC, Ma XM. Dendritic spines in depression: What we learned from animal models. *Neural Plast* 2016; 2016: 8056370.
18. Liu D, Wang Z, Gao Z, Xie K, Zhang Q, Jiang H, et al. Effects of curcumin on learning and memory deficits, BDNF, and ERK protein expression in rats exposed to chronic unpredictable stress. *Behav Brain Res* 2014; 271: 116–21.
19. Snyder JS, Soumier A, Brewer M, Pickel J, Cameron HA. Adult hippocampal neurogenesis buffers stress responses and depressive behaviour. *Nature* 2011; 476(7361): 458–61.
20. Kirby ED, Muroy SE, Sun WG, Covarrubias D, Leong MJ, Barchas LA, et al. Acute stress enhances adult rat hippocampal neurogenesis and activation of newborn neurons via secreted astrocytic FGF2. Fernald R, editor. *eLife*. 2013; 2: e00362.
21. Toni N, Schinder AF. Maturation and functional integration of new granule cells into the adult hippocampus. *Cold Spring Harb Perspect Biol* 2016; 8(1): a018903.
22. Drew LJ, Fusi S, Hen R. Adult neurogenesis in the mammalian hippocampus: Why the dentate gyrus? *Learn Mem* 2013; 20(12): 710–29.

Gingipain Injection Affects Intestinal Oxidant-Antioxidant Status and Alkaline Phosphatase in Overfed Zebrafish

Gizem Gunduz¹ , Merih Beler² , Ismail Unal² , Derya Cansiz³ , Ebru Emekli-Alturfan⁴ , Kemal Naci Kose⁵ 

¹Department of Periodontology, Institute of Health Sciences, Marmara University, Turkiye

²Department of Biochemistry, Institute of Health Sciences, Marmara University, Turkiye

³Department of Biochemistry, Faculty of Medicine, Istanbul Medipol University, Turkiye

⁴Department of Biochemistry, Faculty of Dentistry, Marmara University, Turkiye

⁵Department of Periodontology, Faculty of Dentistry, Marmara University, Turkiye

ORCID ID: G.G. 0000-0003-1282-1175; M.B. 0000-0002-3828-4630; İ.Ü. 0000-0002-8664-3298; D.C. 0000-0002-6274-801X; E.E.A. 0000-0003-2419-8587; K.N.K. 0000-0002-0423-8011

Cite this article as: Gunduz G, Beler M, Unal I, Cansiz D, Emekli-Alturfan E, Kose KN. Gingipain injection affects intestinal oxidant-antioxidant status and alkaline phosphatase in overfed zebrafish. *Experimed* 2023; 13(2): 80-85.

ABSTRACT

Objective: *Porphyromonas gingivalis* (*P. gingivalis*), a major periodontopathogen, is associated with overfeeding disorders, including metabolic syndrome. Gingipains are one of the most powerful endotoxins of *P. gingivalis*. Our aim was to reveal the effects of gingipain injections on the intestinal oxidant-antioxidant status and alkaline phosphatase (ALP) activity in overfed zebrafish.

Materials and Methods: Four groups of healthy adult zebrafish were placed in random tanks as C: Control (n=15); GP: Gingipain (n=15); OF: Overfeeding (n=15); and OF+GP: Overfeeding+Gingipain (n=15) groups. At the end of the experiment, levels of intestinal lipid peroxidation (LPO) and ALP, glutathione S-transferase (GST), and catalase (CAT) activities were evaluated.

Results: Intestinal LPO was significantly lower in the GP and OF groups compared to C. Gingipain injection in OF (OF+GP) significantly elevated LPO when compared to C, GP, and OF groups. ALP activities decreased significantly in the GP, OF, and OF+GP compared to C. GST activities increased significantly in the GP when compared to C. Decreased GST activities were observed in the OF and OF+GP. This decrease was less in OF+GP. CAT activities significantly decreased in all groups when compared to C.

Conclusion: Our findings demonstrate that gingipain injection alters the ALP activity and intestinal oxidant-antioxidant status in overfed zebrafish.

Keywords: Gingipain, zebrafish, oxidative stress

INTRODUCTION

Porphyromonas gingivalis (*P. gingivalis*), a gram-negative anaerobic bacteria, is involved in the etiology of periodontitis. Periodontitis is generally characterized by bacteria-induced inflammation, which damages the tissues around teeth resulting in teeth loss. This strong keystone periodontopathogen, highly related to severe periodontitis, is an effective colonizer of the oral epithelium. *P. gingivalis*

can infiltrate periodontal tissues and get over the host's immune response. Using a panel of virulence factors, it destabilizes innate immunological and inflammatory responses (1). Capsule, lipopolysaccharide (LPS), fimbriae, and cysteine proteases are some listed virulence factors of *P. gingivalis* (2).

P. gingivalis' extracellular cysteine proteinases, known as gingipains, are major endotoxins among these virulence

Corresponding Author: Kemal Naci Köse **E-mail:** kemkose@superonline.com

Submitted: 24.03.2023 **Revision Requested:** 24.04.2023 **Last Revision Received:** 02.05.2023 **Accepted:** 05.05.2023 **Published Online:** 03.08.2023



Content of this journal is licensed under a Creative Commons Attribution-NonCommercial 4.0 International License.

factors. The gingipains are composed of Lys-gingipain (Kgp) and Arg-gingipain (Rgp) (RgpA and RgpB). Gingipain R is specific for arginine, while gingipain K is specific for lysine residues. Gingipains cleave amino acid chains right after lysine or arginine residues at the C-terminal region. In the physiology of the bacteria, gingipains' proteolytic activity is critical for adhering to host surfaces, obtaining nutrition through protein degradation, and promoting further colonization. While present in circulation, gingipains are also associated with fibrin(ogen)olytic activity and can interact with and degrade plasma proteins (3). Gingipains are responsible for 85% of *P. gingivalis*' extracellular proteolytic activities and play a major role in periodontitis. They activate host matrix metalloproteinases, inactivate immune defense by degrading immunological components, and cleave immune cell receptors, causing immune dysregulation and inflammation (2).

P. gingivalis and its endotoxins, including gingipains are detected in circulation and organ lesions (4, 5). The host defense molecules produced against these endotoxins together with bacteria itself play a significant role in the relationship between systemic diseases and periodontitis (6). The current trend topic for periodontal research is the connection between periodontitis and metabolic syndromes, including obesity and diabetes mellitus (7, 8). Recent research has also suggested that *P. gingivalis* cause an imbalance in the microbiota of intestinal tissues and exacerbate metabolic problems (9).

The metabolic syndrome, formerly referred to as insulin resistance, is a group of risk factors including elevated triglycerides and fasting glucose, reduced high-density lipoprotein, high blood pressure and abdominal obesity that increase the risk of type 2 diabetes mellitus (T2D), cardiovascular diseases and even death. In metabolic syndrome, inflammation in adipose tissues and imbalance in intestinal flora are thought to be possible reasons in this abnormal systemic status. As a consequence of continuous exposure to high-fat diets, the composition of gut microbiota is altered and the intestinal mucosa barrier is damaged, allowing enterotoxins to enter systemic circulation. Rapid adipocyte hypertrophy caused tissue hypoxia and induced elevated adipokines, including tumor necrosis factor-alpha (TNF- α) and interleukin-6 (IL-6), stimulating macrophages to release pro-inflammatory substances resulting in increased systemic inflammation and insulin resistance (9).

Intestinal alkaline phosphatase (ALP) is a major player in maintaining intestinal homeostasis and health. Obesity is one of the chronic inflammatory conditions that have been linked to altered ALP expression. Intestinal ALP is essential in the activation of bacterial Lipopolysaccharides (LPS) through dephosphorylation of its lipid A moiety, resulting in a non-toxic monophosphoryl section. This dephosphorylated monophosphoryl lipid A is not capable of forming a complex with the host's toll like receptor 4 (TLR4) (10).

Oxidative stress, the imbalance between oxidants and anti-oxidants, as a result of increased free radicals is involved in the molecular mechanisms underlying many diseases. In order to countervail these harmful molecules, the anti-oxidant enzymes including catalase (CAT), superoxide dismutase (SOD), glutathione S-transferase (GST) and glutathione peroxidase in addition to antioxidant molecule, glutathione (GSH) are produced.

The increased oxidative stress is considered to be an essential factor in the relation between periodontitis and over-eating induced-metabolic syndrome. Intestinal homeostasis and health are also involved in the molecular mechanisms related with obesity and metabolic syndrome. Increased serum Reactive oxygen species (ROS) are present in these conditions, and a pro-inflammatory state is expected to have a reciprocal influence on the molecular mechanisms (7). Patients with periodontitis may experience greater levels of oxidative stress induced-inflammation due to the deranged endogenous antioxidant defense system driven by the overproduction of lipid peroxidation products at inflammatory sites (11).

Due to their various benefits, including their small size, brief life cycle, availability in huge numbers, and low maintenance requirements, zebrafish have become a prominent vertebrate model organism for biomedical research. Zebrafish are used in numerous areas, including genetics, biomedicine, neuroscience, toxicology, pharmacology, as well as the modeling of human disease (12). Overfeeding-caused metabolic syndrome diseases such as obesity and diabetes have been well documented in zebrafish models as well (13-15). *P. gingivalis* and gingipains related research have been recently conducted in zebrafish, but in these studies and other animal models, the specific effects of gingipains have not yet been explored. Despite *P. gingivalis*' many other virulence factors such as LPS, capsule, and fimbria, which all create a cumulative effect in bacterias' pathogenicity, it is important to underline the specific effects of gingipain itself in order to reveal this powerful endotoxins' toxicity (16-18). Here in this study, our aim was to assess the impact of gingipain injections on the intestinal oxidant-antioxidant status and ALP activity in overfed zebrafish to explore the relationship between periodontopathogens' virulence factors and metabolic diseases and to underline the role of gingipain in these complicated pathological mechanisms. We also assessed intestinal ALP because of its regulatory role in intestinal homeostasis in the case of overfeeding situations, which is an inflammatory condition related with altered ALP expression.

MATERIALS AND METHODS

Animals and Treatment

The animal experiments conducted in this study were performed according to the European Communities Council Directive of 24 November 1986 (86/609/EEC). The entire procedures used were authorized by the Marmara University Animal Care and Use Committee (38.2021mar). According to the ARRIVE (Animal Research: Reporting of *in Vivo* Experiments)

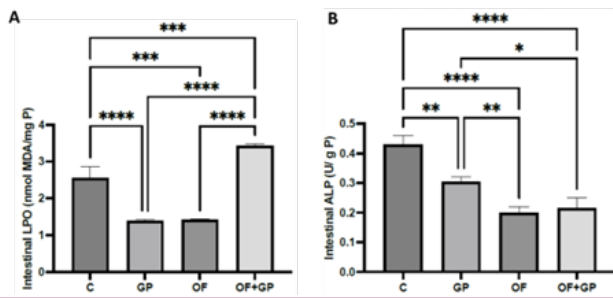


Figure 1. A: LPO levels **B:** ALP activities of the groups. Values are given as means \pm SD; n= 6. **** p<0.0001; *** p<0.001, ** p<0.01; * p<0.05. LPO: Lipid peroxidation, ALP: Alkaline phosphatase, C: Control; GP: Gingipain, OF: Overfeeding, OF+GP: Overfeeding+Gingipain,

guidelines, care was taken to utilize as few animals as possible in the research. Zebrafish (AB/AB strain, wild type) were kept in an aquarium rack system (ZebTEC, Tecniplast, Italy) at a 14/10-hour light/dark cycle and $27\text{--}28 \pm 1^\circ\text{C}$ temperature. Four groups of zebrafish (4-6 months old) were placed at random as C: Control (n=15); GP: Gingipain (n=15); OF: Overfeeding (n=15); and OF+GP: Overfeeding+Gingipain (n=15) groups. The control group was fed with 20 mg of fish food/fish/day, while the overfed zebrafish groups were fed with 120 mg/fish/day of commercial fish food (3.39 kcal/g; TetraMine; Tetra; Germany) over six daily feeding periods using an automated feeding system (Yinsheng T8800; Yinsheng; China). Overfeeding procedure was continued for 15 days. The content of tetramine consisted of a minimum of 51% crude protein, 11% crude oil, 2.3% calcium, 1.5% phosphorus and a maximum of 3% crude fiber, 6.5% moisture and 15% ash. The granule proportions of tetramine were between 0.65 mm and 0.36 mm. The tanks were cleaned and filled with fresh water daily. Gingipain (MyBioSource, Inc., USA, MBS969681, Recombinant *P. gingivalis* Gingipain R1 (rgpA), partial) at 186 nmol/L was intraperitoneally injected into fish in the GP group. Gingipain dosages were chosen and

applied in accordance with range finding research (19). 6 hours after injection applications the zebrafish were sedated and euthanized. Intestinal tissues of the zebrafish were taken, and for upcoming analyses, replicate samples of the tissues were made.

Biochemical Analyses

The total protein concentrations were measured using the Lowry et al. method, and the findings were provided per protein (20). Malondialdehyde (MDA) levels were measured using the Yagi method, and they were analyzed as thiobarbituric acid reactive compounds that are formed as byproducts of lipid peroxidation (LPO) (21). CAT activity was assessed by using the modified method of Aebi (22). For the conjugation of GSH, GST is required, and the activity of GST was measured using a spectrophotometer at 340 nm (23). ALP activity was measured according to Walter and Schutt method (24).

Statistical Analyses

For the statistical analyses GraphPad Prism 9.0 (GraphPad Software, San Diego, USA) was used and the data were presented as mean \pm standard deviation. Dunn’s multiple comparison test was run after the Kruskal Wallis test to compare the data. The Pearson correlation test was applied to evaluate the relationship between the oxidant and antioxidant parameters. Significant data were defined as those with a p-value lower than 0.05 (p<0.05).

RESULTS

When compared with the control group, overfeeding and gingipain injections yielded a significant decrease in intestinal LPO (p<0.001 and p<0.0001, respectively). However, gingipain injections increased LPO level significantly in overfed zebrafish (OF+GP) when compared to the GP, OF, and control groups, (p<0.0001, p<0.001, and p<0.001, respectively) (Figure 1A).

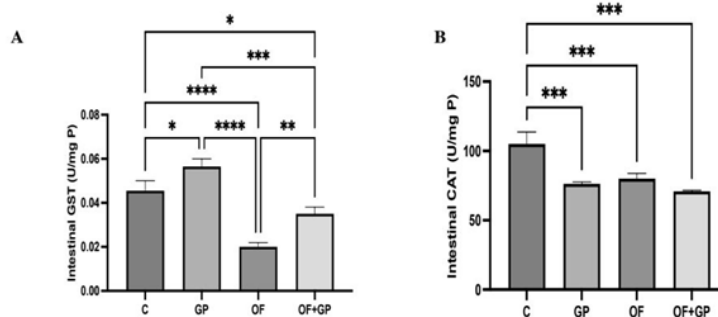


Figure 2. A: GST **B:** CAT activities of the groups. Values are given as means \pm SD; n= 6. **** p<0.0001; *** p<0.001, ** p<0.01; * p<0.05. GST: Glutathione S-transferase, CAT: Catalase, C: Control; GP: Gingipain, OF: Overfeeding, OF+GP: Overfeeding+Gingipain

Intestinal ALP activities decreased significantly by gingipain injections and overfeeding in all three groups (GP, OF, and OF+GP) when compared to the control group ($p < 0.01$, $p < 0.0001$, and $p < 0.0001$, respectively) (Figure 1B).

Intestinal GST activities were significantly elevated by gingipain injections when compared with the control group ($p < 0.05$). However, decreased GST activities were observed in the OF and OF+GP groups ($p < 0.0001$ and $p < 0.05$, respectively). Gingipain injections led to increased GST activities in the overfed zebrafish (OF+GP) ($p < 0.01$) (Figure 2A).

Intestinal CAT activities decreased significantly by gingipain injections and overfeeding in all three groups (GP, OF, and OF+GP) when compared with the control group ($p < 0.001$). No significant change was observed among GP, OF, and OF+GP (Figure 2B).

In the GP group, LPO was positively correlated with CAT activity ($r = 1$; $p < 0.0001$), and negatively correlated with GST activity ($r = -1$; $p < 0.0001$). In the OF group, LPO was positively correlated with GST activity ($r = 1$; $p < 0.0001$); whereas a negative correlation was found between LPO and CAT activity in the same group ($r = -1$; $p < 0.0001$). In the OF+GP group, LPO was negatively correlated with CAT and GST activities ($r = -1$; $p < 0.0001$).

DISCUSSION

P. gingivalis and one of its most significant endotoxins, gingipain, have been detected in organs and the circulatory system. The inhibition of gingipains with the specific inhibitors in *P. gingivalis* infected mice reduced neuroinflammation and brain infection (4). Oral administration of *P. gingivalis* exacerbates the severity of drug-induced colitis in mice (5). These and many other data demonstrate that *P. gingivalis*, key periodontopathogen, and its endotoxins are associated with many systemic disease pathologies. The current trend topic for periodontal research is the relation between periodontitis and metabolic syndromes, including obesity and diabetes mellitus, which are related with overfeeding (7, 8). Many studies about the relation with periodontopathic bacteria and intestinal disorders have indicated that *P. gingivalis* generate the dysbiosis of gut microbiota resulting in the aggregation of metabolic disorders, recently (9).

Dynamic relationships between the intestinal epithelium, the microbiota, and the human immune system are necessary for intestinal homeostasis. Intestinal homeostasis is maintained by a variety of regulatory mechanisms, and a malfunction in these pathways may lead to the chronic inflammatory pathological evident in inflammatory bowel disease (25).

The oral administration of *P. gingivalis* dramatically worsened colitis in the experimental colitis model. By lowering the expression of tight junction proteins *in vivo*, the ingested *P. gingivalis* damaged the colonic epithelial barrier in mice. The disruption of the epithelial barrier specific to *P. gingivalis* was

shown by *in vitro* permeability experiments employing the intestinal epithelial cell line (26).

In this study, we wanted to assess the impacts of gingipain injection on the intestinal oxidant-antioxidant status and ALP activity in overfed zebrafish. We found that gingipain injections decreased intestinal ALP activity. Through interactions with the local microbiota, nutrition and the gut, intestinal ALP has an important function in intestinal homeostasis and health. The function of intestinal ALP in the intestine is to dephosphorylate extracellular nucleotides like uridine diphosphate as well as harmful microbial ligands such as LPS. Intestinal ALPs' capacity to control the microbial environment by establishing a complicated interaction between the microbiota, food, and the intestinal mucosal surface is also crucial in these issues. The gut microbiota and homeostasis can be affected by overfeeding because it changes intestinal ALP expression and activity (27).

Obesity is one of the chronic inflammatory conditions that have been linked to altered intestinal ALP expression (10). The results of our study showed decreased intestinal ALP activity in the overfed group. This finding indicates the diminished protective effect of intestinal ALP due to overfeeding on intestinal hemostasis.

In this study, the activities of CAT and GST were evaluated as they are the main antioxidant enzymes that might detoxify free radicals in the case of GP injection and overfeeding. CAT enzymes defend cells against free radical damage by degrading hydrogen peroxide (22), and GSTs may detoxify the end products of LPO and they can prevent the formation of lipid hydroperoxides (23).

Gingipain injections decreased intestinal CAT activity and LPO in the intestines. The reduction in CAT activity may be associated with the use of CAT to inhibit the increase in LPO associated with gingipain toxicity-induced inflammation. Similarly, the decreased LPO levels in the OF group may be associated with decreased CAT activity in the same group due to its use as an antioxidant to prevent the increase in LPO, consistent with the negative correlation between LPO and CAT observed in this group. Decreased LPO in the GP injected group may also be attributed to the substantial increase in the GST activities in the same group. In order to combat foreign compounds or oxidative stress products, GSTs catalyze the conjugation of reduced glutathione, resulting in the formation of less reactive molecules that are easily eliminated (28). Accordingly, in our study, increased GST in the gingipain-injected group may be suggested to prevent the increase in LPO levels due to gingipain injection. Decreased GST activity in the overfed group is consistent with the reported decrease in the adipose tissue GST enzyme content of high fat fed mice (29). However, gingipain injections in the overfed group caused an elevation in the GST activities to overcome oxidative stress induced by gingipain, as evidenced by increased LPO in the same group. Moreover, gingipain injections caused a significant elevation in GST activity, whereas overfeeding caused a reduction in

intestinal GST activity. Lower GST activity in the gingipain-injected overfed group, when compared with the gingipain-injected group, demonstrated that overfeeding diminished antioxidant response and even the gingipain challenge was not enough to augment this impairment.

As far as we are aware, there are only a few studies that have used gingipain *in vivo* models directly (18). It would be advantageous to increase the number of studies on the direct use of gingipain in zebrafish, given the benefits of this animal model, including their use in toxicological studies and the modelling of systemic diseases. Moreover, to our knowledge, this is the first study to report the effects of gingipain injections on the intestinal oxidant-antioxidant status and ALP activity in overfed zebrafish. Our study showed that gingipain disrupts the oxidant-antioxidant balance and ALP activity in the intestines due to overnutrition and provided important information on the effects of periodontal pathogens on intestinal health in metabolic diseases. We believe that our findings will guide future studies related to the connection of systemic diseases and periodontitis pathology.

Ethics Committee Approval: This study is approved by of Marmara University Animal Experiments Local Ethics Committee (38.2021mar).

Authors' Contributions: Conception/Design of Study- G.G., E.E.A., K.N.K.; Data Acquisition – G.G., M.B.; Data Analysis/Interpretation – G.G., M.B., İ.Ü., D.C., E.E.A., K.N.K.; Drafting Manuscript– G.G.; Critical Revision of Manuscript- E.E.A., K.N.K.; Final Approval and Accountability– G.G., M.B., İ.Ü., D.C., E.E.A., K.N.K.

Conflicts of Interests: The authors declare that they have no competing interests.

Financial Disclosure: This project was supported by Marmara University Scientific Research and Project Commission, Project No: TDK-2021- 10420.

REFERENCES

1. Mysak J, Podzimek S, Sommerova P, Lyuya-Mi Y, Bartova J, Janatova T, et al. Porphyromonas gingivalis: Major periodontopathic pathogen overview. J Immunol Res 2014; 2014: 476068.
2. Xu W, Zhou W, Wang H, Liang S. Roles of Porphyromonas gingivalis and its virulence factors in periodontitis. Adv Protein Chem Struct Biol 2020; 120: 45-84.
3. Nunes JM, Fillis T, Page MJ, Venter C, Lancry O, Kell DB, et al. Gingipain R1 and lipopolysaccharide from Porphyromonas gingivalis have major effects on blood clot morphology and mechanics. Front Immunol 2020; 11: 1551.
4. Dominy SS, Lynch C, Ermini F, Benedyk M, Marczyk A, Konradi A, et al. Porphyromonas gingivalis in Alzheimer’s disease brains: Evidence for disease causation and treatment with small-molecule inhibitors. Sci Adv 2019; 5(1): eaau3333.
5. Tsuzuno T, Takahashi N, Yamada-Hara M, Yokoji-Takeuchi M, Sulijaya B, Aoki-Nonaka Y, et al. Ingestion of Porphyromonas gingivalis exacerbates colitis via intestinal epithelial barrier disruption in mice. J Periodontal Res 2021; 56(2): 275-88.
6. Mei F, Xie M, Huang X, Long Y, Lu X, Wang X, et al. Porphyromonas gingivalis and its systemic impact: Current status. Pathogens 2020; 9(11): 944.

7. Bullon P, Morillo J, Ramirez-Tortosa MC, Quiles J, Newman H, Battino M. Metabolic syndrome and periodontitis: Is oxidative stress a common link? J Dent Res 2009; 88(6): 503-18.
8. Nibali L, Tatarakis N, Needleman I, Tu Y-K, D’Aiuto F, Rizzo M, et al. Association between metabolic syndrome and periodontitis: A systematic review and meta-analysis. J Clin Endocrinol Metab 2013; 98(3): 913-20.
9. Dong Z, Lv W, Zhang C, Chen S. Correlation analysis of gut microbiota and serum metabolome with porphyromonas gingivalis-induced metabolic disorders. Front Cell Infect Microbiol 2022; 12: 858902.
10. Molnár K, Vannay Á, Szebeni B, Bánki NF, Sziksz E, Cseh Á, et al. Intestinal alkaline phosphatase in the colonic mucosa of children with inflammatory bowel disease. World J Gastroenterol 2012; 18(25): 3254.
11. Panjamurthy K, Manoharan S, Ramachandran CR. Lipid peroxidation and antioxidant status in patients with periodontitis. Cell Mol Biol Lett 2005; 10(2): 255-64.
12. Karaman GE, Emekli-Alturfan E, Akyüz S. Zebrafish; an emerging model organism for studying toxicity and biocompatibility of dental materials. Cell Mol Biol (Noisy-le-grand) 2020; 66(8): 41-6.
13. Oka T, Nishimura Y, Zang L, Hirano M, Shimada Y, Wang Z, et al. Diet-induced obesity in zebrafish shares common pathophysiological pathways with mammalian obesity. BMC physiol 2010; 10(1): 1-13.
14. Dandin E, Üstündağ ÜV, Ünal İ, Ateş-Kalkan PS, Cansız D, Beler M, et al. Stevioside ameliorates hyperglycemia and glucose intolerance, in a diet-induced obese zebrafish model, through epigenetic, oxidative stress and inflammatory regulation. Obes Res Clin Pract 2022; 16(1): 23-9.
15. Zang L, Shimada Y, Nishimura Y, Tanaka T, Nishimura N. A novel, reliable method for repeated blood collection from aquarium fish. Zebrafish 2013; 10(3): 425-32.
16. Widziolok M, Prajsnar TK, Tazzyman S, Stafford GP, Potempa J, Murdoch C. Zebrafish as a new model to study effects of periodontal pathogens on cardiovascular diseases. Sci Rep 2016; 6(1): 36023.
17. Farrugia C, Stafford GP, Potempa J, Wilkinson RN, Chen Y, Murdoch C, et al. Mechanisms of vascular damage by systemic dissemination of the oral pathogen Porphyromonas gingivalis. FEBS J 2021; 288(5): 1479-95.
18. Wilensky A, Potempa J, Hourri-Haddad Y, Shapira L. Vaccination with recombinant RgpA peptide protects against Porphyromonas gingivalis-induced bone loss. J Periodontal Res 2017; 52(2): 285-91.
19. Kose K, Gündüz G, Beler M, Emekli-Alturfan E. Inflammatory gene expression in response to gingipain in zebrafish. The 26th International Congress of Turkish Dental Association, September 8-11, J Clin Sci (Supplements), 2022; 11(3): 596-597.
20. Lowry OH. Protein measurement with the Folin phenol reagent. J Biol Chem 1951; 193: 265-75.
21. Yagi K. Assay for blood plasma or serum. Methods Enzymol 1984; 105: 328-31.
22. Aebi H. Catalase in vitro. Methods Enzymol 1984; 105: 121-6.
23. Habig WH, Pabst MJ, Jakoby WB. Glutathione S-transferases: The first enzymatic step in mercapturic acid formation. J Biol Chem 1974; 249(22): 7130-9.
24. Walter K, Schütt C. Acid and alkaline phosphatase in serum (two point method). Methods of Enzymatic Analysis. Vol. 2. Bergmeyer HU editor, Boca Raton, FL, USA: Verlag Chemie GmbH; 1974. p. 856-60.
25. Maloy KJ, Powrie F. Intestinal homeostasis and its breakdown in inflammatory bowel disease. Nature 2011; 474(7351): 298-306.

26. Tsuzuno T, Takahashi N, Yamada-Hara M, Yokoji-Takeuchi M, Sulijaya B, Aoki-Nonaka Y, et al. Ingestion of *Porphyromonas gingivalis* exacerbates colitis via intestinal epithelial barrier disruption in mice. *J Periodontal Res* 2021; 56(2): 275-88.
27. Estaki M, DeCoffe D, Gibson DL. Interplay between intestinal alkaline phosphatase, diet, gut microbes and immunity. *World J Gastroenterol* 2014; 20(42): 15650.
28. Röth E, Marczin N, Balatonyi B, Ghosh S, Kovács V, Alotti N, et al. Effect of a glutathione S-transferase inhibitor on oxidative stress and ischemia-reperfusion-induced apoptotic signalling of cultured cardiomyocytes. *Exp Clin Cardiol* 2011; 16(3):92-6.
29. Frohnert BI, Bernlohr DA. Glutathionylated products of lipid peroxidation: a novel mechanism of adipocyte to macrophage signaling. *Adipocyte* 2014; 3(3): 224-9.

Evaluation of DNA Microarray in Biomarker Detection in Cell-free DNA from Colorectal Cancer Cell Lines: A Proof-of-Concept Study

Hasan Huseyin Kazan^{1,2} , Ceyhan Piril Karahan³ , Ekin Celik⁴ , Ahmet Caglar Ozketen⁵ , Duygu Birgucu Cagil⁶ , Mehmet Ali Ergun⁷ 

¹Department of Medical Genetics, Faculty of Medicine, Near East University, Mersin 10, Turkiye

²DESAM Research Institute, Near East University, Mersin 10, Turkiye

³Department of Biology, Selcuk University, Konya, Turkiye

⁴Department of Medical Biology, Faculty of Medicine, Kirsehir Ahi Evran University, Kirsehir, Turkiye

⁵Department of Chemistry, Middle East Technical University, Ankara, Turkiye

⁶Department of Biology, Ankara University, Ankara, Turkiye

⁷Department of Medical Genetics, Faculty of Medicine, Gazi University, Ankara, Turkiye

ORCID ID: H.H.K. 0000-0001-7936-8606; C.P.K. 0009-0003-2960-6647; E.C. 0000-0003-1966-3907; A.C.O. 0000-0001-6482-6918;

D.B.C. 0009-0006-7526-5611; M.A.E. 0000-0001-9696-0433

Cite this article as: Kazan HH, Karahan CP, Celik E, Ozketen AC, Birgucu Cagil D, Ergun MA. Evaluation of DNA microarray in biomarker detection in cell-free DNA from colorectal cancer cell lines: A proof-of-concept study. *Experimed* 2023; 13(2): 86-92.

ABSTRACT

Objective: DNA microarray is a powerful method to identify genomic anomalies including small insertions, duplications and/or deletions. This method is widely used in routine genetic screening for explaining the genetic background of certain phenotypes, for example, cancer. Cell-free DNA (cfDNA), which is an approach that may give information about the somatic tissues in peripheral blood, is another popular method used in routine genetic screening to understand the background of particular phenotypes, one of which is cancer. There is limited available research that investigates the involvement of these two approaches to decipher novel cancer biomarkers in the literature. However, detection of cancer biomarkers, especially non-invasive types, has been of great interest to research groups.

Materials and Methods: In the present study, we used colorectal cancer as a model tumor to figure out whether we could determine definite biomarkers from cfDNA using DNA microarray methodology. We isolated cfDNA from the cell-free mediums of the cultures of colorectal cancer cell lines in the presence of the control group which was the healthy epithelial colon cell line.

Results: Our results underlined significant alterations that were deletions and/or duplications in some of the genomic regions in a cell line-specific manner.

Conclusion: We propose that DNA microarray could be used to assess the sub-types of certain cancers in a non-invasive manner using cfDNA approaches.

Keywords: cfDNA, carcinogenesis, colorectal cancer, DNA microarray, biomarker

INTRODUCTION

Colorectal cancer (CRC) is one of the most widespread cancers estimated by the Global Cancer Observatory listed in the 'cancer today' data of 2020 (1). CRC is in third place for the number of incidences; however, it ranks second in terms of mortality rate (2). Considering the estimated

number of 1.9 million cases annually, this notorious disease devastates the economy and life expectancy worldwide. The early diagnosis of the tumorigenesis and profiling the mutations may increase the survival rate by improving the chance to fight back. It has been reported that only 30-40% of the cases were diagnosed at early stages (3). Hence,

Corresponding Author: Hasan Huseyin Kazan **E-mail:** hasanhuseyinkazan@gmail.com

Submitted: 07.03.2023 **Revision Requested:** 24.03.2023 **Last Revision Received:** 30.05.2023 **Accepted:** 05.06.2023 **Published Online:** 04.08.2023



Content of this journal is licensed under a Creative Commons Attribution-NonCommercial 4.0 International License.

there is a continuous need for novel diagnostic processes to detect the disease in the initial phases.

Current screening processes for CRC involve analyzing the presence of blood in stool samples, fecal immunochemical tests and colonoscopies (4). When the result is positive, a biopsy takes place to profile the tumor. Nevertheless, the heterogeneity of cancer remains a big challenge to identify mutations (5). Testing blood samples or other body fluids could decrease the compliance of patients. Cell-free DNA (cfDNA) is one of the most promising macromolecules found in body fluids such as blood, saliva and urine (6). It originates from apoptotic, necrotic, or secretory pathways of both healthy and cancer cells of the body (4). These cleaved small DNA sequences contain biomarkers to identify and characterize heterogeneous tumor cells without blockage by tissue-specific boundaries. Therefore, cfDNA has been targeted and exploited by several studies to detect markers of cancers for early diagnosis. In these reports, next-generation sequencing (NGS), real-time polymerase chain reaction (RT-PCR) or droplet digital PCR (ddPCR) have been employed to identify the markers (7-9).

DNA microarray is a robust strategy for the identification and high-throughput screening of genomic anomalies including point mutations, chromosomal alterations such as deletions, and insertions, and copy number variations (CNVs). Microarray tools provide advantages in cancer diagnosis, classification and determination of treatment options (10, 11). Therefore, combining DNA microarray strategy with cfDNA approach would be a vigorous tactic to identify and analyze the markers embedded in cfDNA without meddling with tumor heterogeneity, tissue type and time points. Large-scale screening of cancer markers at any time interval could be possible with this robust, flexible and effortless method using only body fluids.

The present study aimed to clarify any possible markers in the cfDNAs obtained from different CRC cell lines using DNA microarray approach. Up to now, this is the first study assessing biomarker availability by combining both cfDNA and DNA microarray approaches.

MATERIALS AND METHODS

Cell Lines and Cell Culture

In the present study, sporadic colorectal cancer cell lines, LIM1863; colorectal carcinoma cell lines, HCT116 and CACO-2; and colorectal adenocarcinoma cell lines with epithelial morphology HT-29 were used in the presence of normal colon fibroblast cell lines CCD-18Co. All cells were grown in RPMI 1640 medium (Thermo Fischer, USA) in the presence of 1% penicillin/streptomycin (Thermo Fischer, USA) and 10% fetal bovine serum (FBS; Thermo Fischer, USA) in an incubator under 37°C and 5% CO₂ conditions. Cells were routinely passaged when they reached 80% confluency. All experiments were performed when the confluency was 80%.

Isolation of cfDNA

cfDNAs were isolated from the mediums in which the cells were cultured. When the cells reached 80% confluency, the medium on the cells were carefully obtained. Next, medium was slightly centrifuged at 200 g for 5 min to pellet the remaining cells. The supernatants were used for cfDNA isolation using a ZipPrime cfDNA isolation kit (ZipPrime Ltd., Turkiye). In short, 1 ml of the medium was lysed by pre-heated lysis buffer containing proteinase K (Thermo Scientific, USA). Then, the lysate was mixed by a binding solution including binding beads, and shaken for 10 min at room temperature. After mixing, the supernatants were removed with the help of a magnetic rack, and the beads were washed with washing solutions twice. Finally, the beads were dried and re-suspended with 20 µl of the elution buffer, and the supernatants containing cfDNA were obtained. The concentrations and purities of the isolated cfDNAs were determined by both NanoDrop (NanoDrop ND-1000; Thermo Scientific, USA) via optical density ratios (OD260/280 and OD260/230), and Qubit 4 Fluorometer (Thermo Scientific, USA).

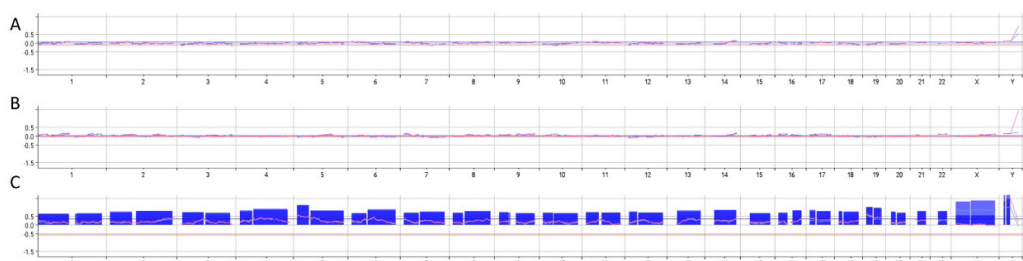


Figure 1. Comparison of the microarray results obtained from CCD-18Co cfDNA with the reference and assessment of genomic DNA (gDNA) contamination. The cfDNAs from CCD-18Co cells were isolated at three different culturing processes. One of them was used as the reference for all cell groups while the others (A and B) were assessed as a study group. As a further control, one of the cfDNAs was deliberately contaminated by commercial human reference DNA and a microarray was performed after whole genome amplification (WGA) step (C). Blue bars correspond to the amplifications of the regions.

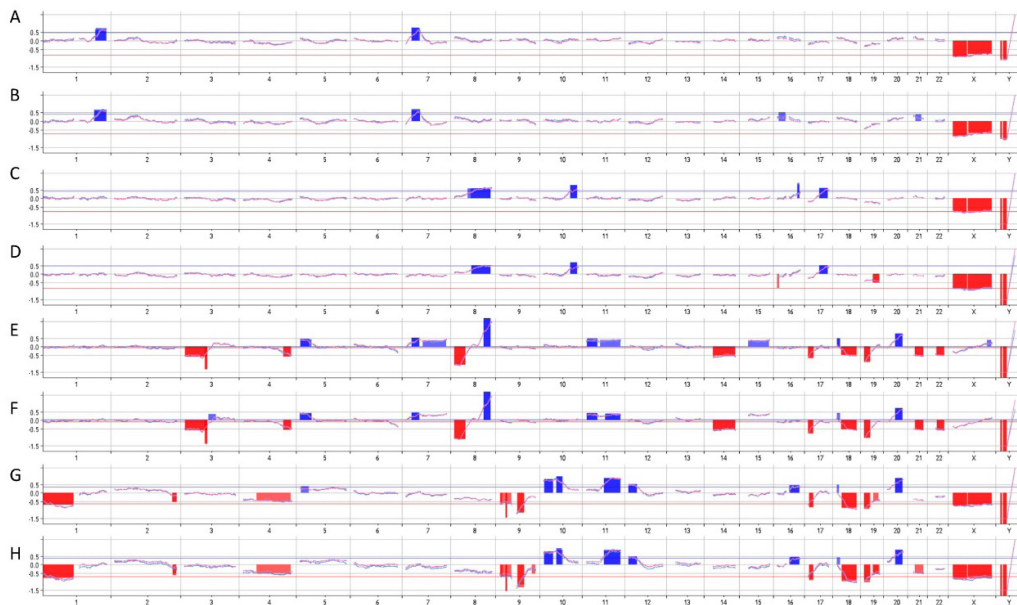


Figure 2. DNA microarray results from cfDNAs obtained from LIM1863 (A-B), HCT116 (C-D), HT-29 (E-F) and CACO-2 (G-H) cells. Red bars point to the losses while blue ones underline the gains.

Whole Genome Amplification (WGA) and DNA Microarray

The isolated cfDNAs were whole-genome amplified using REPLI-g WGA kit (Qiagen, Germany) according to the supplier’s instructions. The amplification was checked with 1% agarose gel. WGA products were labeled with Cyanine3 (Cy3) or Cyanine5 (Cy5) fluorophores at 37°C for 2 h. After the purification step, the labeled DNAs were hybridized using GenetiSure Pre-Screen 8x60K slides (Agilent Technologies, Inc., USA) at 67°C for 16 h. After the washing and drying steps, the slides were scanned by a Sure Scan Microarray Scanner (Agilent Technologies, Inc., USA). The data were analyzed by CytoGenomics Single Cell Analysis software (Agilent Technologies, Inc., USA). All annotations were according to hg19.

Statistical Analyses

The obtaining mediums and cfDNA isolations were duplicated at different periods and thus each sample was run twice. For aberration detection, the log2 ratio was set to default as 0.35 for amplification/gain and -0.45 for deletion/loss as proposed by the application note of the system (12).

RESULTS

Characterization of Isolated cfDNAs

The cfDNAs isolated from the culture mediums of the cells were fluorescently quantified and the concentrations were determined between 1.51-25.3 ng/μl. The gDNA contamination was followed by deliberately addition of gDNA into one of isolated cfDNAs and performing DNA microarray by this

sample. According to the results (Figure 1), possible availability of gDNA bring about remarkable copy gains compared to non-contaminated samples, underlying there were not any gDNA contamination in the study group.

Comparison of CNVs between the cfDNAs

After the DNA microarray step, the chromosomal segments were compared to detect the common and differentiated CNVs between the cfDNAs isolated from the cell lines (Figure 2). The results underlined that some CNVs listed in the Table 1 were specific to each cell line while others were common between the cell lines as a combination of LIM1863& HT-29, HCT116& HT-29 and HT-29& CACO-2 by same loss or gain patterns (Table 2).

DISCUSSION

CRC is one of the deadliest cancer types worldwide and the number of patients with CRC were predicted to approximately be doubled by 2040. CRC subtypes are traditionally classified according to the segment of cancer location; nonetheless, they have more complicated molecular classifications. The molecularly classified subtypes have been shown to associate with clinical outcomes. However, these subtype definitions are limited to a picture of the clinical outcome and further approaches are still needed (13).

cfDNA consists of the small DNA segments that are released by the cells into the circulatory system. In cancer, cfDNA may consist of tumor-derived DNA sequences, which could serve as a platform for biomarkers for the detection and monitoring of cancer and therapy. Numerous studies have frequently focused on cfDNA-based biomarker detection using several

Table 1. The differentially affected regions by gains or losses for each cell line.

Cell line	Chr	Start-Stop	Cytoband	Size (kb)	Gain/Loss
LIM1863	1	206075579-248563836	q32.1 - q44	42,488.258	Gain
	7	23194747-23822183	p15.3	627,436	
HCT116	8	67352994-142205781	q13.1 - q24.3	74,852.788	Gain
	10	104003117-131291788	q24.32 - q26.3	27,288.672	
	17	43120016-77220974	q21.31 - q25.3	34,100.959	
HT-29	5	1130129-45142098	p15.33 - p12	44,011.97	Gain
	11	2909874-44075140	p15.4 - p11.2	41,165.267	
	3	1464291-90273445	p26.3 - p11.1	88,809.155	
	8	215827-43407979	p23.3 - p11.1	43,192.153	Loss
	14	19849591-107152122	q11.2 - q32.33	87,302.532	
	21	14420615-48022981	q11.2 - q22.3	33,602.367	
	22	21240223-51170223	q11.21 - q13.33	29,930.001	
CACO-2	1	746608-121150012	p36.33 - p11.2	120,403.405	Loss
	2	226945229-242938241	q36.3 - q37.3	15,993.013	
	4	53656120-157605164	q12-q32.1	103,949.045	
	9	3022488-12155545	p24.2 - p23	9,133.058	
		23915540-30045342	p21.3 - p21.1	6,129.803	
	10	69430459-97151185	q21.11 - q22.32	27,720.727	Gain
		3314825-38219750	p15.2 - p11.1	34,904.926	
		49954828-72912411	q11.23 - q22.1	22,957.584	
	12	792951-34285770	p13.33 - p11.1	33,492.82	Gain
16	51171823-87138780	q12.1 - q24.2	35,966.958		

Table 2. The same regions affected by gains or losses for the cell lines.

Cell lines	Chr	Start-Stop	Cytoband	Size (kb)	Gain/Loss
LIM1863& HT-29	7	23822183-52965122	p15.3 - p12.1	29,142.94	Gain
HCT116& HT-29	8	115281701-142205810	q23.3 - q24.3	26,924.11	Gain
HT-29& CACO-2	4	157605164-187638862	q32.1 - q35.2	30,033.699	Loss
	11	73712308-134790190	q13.4 - q25	61,077.883	Gain
	17	44684-21180656	p13.3 - p11.2	21,135.973	Loss
	18	861334-10532357	p11.32 - p11.22	9,671.024	Gain
		20663689-77954136	q11.2 - q23	57,290.448	Loss
	19	277373-23035449	p13.3 - p12	22,758.077	Loss
	20	31257259-60346875	q11.21 - q13.33	29,089.617	Gain

high-throughput methods such as NGS (14-17). However, the drawbacks of the NGS systems, such as high cost and time requirements, restrict the wide applicability of the approach (18). Therefore, other high-throughput methods including the DNA microarray approach should be widespread. Huge chromosomal structural alterations and CNVs have extensively been linked to carcinogenesis, pointing out the importance of DNA microarray method in the detection and monitoring of cancer (19).

Although two phenomena, cfDNA, and DNA microarray, have been separately evaluated in cancer studies, recent efforts have focused on the combination of these approaches. For instance, Azad et al. showed the androgen receptor gene anomalies using cfDNA and DNA microarray in patients with prostate cancer (20). Similarly, the product notes of the Agilent Company presented a detailed protocol for the assessment of the power of the DNA microarray on the single-cell level (12). However, none of the studies focused on the sub-typing of specific cancer by the combination of DNA microarray and cfDNA. As a part of an ongoing study, we aimed to evaluate the efficacy of the DNA microarray method on cfDNAs isolated from the medium of the CRC cell lines; suspension sporadic colorectal cancer cell lines; LIM1863; adherent colorectal carcinoma cell lines HCT116 and CACO-2; and adherent colorectal adenocarcinoma cell lines with epithelial morphology HT-29, in the presence of adherent normal colon fibroblast cell line CCD-18Co. The properties of these cell lines, especially secretome profiles have been proven to be distinguishable at the molecular level (21, 22), underlying diversity in the genetic background. Hence, it may be possible to sub-type these cells according to differences in the cfDNA profiles.

In this study, we isolated cfDNAs from the mediums where the cells were grown. Accordingly, we removed the cells by centrifugation and used cell-free medium to obtain cfDNAs. Although we did not perform the size analyses to clearly ensure the isolation of cfDNAs, whose size was about 160 bp (16), we confirmed the lack of genomic DNA (gDNA) owing to the centrifugation step and the concentrations of isolated DNA, which were in a range of 1.51-25.3 ng/μL. Moreover, a recent study underlined that the mediums on the cells could contain mitochondria and intact mitochondrial DNA (23); therefore, a size analysis of cfDNA would not be a practical approach to prove the purity of the cfDNA. To further ensure the lack of the gDNA, additionally, we analyzed the cfDNA from the reference cell line, CCD-18Co, whose cfDNAs were separately isolated from the reference one. The involvement of gDNA in the cfDNA was proved to alter the DNA microarray results (12). However, we did not realize any differences in the CCD-18Co duplicates compared to the reference well (Figures 1A and B). This result may demonstrate the lack of gDNA contamination in the cfDNA samples. Importantly, when gDNA was deliberately contaminated into the isolated cfDNAs, the array results were completely problematic showing significant amplification of all chromosomes (Figure 1C). This result also proved that the cfDNAs were gDNA-free.

Next, we conducted a DNA microarray from cfDNAs obtained from different CRC cell lines compared to that of the reference cell line, CCD-18Co in the presence of biological controls for each cell line. According to the results, the cfDNAs had losses and gains distinguishable between the cell lines (Figure 2), which could be used to *in vitro* determine the subtypes of the CRC phenotypes. Although the amplified or lost regions were highly similar to each other, some regions (for example chromosome 16 for the HCT116 cell line); (Figures 2C and D) was drastically different between the replicas, clarifying that these regions should not be evaluated for subtyping purposes. Notably, there was a huge diversity of the sex chromosome for all cell lines. The system aims to determine the sex of the sample using sex chromosome-dependent probes. According to the American Type Culture Collection (ATCC) and The Cellosaurus databases, LIM1863 and HT-29 originate from female patients while HCT116 and CACO-2 from male ones. Nonetheless, our results did not correspond to the relative sex phenotypes. The success rate of the DNA microarray systems in properly detecting the sex chromosome has been reported to be low (24). Still, the problem with the sex chromosomes would be the result of DNA microarray application on cfDNA and requires further studies. Our propose was not about to examine the sex chromosomes in the present study.

When the common variations between the replicas were evaluated, specific affected chromosome regions were distinguishable between the cell lines. The regions were evaluated comparatively and the differentially altered regions are listed in Table 1, which could be used as a biomarker for subtyping of the CRC. Despite not being for all cell lines, the regions listed in Table 2 were common between the cell lines. Accordingly, the chromosomes of the LIM1863 and HCT116 were shown to be minimally affected while those of HT-29 and CACO-2 cells had dramatic alterations by the cfDNA screening. Chromosomal characterization by gDNA of the CRC cell lines including HCT116, HT-29, and CACO-2 has previously been carried out, and cellular and chromosomal differences were well-reported and showed the remarkable diversity between the cell lines (25), which may confirm the results of the present study. Moreover, these cell lines could be classified according to their differentiation properties and HT-29, and CACO-2 cells compared to LIM1863 and HCT116 have higher differentiation capabilities (26). For particular cell types, differentiation was shown to induce cell death (27) and the association between differentiation and cell death is well documented (28).

When the differentially affected regions (Table 1) were examined by the gene information, 656 genes were seen to have higher copies for the cfDNAs from the LIM1863 cell line. When the pathways were analyzed for these genes by Reactome Database (29), most of the gene-encoded proteins had a role in the olfactory signaling pathway that was already linked to carcinogenesis (30). For the HCT116 cell line, 1720 genes were amplified and the products of these genes mainly had a role in fibroblast growth factor receptor 2 (FGFR2) mutant receptor activation corresponding to colorectal cancer in the literature

(31). In the approximately 5.5 thousand affected genes for the HT-29 cell line, 993 genes whose products acted normally in the olfactory signaling pathway were amplified while 4654 genes whose products were involved predominantly in cellular inflammation, Fc gamma receptor (FCGR) activation and phagocytosis associating with systemic inflammatory clearance lost copies. For CACO-2 cells, similar to HT-29, about 5.5 thousand genes were affected. Of those genes, 1710 of them gained copies and the products of these genes had a role primarily in response to metal ions triggering the carcinogenesis (32), 3792 genes whose products participated in the inhibition of signaling by overexpressed epidermal growth factor receptor (EGFR) that lost copies, putatively to overcome EGFR-targeted strategies. Overall, the products of all affected genes were actualized to directly or indirectly associate with carcinogenesis as expected.

CONCLUSION

The importance of the cfDNA has been well-documented in CRC patients (33-35). However, cfDNAs from patients and/or cell lines should be re-evaluated to diagnose, follow up or treat the CRC by combining diverse approaches. Accordingly, the present study points to the combination of the cfDNA and DNA microarray approaches to find biomarkers specific to subtypes of the CRC cell lines for the first time. Still, further studies are needed to totally explore the potential of these approaches.

Ethics Committee Approval: Ethical approval is not required as the study was performed on cell lines.

Authors' Contributions: Conception/Design of Study – H.H.K., E.C., M.A.E.; Data Acquisition – D.B.C.; Performing experiments – C.P.K., D.B.C.; Data Analysis/Interpretation – A.C.O., H.H.K.; Drafting Manuscript – H.H.K., A.C.O., E.C.; Critical Revision of Manuscript – D.B.C., H.H.K., A.C.O., E.C.; Final Approval and Accountability– H.H.K, E.C., A.C.O., M.A.E.

Conflicts of Interest: The authors declare no conflict of interest.

Financial Disclosure: The authors declare that this study has received no financial support.

REFERENCES

1. Ferlay J, Ervik M, Lam F, Colombet M, Mery L, Piñeros M, et al. Global cancer observatory: Cancer today. Lyon, France: International Agency for Research on Cancer 2020. Available from: <https://gco.iarc.fr/today>, accessed 01 February 2023
2. Sung H, Ferlay J, Siegel RL, Laversanne M, Soerjomataram I, Jemal A, et al. Global cancer statistics 2020: GLOBOCAN estimates of incidence and mortality worldwide for 36 cancers in 185 countries. *CA: Cancer J Clin* 2021; 71(3): 209-49.
3. Colorectal cancer facts & figures. American Cancer Society 2020-2022. Published online, 48.
4. Petit J, Carroll G, Gould T, Pockney P, Dun M, Scott RJ. Cell-free DNA as a diagnostic blood-based biomarker for colorectal cancer: a systematic review. *J Surg Res* 2019; 236: 184-97.
5. Osborne JM, Wilson C, Moore V, Gregory T, Flight I, Young GP. Sample preference for colorectal cancer screening tests: blood or stool? *Open J Prev Med* 2012; 02(03): 326–31.
6. Bronkhorst AJ, Ungerer V, Holdenrieder S. The emerging role of cell-free DNA as a molecular marker for cancer management. *Biomol Detect Quantif* 2019; 17: 100087.
7. Alborelli I, Generali D, Jermann P, Cappelletti MR, Ferrero G, Scaggiante B, et al. Cell-free DNA analysis in healthy individuals by next-generation sequencing: a proof of concept and technical validation study. *Cell Death Dis* 2019; 10(7): 534.
8. Seki Y, Fujiwara Y, Kohno T, Takai E, Sunami K, Goto Y, et al. Picoliter-droplet digital polymerase chain reaction-based analysis of cell-free plasma DNA to assess EGFR mutations in lung adenocarcinoma that confer resistance to tyrosine-kinase inhibitors. *Oncologist* 2016; 21(2): 156-64.
9. Palande V, Shay DR, Frenkel-Morgenstern MI. Detection of cell-free DNA in blood plasma samples of cancer patients. *JoVE* 2020; 9(163): e61449.
10. Selvaraj S, Natarajan J. Microarray data analysis and mining tools. *Bioinformatics* 2011; 6(3): 95.
11. Miller MB, Tang YW. Basic concepts of microarrays and potential applications in clinical microbiology. *Clin Microbiol Rev* 2009; 22(4): 611-33.
12. Costa P, Novorodovskaya N, Basehore S, Fulmer-Smentek S. Single cell copy number screening using the GenetiSure Pre-Screen kit. Application Note. Agilent Technologies, Inc. 2014. USA, 5991-5325EN.
13. Xi Y, Xu P. Global colorectal cancer burden in 2020 and projections to 2040. *Transl Oncol* 2021; 14(10): 101174.
14. Yan YY, Guo QR, Wang FH, Adhikari R, Zhu ZY, Zhang HY, et al. Cell-free DNA: hope and potential application in cancer. *Front Cell Dev Biol* 202; 9: 639233.
15. Cisneros-Villanueva M, Hidalgo-Pérez L, Rios-Romero M, Cedro-Tanda A, Ruiz-Villavicencio CA, Page K, et al. Cell-free DNA analysis in current cancer clinical trials: a review. *Br J Cancer* 2022; 126(3): 391-400.
16. Song P, Wu LR, Yan YH, Zhang JX, Chu T, Kwong LN, et al. Limitations and opportunities of technologies for the analysis of cell-free DNA in cancer diagnostics. *Nat Biomed Eng* 2022; 6(3): 232-45.
17. Barault L, Amatu A, Siravegna G, Ponzetti A, Moran S, Cassingena A, et al. Discovery of methylated circulating DNA biomarkers for comprehensive non-invasive monitoring of treatment response in metastatic colorectal cancer. *Gut* 2018; 67(11): 1995-2005.
18. Meldrum C, Doyle MA, Tothill RW. Next-generation sequencing for cancer diagnostics: a practical perspective. *Clin Biochem Rev* 2011; 32(4): 177.
19. Taylor BS, Barretina J, Socci ND, DeCarolis P, Ladanyi M, Meyerson M, et al. Functional copy-number alterations in cancer. *PLoS One* 2008; 3(9): e3179.
20. Azad AA, Volik SV, Wyatt AW, Haegert A, Le Bihan S, Bell RH, et al. Androgen receptor gene aberrations in circulating cell-free DNA: Biomarkers of therapeutic resistance in castration-resistant prostate CancerAR gene aberrations in circulating cell-free DNA. *Clin Cancer Res* 2015; 21(10): 2315-24.
21. Mathivanan S, Ji H, Tauro BJ, Chen YS, Simpson RJ. Identifying mutated proteins secreted by colon cancer cell lines using mass spectrometry. *J Proteomics* 2012; 76: 141-9.
22. Cevenini A, Orrù S, Imperlini E. Secretome proteomic approaches for biomarker discovery: an update on colorectal cancer. *Medicina* 2020; 56(9): 443.
23. Dache ZA, Otandault A, Tanos R, Pastor B, Meddeb R, Sanchez C, et al. Blood contains circulating cell-free respiratory competent mitochondria. *FASEB J* 2020; 34(3): 3616-30.

24. Yatsenko SA, Shaw CA, Ou Z, Pursley AN, Patel A, Bi W, et al. Microarray-based comparative genomic hybridization using sex-matched reference DNA provides greater sensitivity for detection of sex chromosome imbalances than array-comparative genomic hybridization with sex-mismatched reference DNA. *J Mol Diagn* 2009; 11(3): 226-37.
25. Kleivi K, Teixeira MR, Eknæs M, Diep CB, Jakobsen KS, Hamelin R, et al. Genome signatures of colon carcinoma cell lines. *Cancer Genet Cytogenet* 2004; 155(2): 119-31.
26. Williams CS, Bernard JK, Demory Beckler M, Almohazey D, Washington MK, Smith JJ, et al. ERBB4 is over-expressed in human colon cancer and enhances cellular transformation. *Carcinogenesis* 2015; 36(7): 710-8.
27. Doyle BT, O'Neill AJ, Fitzpatrick JM, Watson RW. Differentiation-induced HL-60 cell apoptosis: a mechanism independent of mitochondrial disruption? *Apoptosis* 2004; 9: 345-52.
28. Bell RA, Megeney LA. Evolution of caspase-mediated cell death and differentiation: Twins separated at birth. *Cell Death Differ* 2017; 24(8): 1359-68.
29. Gillespie M, Jassal B, Stephan R, Milacic M, Rothfels K, Senff-Ribeiro A, et al. The reactome pathway knowledgebase 2022. *Nucleic Acids Res* 2022; 50(D1): D687-92.
30. Chung C, Cho HJ, Lee C, Koo J. Odorant receptors in cancer. *BMB Rep* 2022; 55(2): 72.
31. Matsuda Y, Ueda J, Ishiwata T. Fibroblast growth factor receptor 2: expression, roles, and potential as a novel molecular target for colorectal cancer. *Pathol Res Int* 2012: 1-8.
32. Tokar EJ, Benbrahim-Tallaa L, Waalkes MP. Metal ions in human cancer development. *Met Ions Life Sci* 2011; 8: 375-401.
33. Spindler KL, Boysen AK, Pallisgård N, Johansen JS, Taberero J, Sørensen MM, et al. Cell-free DNA in metastatic colorectal cancer: a systematic review and meta-analysis. *Oncologist* 2017; 22(9): 1049-55.
34. Strickler JH, Loree JM, Ahronian LG, Parikh AR, Niedzwiecki D, Pereira AA, et al. Genomic landscape of cell-free DNA in patients with colorectal cancer: cell-free dna sequencing in colorectal cancer. *Cancer Discov* 2018; 8(2): 164-73.
35. Vymetalkova V, Cervena K, Bartu L, Vodicka P. Circulating cell-free DNA and colorectal cancer: a systematic review. *Int J Mol Sci* 2018; 19(11): 3356.

Cyclosporine Treatment Increases the ACE/ACE2 Ratio in Adipose Tissue and Aorta

Samed Emre Darilmaz¹ , Ilknur Bingul¹ , Merva Soluk-Tekkesin² , Nergis Demir³ , Seldag Bekpinar¹ 

¹Department of Medical Biochemistry, Istanbul Faculty of Medicine, Istanbul University, Istanbul, Turkiye

²Department of Pathology, Institute of Oncology, Istanbul University, Istanbul, Turkiye

³Academi Molgen Biotechnology, Istanbul, Turkiye

ORCID ID: S.E.D. 0000-0001-5795-4890; I.B. 0000-0002-6432-3541; M.S.T. 0000-0002-7178-3335; N.D. 0000-0001-9243-7450; S.B. 0000-0002-2069-7330

Cite this article as: Darilmaz SE, Bingul I, Soluk-Tekkesin M, Demir N, Bekpinar S. Cyclosporine treatment increases the ACE/ACE2 ratio in adipose tissue and aorta. *Experimed* 2023; 13(2): 93-96.

ABSTRACT

Objective: The renin-angiotensin system (RAS) mainly functions in the regulation of vascular tone. Since the perfusion and storage capacity of adipose tissue is largely dependent on vessel density and tone, factors that modulate vasoactive RAS components may affect adipose tissue metabolism. Cyclosporine, an immunosuppressive drug, has some detrimental effects on the vascular system and kidneys by modulating the components of the RAS. However, the effect of cyclosporine on adipose tissue is still not clear. In this study, the impact of cyclosporine on mRNA expressions of some "RAS components" in the aorta and epididymal adipose tissue of rats were investigated.

Materials and Methods: Rats were injected subcutaneously with cyclosporine at a dose of 25 milligrams per kilogram per day for 1 week. Angiotensin II, angiotensin (1-7), blood urea nitrogen and creatinine levels were examined in serum samples of rats. mRNA expressions of RAS components in the aorta and epididymal adipose tissue, and hypoxia-inducible factor-1 (HIF-1) and vascular endothelial growth factor (VEGF) in epididymal adipose tissue were determined. In addition, histopathological examinations of the adipose tissue were performed.

Results: Cyclosporine administration significantly suppressed the expression of angiotensin-converting enzyme 2 (ACE2) in both the aorta and adipose tissue. Accordingly, it caused a significant increase in the ACE/ACE2 ratio. However, it did not affect the adipose tissue HIF-1 and VEGF expressions. When examined histopathologically, no change was observed in the vascular density of adipose tissue due to cyclosporine.

Conclusion: It was thought that the increase in the ACE/ACE2 ratio might be an adaptation that protects the adipose tissue against the systemic effect of cyclosporine.

Keywords: Cyclosporine, adipose tissue, angiotensin-converting enzyme 2, vascular density

INTRODUCTION

Cyclosporine is an immunosuppressant medication used in clinical practice to prevent organ graft rejection and to treat autoimmune diseases. However, this drug shows additional effects on non-immune cell populations and may adversely affect the vascular system and kidneys (1).

It has been reported that upregulation of the vasoconstrictive renin-angiotensin system (RAS) and endothelin-1, inhibition of nitric oxide (NO)-dependent vasodilation, and also increasing the formation of free radicals are effective in the hypertensive and nephrotoxic effects of cyclosporine (1).

Corresponding Author: Seldag Bekpinar **E-mail:** bekpinar@istanbul.edu.tr

Submitted: 03.05.2023 **Revision Requested:** 24.05.2023 **Last Revision Received:** 25.05.2023 **Accepted:** 05.0.2023 **Published Online:** 26.07.2023



Content of this journal is licensed under a Creative Commons Attribution-NonCommercial 4.0 International License.

Table 1. Serum parameters of control and cyclosporine-treated rats.

	CONTROL (n=7)	CYCLOSPORINE (n=9)
Ang-II (pg/mL)	66 ± 2.7	61 ± 5.0
Ang 1-7 (pg/mL)	59 ± 1.6	48 ± 3.1 ^a

Note: Values are means ± SEM. In statistical evaluations, a Mann–Whitney U test were used. The unpaired Student's t-test was used for equal variances.

Ang-II, angiotensin II; Ang (1-7), angiotensin (1-7).

^a: p < 0.05 compared with the control group.

Table 2. Vascular density score in epididymal adipose tissue in control and cyclosporine-treated rats.

	Vascular density score
Control group	10.83 ± 0.74
Cyclosporine-treated group	12.25 ± 0.62

Note: Values are mean ± SEM (n = 7–9 in each group). Vessels in three different areas of adipose tissue section of each rat were counted and averaged. In statistical evaluations, a Mann–Whitney U test were used.

Angiotensin II (Ang-II), which is synthesized by catalysis of angiotensin-converting enzyme (ACE), exhibits a vasoconstrictive effect when it interacts with the Ang-II type-1 receptor (AT1R), whereas a vasodilator effect is observed by interacting with the Ang-II type-2 receptor (AT2R). Moreover, angiotensin (1-7), synthesized by angiotensin-converting enzyme-2 (ACE2) enzymatic activity, has a vasodilator effect when it binds to the Ang (1-7) receptor (Mas R). The antagonistic effects of RAS components are crucial in the regulation of vascular tone and perfusion of the relevant organ.

RAS components also exert a crucial role in adipose tissue metabolism in an autocrine or paracrine manner (2,3). It has been reported that RAS components with vasoconstrictive effects are largely responsible for hypertension that seen in obese individuals (2, 3).

Although its apparent effects on the vascular system and kidneys are known, how cyclosporine affects adipose tissue metabolism has not been studied much. In a study administering to rats by gavage for six weeks, cyclosporine was reported to decrease glucose uptake into adipocytes, increase lipolysis and suppress lipogenesis (4).

In this study, we aimed to elucidate the effect of cyclosporine administration to rats for 1 week in mRNA expressions of RAS components in both epididymal adipose tissue and the aorta. In addition, we also elucidated the vascular density and the mRNA expressions of HIF-1 and VEGF in adipose tissue.

MATERIALS AND METHODS

Animals

In this study, sixteen male Wistar rats weighing approximately 350 grams, provided by the Bezmialem University, Experimental Medical Research Institute were housed in a stainless cage (three to four per cage) with temperature and light control (12 h dark/12 h dark) and received a standard pellet diet. The experimental procedures were implemented according to the order of Bezmialem University, Animal Experiments Local Ethics Committee (Date: 28.02.2019, No: 33).

Experimental Design

Cyclosporine group (n=9): Cyclosporine A (Sandimmune, Novartis, Switzerland) was prepared in ethanol (94%) and polyoxyethylated castor oil and a dose of 25 mg/kg was applied subcutaneously once daily during the one-week experimental period, according to previous studies (5).

Control group (n=7): Rats were exposed to daily subcutaneous injections of Cremophore EL: alcohol (2:1) as a vehicle during the one-week experimental period.

Samples

Rats were given ketamine (35 mg/kg, Pfizer, USA) and xylazine HCl (15 mg/kg, Bioveta, Czech Republic) intraperitoneally for anaesthesia, and euthanized after an overnight fasting. Blood samples were taken from their hearts into tubes; thereafter, sera were obtained by centrifugation.

The thoracic aorta and epididymal adipose tissue samples were isolated from each rat.

Determination of Ang-II, Ang (1-7), Blood Urea Nitrogen (BUN) and Creatinine in Serum

Ang-II and Ang (1-7) (Rat ELISA kit; Ang II #101212; Ang (1-7) #101211; Abbkine, Inc., China), as well as BUN and creatinine (Roche Cobas auto-analyzer) levels in sera were determined.

Determination of mRNA Expressions in the Aorta and Adipose Tissue

AT1R, ACE, and ACE2 mRNA expressions in the aorta and ACE, ACE2, HIF-1 and VEGF mRNA expressions in the epididymal fat sample were measured. A commercial kit (NucleoSpin RNA Isolation Kit, #740955, Macherey-Nagel, Germany) was used for the RNA purification. Following that procedure, 5 ng purified RNA was also used to synthesize the cDNA samples (cDNA Synthesis Kit; #PCR511, Script, Jena-Bioscience GmbH, Jena, Germany). After the cDNA acquisition, quantitative real time-polymerase chain reaction (qRT-PCR) was carried out by using the qPCR Sybr Green Master Mix kit from Jena Bioscience (#PCR372, GmbH, Jena, Germany) with the following primers of AT1R (NM_004835, F:5'-TTCACCTGCCTCAGGATCT-3'; R:5'-CCAGACCCACCAATCCA TCC-3');

ACE (NM_000789, F:5'-CGTCCACCGTTACCAGACAA-3'; R:5'-TTGGCCTCTGCGTATTCGTT-3');
ACE2 (NM_021804, F:5'-GAATGCGACCATCAAGCGTC-3'; R:5'-CAAGCCCAGAGCCTACGATT-3');
VEGF (NM_001025366, F:5'-GCACTGGACCTGGTTTAC-3'; R:5'-GGGTCTCAATTGGACGGCAA-3') and
HIF-1 (NM_001530, F:5'-ATGTACCCTAACAAGCCGGG-3'; R:5'-AAGCACGTCATAGCGGTTT-3')(LGCBiosearchTechnologies, Denmark) in a Biorad-CFX Connect device (California-USA). The relative mRNA expressions were calculated with the method of $2^{-\Delta\Delta CT}$. The expression of mRNA of glyceraldehyde-3-phosphate dehydrogenase (GAPDH), an internal control, was used to adjust the analytical data.

Histopathological Examination

Samples of epididymal adipose tissue were preserved in a 10% buffered formalin solution, which was then paraffin blocked. Hematoxylin-eosin stained preparations were observed morphologically under a light microscope. For scoring of the vascular density, three different areas were chosen, and then the number of vessels was counted and vascular density was calculated by dividing the total number of vessels by three.

Statistical Analyses

The statistical analyses were implemented by using the Statistical Package for The Social Sciences (21.0; SPSS Inc., Chicago, IL-USA) program, unpaired Student's ttest or Mann-Whitney Utest, according to data distribution. Correlations were evaluated by Pearson's test. When p-values are less than 0.05, they were considered significant.

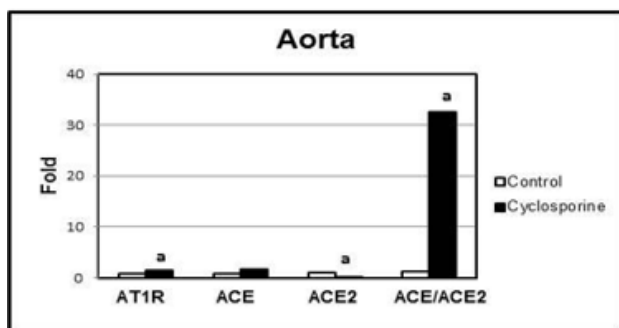


Figure 1. The impact of cyclosporine on mRNA expressions of RAS components in rat aorta

Values are given as mean \pm SEM (n=7-9 for each group).

a: p < 0.05; compared to the control. AT1R, angiotensin-II type-1 receptor; ACE, angiotensin-converting enzyme; ACE2, angiotensin-converting enzyme-2

RESULTS

Cyclosporine administered daily for one week into animals at a dose of 25 mg/kg, did not affect renal function; BUN and creatinine levels in serum did not change (Cyclosporine: 24.7 ± 1.1 mg/dL - Control: 25.6 ± 4.7 and Cyclosporine: 0.36 ± 0.01 mg/dL - Control: 0.31 ± 0.03 respectively). While serum Ang- II levels were not affected by cyclosporine treatment, Ang (1-7) levels decreased (Table 1).

Cyclosporine treatment in aortic tissue significantly increased the mRNA expression of AT1R. However, a significant decrease in ACE2 expression and an increased ACE/ACE2 ratio were observed (Figure 1).

A significant cyclosporine-induced decrease in ACE2 expression was also found in adipose tissue, resulting in a marked increase in the ACE/ACE2 ratio. However, AT1R and ACE expressions remained unchanged with cyclosporine treatment (Figure 2). To evaluate the effect of cyclosporine on adipose tissue perfusion, we examined histopathologically the vascular density and RNA expressions of HIF-1 and VEGF. We did not detect any change in these parameters due to cyclosporine (Figures 2 and 3, Table 2).

But interestingly, a significant negative correlation was found between ACE/ACE2 ratio and HIF-1 in adipose tissue ($r = -0.651$, $p = 0.009$).

DISCUSSION

The effect of the administration of 25 mg/kg cyclosporine to rats for one week on mRNA expressions of RAS components in the aorta and epididymal adipose tissue were investigated in the current study. In the aorta, this immunosuppressive drug caused an increase in AT1R and a decrease in ACE2 expression and a marked increase in the ACE/ACE2 ratio. In addition,

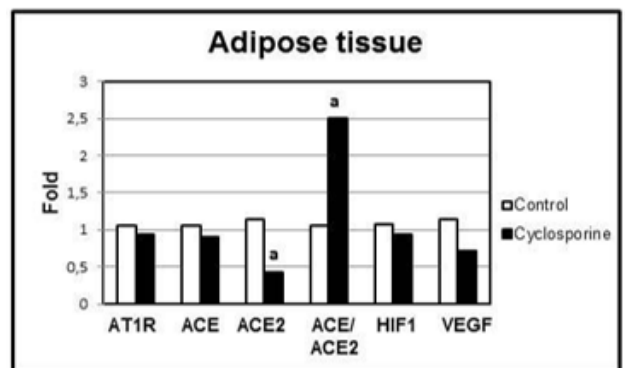


Figure 2. The impact of cyclosporine on mRNA expressions of RAS, HIF-1 and VEGF in rat epididymal adipose tissue

Values are given as mean \pm SEM (n=7-9 for each group).

a: p < 0.05; compared to the control. AT1R, angiotensin-II type-1 receptor; ACE, angiotensin-converting enzyme; ACE2, angiotensin-converting enzyme-2, HIF-1, hypoxia-inducible factor-1; VEGF, vascular endothelial growth factor

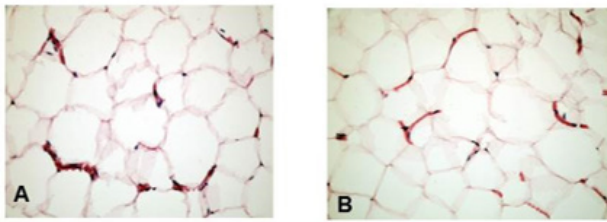


Figure 3. The representative images of the epididymal adipose tissue stained by hematoxylin-eosin (n=7-9 in each group). Control (A) and cyclosporine (B) groups have a similar appearance. Thin vessel sections were observed between adipocytes. (Original magnification×400)

serum Ang-II levels remained unchanged, but Ang (1-7) levels were found to be low in the cyclosporin group. Our findings showed that at least in part that cyclosporine has a systemic vasoconstrictive effect, as previously described (1, 6, 7).

Adipose tissue is a highly vascularized organ. Beyond supplying oxygen and nutrients, the vascular system carries a variety of cytokines, growth factors, and hormones to and from adipose tissue. Any modulation of vessel density and vessel diameter of adipose tissue affects tissue perfusion and function. The main transcription factor regulated by oxygen homeostasis and hypoxia is HIF-1. Under hypoxic conditions, HIF-1 activates the transcription of genes facilitating metabolic adaptation to hypoxia such as glycolytic enzymes, vascular endothelial growth factor, etc. (8)

In our study investigating the effect on some vasoactive RAS components and hypoxic parameters in adipose tissue, it was found that cyclosporine decreased ACE2 expression and increased the ACE/ACE2 ratio. However, HIF-1 and its target gene VEGF expressions were not affected by this drug. Furthermore, no change was observed histopathologically in the vascular density of adipose tissue due to cyclosporine. But interestingly, a marked inverse association was detected between the ACE/ACE2 ratio and HIF-1 in adipose tissue.

It is well known that the increase in systemic blood pressure passively dilates the vessels in the resistant arteries and arterioles embedded within the parenchyma. To compensate for this expansion, the smooth muscle cells of the vessel contract and try to return the vessel diameter to its initial state. This reactive contraction, called the myogenic response, counteracts the effect of a change in systemic pressure on tissue perfusion (9, 10). Multiple mechanisms have been reported to mediate the myogenic response depending on their location in the body (9). In a study conducted in cerebral resistant arteries, the role of AT1R activation in the pressure-induced myogenic response was indicated (11).

According to our findings, the increase in ACE/ACE2 ratio observed due to cyclosporine in our study may be related to the myogenic adaptation that protects the adipose tissue against the systemic effect of cyclosporine.

Ethics Committee Approval: This study is approved by Bezmialem University, Animal Experiments Local Ethics Committee (Date: 28.02.2019, No: 33).

Authors' Contributions: Conception/Design of Study – S.B, I.B.; Data Acquisition – S.B., I.B.; Data Analysis/Interpretation – S.B., I.B., E.D.; Drafting Manuscript– I.B.; Critical Revision of Manuscript- S.B.; Final Approval and Accountability– I.B.; Technical or Material Support- E.D., I.B.; M.S.T, N.D.; Supervision- S.B.

Conflicts of Interest: The authors declare no conflict of interest.

Financial Disclosure: The authors declare that this study has received no financial support.

REFERENCES

- Hoková L, Málek I, Kopkan L, Kautzner J. Pathophysiological mechanisms of calcineurin inhibitor-induced nephrotoxicity and arterial hypertension. *Physiol Res* 2017; 66: 167-80.
- Cassis LA, Police SB, Yiannikouris F, Thatcher SE. Local adipose tissue renin-angiotensin system. *Curr Hypertens Rep* 2008; 10: 93-8.
- Slamkova M, Zorad S, Krskova K. Alternative renin-angiotensin system pathways in adipose tissue and their role in the pathogenesis of obesity. *Endocr Regul* 2016; 50: 229-40.
- Fuhrmann A, Lopes P, Sereno J, Pedro J, Espinoza DO, Pereira MJ, et al. Molecular mechanisms underlying the effects of cyclosporin A and sirolimus on glucose and lipid metabolism in liver, skeletal muscle and adipose tissue in an in vivo rat model. *Biochem Pharmacol* 2014; 88: 216-28.
- Damiano S, Trepiccione F, Ciarcia R, Scanni R, Spagnuolo M, Maco I, et al. A new recombinant MnSOD prevents the cyclosporine A-induced renal impairment. *Nephrol Dial Transplant* 2013; 28(8): 2066-72.
- Porter G A, Bennett WM, Sheps SG. Cyclosporine-associated hypertension. *National High Blood Pressure Education Program. Arch Intern Med* 1990; 150(2): 280-3.
- Marienhagen K, Lehner F, Klemptner J, Hecker H, Borlak J. Treatment of cyclosporine induced hypertension: Results from a long-term observational study using different antihypertensive medications. *Vascul Pharmacol* 2019; 115: 69-83.
- Ye J. Emerging role of adipose tissue hypoxia in obesity and insulin resistance. *Int J Obes (Lond)* 2009; 33: 54-66.
- Jackson WF. Myogenic tone in peripheral resistance arteries and arterioles: The pressure is on! *Front Physiol* 2021; 12: 699517.
- Roman RJ, Van Dokkum RP. Commentary on the special issue on the impact of myogenic tone in health and disease. *Curr Vasc Pharmacol* 2014; 12: 779.
- Gonzales AL, Yang Y, Sullivan MN, Sanders L, Dabertrand F, Hill-Eubanks DC, et al. A PLCγ1-dependent, force-sensitive signaling network in the myogenic constriction of cerebral arteries. *Sci Signal* 2014; 7: ra49.

Characterization of Rubidium-Based Nanoparticles by Green Synthesis and Their Effect on Colorectal Cancer Cells

Dilsad Ozerkan¹ , Ishak Afsin Kariper² 

¹Department of Genetic and Bioengineering, Faculty of Engineering and Architecture, Kastamonu University, Kastamonu, Turkiye

²Department of Science Education, Faculty of Education, Erciyes University, Kayseri, Turkiye

ORCID ID: D.O. 0000-0002-0556-3879; I.A.K. 0000-0001-9127-301X

Cite this article as: Ozerkan D, Kariper IA. Characterization of rubidium-based nanoparticles by green synthesis and their effect on colorectal cancer cells. *Experimed* 2023; 13(2): 97-102.

ABSTRACT

Objective: Colorectal cancers pose a major threat along with increasing morbidity and mortality to human health worldwide. Therefore, it is crucial to develop effective and safe methods for tumor therapy. In recent years, nanoparticles have emerged as successful candidates for drug delivery into tumor tissues. The particle size of nanoparticles (NPs) is of great importance for passive tumor targeting. Therefore, in this study, we aimed to synthesize and characterize rubidium-based nanoparticles (RbNPs) from the moss *Abietinella abietina* (AA) and determine their anticancer effects on colorectal carcinoma cell line (HCT116).

Materials and Methods: A field emission scanning electron microscope (FESEM), dynamic light scattering (DLS), energy dispersive X-ray analysis (EDX), UV/VIS and fourier transform infrared (FTIR) spectrophotometers were used to characterize the RbNPs. To study the cytotoxicity, a sulforhodamine B (SRB) assay was performed in colorectal carcinoma cell cultures.

Results: As a result, RbNPs- AA developed with an average particle size of about 70 nm. RbNPs- AA proved to be cytotoxic at lower doses than free AA, as it decreased cell viability at half the amount of free AA (14.25 µg/mL).

Conclusion: The availability of RbNPs, particularly for the treatment of colorectal cancer, is evidenced by the fact that all the data collected are highly relevant.

Keywords: Colorectal cancer, rubidium nanoparticles, green synthesis

INTRODUCTION

Besides gastrointestinal cancers, colorectal carcinoma (CRC) is the third most common malignancy and the third leading cause of cancer-related deaths worldwide (1). The most common therapies for CRC include surgery, chemotherapy and radiotherapy for all stages of the disease, and adjuvant and neoadjuvant therapy for advanced stages (2). The fact that symptoms follow a similar course to other bowel diseases and that CRC is not diagnosed until the 3rd and 4th stages, with no response to the treatments used or resistance to treatment, reduces the survival rate for this disease.

Although many alternative methods have been explored, progress is still in its infancy. Tumor-targeted nanostructure systems are therefore heavily involved in cancer research studies (3, 4). In the last 20 years, the environmentally friendly production of chemicals for a sustainable future has been the subject of extensive research worldwide. The choice of an environmentally friendly solvent, an effective reducing agent, and an effective stabilizing agent are the three most important requirements for the production of nanomaterials. However, the biosynthetic method is considered a safe and environmentally friendly green method for the synthesis of nanoparticles for medical purposes. Generally, the chemical methods

Corresponding Author: Dilşad Özerkan **E-mail:** dilsadokan@gmail.com

Submitted: 19.04.2023 **Revision Requested:** 16.05.2023 **Last Revision Received:** 27.05.2023 **Accepted:** 14.06.2023 **Published Online:** 28.07.2023



Content of this journal is licensed under a Creative Commons Attribution-NonCommercial 4.0 International License.

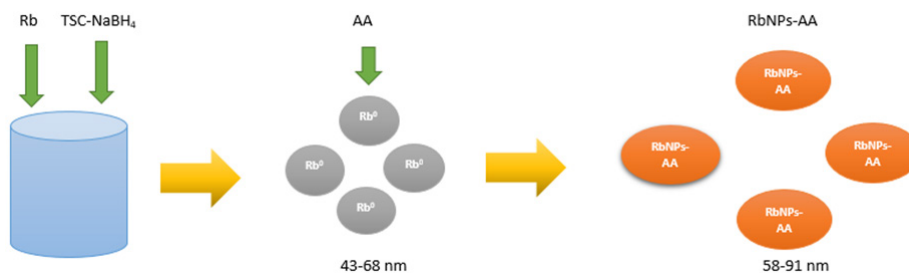


Diagram 1. Preparation of RbNPs and RbNPs-AA

used are expensive and involve the use of hazardous and harmful chemicals that pose many risks to the environment (4). Researchers around the world are constantly working on environmentally friendly production techniques that use green nanotechnology to develop highly effective, non-toxic, and environmentally safe products (5). Nanocarriers used in biology and medicine should have low or no toxicity and be easy to integrate and degrade (6). Metallic nanoparticles can easily cross biological barriers and penetrate into human tissues through the pores of the skin. They can bind to proteins and nucleic acids, be absorbed into cell membranes, enter the nucleus and alter the activities of cells, and exhibit greater cellular activity due to their small size and large surface area (7, 8).

The oldest plants, called bryophytes, which can be used in green synthesis, can adapt to a wide range of environmental conditions. They generally have inadequate growth and defense systems. Therefore, liverworts depend on the metabolic processes of secondary metabolites for both survival and environmental protection (9). In addition, some components of the mosses inhibit tumor growth and show an anticarcinogenic effect on various cancer cell lines (10). *Abietinella abietina* (AA) is a moss species from the Thuidiaceae family (11). The discovery of the antileukaemic activity of P-388 in the ethanol extract of *Claopodium crispifolium*, which belongs to the Thuidiaceae family, led to more mosses being collected and studied in 1980 and 1981 (12). Recently, in our work, we investigated different mosses with different extraction solutions, including the cytotoxic effect of AA on the 5-fluorouracil (5-FU) selected CD24+ colon cancer cells. In comparison to many different extracts of AA, the ethanol extract showed the highest cytotoxicity and decreased the Rho123 low cell population in 5-FU resistant HCT116 colon cancer cells (13). Therefore, we wanted to continue this study and analysed the efficacy of ethanol extract of *i* with a nanocarrier at this time. For this reason, rubidium metal-based nanoparticles (RbNPs) were synthesized using AA moss by green synthesis technique and their effects on colon cancer cells (HCT116) were evaluated after their characterization in this study.

MATERIALS AND METODS

Rubidium dinitrate ($Rb(NO_3)_2$), Sodium borohydride ($NaBH_4$) and trisodium nitrate ($Na_3C_6H_5O_7$) (Sigma Aldrich) were used for RbNPs. $NaHCO_3$ (Sigma), Dulbecco's modified eagle medium (DMEM; Sigma), dimethyl sulfoxide (DMSO) (Sigma) and fetal bovine serum (FBS) were used for cell culture assays.

Liverwort Extraction

AA was freeze-dried, and its extracts were obtained. Absolute ethyl alcohol, which has a boiling point of 78.37 °C and a relative polarity of 0.654, was utilized as the dissolvent. A sample-to-solvent ratio of 1:50 was used in the extraction. All of the process was done in the Soxhlet apparatus. After 24 h extraction, the solutions were completely evaporated in a rotary evaporator (Heidolph) at 40°C under a vacuum. For analysis, the powdered dry extracts were diluted with DMSO.

Preparation of RbNPs and RbNPs-AA

Stock solutions of 0.1 mM $Rb(NO_3)_2$, 4.3×10^{-3} M $Na_3C_6H_5O_7$, and 2×10^{-3} M $NaBH_4$ were prepared. First, 2 mL of $Rb(NO_3)_2$ was mixed with 24 mL of $Na_3C_6H_5O_7$ and 24 mL of $NaBH_4$ for 15 min. at 60 °C. The mixture was then shaken for an additional 15 min. at 90 °C. The obtained RbNPs stock solution was diluted with the extract of 1 mg/mL AA prepared in an aqueous medium (Diagram 1).

Dynamic Light Scattering (DLS) and Zeta Sizer Analysis

Zetasizer measurements were performed at 22-23°C DLS evaluation with the Zetasizer Nano ZS using a 4 mW He-Ne laser at a wavelength of 633 nm and a detection angle of 173 °C.

Energy Dispersive X-Ray (EDX)-Field Emission Scanning Electron Microscope (FESEM) analysis

RbNPs and RbNPs-AA samples were trickled onto a glass substrate and covered with Au/Pd at a thickness of 450 nm using a small Polaron sc 7620 sputter coater, then analysed by FESEM and EDX. To image liquid samples for analysis, samples were dropped onto glass substrates, dried, and then placed on the instrument.

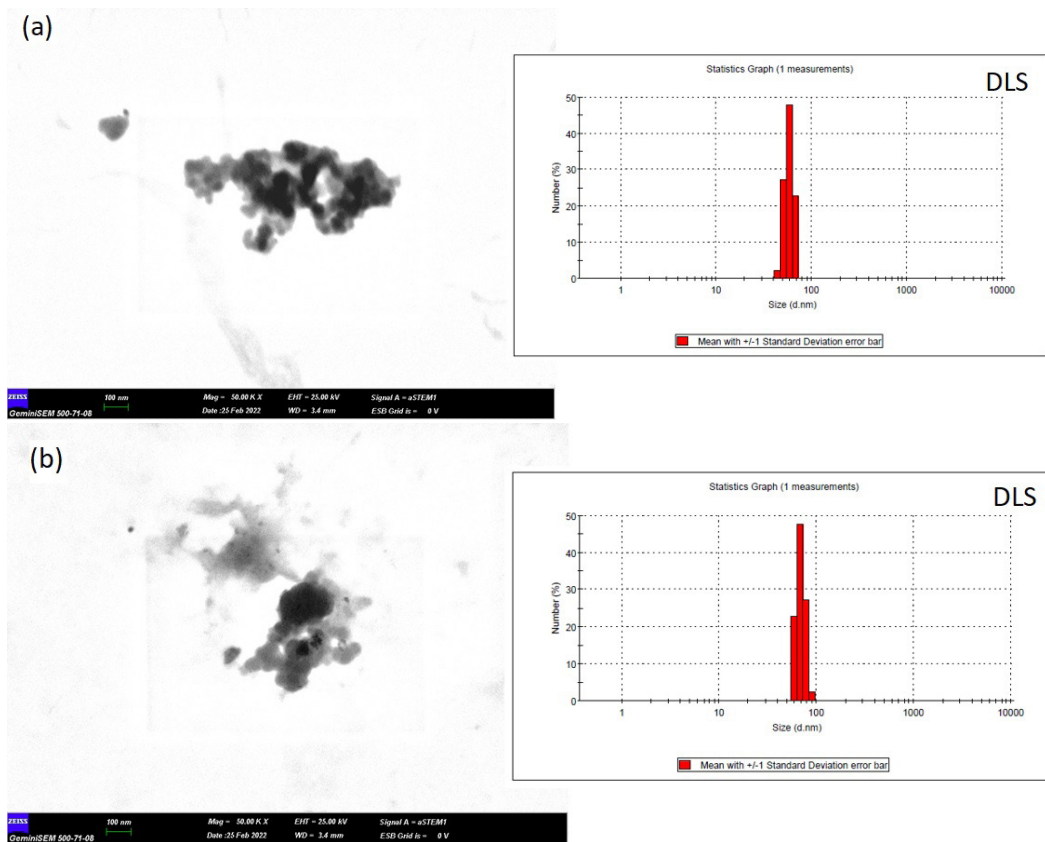


Figure 1. FESEM images and DLS particle size distribution of (a) RbNPs and (b) RbNPs-AA.

Fourier Transform Infrared (FTIR) Analysis of RbNPs and RbNPs-AA

FTIR analyses of the samples were performed using a Perkin Elmer Spectrum (400 FT-IR/FT-FIR Spectrometer Spotlight 400 Imaging System).

Absorption Measurements

The Hach Lange DR 5000 spectrophotometer was used to evaluate the absorbance of aqueous solutions of plastics. Water was used as a reference for measurements in the wavelength range 200-1100 nm.

Preparation of Colorectal Carcinoma Cell Line

A total of 1×10^5 cells/mL (ATCC® CCL-247™) cells were cultured in DMEM containing 10% FBS and 1% penicilin/streptomycin and incubated at 37 °C in an incubator containing 5% CO₂ for 48 hours.

Effects of AA and RbNPs-AA on the Cell Viability on HCT116 with Sulforhodamine B (SRB) Assay

SRB is a fluorescent dye that is used to quantify cellular proteins in cultivated cells as well as laser-induced fluorescence. The SRB test determines the volume of all proteins and connects it with the number of cells based on the dye's affinity for amino acids

in proteins in cells (14). For this aim, lyophilized extract stock solutions were prepared in DMSO and then diluted with six different doses of free AA and RbNPs-AA (114, 57, 28.5, 14, 25,

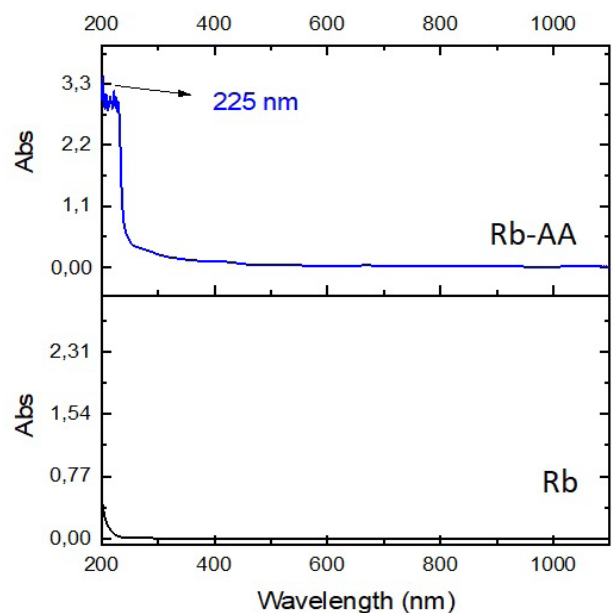


Figure 2. UV-VIS measurement results of RbNPs.

7.125, and 3.56 µg/mL) before being administered to HCT116 cells and cultured for 48 hours at 37°C in a 5% CO₂ incubator. After 48 hours, the antiproliferative effect of free AA and RbNPs-AA against colon cancer cells was performed. Dose-response curves were generated to determine the IC₅₀ of a compound (the concentration that prevents 50% of cells from growing). Using the Graphpad Prism 5 tool, the efficacy of the extracts was compared using this metric.

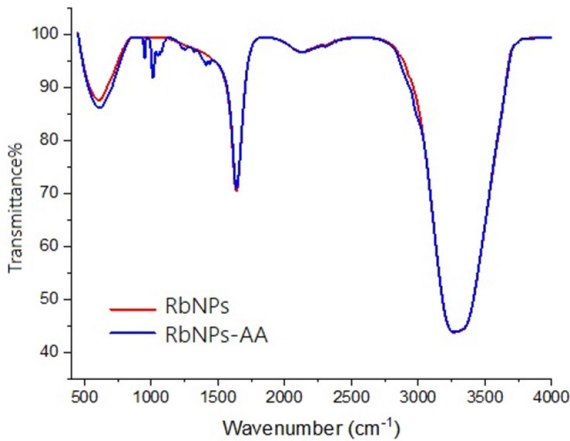


Figure 3. The FTIR data of RbNPs, and RbNPs-AA extract.

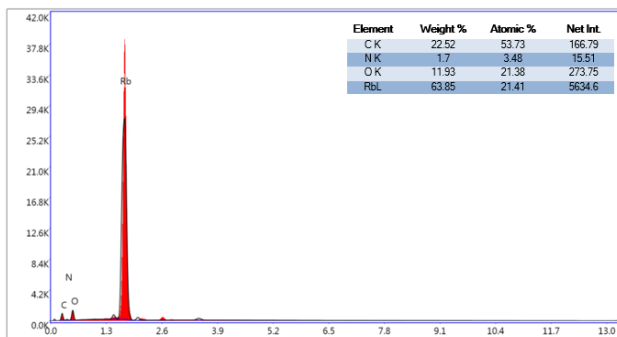


Figure 4. EDX analysis of RbNPs-AA.

RESULTS

In the present work, the size distributions of two RbNPs are compared. The RbNPs produced ranged from 43.82 nm to 68.06 nm, as shown by the DLS data in Figure 1. The approximate particle size is 58 nm on average. The particle diameters of the AA extract linked to RbNPs varied from 58.77 nm to 91.28 nm. FESEM evaluation shows that although the nanoparticles stick together after solvent evaporation, particles between 50 nm and 60 nm are easily visible. In contrast, RbNPs-AA extracts discolored the soil and made it difficult to distinguish particles below 100 nm (Figure 1). This is due to the fact that the amine groups in the extract structure of AA contain dye features.

In the studies of UV-VIS, no pronounced RbNPs absorption peak was detected in the visible spectrum. However, in the composition with the AA extract, strong peaks were detected near the ultra-UV region of 205-225 nm (Figure 2).

In Figure 3, the first peak was shown at 3276 cm⁻¹ for the -OH band, the second peak was measured at 1645 cm⁻¹ for the carboxylate group of Na₃C₆H₅O₇, the band for -CH vibrations at lower wavelengths. Shifts were observed for RbNPs-AA compared to RbNPs. In the RbNPs-AA extract, the -OH vibrational band shifted from 3276 cm⁻¹ to 3242 cm⁻¹ due to the amine groups in the structure. Moreover, characteristic vibrational peaks such as -CN stretching, -OH bending, -CH bending, -CO stretching between 1634-1007-934 cm⁻¹ were measured in the RbNPs-AA group.

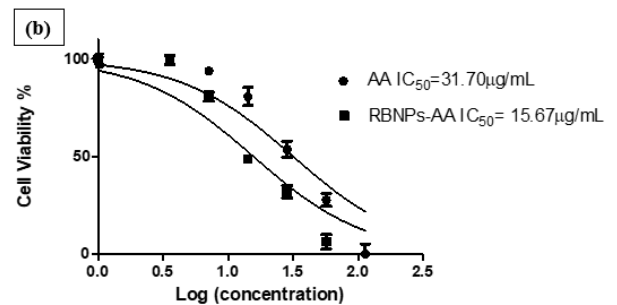
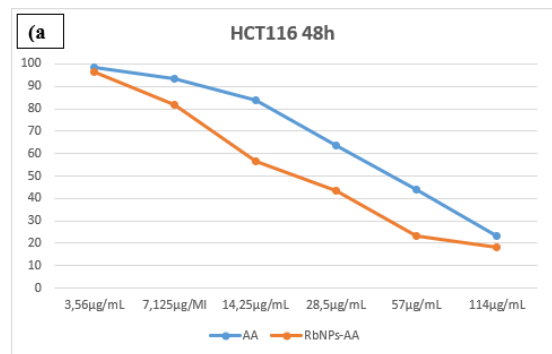


Figure 5a. The results of cell viability percentages of RbNPs-AA and free AA. **b.** IC₅₀ values of RbNPs-AA and free AA.

AA extract had 53.73% carbon, 3.48% nitrogen and 21.38% oxygen, while RbNPs contained 21.41% Rb according to EDX analysis. A very high percentage of the carrier RbNPs was found in the structure (Figure 4).

The effects of nanoparticles on cancer cell viability are determined by cytotoxicity analysis. In this way, the effectiveness of nanoparticles on cells can be better understood. Therefore, the SRB assay was used in this study, which is the preferred cytotoxicity assay. Accordingly, RbNPs-AA inhibited cell viability at half the dose of free AA (14.25 µg/mL) (Figure 5a). When IC₅₀ values were compared, RbNPs-AA was found to be more cytotoxic (Figure 5b).

DISCUSSION

To prepare nanoscale pharmaceutical preparations, anticancer drugs have recently been combined with nanoscale matrix materials by covalent chemical bonding, non-covalent chemical interactions (15), encapsulation by hydrophobic interactions, and encapsulation. The water solubility of drugs, distribution in tissues, and *in vivo* pharmacokinetics can be altered using matrix materials, and absorption in cells is also significantly enhanced (16). As a key factor in each stage of nanoparticle packaging, particle size is a crucial characteristic of nanoparticles (17). According to studies (18, 19), small nanoparticles have the advantage of penetrating into tumor tissues, while larger nanoparticles can passively enter the blood and aggregate near tumor blood vessels due to their increased permeability and retention (EPR). The presence of an extracellular matrix (ECM) and anomalous interstitial fluid pressure (IFP) have also been discovered as physiological barriers that contribute to osmotic barriers (20). The force that drives the diffusion of nanomedicines from blood vessels into the tumor is undermined by increased IFP in the tumor, resulting in a lower pressure differential between them (21). A thick barrier that restricts the passage of nanomaterials to the tumor core is formed by the ECM, which includes very active macromolecules that envelop cancer tissue (20). Therefore, it is inconvenient for large nanoparticles to pass through blood vessels and reach the distal end of cancer cells, especially in desmoid tumors that are enclosed by the thick tumor tissue and lack of blood vessels. In another experiment, it was found that 300 nm liposomes enhance the efficacy of surface modification but do not enter the tumor as well as 100 nm liposomes. Clearly, the small particle size of the nanocarrier contributes to a longer half-life of the drug and better tumor penetration. In addition, tumors are prone to collect nanoparticles that have substantial permeability and are below 70 nm in size (22). The average particle size of RbNPs-AA is 70 nm. Thus, the nanoparticle sizes found in this work are quite perfect. In addition, it is possible to determine the size of the particles using XRD patterns and the change in band gap absorption in the UV-VIS spectrum. The strong peaks of RbNPs-AA near the ultra-UV region of 205-225 nm is due to the absorption peaks of the electronic π -* transitions in the AA-extract structure originating from the carboxyl and amine groups (23). FTIR analysis uses infrared beam to scan samples to describe inorganic, organic, and molecular components. A change in chemical structure can be easily detected by changes in the typical pattern of absorption bands. FTIR is useful in defining and identifying unidentified compounds, detecting additions, finding impurities in a substance, and detecting degradation and oxidation (24). While the characteristic vibrational peak of RbNPs was seen at 596 cm^{-1} , it was simultaneously found that this vibrational signal shifted to 607 cm^{-1} after AA extraction charge (25). On the other hand, for a thorough chemical evaluation of nanoparticles, EDX has proven to be an effective and quite fast characterization technique (26). In this study significant results were detected by EDX analyzes.

Currently, there are very few studies on the preparation of RbNPs. Rubidium chloride (RbCl)-doped magnesium oxide (MgO) nanoparticles were prepared by Suba et al. (27), using grape juice, and they discovered that these RbNPs have antibacterial properties. A new class of Rb-containing bioactive glass nanoparticles (Rb-BGNs) with particle sizes below 100 nm was prepared in another study, and the results suggested that Rb-BGNs could be effective bioactive fillers for bone regeneration applications (28). According to Khorshid et al. (29), PMF, cesium, and rubidium nanoparticles were found to increase apoptosis in A549 lung cancer cells.

CONCLUSION

In summary, we have synthesized very small RbNPs with AA extract. The green synthesis approach has remarkable properties suitable for anticancer purposes. This is because the lower dosage of RbNPs-AA, which we used for this study in contrast to the free AA group, proved to be two-fold cytotoxic to colon cancer cells. Bryophytes are plants that do not have to be grown laboriously all over the world, are abundant and contain a lot of bioactive substances. Therefore, they are of great importance for anticancer drug/active substance content. Furthermore, very detailed studies on rubidium nanocarriers have not yet been carried out. So, the efficacy of RbNPs prepared in our work using the green synthesis approach will serve as a model for further studies. Besides, the isolation of biologically active substances from moss extracts could be useful in further investigations of agents providing protection against colorectal cancer.

Acknowledgement: The *Abietinella abietina* moss specimens used in the study were obtained from the personal herbarium of Kerem Canlı. We would like to thank him for his invaluable input and support throughout the research process.

Ethics Committee Approval: Ethics committee approval is not required for cell culture studies in the article.

Authors' Contributions: Conception/Design of Study – D.O., I.A.K.; Data Acquisition – D.O., I.A.K.; Data Analysis/Interpretation – D.O., I.A.K.; Drafting Manuscript – D.O., I.A.K.; Critical Revision of Manuscript – D.O., I.A.K.; Final Approval and Accountability – D.O., I.A.K.

Conflict of Interest: Authors declared no conflict of interest.

Financial Disclosure: The authors declare that this study has received no financial support.

REFERENCES

1. Xi Y, Xu P. Global colorectal cancer burden in 2020 and projections to 2040. *Transl Oncol* 2021; 14(10): 101174.
2. Saraiva MR, Rosa I, Claro I. Early-onset colorectal cancer: A review of current knowledge. *World J Gastroenterol* 2023; 29(8): 1289-303.
3. Bonelli J, Velasco-de Andrés M, Isidro N, Bayó C, Chumillas S, Carrillo-Serradell L, et al. Novel tumor-targeted self-nanostructured and compartmentalized water-in-oil-in-water polyurethane-polyurea nanocapsules for cancer theragnosis. *Pharmaceutics* 2022; 15(1): 58.
4. Nath D, Banerjee P. Green nanotechnology - a new hope for medical biology. *Environ Toxicol Pharmacol* 2013; 36(3): 997-1014.

5. Shahverdi AR, Fakhimi A, Shahverdi HR, Minaian S. Synthesis and effect of silver nanoparticles on the antibacterial activity of different antibiotics against *Staphylococcus aureus* and *Escherichia coli*. *Nanomedicine* 2007; 3(2): 168-71.
6. Makarov VV, Love AJ, Sinitynsya OV, Makarova SS, Yaminsky IV, Taliansky ME, et al. "Green" Nanotechnologies: Synthesis of metal nanoparticles using plants. *Acta Naturae* 2014; 6: 35.
7. Ritter SK. EPA Data suggest green success. *Chemical & Engineering News*. 2015; 93: 32–3.
8. Nasrollahzadeh M, Issaabadi Z, Sajadi SM. Green synthesis of a Cu/MgO nanocomposite by *Cassythia filiformis* L. extract and investigation of its catalytic activity in the reduction of methylene blue, congo red and nitro compounds in aqueous media. *RSC Adv* 2018; 8: 3723–35.
9. Clayton WA, Albert NW, Thrimawithana AH, McGhie TK, Deroles SC, Schwinn KE. et al. UVR8-mediated induction of flavonoid biosynthesis for UVB tolerance is conserved between the liverwort *Marchantia polymorpha* and flowering plants. *Plant J* 2018 ; 96: 503–17.
10. Bandyopadhyay A, Dey A. The ethno-medicinal and pharmaceutical attributes of Bryophytes: A review. *Phytomed Plus* 2022; 2: 100255.
11. "*Abietinella abietina* var. *abietina/histicosa*". Royal Botanic Garden Edinburgh. Retrieved 2023-05-18. Available from: URL: <https://www.britishbryologicalsociety.org.uk/wp-content/uploads/2020/12/Abietinella-abietina-var.-abietina-histicosa.pdf>.
12. Spjut RW, Suffness M, Cragg GM, Norris DH. Mosses, hornworts and liverworts screened for antitumor activity. *Economic Botany* 1986; 40: 310-38.
13. Özerkan D, Erol A, Altuner EM, Canlı K, Kuruca DS. Some bryophytes trigger cytotoxicity of stem cell-like population in 5-fluorouracil resistant colon cancer cells. *Nutr Cancer* 2022; 74(3): 1012-22.
14. Orellana EA, Kasinski AL. Sulforhodamine B (SRB) assay in cell culture to investigate cell proliferation. *Bio Protoc* 2016; 6: 21.
15. Andrežalová L, Országhová Z. Covalent and noncovalent interactions of coordination compounds with DNA: An overview. *J Inorg Biochem* 2021; 225: 111624.
16. Sourı M, Soltani M, Moradi Kashkooli F, Shahvandi MK. Engineered strategies to enhance tumor penetration of drug-loaded nanoparticles. *J Control Release* 2022; 3(41): 227–46.
17. Yadav KS, Dalal DC. The heterogeneous multiscale method to study particle size and partitioning effects in drug delivery. *Comput Math Appl* 2021; 92: 134–48.
18. Ikeda-Imafuku M, Wang LLW, Rodrigues D, Shaha S, Zhao Z, Mitragotri S. Strategies to improve the EPR effect: A mechanistic perspective and clinical translation. *J Control Release* 2022; 345: 512–36.
19. Fang J, Islam W, Maeda H. Exploiting the dynamics of the EPR effect and strategies to improve the therapeutic effects of nanomedicines by using EPR effect enhancers. *Adv Drug Deliv Rev* 2020; 157: 142–60.
20. Liu Y, Zhou J, Li Q, Li L, Jia Y, Geng F. et al. Tumor microenvironment remodeling-based penetration strategies to amplify nanodrug accessibility to tumor parenchyma. *Adv Drug Deliv Rev* 2021; 172: 80–103.
21. Zi Y, Yang K, He J, Wu Z, Liu J, Zhang W. Strategies to enhance drug delivery to solid tumors by harnessing the EPR effects and alternative targeting mechanisms. *Adv Drug Deliv Rev* 2022; 114449.
22. Xu J, Song M, Fang Z, Zheng L, Huang X, Liu K. Applications and challenges of ultra-small particle size nanoparticles in tumor therapy. *J Control Release* 2023; 353: 699–712.
23. Jiao Y, Meng F, Zhu G, Ran LZ, Jiang YF, Zhang Q. Synthesis of a novel p-hydroxycinnamic amide with anticancer capability and its interaction with human serum albumin. *Exp Ther Med* 2019; 17: 1321–29.
24. Titus D, James Jebaseelan Samuel E, Roopan SM. Nanoparticle characterization techniques. Shukla AK, Iravani S, editors. *Micro and nano technologies, green synthesis, characterization and applications of nanoparticles*. Elsevier; 2019. p. 303–19.
25. Fissan H, Ristig S, Kaminski H, Asbach C, Epple M. Comparison of different characterization methods for nanoparticle dispersions before and after aerosolization. *Analytical Methods* 2014; 6: 7324–34.
26. Rades S, Hodoroaba VD, Salge T, Wirth T, Lobera MP, Labrador RH. High-resolution imaging with SEM/T-SEM, EDX and SAM as a combined methodical approach for morphological and elemental analyses of single engineered nanoparticles. *RSC Adv* 2014; 4: 49577–87.
27. Suba A, Selvarajan P, Jebaraj Devadasan J. Rubidium chloride doped magnesium oxide nanomaterial by using green synthesis and its characterization. *Chem Phys Lett* 2022; 793: 139463.
28. Ouyang S, Zheng K, Huang Q, Liu Y, Boccaccini AR. Synthesis and characterization of rubidium-containing bioactive glass nanoparticles. *Mater Lett* 2020; 273: 127920.
29. Khorshid FA, Raouf GA, El-Hamidy SM, Al-amri GS, Alotaibi NA. PMF, cesium & rubidium nanoparticles induce apoptosis in A549 cells. *Life Sci J* 2011; 8(3): 534-42.

Comparison of Gene Expression Levels in the p53 Pathway in Blood and Bone Marrow of Healthy Individuals

Aynur Daglar Aday¹ , Gozde Oztan² , Ilknur Suer^{1,3} 

¹Division of Medical Genetics, Department of Internal Medicine, Istanbul Faculty of Medicine, Istanbul University, Istanbul, Turkiye

²Department of Medical Biology, Istanbul Faculty of Medicine, Istanbul University, Istanbul, Turkiye

³Department of Medical Genetics, Istanbul Faculty of Medicine, Istanbul University, Istanbul, Turkiye

ORCID ID: A.D.A. 0000-0001-8072-0646; G.O. 0000-0002-2970-1834; I.S. 0000-0003-1954-4190

Cite this article as: Daglar Aday A, Oztan G, Suer I. Comparison of gene expression levels in the p53 pathway in blood and bone marrow of healthy individuals. *Experimed* 2023; 13(2): 103-108.

ABSTRACT

Objective: A bone marrow (BM) sample is largely used in the diagnosis and prognosis follow-up of many hematological malignancies. BM aspiration is a more risky and laborious technique compared to blood collection. Together with publications in which the expression levels in BM and peripheral blood (PB) are correlated for many genes, there are also conflicting publications. This may also be due to the physiological and disease state. In this study, we aimed to compare the BM and PB expression levels of genes in the p53 pathway in healthy individuals.

Materials and Methods: The study comprised 23 healthy individuals. The expressions of 22 genes in the p53 pathway were analyzed using the RT²-profiler polymerase chain reaction (PCR) array. The expression levels were normalized to the reference gene β -actin. Then the mRNA expression levels between PB and BM sample groups were compared.

Results: The expression levels of the 20 genes studied were similar between the two groups. Only *GADD45* and *PTX3* genes were differentially expressed between PB and BM sample groups ($p=0.003$ and $p=0.033$, respectively) and those two gene expression levels were strongly correlated ($r=0.886$, $p<0.0001$).

Conclusion: When the expressions of 20 genes other than the *GADD45* and *PTX3* in our panel were evaluated, we suggest that PB largely reflects the p53 pathway gene expression levels in the BM. Therefore, PB may be preferred as an alternative to invasive BM in the analysis of these 20 genes in patients with hematological malignancies.

Keywords: p53 pathway, bone marrow, peripheral blood

INTRODUCTION

The canonical functions of p53 in cell division, DNA repair, cellular senescence, and cell death are well-known (1). Recent studies have shown that wild-type and mutant p53 are involved in amino acid, nucleotide, and lipid metabolism, as well as other major metabolisms such as oxidative phosphorylation, glycolysis, and redox homeostasis (2, 3). From a metabolic point of view, the p53 pathway should be considered as a non-linear pathway. Furthermore, the

complex metabolic network controlled by p53 regulators and the function of p53 in these mechanisms is not fully understood (3).

Peripheral blood (PB) material includes plasma and blood cells (erythrocytes, platelets, leukocytes). Apart from blood cells, plasma contains sugar, fat, salt, and water. Blood carries nutrients and oxygen to the cells, as well as removing waste from the cells (4). PB is used in many diagnostic tests because it can be collected less invasively than most other

Corresponding Author: Gözde Öztan **E-mail:** gozdeoztan@istanbul.edu.tr

Submitted: 16.04.2023 **Revision Requested:** 23.05.2023 **Last Revision Received:** 26.05.2023 **Accepted:** 16.06.2023 **Published Online:** 07.08.2023



Content of this journal is licensed under a Creative Commons Attribution-NonCommercial 4.0 International License.

body materials and obtaining blood is both easier and less risky compared to bone marrow (BM) collection (5). BM is localized

within the bone and is responsible for the production of blood cells. Hip and scapula bones are frequently preferred sites for

Table 1. Comparison of expressions of p53 pathway genes between bone marrow and peripheral blood samples.

Gene	Groups	Number of participants	Relative expression (mean ± SD)	Fold change	p-value
BAX	BM	8	0.3273 ± 0.91941	1.15	0.353
	PB	15	0.0036 ± 0.00072		
CDKN2A	BM	8	0.0005 ± 0.00138	0.72	0.330
	PB	15	0.0000 ± 0.00001		
APAF1	BM	8	0.0084 ± 0.01071	1.94	0.456
	PB	15	0.0054 ± 0.00073		
ATM	BM	8	0.0021 ± 0.00414	2.03	0.430
	PB	15	0.0009 ± 0.00034		
ATR	BM	8	0.0016 ± 0.00342	1.13	0.309
	PB	15	0.0003 ± 0.00008		
CASP9	BM	8	0.0026 ± 0.00513	1.46	0.432
	PB	15	0.0011 ± 0.00016		
CDK4	BM	8	0.0036 ± 0.00623	0.68	0.249
	PB	15	0.0009 ± 0.00021		
CDKN1A	BM	8	0.0021 ± 0.00273	2.47	0.850
	PB	15	0.0019 ± 0.00060		
CHEK2	BM	8	0.0031 ± 0.00763	0.40	0.316
	PB	15	0.0002 ± 0.00005		
E2F1	BM	8	0.0007 ± 0.00081	0.46	0.066
	PB	15	0.0001 ± 0.00006		
E2F3	BM	8	0.0021 ± 0.00126	0.99	0.286
	PB	15	0.0016 ± 0.00023		
MCL1	BM	8	0.0781 ± 0.05242	0.98	0.350
	PB	15	0.0593 ± 0.01336		
MDM2	BM	8	0.0165 ± 0.03737	1.09	0.393
	PB	15	0.0045 ± 0.00103		
MDM4	BM	8	0.0013 ± 0.00183	1.31	0.555
	PB	15	0.0009 ± 0.00031		
PTEN	BM	8	0.0196 ± 0.01991	0.91	0.362
	PB	15	0.0127 ± 0.00146		
RB1	BM	8	0.0281 ± 0.07244	0.42	0.336
	PB	15	0.0016 ± 0.00036		
P53	BM	8	0.0482 ± 0.12947	0.64	0.353
	PB	15	0.0027 ± 0.00052		
BCL2	BM	8	0.3217 ± 0.90720	0.38	0.351
	PB	15	0.0009 ± 0.00035		
CHEK1	BM	8	0.0091 ± 0.02359	0.09	0.315
	PB	15	0.0001 ± 0.00002		
GADD45	BM	8	0.0011 ± 0.00063	0.10	0.003
	PB	15	0.0001 ± 0.00002		
PCNA	BM	8	0.0263 ± 0.04768	0.23	0.202
	PB	15	0.0026 ± 0.00059		
PTX3	BM	8	0.0035 ± 0.00357	0.06	0.033
	PB	15	0.0002 ± 0.00009		

PB: Peripheral blood; BM: Bone marrow

BM extraction (6). BM aspiration from these regions is highly invasive and local anesthesia is applied during the procedure. It has been reported that these anesthetics may have side effects that lead to various neurodevelopmental disorders, particularly in children (7). Allogeneic hematopoietic stem cell transplantation in adults with hematological malignancies is increasingly performed using PB-derived stem cells rather than BM. It is possible to donate PB-derived stem cells for convenience and safety reasons as well as logistical reasons, which have been behind the growth of this stem cell source (8).

Gene expression analyses in samples from PB mononuclear cells and different tissues are not always the same. Results from a single tissue are not sufficient to explain how expression changes affect complex biological systems in human beings (9). Limited studies compare PB and BM samples in terms of expression patterns. As a result of our detailed investigation, no study was present in the literature comparing the p53 pathway gene expression levels in healthy individuals. *HMG-CoA reductase gene (HMGCR)* and *low-density lipoprotein receptor (LDLR)* gene expressions in the PB and BM samples of myelodysplastic syndrome (MDS) patients have been reported to be upregulated similarly when compared to blood samples of healthy controls (10). Apoptosis stimulating effect of p53 protein 2 (*ASPP2*) gene expression in PB and BM samples from chronic lymphoblastic leukemia (CLL) patients has been reported to be downregulated in the same way when compared to blood samples from healthy controls. In the same study, it was shown that the level of gene expression in the PB and BM samples of the patients were similar (11).

The p53 pathway genes, mainly p53, respond to stress during cell division (12). However, tumor protein p53 (TP53) is the most frequently genetically altered gene in both solid and hematological cancers (13). Other genes involved in

this pathway have not been elucidated as p53. In order to understand the similar and different aspects of PB and BM aspirate materials in terms of p53 pathway genes, we aimed to compare the differential expression patterns of 22 genes ATM serine/threonine kinase (*ATM*), Bcl-2 associated X-protein (*BAX*), cyclin-dependent kinase 4 (*CDK4*), cyclin dependent kinase inhibitor 2A (*CDKN2A*), checkpoint kinase 1 (*CHEK1*), checkpoint kinase 2 (*CHEK2*), cyclin dependent kinase inhibitor 1A (*CDKN1A*), Ataxia Telangiectasia and Rad3 related (*ATR*), growth arrest and DNA damage inducible alpha (*GADD45A*), mouse double minute 2 homolog (*MDM2*), mouse double minute 4 (*MDM4*), proliferating cell nuclear antigen (*PCNA*), retinoblastoma 1 (*RB1*), caspase 9 (*CASP9*), tumor protein P53 (*TP53*), B-cell lymphoma 2 (*BCL2*), apoptotic peptidase activating factor 1 (*APAF1*), E2F transcription factor 1 (*E2F1*), E2F transcription factor 3 (*E2F3*), myeloid cell leukemia 1 (*MCL1*), pentraxin 3 (*PTX3*), phosphatase and tensin homolog (*PTEN*) selected from the p53 pathway involved in cell growth, proliferation, differentiation, DNA repair and apoptosis processes.

MATERIALS AND METHODS

Samples

PB and BM samples were collected in sterile tubes containing EDTA, after obtaining written informed consent from 23 healthy volunteers. PB samples were taken from healthy hospital personnel without a history of leukemia, and BM samples were taken from BM transplantation donor candidates in the Istanbul University Faculty of Medicine, Department of Hematology. The median age of 50.95 years was observed among 10 males (43.4%) and 13 females (56.5%). The study protocol was designed in accordance with the Declaration of

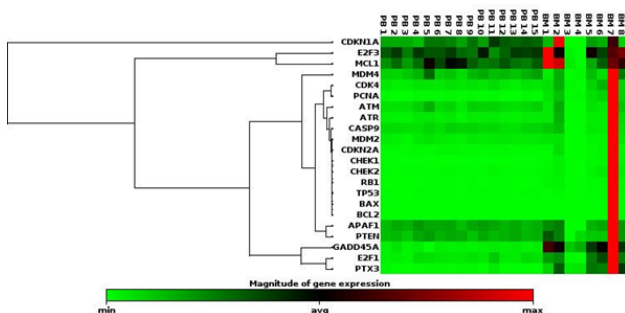


Figure 1. The average of the fold change for PB and BM samples were shown in heatmap graphs. The heat map is a graphical representation of the RT²-PCR array's findings about the differential regulation of gene expression between the peripheral blood and bone marrow samples. The intensity of the colors reveals the degree of change in gene expression. Low gene expression (ratio<1) in PB samples is shown in green. Genes with a ratio close to 1 are shown as black squares. Gene expression in the red squares is greater than in the BM samples (ratio>1).

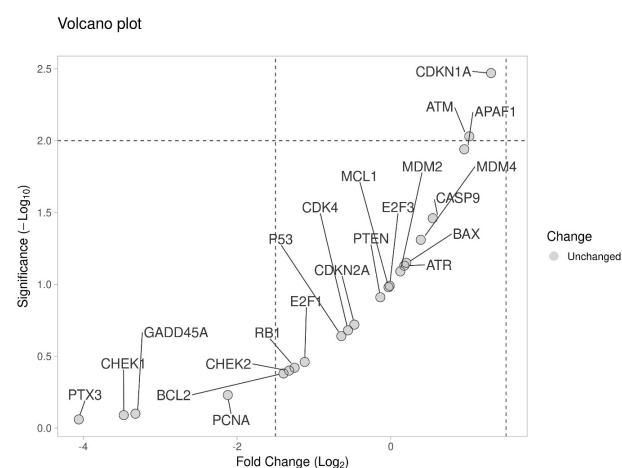


Figure 2. A volcano plot was generated showing the gene expressions of BM samples versus PB samples. Distributions of fold changes in gene expression are shown using volcano plots. BM samples compared with PM samples. p-values less than 0.05 and absolute fold changes of 2 were considered significant. No significant variation in fold alterations of genes was observed.

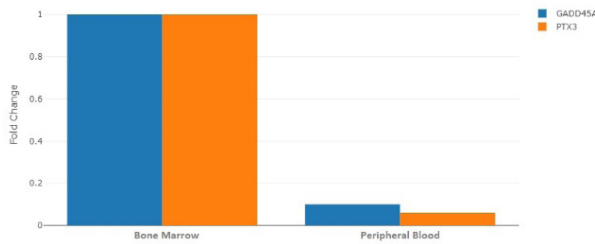


Figure 3. Comparison of the *GADD45* and *PTX3* gene expression in PB and BM samples. Fold-change ($2^{-\Delta\Delta CT}$) is the ratio of the normalized gene expression ($2^{-\Delta CT}$) in the PB sample to the normalized gene expression ($2^{-\Delta CT}$) in the BM sample. Fold-change values higher than one indicate a positive regulation, also known as an up-regulation, whereas fold-change values lower than one indicate a negative regulation, also known as a down-regulation.

Helsinki. The study was conducted with the ethical approval obtained from the Clinical Research Ethics Committee of Istanbul University Faculty of Medicine (E-29624016-050.99-876968/ May 9, 2022).

RNA Isolation and cDNA Synthesis

Total RNA from whole blood and BM samples were extracted using the QiaAmp RNA Blood Mini Kit (Qiagen, USA). RNA quality and quantity were measured using NanoDrop 2000c spectrophotometer (Thermo Fisher Scientific, USA). A template of 1 µg of total RNA was used in cDNA synthesis. cDNA synthesis was performed on a LightCycler 480 II platform using Qiagen RT²HT First Strand Kit (Qiagen, USA).

Expression Analysis via qRT-PCR Array

qRT-PCR array using a custom RT²-Profiler PCR array (CAPH_133446F; cat no. 330131/12 plate) was conducted to analyze the mRNA expressions of 22 genes involved in proliferation, differentiation, cell cycle, DNA repair, and apoptosis processes intervened by the p53 pathway. The study was carried out on a LightCycler 480 II platform using SYBR Green master mix and 1 µl cDNA sample. The gene expression levels were analyzed and normalized with the β-actin housekeeping gene. The Livak method was used to calculate relative gene expression levels (14).

Statistical Analysis

Statistical analysis was carried out using the SPSS package program, version 21. Statistical analysis of the expression levels of the genes in the BM aspirate and PB was carried out using the Student's t-test. Pearson correlation analysis was conducted to determine the expression correlations of genes that were statistically significant between the groups. $p < 0.05$ was determined as the cut-off value for statistical significance.

RESULTS

Two of the p53 pathway genes (*GADD45* and *PTX3*) we investigated in our study were found to have different expression levels between BM and PB. The fold change in expression of these two genes between the groups (BM/PB) was 0.1 and 0.06, respectively. It was found that *GADD45A* and *PTX3* gene expressions were significantly decreased in BM samples compared to PB samples ($p=0.003$ and $p=0.033$, respectively) (Table 1). However, there was no statistical difference in the expression levels of *APAF1*, *ATM*, *BAX*, *CDKN1A*, *CDKN2A*, *MDM2*, *MCL1*, *MDM4*, *PTEN*, *CASP9*, *ATR*, *CHEK2*, *E2F1*, *E2F3*, *RB1*, *TP53*, *BCL2*, *CDK4*, *CHEK1*, and *PCNA* genes between the two groups (Table 1). The averages of the fold change for PB and BM samples were shown in heatmap graphs (Figure 1). A volcano plot was generated showing the gene expressions of BM samples versus PB samples (Figure 2). Comparison of the gene expressions of the genes that are differentially expressed (*GADD45*, *PTX3*) are shown in the bar graph (Figure 3).

According to the results of the Pearson correlation analysis, it was observed that the *GADD45* gene showed a high correlation with the expressions of the *APAF1*, *ATR*, *CDK4*, *E2F1*, *PTEN*, *PCNA*, *PTX3* genes ($r=0.7$; $p < 0.001$). In addition, the *PTX3* gene showed a high correlation with the expressions of *BAX*, *CDKN2A*, *APAF1*, *ATM*, *ATR*, *CASP9*, *CDK4*, *CHEK2*, *E2F1*, *MDM2*, *MDM4*, *PTEN*, *RB1*, *TP53*, *BCL2*, *CHEK1*, *GADD45* and *PCNA* genes ($r=0.7$; $p < 0.001$). The correlation between *GADD45* and *PTX3* was quite high ($r=0.886$, $p < 0.0001$).

DISCUSSION

Transcription factor p53, which is one of the major tumor suppressor genes, affects the expression of many genes by targeting more than thousands of sites (15). p53 plays a role in the regulation of many cellular metabolic functions. In addition, p53 is also involved in various processes, including the regulation of growth factors and reactive oxygen species, which have an impact on cancer pathogenesis (16). Disturbances in the p53 pathway play a more active role in some hematological cancers like chronic lymphoblastic leukemia (CLL) and multiple myeloma (17, 18). Hematological cancers are malignancies of BM-derived cells. BM aspiration biopsy, which is important in the diagnosis and routine follow-up of patients, is an invasive technique that is very uncomfortable for the patient and has risks compared to PB collection. It is very important to determine the expression patterns of p53 pathway genes in PB and BM, as they may contribute to the same mechanisms. To the best of our knowledge, our study is the first to compare the differences in mRNA levels and correlations of p53 pathway genes between PB and BM samples.

However, there are various studies in the literature investigating different gene expression states in PB and BM samples of patients with hematological cancers. Crassini et al. examined the expression profile of 260 genes in PB, BM, and lymph node-derived CLL cells. They reported that approximately half of these

genes were reduced in PB-induced CLL cells compared to other groups (19). In another study comparing the expression levels of PB and BM samples taken from CLL patients, it was stated that there was not much difference in *Bcl-2*, *ADAM29*, *Mcl-1*, *ZAP70*, and *LPL* genes in this sense (20). In their study on acute myeloid leukemia patients, Sakhinia et al. did not find any difference in the expression of some genes (*leptin receptor*, *CD33*, *adipsin*, *proteoglycan 1*, *MB-1*, *cyclin D3*, *hSNF2b*, *proteasome iota*, *HkrT-1*, and *E2A*), but they found significant changes in the expression of some other genes *c-myb*, *HOXA9*, *LYN*, *cystatin c* and *LTC4s* (21). In a study conducted on patients with chronic myeloid leukemia, it was reported that BCR-ABL transcript levels were correlated in PB and BM samples, and PB could be used instead of BM in routine monitoring (22). Moreover, van Leeuwen-Kerkhoff et al. reported that *MRC1*, *CSF3R*, *XCR1*, *CLEC9A* and *IRF8KI* gene expressions were correlative in BM and PB-derived myeloid dendritic cell subgroups (23).

Low fold change value detected in *GADD45* and *PTX3* genes and the presence of insignificant gene expression levels in other p53 pathway genes may indicate the similarity of PB and BM with respect to p53 pathway gene expressions.

Members of the *GADD45* family, which are defined as stress sensors, are triggered by environmental stress such as inflammatory cytokines and genotoxic agents (24, 25). They also regulate genomic stability, senescence, cell survival and apoptosis (24). Apoptosis is induced when DNA damage is fatal or *GADD45A* arrests cell cycle progression. The hematopoietic system might benefit from *GADD45A*'s ability to induce terminal differentiation in damaged stem and progenitor cells, as well as DNA repair and genomic stabilization (26). The impact of *GADD45* proteins on tumor growth depends on the molecular structure of the activated oncogene, as well as the cell type in which it is expressed and the signaling pathways with which it is currently interacting (25). Exemplarily, *GADD45a* is both expressed independently of p53 and is a p53 target gene (27).

The second gene, *PTX3* which is a multifunctional protein, plays an important role in immunity, inflammation, and extracellular matrix organization/remodeling (28). In studies investigating the role of *PTX3*, it has been reported that it is expressed in different cells such as macrophages, neutrophils, and smooth muscle cells (29). According to the data we obtained from our study, a strong correlation was identified between *GADD45* and *PTX3* gene expression levels. Because of the similar mRNA levels between PB and BM, we think that PB may reflect the BM expression pattern for the other p53 pathway genes we analyzed.

As a limitation of our current study, the number of the participants was relatively small, that's why it should be considered as a preliminary study and should be confirmed by further studies encompassing larger PB and BM groups.

In this present study that aimed to compare the expression levels of the important genes in the p53 pathway, we detected a statistically significant difference between the expression patterns of only two genes (*GADD45A*, *PTX3*) in the PB and

BM out of 22 genes. The fact that no statistically significant difference was observed in the expression of the other 20 genes in both groups suggested that these two groups may have similar characteristics in terms of p53 pathway genes. Therefore, a PB sample, which is easier and less invasive to obtain, may be a convenient alternative to examine the expressions of genes in the p53 pathway instead of the BM sample.

Ethics Committee Approval: This study was approved by Clinical Research Ethic Committee of Istanbul Faculty of Medicine (E-29624016-050.99-876968/ May 9, 2022).

Authors' Contributions: Conception/Design of Study – A.D.A., G.O., I.S.; Data Acquisition – A.D.A., G.O., I.S.; Data Analysis/Interpretation – A.D.A., G.O., I.S.; Drafting Manuscript– A.D.A., G.O., I.S.; Critical Revision of Manuscript- A.D.A., G.O., I.S.; Final Approval and Accountability– A.D.A., G.O., I.S.

Note: All authors have contributed equally to this work.

Conflict of Interest: Authors declared no conflict of interest.

Financial Disclosure: The authors declare that this study has received no financial support.

REFERENCES

1. Kruiswijk F, Labuschagne CF, Vousden KH. p53 in survival, death and metabolic health: a lifeguard with a licence to kill. *Nat Rev Mol Cell Biol* 2015; 16(7): 393-405.
2. Lacroix M, Riscal R, Arena G, Linares LK, Le Cam L. Metabolic functions of the tumor suppressor p53: Implications in normal physiology, metabolic disorders, and cancer. *Mol Metab* 2020; 33: 2-22.
3. Lahalle A, Lacroix M, De Blasio C, Cissé MY, Linares LK, Le Cam L. The p53 pathway and metabolism: The tree that hides the forest. *Cancers (Basel)* 2021; 13(1): 133.
4. Cowin SC, Cardoso L. Blood and interstitial flow in the hierarchical pore space architecture of bone tissue. *J Biomech* 2015; 48(5): 842-54.
5. Schraw JM, Woodhouse JP, Bernhardt MB, Taylor OA, Horton TM, Scheurer ME, et al. Comparison of the blood, bone marrow, and cerebrospinal fluid metabolomes in children with b-cell acute lymphoblastic leukemia. *Sci Rep* 2021; 11(1): 19613.
6. Lucas D. Structural organization of the bone marrow and its role in hematopoiesis. *Curr Opin Hematol* 2021; 28(1): 36-42.
7. Banerjee P, Rossi MG, Angheliescu DL, Liu W, Breazeale AM, Reddick WE, et al. Association between anesthesia exposure and neurocognitive and neuroimaging outcomes in long-term survivors of childhood acute lymphoblastic leukemia. *JAMA Oncol* 2019; 5(10): 1456-63.
8. Holtick U, Albrecht M, Chemnitz JM, Theurich S, Shimabukuro-Vornhagen A, Skoetz N, et al. Comparison of bone marrow versus peripheral blood allogeneic hematopoietic stem cell transplantation for hematological malignancies in adults - a systematic review and meta-analysis. *Crit Rev Oncol Hematol* 2015; 94(2): 179-88.
9. Pinhel MAS, Noronha NY, Nicoletti CF, Quinhoneiro DCG, Oliveira BAP, Cortes-Oliveira C, et al. Comparison of gene expression profile between blood cells and white adipose tissue of patients with obesity. *Nutr Hosp* 2017; 34(3): 608-12.

10. Ellis MH, Baraf L, Shaish A, Har-Zahav A, Harats D, Ashur-Fabian O. Alteration of lipids and the transcription of lipid-related genes in myelodysplastic syndromes via a TP53-related pathway. *Exp Hematol* 2012; 40(7): 540-7.
11. Schittenhelm MM, Illing B, Ahmut F, Rasp KH, Blumenstock G, Döhner K, et al. Attenuated expression of apoptosis stimulating protein of p53-2 (ASPP2) in human acute leukemia is associated with therapy failure. *PLoS One* 2013; 8(11): e80193.
12. Harris SL, Levine AJ. The p53 pathway: positive and negative feedback loops. *Oncogene* 2005; 24(17): 2899-908.
13. Kandoth C, McLellan MD, Vandin F, Ye K, Niu B, Lu C, et al. Mutational landscape and significance across 12 major cancer types. *Nature* 2013; 502(7471): 333-9.
14. Livak KJ, Schmittgen TD. Analysis of relative gene expression data using real-time quantitative PCR and the 2(-Delta Delta C(T)) Method. *Methods* 2001; 25(4): 402-8.
15. Simabuco FM, Morale MG, Pavan ICB, Morelli AP, Silva FR, Tamura RE. p53 and metabolism: from mechanism to therapeutics. *Oncotarget* 2018; 9(34): 23780-823.
16. Hanahan D, Weinberg RA. The hallmarks of cancer. *Cell* 2000; 100(1): 57-70.
17. Ilknur S, Aynur A, Sariman M, Mesut A, Hindilerden IY, Ekmekci SS, et al. Dysregulation of MS4A3 and PRDX5 gene expression in multiple myeloma patients. *Int J Hem Oncol* 2021; 31(4): 205-13.
18. Öztan G, Aktan M, Palanduz S, İşsever H, Öztürk S, Nikerel E, et al. Relationship between chromosomal aberrations and gene expressions in the p53 pathway in chronic lymphocytic leukemia. *Balkan J Med Genet* 2020; 23(1): 15-24.
19. Crassini KR, Shen Y, Christopherson R, Stevenson WS, Mulligan S, Best OG. Analysis of mRNA expression in peripheral, bone marrow and lymph node derived CLL Cells using the nanosting ncounter platform. *Blood* 2017; 130(1): 4279.
20. Wiestner A, Marti GE, Billings EM, Liu H, Lee E, White T, et al. Differential gene expression in CLL cells from bone marrow and peripheral blood suggests a role of bone marrow stroma in leukemic cell proliferation. *Blood* 2005; 106(11): 708.
21. Sakhinia E, Farahangpour M, Tholouli E, Liu Yin JA, Hoyland JA, Byers RJ. Comparison of gene-expression profiles in parallel bone marrow and peripheral blood samples in acute myeloid leukaemia by real-time polymerase chain reaction. *J Clin Pathol* 2006; 59(10): 1059-65.
22. Jiang Q, Zhao XY, Qin YZ, Liu YR, Lai YY, Jiang B, et al. The differences and correlations of BCR-ABL transcripts between peripheral blood and bone marrow assays are associated with the molecular responses in the bone marrow for chronic myelogenous leukemia. *Am J Hematol* 2012; 87(12): 1065-9.
23. Van Leeuwen-Kerkhoff N, Lundberg K, Westers TM, Kordasti S, Bontkes HJ, Lindstedt M, et al. Human bone marrow-derived myeloid dendritic cells show an immature transcriptional and functional profile compared to their peripheral blood counterparts and separate from Slan+ non-classical monocytes. *Front Immunol* 2018; 9: 1619.
24. Guo D, Zhao Y, Wang N, You N, Zhu W, Zhang P, et al. GADD45g acts as a novel tumor suppressor, and its activation suggests new combination regimens for the treatment of AML. *Blood* 2021; 138(6): 464-79.
25. Liebermann DA, Tront JS, Sha X, Mukherjee K, Mohamed-Hadley A, Hoffman B. Gadd45 stress sensors in malignancy and leukemia. *Crit Rev Oncog* 2011; 16(1-2): 129-40.
26. Wingert S, Thalheimer FB, Haetscher N, Rehage M, Schroeder T, Rieger MA. DNA-damage response gene GADD45A induces differentiation in hematopoietic stem cells without inhibiting cell cycle or survival. *Stem Cells* 2016; 34(3): 699-710.
27. Yamasawa K, Nio Y, Dong M, Yamaguchi K, Itakura M. Clinicopathological significance of abnormalities in Gadd45 expression and its relationship to p53 in human pancreatic cancer. *Clin Cancer Res* 2002; 8(8): 2563-9.
28. Garlanda C, Bottazzi B, Magrini E, Inforzato A, Mantovani A. PTX3, a humoral pattern recognition molecule, in innate immunity, Tissue Repair, and Cancer. *Physiol Rev* 2018; 98(2): 623-39.
29. Inoue K, Kodama T, Daida H. Pentraxin 3: A novel biomarker for inflammatory cardiovascular disease. *Int J Vasc Med* 2012; 2012: 657025.

Investigation of the Toxicologic and Biochemical Effects of Silk Fibroin/Gold Nanoparticles-Based Nanofiber Using Zebrafish Embryos

Ozan Ozcan¹ , Ismail Unal¹ , Elif Tufan¹ , Ebru Emekli-Alturfan² , Tugba Tunali-Akbay² 

¹Department of Biochemistry, Institute of Health Sciences, Marmara University, Istanbul, Turkiye

²Department of Basic Medical Sciences, Biochemistry, Faculty of Dentistry, Marmara University, Istanbul, Turkiye

ORCID ID: O.O. 0000-0003-0523-1732; I.U. 0000-0002-8664-3298; E.T. 0000-0003-0684-3693; E.E.A. 0000-0003-2419-8587;

T.T.A. 0000-0002-2091-9298

Cite this article as: Ozcan O, Unal I, Tufan E, Emekli-Alturfan E, Tunali-Akbay T. Investigation of the toxicologic and biochemical effects of silk fibroin/gold nanoparticles-based nanofiber using zebrafish embryos. *Experimed* 2023; 13(2): 109-114.

ABSTRACT

Objective: This study aimed to test the toxicity of silk fibroin (SF) / gold nanoparticles (AuNPs)-based nanofiber by using zebrafish embryos as an alternative animal model.

Materials and Methods: Nanofiber was fabricated via electrospinning. The zebrafish embryos were divided into four groups as control, 3,4-dichloroaniline (DCA) treated, one day SF/AuNPs treated (1D), and seven days SF/AuNPs treated (7D) group. The SF/AuNPs nanofiber was incubated in the medium for one day and seven days. Following incubation, the embryos were placed in the mediums and their development was monitored 72 hours post-fertilization. In the zebrafish embryos, levels of malondialdehyde (MDA), nitric oxide (NO), activities of superoxide dismutase (SOD) and glutathione-S-transferase (GST) were detected.

Results: Compared to the control group, there was no change in the hatching and mortality rates in the 1D and 7D groups. In the DCA group, the mortality rate was higher than the controls. In the 1D and 7D groups, MDA and NO were higher than the control but lower than the DCA group. SOD and GST activities decreased compared to the control.

Conclusion: SF/AuNPs-based nanofiber did not affect the hatchability and mortality of embryos but increased oxidant damage, therefore it is thought that this oxidant effect of SF/AuNPs-based nanofibers may provide antibacterial properties.

Keywords: Silk fibroin, gold nanoparticles, zebrafish embryos, oxidant-antioxidant status, toxicity

INTRODUCTION

The development of functional nanofiber-based membranes has gained considerable interest due to their distinctive features like high level porosity, high surface area-to-volume ratio, and excellent biocompatibility (1). In this study, gold nanoparticles (AuNPs)-added silk fibroin (SF)-based nanofiber membranes were prepared. Among various materials studied for nanofibrous membranes, SF has attracted interest due to its biodegradability and low immunogenicity. SF is a natural protein produced by a variety of spiders and insect species that has remarkable

strength, toughness, and flexibility (2). Human epithelial, fibroblast, keratinocyte, and osteoblast cells from a variety of tissues may adhere to, spread out, and develop when placed in three-dimensional SF nets. (3). SF has been utilized in bioengineering delivery systems for drugs, and delivery of therapeutics to cancer cells (4). SF has high biocompatibility, controlled degradability, structural integrity, and diverse process ability, these features make SF a desirable and valuable candidate for use in tissue science and delivery systems for drugs (5). Furthermore, SF nanofibers have been found to exhibit antioxidant effects, which can further support the wound-healing process

Corresponding Author: Tuğba Tunali Akbay **E-mail:** ttunali@marmara.edu.tr

Submitted: 24.05.2023 **Revision Requested:** 16.06.2023 **Last Revision Received:** 16.06.2023 **Accepted:** 21.06.2023 **Published Online:** 26.07.2023



Content of this journal is licensed under a Creative Commons Attribution-NonCommercial 4.0 International License.

(6). The addition of AuNPs to SF may exhibit bioactivities that could be used in biomedical applications. From a biological standpoint, the toxicity of AuNPs is crucial (7). In this case, the preparation of AuNPs, the dose and toxicity of AuNPs in products such as wound dressings in which nanoparticles are used needs to be considered. Following investigation of AuNPs in fibroblasts, epithelial cells, and macrophages, there was substantial concern that small AuNPs (dcore 2.0nm), which are more redox-reactive than bigger AuNPs, would have significant toxicity. However, further *in vitro* and *in vivo* studies have revealed that AuNPs, regardless of core diameter, are not acutely hazardous or toxic (8).

However, some studies state the AuNPs-induced reactive oxygen species production causes toxic effects on the DNA, cell nucleus, and mitochondria (9). Researchers have difficulty due to a lack of understanding of the mechanisms involved in the reduction stability and effects of biosynthesized gold nanoparticles (10). In this study gold nanoparticles were synthesized by using green chemistry techniques to decrease their hazardous effects and mixed with the SF to fabricate SF/AuNPs hybrid electrospun nanofiber.

The production of hybrid nanofibers containing gold nanoparticles are an important option in the invention of clean, nontoxic, and sustainable products with significant benefits over previous methods (11). Therefore, in this study, the possible toxicity of SF/AuNPs-based nanofibers was tested using zebrafish embryos focusing on the oxidant-antioxidant system when used as a wound dressing material.

MATERIALS AND METHODS

SF Preparation

SF was synthesized according to Zhu et al. (12). To degum the silk from sericin, Bombyx mori silk cocoons (5g) were cut into portions and boiled for thirty minutes in a 0.02 M sodium carbonate solution. The degummed silk was washed with deionized water and dried before being dissolved for four hours in 9.3 M LiBr solution and then dialyzed against deionized water for 72 hours to remove the LiBr. The obtained SF was centrifuged at 9,500xg and kept in 4°C.

AuNPs Preparation

AuNPs were prepared by using green chemistry. Collected fresh strawberry leaves were dried in a cool and shaded area. The dried strawberry leaves were then pulverized in a mortar. To ensure an equal size of the particles, the powder was sieved with a pore size of approximately 0.08mm sieve. 0.4 grams of strawberry leaf powder was mixed with deionized water and heated at 80°C for 20 minutes to create an aqueous extract. The plant extract was cooled to room temperature, and a simple centrifugation process was employed to remove the plant debris. A 1mM concentration of HAuCl₄ (chloroauric acid) solution was used to obtain gold nanoparticles. The 1mM HAuCl₄ solution was heated to 100°C. The strawberry leaf

extract was added to the boiling gold solution. Heating was continued until the prepared solution reached a dark red color. After the color change in approximately one to five seconds, the prepared solution was cooled to room temperature (13).

Preparation of SF /AuNP Nanofiber

10% SF in formic acid was mixed with 1% gold nanoparticles. This hybrid mixture was used to produce nanofiber. The optimized conditions for the electrospinning were determined as 25.5 kV electrical power, the flow rate in the feeding unit was 0.15mL per minute, the collector rotation speed was 200 rpm and the distance between the nozzle and the collector was 13.7 cm.

Development of Zebrafish Embryos

The zebrafish (AB/AB strain, wild type) was kept in an environment which was free of disease under controlled care. The zebrafish were maintained in an aquarium racking mechanism (ZebTEC, Italy) between 26-28°C. They were fed with commercial powdered fish meal twice a day, mixed with live saltwater shrimp. All studies were conducted in 0.018 mg/L sea salt solution which was prepared with reverse osmosis water (Instant Ocean™, USA). For all experiments, reverse osmosis water supplemented with 0.018 mg/L sea salt (Instant Ocean™, USA) was used. After natural breeding, fertilized embryos were obtained, cultured, and classified based on development time and characteristic morphology using a Zeiss Discovery V8 stereomicroscope (Germany) (14).

Experimental Design of Zebrafish Embryo Groups

Zebrafish embryos were divided into four groups as control, 3,4-Dichloroaniline (DCA, Fluka, Steinheim, Germany), one-day (1D) and seven-day incubation (7D) groups. No treatment was applied to the embryo medium of the control group. In the DCA group, 4mg DCA/L was added to the embryo medium. In the 1D incubation group, 3x3cm SF/AuNPs based nanofiber was, continuously shaken in the embryo medium for 24 hours, and in the 7D incubation group 3x3 cm SF/AuNPs based nanofiber was continuously shaken in the embryo medium for seven days. Embryos were exposed to four different embryo mediums and monitored for 72 hours post-fertilization (hpf).

Biochemical Analysis

Preparation of Zebrafish Embryos for Biochemical Analysis

Biochemical analyses were conducted on the zebrafish embryos. The embryos were produced as five biological replicates of zebrafish embryos (100 embryos/pool) through the use of 72 hours post-fertilization (hpf) zebrafish. One milliliter phosphate-buffered saline (PBS) was used to homogenize 100 embryos in each pool and then the pools were centrifuged. Biochemical analysis was performed using the supernatant.

Lipid Peroxidation and Nitric Oxide (NO) Levels

The Ledwozyw method was used to measure the level of malondialdehyde (MDA), which serves as a lipid peroxidation end product, using thiobarbituric acid reactive substances (15). The MDA level was presented as nmol MDA/mL.

The NO measurement was conducted using the Miranda et al. method (16). In the NO determination, vanadium (III) chloride was used to reduce nitrate to nitrite. Under acidic conditions, the nitrite produced reacts with sulfonyl amide and N-(1-naphthyl) ethylenediamine dihydrochloride, forming a complex diazonium compound. The intensity of the resulting complex was measured at 540nm. The results were presented as $\mu\text{mol NO/mL}$.

Superoxide Dismutase (SOD) and Glutathione-S-Transferase (GST) Activities

The SOD activity was measured with a method that consist on the potential of SOD to enhance the effects of riboflavin-sensitized photooxidation of o-dianisidine. The resulting product's absorbance was determined at 460nm. The net absorbance was calculated by comparing the absorbance values at zero and eight minutes of illumination. The SOD activity was presented as U/mL (17).

The GST activity was measured using the Habig et al. method. The absorbance of the formed product was detected at 340nm wavelength using a spectrophotometer (18).

Statistical Analysis

One-way analysis of the variance (ANOVA) and post hoc Tukey's multiple comparison tests were used to analyze the differences between the groups using the Graph Pad 8 (GraphPad Software, La Jolla, CA, USA). $p < 0.05$ was considered significant.

RESULTS

Development, Mortality and Hatching Rates of the Embryos

The mortality rates of zebrafish embryos at 72 hpf were presented in Figure 1. The mortality rate was significantly increased in embryos exposed to DCA when compared to the control group. Mortality rates in the 1D and 7D exposure groups were not significantly changed when compared to the control group. The hatching rates of zebrafish embryos at 72 hpf are presented in Figure 2. There was no significance between the hatching rates of all groups.

Lipid Peroxidation and NO Levels

The MDA and NO levels significantly increased in all groups when compared to the control group (Figure 3). The MDA and NO levels of the 1D and 7D groups were significantly lower than the DCA group (Figure 3).

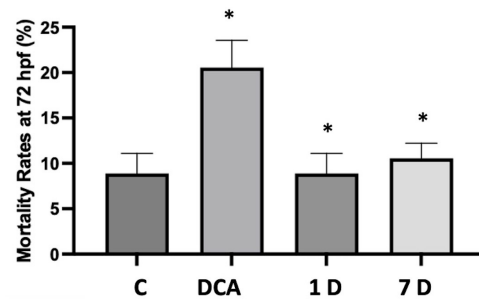


Figure 1. The mortality rates of zebrafish embryos exposed to DCA and also SF/AuNPs for 1 day (1D) and 7 days (7D) were measured at 72 hours post-fertilization (hpf).

C: Control

DCA: 3,4-Dichloroaniline

1D: Silk fibroin/gold nanoparticles treatment at day 1

7D: Silk fibroin/gold nanoparticles treatment at day 7.

* $p < 0.05$ significantly different from the control group (C).

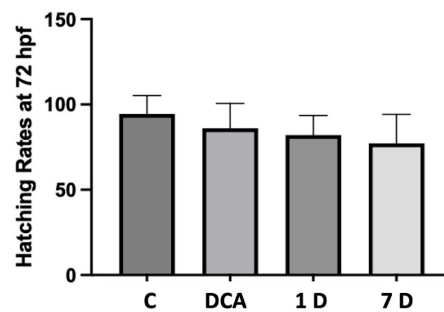


Figure 2. The hatching rates of zebrafish embryos exposed to DCA and also SF/AuNPs for 1 day (1D) and 7 days (7D) were measured at 72 hours post-fertilization (hpf).

C: Control

DCA: 3,4-Dichloroaniline

1D: Silk fibroin/gold nanoparticles treatment at day 1

7D: Silk fibroin/gold nanoparticles treatment at day 7.

SOD and GST Activities

The SOD activity in all groups was lower than the control group (Figure 4). The GST activity was significantly decreased in the DCA and 1D groups when compared to the control group, while the 7D group showed similar GST activity to the control group (Figure 4).

Discussion

In health-related products, gold nanoparticles and SF-based products continue to generate great attention. However, since there are dilemmas related to products containing these substances in the studies, assessing the potential toxicity

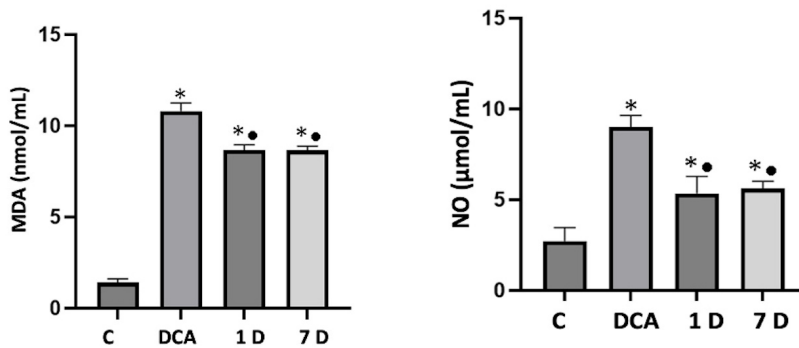


Figure 3. Malondialdehyde and nitric oxide levels of zebrafish embryos at 72 hpf.

C: Control

DCA: 3,4-Dichloroaniline

1D: Silk fibroin/gold nanoparticles treatment at day 1

7D: Silk fibroin/gold nanoparticles treatment at day 7 * p < 0.05 significantly different from the control group, • p < 0.05 significantly different from the DCA group

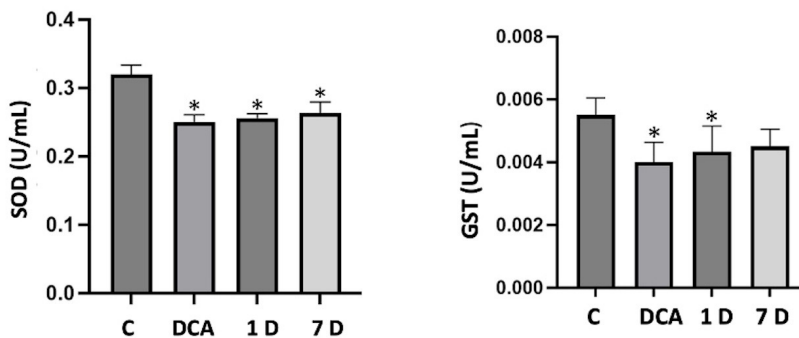


Figure 4. Superoxide dismutase and glutathione-S-transferase activities of zebrafish embryos at 72 hpf.

C: Control

DCA: 3,4-Dichloroaniline

1D: Silk fibroin/gold nanoparticles treatment at day 1

7D: Silk fibroin/gold nanoparticles treatment at day 7 * p < 0.05 significantly different from the control group.

of the SF/AuNPs-based hybrid nanofiber was necessary. Therefore, this study demonstrated the possible toxic and oxidant-antioxidant effects of SF/AuNPs-based nanofibrous membranes. According to the results of this study, the SF/AuNPs-based nanofibers had a nontoxic effect on zebrafish embryos and promoted the healthy development of zebrafish embryos compared to the DCA exposed zebrafish embryos as positive control. Higher hatching rates and lower mortality rates were observed in groups treated with SF/AuNPs-based nanofiber when compared to the DCA-exposed zebrafish embryos. It was revealed that gold nanoparticles do not exhibit any toxicity to zebrafish embryos when compared

to other nanoparticles like silver, copper, and platinum (19). However, there is no research on how gold nanoparticles affect the zebrafish embryos when they form a hybrid with SF. The toxicity of SF/AuNPs hybrid nanofibers depend on several factors, including the characteristics of the nanoparticles, their concentration, exposure duration, and the specific biological system under consideration. While SF is generally considered biocompatible, the addition of gold nanoparticles could potentially introduce new properties and interactions that may affect the toxicity (20).

Exposure to SF/AuNPs-based nanofiber increased lipid peroxidation in the embryos. Under certain conditions, gold

nanoparticles may release and could contribute to oxidative damage. They could induce the generation of reactive oxygen. Excessive production of reactive oxygen species production disrupts the oxidant-antioxidant balance and leads to oxidative stress. The release of gold ions depends on factors such as pH, temperature, and exposure duration (21, 22). In this study, the increased lipid peroxidation level and decreased SOD and GST activities in the zebrafish embryos could be related to the gold nanoparticles released from the hybrid nanofiber. NO is another reactive oxygen species, and the current study found that embryonic NO levels increased in response to DCA and nanofibrous membranes (23). NO is a highly reactive physiological molecule that has been revealed to play a vital function in controlling pre-implantation embryo development (24). Gouge et al. revealed the need for NO in embryos before implantation and suggests that it may play a function in controlling mitosis in them (25). The present findings show that DCA and nanofibrous membrane resulted in higher NO generation in 72 hpf embryos when compared to the control group but this increase in the NO level did not affect the hatching and mortality rate of the zebrafish embryos. The oxidant effect of the SF/AuNPs nanofiber membrane exposed embryo medium showed that gold nanoparticles were released into the medium. This oxidant effect of the membrane could contribute to killing the bacteria by adhering to their surface and could cause oxidant damage to bacteria when used as a wound-healing material. This confirmed that the membrane produced in this study could have antibacterial properties. The dimension, shape, charge, and coating of the surface of gold nanoparticles released to the embryo medium could also influence their oxidant-antioxidant balance (26). The size of the gold nanoparticles that were used in this study was approximately 20 nm. Smaller nanoparticles, especially those below ten nanometers, have greater potential for cellular uptake and interaction and could alter the behavior of gold nanoparticles (27).

In conclusion, while SF is considered biocompatible, the addition of gold nanoparticles introduces a new component that could have an oxidant and therefore antibacterial effect on the hybrid nanofibers. Therefore, a careful evaluation of the specific hybrid nanofiber formulation is necessary to assess its safety and potential toxicity in the intended application.

Ethics Committee Approval: According to the legal regulations in the European Union and in our country, ethical committee approval is not required for the use of embryos and larvae in studies involving zebrafish during the first 120 hours of post-fertilization development. In this study, the research was terminated at 72 hours post-fertilization.

Authors' Contributions: Conception/Design of Study – O.O., T.T.A., E.E.A.; Data Acquisition – E.E.A., I.U., O.O., E.T.; Data Analysis/ Interpretation – T.T.A., E.E.A.; Drafting Manuscript– T.T.A., O.O; Final Approval and Accountability– T.T.A., E.E.A.

Conflicts of Interest: The authors declare no conflict of interest.

Financial Disclosure: This study was funded by a grant from Marmara University Scientific Research Project Department (Project ID: TDK-2022-10384).

REFERENCES

1. Kamoun EA, Loutfy SA, Hussein Y, Kenawy E-RS. Recent advances in PVA-polysaccharide based hydrogels and electrospun nanofibers in biomedical applications: A review. *Int J Biol Macromol* 2021; 187: 755-68.
2. Vidya M, Rajagopal S. Silk fibroin: a promising tool for wound healing and skin regeneration. *Int J Polym Sci* 2021; 2021: 1-10.
3. Unger R, Peters K, Wolf M, Motta A, Migliaresi C, Kirkpatrick C. Endothelialization of a non-woven silk fibroin net for use in tissue engineering: growth and gene regulation of human endothelial cells. *Biomaterials* 2004; 25(21): 5137-46.
4. Tomeh MA, Hadianamrei R, Zhao X. Silk fibroin as a functional biomaterial for drug and gene delivery. *Pharmaceutics* 2019; 11(10): 494.
5. Nguyen TP, Nguyen QV, Nguyen VH, Le TH, Huynh VQN, Vo DVN, et al. Silk fibroin-based biomaterials for biomedical applications: A review. *Polymers* 2019; 11(12): 1933.
6. Huang K, Jinzhong Z, Zhu T, Morsi Y, Aldalbahi A, El-Newehy M, et al. Exploration of the antibacterial and wound healing potential of a PLGA/silk fibroin-based electrospun membrane loaded with zinc oxide nanoparticles. *J Mater Chem B* 2021; 9(5): 1452-65.
7. Jia L, Guo L, Zhu J, Ma Y. Stability and cytocompatibility of silk fibroin-capped gold nanoparticles. *Mat Sci Eng C* 2014; 43: 231-6.
8. Alkilany AM, Lohse SE, Murphy CJ. The Gold standard: gold nanoparticle libraries To understand the nano-bio interface. *Acc Chem Res* 2013; 46(3): 650-61.
9. Shrivastava R, Kushwaha P, Bhutia YC, Flora S. Oxidative stress following exposure to silver and gold nanoparticles in mice. *Toxicol Ind Health* 2016; 32(8): 1391-404.
10. Ahmad T, Iqbal J, Bustam MA, Irfan M, Asghar HMA. A critical review on phytosynthesis of gold nanoparticles: Issues, challenges and future perspectives. *J Clean Prod* 2021; 309: 127460.
11. Rahman A, Chowdhury MA, Hossain N. Green synthesis of hybrid nanoparticles for biomedical applications: A review. *Appl Surf Sci* 2022; 11: 100296.
12. Zhu J, Zhang Y, Shao H, Hu X. Electrospinning and rheology of regenerated Bombyx mori silk fibroin aqueous solutions: The effects of pH and concentration. *Polymer* 2008; 49(12): 2880-5.
13. Sharma R, Gulati S, Mehta S. Preparation of gold nanoparticles using tea: A green chemistry experiment. *J Chem Educ* 2012; 89(10): 1316-8.
14. Karaman GE, Ünal İ, Beler M, Üstündağ FD, Cansız D, Üstündağ ÜV, et al. Toothpastes for children and their detergent contents affect molecular mechanisms of odontogenesis in zebrafish embryos. *Drug Chem Toxicol* 2022: 1-11.
15. Ledwozyw A, Michalak J, Stepień A, Kadziolka A. The relationship between plasma triglycerides, cholesterol, total lipids and lipid peroxidation products during human atherosclerosis. *Clin Chim Acta* 1986; 155(3): 275-83.
16. Miranda KM, Espey MG, Wink DA. A rapid, simple spectrophotometric method for simultaneous detection of nitrate and nitrite. *Nitric Oxide* 2001; 5(1): 62-71.

17. Mylroie AA, Collins H, Umbles C, Kyle J. Erythrocyte superoxide dismutase activity and other parameters of copper status in rats ingesting lead acetate. *Toxicol Appl Pharmacol* 1986; 82(3): 512-20.
18. Habig WH, Jakoby WB. Assays for differentiation of glutathione S-Transferases. *Methods Enzymol* 1981; 77: 398-405.
19. Machado S, González-Ballesteros N, Gonçalves A, Magalhães L, Sárria Pereira de Passos M, Rodríguez-Argüelles MC, et al. Toxicity in vitro and in zebrafish embryonic development of gold nanoparticles biosynthesized using cystoseira macroalgae extracts. *Int J Nanomed* 2021; 16: 5017-36.
20. Xu Z, Shi L, Yang M, Zhu L. Preparation and biomedical applications of silk fibroin-nanoparticles composites with enhanced properties-a review. *Mater Sci Eng C Mater Biol Appl* 2019; 95: 302-11
21. Sani A, Cao C, Cui D. Toxicity of gold nanoparticles (AuNPs): A review. *Biochem Biophys Rep* 2021; 26: 100991
22. Abdal Dayem A, Hossain MK, Lee SB, Kim K, Saha SK, Yang G-M, et al. The role of reactive oxygen species (ROS) in the biological activities of metallic nanoparticles. *Int J Mol Sci* 2017; 18(1): 120.
23. Espey MG, Miranda KM, Thomas DD, Xavier S, Citrin D, Vitek MP, et al. A chemical perspective on the interplay between NO, reactive oxygen species, and reactive nitrogen oxide species. *Ann N Y Acad Sci* 2002; 962(1): 195-206.
24. Pourova J, Kottova M, Voprsalova M, Pour M. Reactive oxygen and nitrogen species in normal physiological processes. *Acta Physiol* 2010; 198(1): 15-35.
25. Thaler CD, Epel D. Nitric oxide in oocyte maturation, ovulation, fertilization, cleavage and implantation: a little dab'll do ya. *Curr Pharm Des* 2003; 9(5): 399-409.
26. Sen GT, Ozkemahli G, Shahbazi R, Erkekoglu P, Ulubayram K, Kocer-Gumusel B. The effects of polymer coating of gold nanoparticles on oxidative stress and DNA damage. *Int J Toxicol* 2020; 39(4): 328-40.
27. Huefner A, Septiadi D, Wilts BD, Patel, II, Kuan WL, Fragniere A, et al. Gold nanoparticles explore cells: cellular uptake and their use as intracellular probes. *Methods* 2014; 68(2): 354-63.

In vitro Antileishmanial Activity of *Lavandula angustifolia* Essential Oil on *Leishmania infantum* Parasites

Zeynep Islek^{1,2} , Fikrettin Sahin¹ 

¹Department of Genetics and Bioengineering, Faculty of Engineering, Yeditepe University, Istanbul, Turkiye

²Department of Pharmaceutical Technology, Faculty of Pharmacy, Istanbul Health and Technology University, Istanbul, Turkiye

ORCID ID: Z.I. 0000-0003-4789-9095; F.S. 0000-0003-1503-5567

Cite this article as: Islek Z, Sahin F. *In vitro* antileishmanial activity of *Lavandula angustifolia* essential oil on *Leishmania infantum* parasites. Experimed 2023; 13(2): 115-120.

ABSTRACT

Objective: Leishmaniasis is an endemic tropical disease that is disseminated through the bite of a sandfly infected with *Leishmania* parasites. Conventional antileishmanial drugs are mainly toxic and can be ineffective; therefore, there is a need for new natural drug candidates. This study investigated the antileishmanial effects of *Lavandula angustifolia* (LA) essential oil on *Leishmania infantum* (*L. infantum*) parasites, and the safety features were tested on RAW264.7 murine macrophages.

Materials and Methods: LA essential oil was produced through the process of hydro-distillation, and its phytochemical content was determined using the gas chromatography-mass spectrometry (GC-MS) analysis. The antileishmanial effects of LA (0.063 to 1 μ L/mL) on *L. infantum* parasites as well as their safety features were assessed on RAW264.7 murine macrophages.

Results: The composition of LA essential oil was detected using GC-MS analysis, including linalool, pinene, 1, 8-cineole, linalyl acetate, and lavandulol. Concentrations at and above 0.5 μ L/mL LA indicated a significant reduction (71% decrease) in the parasite proliferation, and caused a slight reduction in macrophage viability to 70% at 72 h.

Conclusions: The findings revealed the antileishmanial effect of LA on *L. infantum* parasites with relatively less toxicity on macrophages. The promising antileishmanial efficacy highlights the potential for further *in vivo* studies.

Keywords: Antileishmanial therapy, *Lavandula angustifolia*, *Leishmania infantum*, macrophages

INTRODUCTION

Leishmaniasis is a parasitic disease widespread in tropical regions, caused by protozoan parasites classified under the genus *Leishmania*. It significantly affects millions of individuals globally, particularly in developing countries, and is transmitted via the bite of phlebotomine sandflies. More than 20 different *Leishmania* species exhibit the ability to survive as either promastigotes (extracellular form) within sandflies or amastigotes (intracellular form) inside mammalian macrophages (1). According to a report by the World Health Organization in 2018, leishmaniasis is widespread in 98 tropical countries, thereby posing a significant threat to more than 600,000 individuals (2).

There is an annual occurrence of around 1.3 million new cases of leishmaniasis, which manifest in three clinically different forms, including visceral Leishmaniasis, which is generally known as "Kala Azar" and can lead to mortality, if not treated.

The current treatment options available for Leishmaniasis have been reported to contain pentavalent antimonials, conventional amphotericin B (AmpB) deoxycholate, miltefosine, paromomycin, AmpB micelles (Fungizone), and liposomal AmpB (AmBisome) (3–9). However, therapeutic interventions have certain limitations associated with these therapies, such as restricted efficacy against parasites (10), numerous adverse effects owing to low therapeutic

Corresponding Author: Fikrettin Sahin **E-mail:** fsahin@yeditepe.edu.tr

Submitted: 24.05.2023 **Revision Requested:** 14.06.2023 **Last Revision Received:** 14.06.2023 **Accepted:** 23.06.2023 **Published Online:** 04.08.2023



Content of this journal is licensed under a Creative Commons Attribution-NonCommercial 4.0 International License.

index (11), the need for cautious and gradual intravenous administration (e.g. AmpB) (12), and the emergence of drug resistance against the therapy (3, 5, 7, 13– 17). Therefore, there is a need for new drugs with fewer side effects and higher efficacy.

In recent years, researchers have turned their attention to natural products as potential candidates for new drugs (18– 24). The plant *Lavandula*, commonly referred to as lavender, has been utilized for its medicinal properties for centuries. Previous studies demonstrated that lavender exhibits diverse biological activities, including anti-protozoal effects against Leishmaniasis and other protozoan infections (19, 25, 26). Besides, the essential oils of *Lavandula angustifolia* (LA) and *Lavandula intermedia* were assessed for their anti-parasitic properties against protozoans, namely *Giardia duodenalis*, and *Trichomonas vaginalis*, as reported in a previous study (26). In another study, the antileishmanial effects of LA and *Rosmarinus (R.) officinalis* essential oils, as well as their nanoemulsions against *Leishmania major*, were examined by Shokri et al. (2017) (19). Upon treatment of *Leishmania* parasites with different species of lavender, several compounds were investigated in the composition of lavender, such as linalool and linalyl acetate, which displayed a potent antileishmanial activity. This has led to increased interest in exploring lavender as a potential source of new drugs for leishmaniasis.

In this study, LA essential oil (found in Turkish flora) was first obtained by hydro-distillation, and further composition of LA was detected by gas chromatography-mass spectrometry (GC-MS) analysis. Following the investigation of the plant composition, the antileishmanial effect of LA on the growth of *Leishmania infantum* (*L. infantum*) parasites was evaluated together with its safety properties on healthy murine RAW264.7 macrophages at different ranges of concentrations (0.063– 1 µL/mL). Cell culture studies, including cell viability, and morphology were conducted to evaluate the antileishmanial efficacy of LA essential oil.

MATERIALS AND METHODS

Materials

Resazurin sodium salt (R7017 - 1G) was purchased from Sigma-Aldrich, Germany. The flowering aerial tops of LA were collected from Yalova, Turkiye, in May 2022. The plant material was identified by Prof. Dr. Fikretin Sahin.

The Process of Obtaining LA Essential Oil Through Hydro-Distillation

A quantity of 200 grams of herbal material that had been dried and crushed was subjected to distillation with 2 liters of pure water for a duration of 3 h, utilizing a Clevenger-type apparatus.

GC-MS Analysis

The carrier gas in the experiment was helium, which was maintained at a consistent flow rate (1 mL/min). 1 µL sample was introduced into the system via injection. The temperature

program for the GC was established in the following manner: a hold at 50°C for 5 minutes, subsequently a ramp to 250°C at a rate of 5°C/minute, and a subsequent hold for 10 minutes. The transfer line for the mass spectrometer was maintained at 220°C. The mass range of 50 to 650 m/z was used in scan mode, and as a column, DB-Wax 60 m x 0.25mm ID x 0.25 µm was utilized.

Parasite Culture

The *L. infantum* (MHOM/MA/67/ITMAP-263) strain was obtained from Dr. Ana M. Tomás at the University of Porto, Portugal. The cultivation of *L. infantum* promastigotes was performed in RPMI 1640 Glutamax medium, which was supplemented with 10% (v/v) inactivated fetal bovine serum (iFBS), 50 U/mL penicillin, 50 µg/mL streptomycin, and 20 mM HEPES sodium salt at 25°C. The collection of promastigotes was carried out through centrifugation of the pellet at 3000 × g for 10 minutes.

Macrophage Culture

The RAW 264.7 murine macrophage cells (American Type Culture Collection TIB-71) were cultured in DMEM that was supplemented with 10% iFBS, 2 mM L-glutamine, and 100 Units/mL of penicillin and 100 µg/mL of streptomycin. The culture was maintained at a temperature of 37°C in a 5% CO₂. The cells were cultured through regular sub-passaging at 3-day intervals.

The Effect of LA on the Growth of *L. infantum* Promastigotes

The antileishmanial properties of LA essential oil against *L. infantum* were implemented using a resazurin assay, as introduced in Islek et al. (27). Briefly, promastigotes were cultured in 96-well plates at 3x10⁵ cells per well in a completed RPMI medium. The cells were subsequently treated with 0.063– 1 µL/mL of LA essential oil and incubated for 24, 48, and 72 h. Following incubations, the resazurin solution (2.5 mM) was put into each well at a concentration of 10% (v/v), and luminescence intensity was assessed using a UV-Vis spectrophotometer with

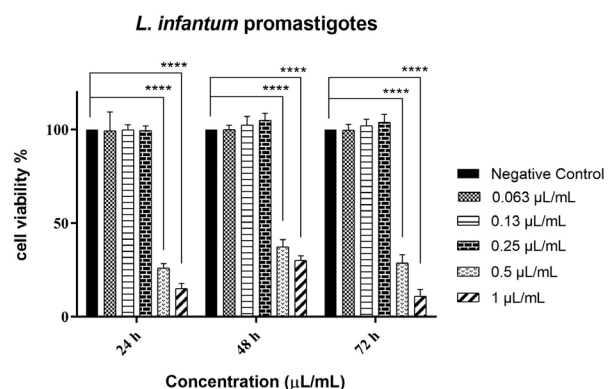


Figure 1. Effect of LA on the growth of *L. infantum* promastigotes. Viability of parasites following 24, 48, and 72 h of treatment with LA essential oil at various concentrations (0.063 to 1 µL/mL).

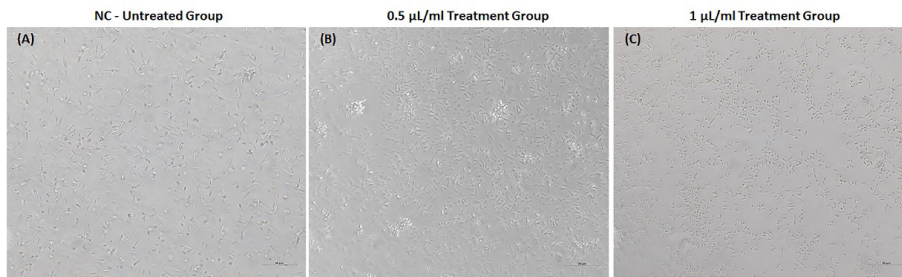


Figure 2. Phase-contrast microscopy images of (A) negative control (NC - untreated *L. infantum* promastigotes), (B) 0.5 µL/mL, and (C) 1 µL/mL LA essential oil treatment groups after 24 h of incubation. Bars correspond to 50 µm.

an excitation (560 nm) and an emission wavelength (590 nm). The viabilities (%) were determined relative to the negative control group, which was not subjected to any treatment. The data underwent analysis through the utilization of GraphPad Prism 8.01 software, following which the values for the 50% inhibitory concentration (IC_{50}) were determined.

Cell Viability Assay on Macrophages

RAW264.7 macrophages were treated with LA essential oil at varying concentrations (0.063 to 1 µL/mL), and viabilities were conducted through the utilization of the resazurin assay. Accordingly, the RAW264.7 cells were harvested in 96-well plates at 10,000 cells per well. Following 24h, the cells were incubated with various concentrations (0.063-1 µL/mL) of LA essential oil for 24, 48, and 72 h. After treatments, the cells were subjected to a 2-h incubation period in a 2.5 mM resazurin solution with a concentration of 10% (v/v), and then the luminescence intensity was assessed by an ultraviolet-visible (UV-Vis) spectrophotometer. The cell viability (%) was determined according to the negative control group. The data underwent analysis using GraphPad Prism 8.01 software.

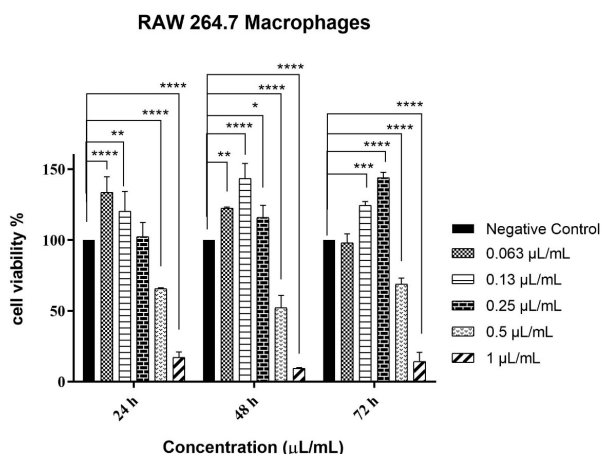


Figure 3. The viability analysis of RAW264.7 murine macrophages treated with LA essential oil at different concentrations (0.063-1 µL/mL) after 24, 48, and 72 h, compared to negative control.

Statistical Analysis

The statistical analysis was conducted utilizing GraphPad Prism Software (version 8.01). The study used statistical analysis by conducting a comparison of data sets using a two-way ANOVA, followed by Tukey's multiple comparison test. The statistical significance of the findings were assessed at different levels of probability, i.e. (*) $p \leq 0.05$, (**) $p \leq 0.01$, (***) $p \leq 0.001$, and (****) $p \leq 0.0001$.

RESULTS

GC-MS Analysis

The GC-MS technique was utilized to determine the phytochemical composition of LA essential oil. As presented in Table 1, linalool was found to be the predominant constituent of the lavender oil at 37%, and it was consistent with the European Pharmacopoeia, in which linalool content should range from 20.0% to 45.0%. In addition, 1,8-Cineole, camphor, and limonene were detected in the lavender oil as 13.8%, 12.7%, and 2.4%, respectively (Table 1), which was found above the criteria of European Pharmacopoeia, whereas 7.7% linalyl acetate was detected as below the criteria. However, the percentage of the 4-terpinol content was found at 3.7%, which was consistent with the value within the range from 1.0 to 8.0% given in the European Pharmacopoeia. Likewise, the content of lavandulol and α -terpineol in lavender oil was detected at 0.5% and 1.5%, respectively, which confirms the quality criteria of obtained lavender oil considering the European Pharmacopoeia (the criteria for lavandulol: min. 0.1%; α -terpineol: max. 2.5%). The chemical quality of the oil utilized was found to be above the specified limitation regarding to the high linalool content (i.e., 37%) (Table 1).

Cell Culture Studies

In vitro Antileishmanial Effect of the LA Essential Oil on *L. infantum* Parasites

The treatment groups of 0.5 and 1 µL/mL exhibited a dose and time-dependent inhibition of parasite proliferation. Treatment with 0.5 µL/mL LA essential oil significantly decreased promastigote viability to 26% ($p \leq 0.0001$) at 24 h, and became nearly 38% and

Table 1. Phytochemical composition and retention time (min) of the hydro-distilled LA essential oil using GC-MS analysis.

Retention index	Retention time (min)	Compounds	Area%
1027	7.98	α-pinene	1.5
1113	10.06	β-pinene	1.1
1212	12.63	limonene	2.4
1224	13.05	1,8-Cineole	13.8
1498	21.98	camphor	12.7
1548	22.51	linalool	37.0
1569	22.61	linalyl acetate	7.7
1593	24.00	4-terpineol	3.7
1679	25.65	lavandulol	0.5
1694	26.24	α-terpineol	1.5

29% at 48, and 72 h ($p \leq 0.0001$), respectively. Upon an increase in the concentration to 1 $\mu\text{L/mL}$, the viability of promastigotes exhibited a significant decrease to 15% (*i.e.*, 15.11%) after 24 h ($p \leq 0.0001$), and became nearly 30% (*i.e.*, 30.09%) and 11% (*i.e.*, 11.01%) at 48 h and 72 h, respectively, as depicted in Figure 1 ($p \leq 0.0001$). However, there was no significant further alteration in the inhibition of the promastigote proliferation at concentrations lower than 0.5 $\mu\text{L/mL}$.

The IC_{50} values were determined for LA essential oil following 24, 48, and 72 h of incubation, as $0.43 \pm 0.089 \mu\text{L/mL}$, $0.46 \pm 0.053 \mu\text{L/mL}$, and $0.47 \pm 0.033 \mu\text{L/mL}$, respectively. The findings demonstrated that 24, 48, and 72 h-incubation of LA essential oil exhibited efficacy against *L. infantum* promastigotes.

Effects of LA Essential Oil on Morphology of *L. infantum* Parasites

In parallel to the parasite viability, phase-contrast microscopy images suggested that treatments with 0.5 and 1 $\mu\text{L/mL}$ concentrations of LA essential oil indicated a dose-dependent reduction in the number of the parasite and transformation from elongated-shape to round-shaped morphologies at 24 h of incubation (Figure 2).

Cytotoxicity of LA Essential Oil on Macrophages

After conducting an *in vitro* assessment of the antileishmanial efficacy of LA essential oil on *L. infantum* promastigotes, the cytotoxicity was assessed on healthy murine RAW264.7 macrophages (Figure 3). As shown in Figure 3, when murine macrophages were treated with LA essential oil at concentrations $\leq 0.25 \mu\text{L/mL}$, cell viability of macrophages remained above 100%, and LA essential oil did not lead to toxicity on macrophages for 24, 48, and 72 h. Besides, the viability was increased to approximately 100%, 116% ($p \leq 0.05$), and 144% ($p \leq 0.0001$) following treatment with 0.25 $\mu\text{L/mL}$

LA essential oil for 24, 48, and 72 h, respectively. Conversely, upon increasing concentration to 0.5 $\mu\text{L/mL}$, the viability was decreased to 66% at 24 h, which became 52% and 70% at 48, and 72 h of incubation, compared to negative control ($p \leq 0.0001$; Figure 3). A minor recovery in cell viability was detected among 48- and 72-h of treatment as ranging from 52% to 70% of cell viability. However, when the macrophages were treated with 1 $\mu\text{L/mL}$ LA essential oil, the macrophage viability was decreased to below 17%, 10%, and 15% at 24, 48, and 72 h, respectively ($p \leq 0.0001$).

The results revealed that 0.5 $\mu\text{L/mL}$ concentration of LA essential oil indicated a significant antileishmanial effect on *L. infantum* parasite proliferation with relatively less toxicity on macrophages.

DISCUSSION

Leishmaniasis, a neglected disease, has affected a significant number of individuals globally and continues to pose significant challenges in terms of drug development. The complexity of the disease, including the difficulty of diagnosis, coupled with limited financial incentives for pharmaceutical companies, has hindered progress in finding effective treatments. Additionally, the available drugs suffer from drawbacks such as high toxicity, prolonged treatment durations, and emerging drug resistance. In contrast to synthetic pharmaceuticals, a greater abundance of natural drug resources exists, and the pursuit of novel drug discovery from natural products and traditional herbal medicine warrants serious consideration. In the present study, the plant-based, potential antileishmanial therapy was examined, such as LA, due to its high biocompatibility, natural properties, and low toxicity in RAW264.7 cells through mitochondrial respiration. In short, LA essential oil was examined by GC-MS

analysis to detect its composition, according to the European Pharmacopoeia, and following the GC-MS analysis, the cell culture studies, including the antileishmanial activity on *L. infantum*, and safety features of the compound on healthy macrophages were examined *in vitro* models.

Accordingly, the composition of LA essential oil was detected by the GC-MS technique, which was consistent with previous reports in the literature (19, 28). Linalool was found to be the main component of lavender oil (37%), which was linked to the characteristic compounds within the composition of LA essential oil, and consistent with the quality criteria of the European Pharmacopoeia (*i.e.*, 20.0 to 45.0%; Table 1). A previous study suggested that the presence of the key ingredients in lavender essential oil, such as linalool, and terpineol can enhance its penetration to the cell membrane (29, 30). Besides that, terpineol has the ability to bind to particular G protein-coupled receptors, leading to an impact on the cAMP and Ca²⁺ concentrations, thus enhancing the activation of corresponding kinases, and ultimately facilitating the manifestation of its biological activities. Antileishmanial efficacy could be linked to the regulation of the kinase domain of calcium-dependent protein kinases (CDPKs) through calcium ions, and CDPK1 exhibits a significant association with the adhesion and invasion processes of protozoons (29).

In the present study, according to the growth inhibition on *L. infantum* promastigotes, the IC₅₀ values were calculated for LA essential oil as 0.47±0.033 µL/mL at 72 h, and 0.5 and 1 µL/mL treatment groups exhibited a dose-dependent inhibition of parasite proliferation (Figure 1). Additionally, RAW264.7 macrophage cytotoxicity studies revealed relatively no observed toxicity toward the host cells at concentrations equal to the IC₅₀ concentrations (Figure 3). Similarly, Yao et al. (2021) stated the antiprotozoal activity of LA essential oil against *Toxoplasma gondii* as dose-dependent within safe concentration ranges, and furthermore, the viability was not significantly reduced by LA essential oil at a 4.48 mg/ml in human foreskin fibroblasts (29). Furthermore, LA, and their nanoemulsions were found to be significantly effective on *L. major* parasites compared to *R. officinalis* essential oils, and conventional pentavalent antileishmanial chemotherapeutic, meglumine antimoniate (19). *Lavender* and *Rosemary* essential oils indicated the activity of *L. major* promastigote with IC₅₀= 0.11 µL/mL, and IC₅₀= 0.26 µL/mL, respectively, after 72 h of incubation (19). In parallel to viability studies, phase-contrast microscopy images demonstrated that 0.5 and 1 µL/mL treatments groups of LA essential oil indicated a dose-dependent reduction in the number of the parasite and transformation from elongated-shape to round-shaped morphologies at 24 h of incubation (Figure 2). The observed inhibitory effect could potentially be attributed to the impact on the morphology of *L. infantum* parasites, associated with the loss of membrane and flagellum integrity, and apoptosis. Nevertheless, the precise mechanism through which essential oils act on *L. infantum* remains uncertain and necessitates further investigation.

CONCLUSION

In short, this study is the first statement on the antileishmanial activity of LA essential oil on *L. infantum* parasites. The present investigation provides preliminary studies of the traditional use of LA for antileishmanial therapy with *in vitro* cell culture analysis. The promising antileishmanial efficacy of lavender essential oil highlights the potential therapy in future *in vivo* studies.

Acknowledgments: We would like to thank Ezgi Taskan for her contribution to the cell viability studies.

Ethics Committee Approval: Ethics committee approval is not required because of no material or experimental animal that would require permission.

Authors' Contributions: Conception/Design of Study – F.S., Z.I.; Data Acquisition – F.S., Z.I.; Data Analysis/Interpretation – Z.I.; Drafting Manuscript– F.S., Z.I.; Critical Revision of Manuscript- F.S., Z.I.; Final Approval and Accountability– F.S., Z.I.

Conflicts of Interest: The authors did not disclose any potential conflicts of interest.

Financial Disclosure: This study was funded by the Department of Genetics and Bioengineering, Yeditepe University.

REFERENCES

1. Rodrigues V, Cordeiro-da-Silva A, Laforge M, Silvestre R, Estaquier J. Regulation of immunity during visceral Leishmania infection. *Parasit Vectors* 2016; 9: 118.
2. Leishmaniasis. [cited 2023 23 May]. Available from <https://www.who.int/news-room/fact-sheets/detail/leishmaniasis>.
3. Sundar S, Chatterjee M. Visceral leishmaniasis - Current therapeutic modalities. *Indian J Med Res* 2006; 123(3), 345–52.
4. Sundar S, Jha TK, Thakur CP, Engel J, Sindermann H, Fischer C, et al. Oral miltefosine for Indian visceral Leishmaniasis. *N Engl J Med* 2002; 347(22), 1739–46.
5. Shyam Sundar. *5 Journal Medicine. English J* 2002; 346(5): 305–10.
6. Köse Ş, Töz SÖ, Lu İCBĞ, Olut A, Korkmaz M, Özbel Y. Case Report : Treatment of Kala- Azar by Amphotericin B lipid complex (ABELCET®). *Türkiye Parazitoloji Dergisi* 2004; 28 (2): 126-8.
7. Murray HW, Berman JD, Davies CR, Saravia NG. Advances in leishmaniasis. *Lancet*. 2005; 366: 1561–77.
8. Tiunan TS, Santos AO, Ueda-Nakamura T, Filho BPD, Nakamura CV. Recent advances in leishmaniasis treatment. *Int J Infect Dis* 2011; 15(8): e525-e532.
9. Aronson N, Herwaldt BL, Libman M, Pearson R, Lopez-Velez R, Weina P, et al. Diagnosis and treatment of leishmaniasis: Clinical practice guidelines by the infectious diseases society of America (IDSA) and the American Society of tropical medicine and hygiene (ASTMH). *Am J Trop Med Hyg* 2017; 96(1): 24–45.
10. Gupta G, Oghumu S, Satoskar AR. Mechanisms of immune evasion in Leishmaniasis. In: *Advances in applied microbiology*. 2013. p. 155–84.
11. Sahar H. Al-Natour. Update in the treatment of cutaneous Leishmaniasis. *J Fam Community* 2009; 16(2): 41–7.
12. Freitas-Junior LH, Chatelain E, Kim HA, Siqueira-Neto JL. Visceral leishmaniasis treatment: What do we have, what do we need and how to deliver it? *Int J Parasitol Drugs Drug Resist* 2012; 2: 11-9.

13. Sundar S, Jha TK, Thakur CP, Mishra M, Singh VP, Buffels R. Single-dose liposomal amphotericin B in the treatment of visceral leishmaniasis in India: A multicenter study. *Clin Infect Dis* 2003; 37(6): 800–4.
14. Ouellette M, Drummel-Smith J, Papadopoulou B. Leishmaniasis: Drugs in the clinic, resistance and new developments. *Drug Resist Updat* 2004; 7(4-5): 257–66.
15. Croft SL, Sundar S, Fairlamb AH. Drug resistance in leishmaniasis. *Clin Microbiol Rev* 2006; 19(1): 111–26.
16. Gupta S, Dube A, Vyas SP. Antileishmanial efficacy of amphotericin B bearing emulsomes against experimental visceral leishmaniasis. *J Drug Target* 2007; 15(6): 437–44.
17. Natera S, Machuca C, Padrón-Nieves M, Romero A, Díaz E, Ponte-Sucre A. *Leishmania* spp.: Proficiency of drug-resistant parasites. *Int J Antimicrob Agents* 2007; 29(6): 637–42.
18. Cavanagh HMA, Wilkinson JM. Biological activities of lavender essential oil. *Phytother Res* 2002; 16(4): 301–8.
19. Shokri A, Saeedi M, Fakhar M, Morteza-Semnani K, Keighobadi M, Hosseini Teshnizi S, et al. Antileishmanial activity of *lavandula angustifolia* and *rosmarinus officinalis* essential oils and nano-emulsions on *leishmania major* (MRHO/IR/75/ER). *Iran J Parasitol* 2017; 12(4): 622–31.
20. Sen R, Chatterjee M. Plant derived therapeutics for the treatment of Leishmaniasis. *Phytomedicine* 2011; 18(12): 1056–69.
21. Soosaraei M, Fakhar M, Hosseini Teshnizi S, Ziaei Hezarjaribi H, Banimostafavi ES. Medicinal plants with promising antileishmanial activity in Iran: A systematic review and meta- analysis. *Ann Med Surg (Lond)* 2017; 21: 63–80.
22. Bahmani M, Saki K, Ezatpour B, Shahsavari S, Eftekhari Z, Jelodari M, et al. Leishmaniosis phytotherapy: Review of plants used in Iranian traditional medicine on Leishmaniasis. *Asian Pac J Trop Biomed* 2015; 5(9): 695-701.
23. Atay I, Kirmizibekmez H, Kaiser M, Akaydin G, Yesilada E, Tasdemir D. Evaluation of in vitro antiprotozoal activity of *Ajuga laxmannii* and its secondary metabolites. *Pharm Biol* 2016; 54(9): 1808–14.
24. Cha JD, Jeong MR, Choi HJ, Jeong S II, Moon SE, Yun S II, et al. Chemical composition and antimicrobial activity of the essential oil of *Artemisia lavandulaefolia*. *Planta Med* 2005; 71(6): 575–7.
25. Sharifi-Rad J, Sureda A, Tenore GC, Daglia M, Sharifi-Rad M, Valussi M, et al. Biological activities of essential oils: From plant chemoeology to traditional healing systems. *Molecules* 2017; 22(1): 70.
26. Moon T, Wilkinson JM, Cavanagh HMA. Antiparasitic activity of two *Lavandula* essential oils against *Giardia duodenalis*, *Trichomonas vaginalis* and *Hexamita inflata*. *Parasitol Res* 2006; 99(6): 722–8.
27. Islek Z, Ucisik MH, Keskin E, Sucu BO, Gomes-Alves AG, Tomás AM, et al. Antileishmanial Activity of BNIPDaoct- and BNIPDanon-loaded Emulsomes on *Leishmania infantum* Parasites. *Front Nanotechnol* 2022; 3: 773741.
28. Hsouna A Ben, Hamdi N. Phytochemical composition and antimicrobial activities of the essential oils and organic extracts from *pelargonium graveolens* growing in Tunisia. *Lipids Health Dis* 2012; 11, 167.
29. Yao N, He JK, Pan M, Hou ZF, Xu JJ, Yang Y, et al. In vitro evaluation of *lavandula angustifolia* essential oil on anti-toxoplasma activity. *Front Cell Infect Microbiol* 2021; 11: 755715.
30. Mantovani ALL, Vieira GPG, Cunha WR, Groppo M, Santos RA, Rodrigues V, et al. Chemical composition, antischistosomal and cytotoxic effects of the essential oil of *Lavandula angustifolia* grown in Southeastern Brazil. *Rev Bras Farmacogn* 2013; 23(6): 877-84.

Cryptotanshinone Protects Against Acute Pulmonary Edema

Umit Yilmaz¹ , Mehmet Demir¹ 

¹Department of Physiology, Faculty of Medicine, Karabuk University, Karabuk, Turkiye

ORCID ID: U.Y. 0000-0003-0248-3483; M.D. 0000-0001-6990-3337

Cite this article as: Yilmaz U, Demir M. Cryptotanshinone protects against acute pulmonary edema. *Experimed* 2023; 13(2): 121-126.

ABSTRACT

Objective: Cryptotanshinone (CTS) is a compound with anti-inflammatory, anti-bacterial, anti-oxidative and anti-aggregant functions. We aimed to determine the effects of CTS on α -naphthylthiourea (ANTU)-induced acute pulmonary edema.

Materials and Methods: In this study, 4 groups (control, sham, ANTU and ANTU+CTS) were established from a total of 40 rats. The ANTU+CTS group received intraperitoneal CTS for seven days, and both ANTU and ANTU+CTS received an ANTU administration for the induction of peripheral effusion. Four hours after the ANTU administration, the rats were subjected to a forced swim test and were decapitated. Swimming times of rats, amount of pleural effusion (PE), lung weight (LW)/body weight (BW), and PE/BW ratios were determined.

Results: At the end of the experiment, PE was not detected in the lungs of control and sham group rats. It was determined that PE, LW/BW and PE/BW were significantly decreased, while swimming time was increased after acute pulmonary edema in the CTS group ($p < 0.05$).

Conclusion: CTS showed a protective effect against acute pulmonary edema, which indicates that it may be used as a new therapeutic agent against pulmonary toxicity.

Keywords: Cryptotanshinone; α -naphthylthiourea, pulmonary edema, pleural effusion, swimming duration

INTRODUCTION

Pleural diseases are extremely common today, affecting 3000 people out of every 1 million people annually. Pleural effusions (PE) constitute an important part of pleural diseases (1). It has been reported that approximately 90% of PE, which constitute an important part of pleural diseases, occur due to congestive heart failure, pneumonia, malignancy, and pulmonary embolism (2). Pulmonary edema occurs as a result of high pressure in the pulmonary microcirculation or an increase in the permeability of the alveolar-capillary barrier, or a combination of both (3). Pulmonary edema is an imbalance between the formation and reabsorption of lung tissue fluid, leading to massive tissue fluid reabsorption by pulmonary lymphatic and venous vessels insufficiency. Pulmonary edema can also be defined as abnormal fluid accumulation in the

extravascular parts of the lung (4). Pulmonary edema is divided into two subgroups as cardiogenic and non-cardiogenic (5). Non-cardiogenic pulmonary edema occurs with increased alveolocapillary permeability as a direct or indirect result of a pathological process (multiple trauma, septic shock, influenza pneumonia, aspiration syndrome) (6). Cardiogenic pulmonary edema is characterized by increased secondary hydrostatic capillary pressure due to increased pulmonary venous pressure (7). Cardiogenic pulmonary edema leads to acute respiratory failure and has a high mortality rate (8).

Cryptotanshinone (CTS) is a lipophilic compound derived from the roots of the plant species *Salvia miltiorrhiza*, which is used in the treatment of cardiovascular diseases, hepatitis, diabetes, and chronic liver failure in China (9). This compound, which has the potential to prevent many

Corresponding Author: Umit Yilmaz **E-mail:** umityilmaz@karabuk.edu.tr

Submitted: 02.06.2023 **Revision Requested:** 06.07.2023 **Last Revision Received:** 06.07.2023 **Accepted:** 11.07.2023 **Published Online:** 04.08.2023



Content of this journal is licensed under a Creative Commons Attribution-NonCommercial 4.0 International License.

diseases, also has anti-inflammatory, antibacterial, anticancer, antioxidative and antiaggregant effects (10-13). The important therapeutic effects of CTS in the treatment of angiogenesis-related diseases by inhibiting endothelial cell proliferation have been emphasized (14). CTS shows antipermeability and antiangiogenic effects, as well as anti-inflammatory properties, in interaction with other cytokines and chemokines (15). It has been suggested that since CTS alleviates pulmonary fibrosis (16), it is a promising drug candidate for the treatment of fibrotic pulmonary diseases (17). In addition, inhalation of CTS is a safe and effective treatment strategy for chronic pulmonary fibrosis. (18). Although CTS has anti-inflammatory effects against acute lung injury, it also has therapeutic effects (19). Moreover, it can efficiently protect pulmonary function and decrease early pulmonary inflammation infiltration in radiation-induced lung injury, and it was found to be more effective than prednisone in alleviating pulmonary fibrosis (20).

For the identification of new therapeutic agents in the treatment of pulmonary edema, the α -naphthylthiourea (ANTU)-induced pulmonary edema model is the most widely used and most similar to the clinicopathological features of pulmonary edema in humans (21). ANTU, a chemical compound derived from thiourea, was first used as a rodenticide, and it causes an increase in pulmonary vascular permeability in the rat, leading to the development of pulmonary edema (22).

To date, several antioxidants have been used as an alternative treatment for the cure of various diseases, including pulmonary edema. The potential of numerous flavonoids isolated from natural sources has been demonstrated against various lung diseases. However, the protective effect of CTS, which is a strong antioxidant substance against acute pulmonary edema, has not been studied so far.

We aimed to determine the effects of CTS on the amount of PE, lung weight (LW)/body weight (BW), and PE/BW ratios and forced swim test time in the lungs of rats with acute pulmonary edema with ANTU.

MATERIALS AND METHODS

The study was performed with the approval of the Karabuk University Medical Faculty Experimental Animals Ethics Committee (Date: 04/10/2022, Decision number: 2022/09/15, Registration number: E-55212866-050.99-174960). A total of 40 male Wistar Albino rats with an average weight of 200-240 grams were included in the study. During the study, the rats were housed in a 12-hour light/12-hour dark cycle and a temperature of $21\pm 2^\circ\text{C}$. The animals were fed *ad libitum* with standard rat pellet feed produced for experimental animals and were given tap water.

Experimental Groups and Experimental Design

Before the experimental stages, all the rats were weighted, and experimental groups were formed from those whose body weights were closest to each other. Experimental groups: They

were randomly divided into 4 groups as control, sham, ANTU and ANTU+CTS (n=10, for each group).

Control: Rats of this group were given CTS solvent (saline containing 1% Tween 80) in a volume of CTS for 7 days from day 1 of the study.

Sham: The rats in this group were given a single intraperitoneal ANTU solvent (olive oil) (Sigma-Aldrich, USA) dose volume of ANTU on the 7th day of the study.

ANTU: The rats of this group were injected with a single dose of ANTU intraperitoneal at a dose of 10 mg/kg dissolved in olive oil (4 mg/mL) on the 7th day of the study.

ANTU+CTS: The rats of this group were administered CTS (10 mg/kg) (Sigma-Aldrich, USA) dissolved in saline containing 1% Tween 80 for 7 days from the 1st day of the study (23-25). Again, the rats in this group were injected with ANTU on the 7th day of the study.

Establishment of Experimental Lung Edema Model with ANTU

Severe pulmonary edema and lung damage were observed in rats injected with ANTU within 4 hours. As a result of this damage, PE formation, LW/BW and PE/BW ratios were found to be increased. Floatation exercises were performed on the rats 4 hours after the ANTU injection.

Forced Swim Test

The forced swim test is commonly used to evaluate fatigue behavior in animal experiments. The pulmonary edema and effusion we created experimentally lead to fatigue and respiratory failure because of the decreased oxygenation capacity and lung compliance of the lungs of rats. The forced swim test was utilized to evaluate the effect of CTS on induced PE.

For the rats to get used to the pool, they were allowed to swim free for 15 minutes the day before the experiment and were dried and returned to their cages. After seven days of CTS and solvent injections, on the 7th day of the experiment (4 hours after the ANTU injection), the rats were subjected to a forced swim test in a plastic pool (90 cm \times 45 cm \times 45 cm) filled with room temperature water. In this test, the depth of the water should have been sufficient to prevent the animals from touching the floor of the pool with their tails. The swimming period was taken as the duration spent by the rats swimming until they exhausted their strength and started struggling. The end point of the strenuous swimming time was accepted as the point where the nose of the rats remained below the water surface for 10 seconds. When obvious signs of fatigue appeared, the animals were removed from the pool, and returned to their cages (26).

Termination of Experiment

Following the swimming exercises, the rats were euthanized by taking blood from the abdominal aorta under anesthesia (intraperitoneal ketamine/xylazine (100 mg/kg / 5 mg/kg). The thorax was opened very carefully, and utmost care was taken not to make the surrounding tissues bleed and not to contaminate the effusion fluid with blood. The effusion fluid was collected from the pleural space with a syringe, and the lungs were carefully isolated and cleaned from the surrounding tissues. The removed lungs were weighed on a precision scale. The amount of PE, LW/BW, and PE/BW ratios were calculated.

Statistical Analyses

Statistical analyses were performed with IBM SPSS 25.0 program. The normal distribution was determined with the Shapiro Wilk test. When the data of the groups did not show normal distribution, the difference between the groups was evaluated with the Kruskal Wallis H test. When statistical significance was detected between groups, multiple/pair comparisons were analyzed with the Bonferroni correction-Mann Whitney U test. $p < 0.05$ was considered significant.

RESULTS

Effect of CTS on PE

It was detected that there was no PE in the lungs of the rats in the control and sham groups, when the study was terminated, and the thorax of rats were opened. Non-hemorrhagic PE with exudate characteristics was determined in the lungs of rats in the ANTU and ANTU+CTS groups. When the pleural effusions of groups were compared; it was determined that the amount of pleural fluid in the ANTU (4.1 ± 0.5 mL) group and ANTU+CTS

(1.8 ± 0.4 mL) groups were statistically significantly higher than in the control and sham groups ($p < 0.05$). In addition, when the ANTU group and ANTU+CTS groups were compared, it was found that the pleural fluid of the ANTU+CTS group was statistically reduced compared to the ANTU group ($p < 0.05$) (Figure 1). It can be said that CTS provides protection against the formation of PE.

Effect of CTS on PE/BW $\times 10^4$

When the PE/BW ratios of the groups were compared; the PE/BW ratio of the ANTU (144.9 ± 3.8) and ANTU+CTS (83.6 ± 1.8) groups was statistically significantly higher than the control and sham groups ($p < 0.05$). However, when ANTU and ANTU+CTS groups were compared in terms of PE/BW ratio, it was determined that CTS statistically significantly reduced the PE/BW weight ratio ($p < 0.05$) (Figure 2).

Effect of CTS on LW/BW $\times 10^4$

By the end of the experiment, when the LW/BW ratios of the groups were compared; the LW/BW ratio of the ANTU (93.6 ± 9.4) and ANTU+CTS (79.7 ± 3.8) groups was statistically significantly higher than the control (47.7 ± 2.6) and sham (46.3 ± 2.4) groups ($p < 0.05$), while it was statistically lower in the ANTU+CTS group than ANTU ($p < 0.05$) (Figure 3).

Effect of CTS on Swimming Time

On the seventh day of the experiment, four hours after ANTU was given to ANTU and ANTU+CTS groups, all experimental groups were given a swimming test. Regarding the swimming times of the groups; it was statistically significantly lower in ANTU (18.8 ± 6.9) and ANTU+CTS (30.2 ± 5.8) than in the control (50.2 ± 5.1) and sham (48.4 ± 4.9) groups ($p < 0.05$). Moreover, the swimming time of the ANTU+CTS group was statistically

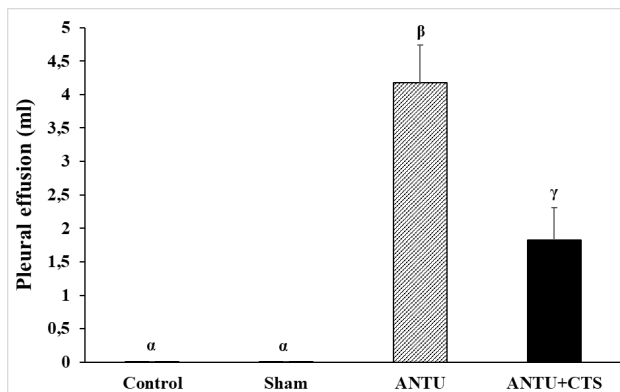


Figure 1. Effect of CTS on PE.

α : There was no significance between the control and sham groups.

β : The ANTU group is significantly higher than the control and sham groups.

γ : The ANTU+CTS group was significantly reduced compared to the ANTU group.

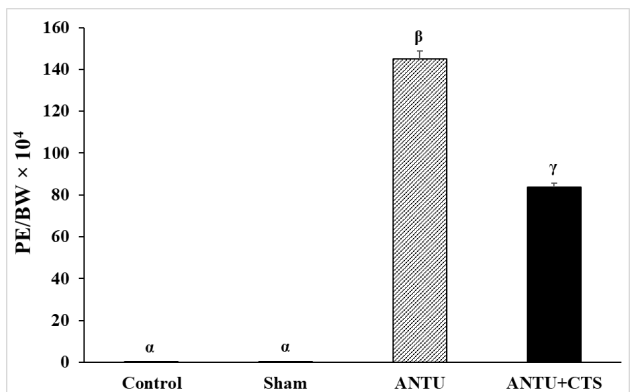


Figure 2. Effect of CTS on PE/BW $\times 10^4$.

α : There was no significance between the control and sham groups.

β : The ANTU group is significantly higher than the control and sham groups.

γ : The ANTU+CTS group was significantly reduced compared to the ANTU group.

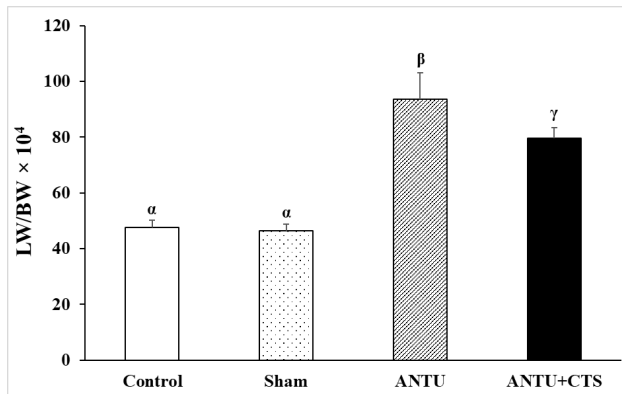


Figure 3. Effect of CTS on LW/BW.
 α: There was no significance between the control and sham groups.
 β: The ANTU group is significantly higher than the control and sham groups.
 γ: The ANTU+CTS group was significantly reduced compared to the ANTU group.

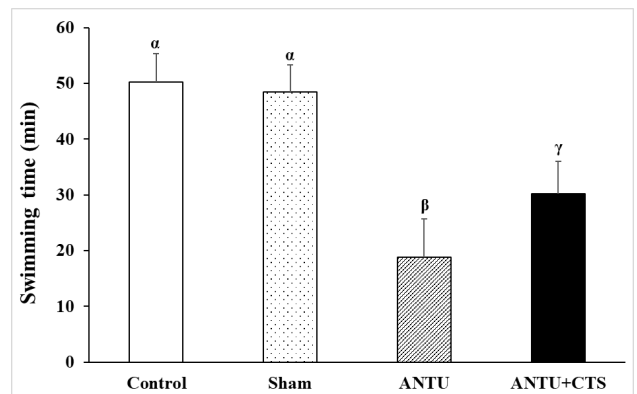


Figure 4. Effect of CTS on swimming time.
 α: There was no significance between the control and sham groups.
 β: The ANTU group is significantly lower than the control and sham groups.
 γ: The ANTU+CTS group was significantly increased compared to the ANTU group.

higher ($p < 0.05$) than ANTU (Figure 4). It can be said that CTS reduces the formation of PE and increases swimming time.

DISCUSSION

ANTU gives rise to acute pulmonary vascular injury in rodents, with the most prominent manifestations including increased lung weight due to PE and pulmonary edema due to damage to endothelial cells and pneumocytes in the lung. Since the effects of ANTU are highly specific to the lungs, it is widely used in generating animal models to investigate the pathology of acute pulmonary edema (27). CTS, a key ingredient derived from *Salvia miltiorrhiza*, has many pharmacological properties such as anti-inflammatory, anti-oxidative, anti-angiogenic, and anti-proliferative properties. CTS is used in the treatment of many diseases including acute lung injury (18). Additionally, orally administered CTS is an alternative treatment agent for pulmonary fibrosis (17). However, its poor oral absorption and sensitivity to light greatly limit its clinical application (28).

Regarding its anti-cancer properties, it has been stated that CTS induces apoptosis in lung cancer cells and inhibits tumor formation in the lung both *in vitro* and *in vivo* (29). Furthermore, CTS prevents invasion/metastasis in non-small cell lung cancer (NSCLC) via inhibiting the expression of carcinogenic microRNAs (30, 31). It has also been stated that CTS potentiates the effects of chemotherapeutic drugs on NSCLC cells through transketolase inhibition both *in vitro* and *in vivo* (32). When this information is compiled, it can be concluded that CTS has suppressive effects on lung cancer, can be used as a treatment agent *in vivo* and *in vitro* studies.

It has been stated that CTS reduces allergic airway inflammation (33), and might be a curative agent for the treatment of asthma (34). Moreover, CTS has been shown to have an anti-inflammatory effect by down-regulating pro-inflammatory

inducible nitric oxide synthase (iNOS) and cyclooxygenase-2 (COX-2) in the mouse macrophage cell line (35). In addition, CTS also performed anti-inflammatory effects specifically by inhibiting COX-2 activity in lipopolysaccharide (LPS)-stimulated pro-monocyte cell line and paw edema model (13). Tang et al. have shown that CTS reduces LPS-induced acute lung injury through its anti-inflammatory effects by inhibiting toll like receptor 4 (TLR4)-mediated nuclear factor kappa B (NF-κB) signaling pathways (36). Moreover, CTS maintain to pulmonary fibrosis by suppressing the cascade of Smad and STAT3 (37). CTS treatment has been shown to reduce radiation-induced lung injury and pulmonary fibrosis in rats by suppressing inflammatory and fibrotic factors (38). Similarly, its inhalation has also been shown to alleviate pulmonary fibrosis; therefore, CTS may be an alternative treatment method in the treatment of pulmonary fibrosis (39).

To date, the effects of CTS have not been examined on pulmonary edema. However, considering the studies on CTS, its protective role in pulmonary diseases and edema is due to its anti-inflammatory effects through inhibition of the inflammatory pathway. In this study, it was determined that the use of CTS improves swimming scores by reducing pleural fluid in the ANTU-induced pulmonary edema model. CTS may have shown a protective effect against pulmonary edema by inhibiting the anti-inflammatory pathway.

CONCLUSION

Our findings have demonstrated that CTS shows a protective effect against ANTU-induced acute pulmonary edema. CTS decreased PE, LW/BW, and PE/BW following pulmonary edema, while increasing swimming time. CTS seems like it may be considered as an alternative treatment approach in the treatment of pulmonary edema following more detailed

studies. The lack of molecular analyses is one of the limiting factors of our study, however, it provides important preliminary information for studies that will attempt to understand the effects of CTS on pulmonary edema with molecular analysis.

Ethics Committee Approval: This study was conducted with the approval of Karabuk University Faculty of Medicine Experimental Animals Ethics Committee (Date: 04/10/2022, Decision Number: 2022/09/15, Registration number: E-55212866-050.99-174960).

Authors' Contributions: Conception/Design of Study- U.Y., M.D.; Data Acquisition – U.Y., M.D.; Data Analysis/Interpretation – U.Y., M.D.; Drafting Manuscript– U.Y.; Critical Revision of Manuscript- U.Y.; Final Approval and Accountability– U.Y., M.D.

Conflict of Interest: Authors declared no conflict of interest.

Financial Disclosure: Authors declared no financial support.

REFERENCES

1. Panjwani A, Salman MR. An uncommon cause of pleural effusion. *Breathe (Sheff)* 2019; 15(2): e84-e9.
2. Marel M, Zrustova M, Stasny B, Light RW. The incidence of pleural effusion in a well-defined region. Epidemiologic study in central Bohemia. *Chest* 1993; 104(5): 1486-9.
3. Riedel M. Noncardiogenic pulmonary edema. *Ceskoslovenska fysiologie* 1996; 45(2): 112-9.
4. MacIver DH, Clark AL. The vital role of the right ventricle in the pathogenesis of acute pulmonary edema. *Am J Cardiol* 2015; 115(7): 992-1000.
5. Glaus T, Schellenberg S, Lang J. Cardiogenic and non cardiogenic pulmonary edema: pathomechanisms and causes. *Schweiz Arch Tierheilkd* 2010; 152(7): 311-7.
6. Rapin M, Lemaire F. Les oedèmes pulmonaires non hémodynamiques [Non cardiogenic pulmonary edema]. *Sem Hop* 1979; 55(7-8): 331-4.
7. Alwi I. Diagnosis and management of cardiogenic pulmonary edema. *Acta Med Indones* 2010; 42(3): 176-84.
8. Wang Y-J, Liao C-Y, Kao C-W. Nursing assessment and management of patients with cardiogenic pulmonary edema. *Hu Li Za Zhi* 2012; 59(1): 24.
9. Yu XY, Lin SG, Chen X, Zhou ZW, Liang J, Duan W, et al. Transport of cryptotanshinone, a major active triterpenoid in *Salvia miltiorrhiza* Bunge widely used in the treatment of stroke and Alzheimer's disease, across the blood-brain barrier. *Curr Drug Metab* 2007; 8(4): 365-78.
10. Kim SY, Moon TC, Chang HW, Son KH, Kang SS, Kim HP. Effects of tanshinone I isolated from *Salvia miltiorrhiza* bunge on arachidonic acid metabolism and in vivo inflammatory responses. *Phytother Res* 2002; 16(7): 616-20.
11. Park IJ, Kim MJ, Park OJ, Park MG, Choe W, Kang I, et al. Cryptotanshinone sensitizes DU145 prostate cancer cells to Fas(APO1/CD95)-mediated apoptosis through Bcl-2 and MAPK regulation. *Cancer Lett* 2010; 298(1): 88-98.
12. Lee WY, Liu KW, Yeung JH. Reactive oxygen species-mediated kinase activation by dihydrotanshinone in tanshinone-induced apoptosis in HepG2 cells. *Cancer Lett* 2009; 285(1): 46-57.
13. Jin DZ, Yin LL, Ji XQ, Zhu XZ. Cryptotanshinone inhibits cyclooxygenase-2 enzyme activity but not its expression. *Eur J Pharmacol* 2006; 549(1-3): 166-72.
14. Chen Q, Zhuang Q, Mao W, Xu XM, Wang LH, Wang HB. Inhibitory effect of cryptotanshinone on angiogenesis and Wnt/beta-catenin signaling pathway in human umbilical vein endothelial cells. *Chin J Integr Med* 2014; 20(10): 743-50.
15. Tang S, Shen XY, Huang HQ, Xu SW, Yu Y, Zhou CH, et al. Cryptotanshinone suppressed inflammatory cytokines secretion in RAW264.7 macrophages through inhibition of the NF-kappaB and MAPK signaling pathways. *Inflammation* 2011; 34(2): 111-8.
16. Zhang Q, Gan C, Liu H, Wang L, Li Y, Tan Z, et al. Cryptotanshinone reverses the epithelial-mesenchymal transformation process and attenuates bleomycin-induced pulmonary fibrosis. *Phytother Res* 2020; 34(10): 2685-96.
17. Zhang Y, Lu W, Zhang X, Lu J, Xu S, Chen S, et al. Cryptotanshinone protects against pulmonary fibrosis through inhibiting Smad and STAT3 signaling pathways. *Pharmacol Res* 2019; 147: 104307.
18. Wang X, Wan W, Lu J, Zhang Y, Quan G, Pan X, et al. Inhalable cryptotanshinone spray-dried swellable microparticles for pulmonary fibrosis therapy by regulating TGF-beta1/Smad3, STAT3 and SIRT3 pathways. *Eur J Pharm Biopharm* 2022; 172: 177-92.
19. Tang Y, Chen Y, Chu Z, Yan B, Xu L. Protective effect of cryptotanshinone on lipopolysaccharide-induced acute lung injury in mice. *Eur J Pharmacol* 2014; 723: 494-500.
20. Jiang Y, You F, Zhu J, Zheng C, Yan R, Zeng J. Cryptotanshinone Ameliorates Radiation-Induced Lung Injury in Rats. *Evid Based Complement Alternat Med* 2019; 2019: 1908416.
21. Markov AK, Causey AL, Didlake RH, Lemos LB. Prevention of alpha-naphthylthiourea-induced pulmonary edema with fructose-1,6-diphosphate. *Exp Lung Res* 2002; 28(4): 285-99.
22. Richter CP. The physiology and cytology of pulmonary edema and pleural effusion produced in rats by alpha-naphthyl thiourea (ANTU). *J Thoracic Surg* 1952; 23(1): 66-91.
23. Park OK, Choi JH, Park JH, Kim IH, Yan BC, Ahn JH, et al. Comparison of neuroprotective effects of five major lipophilic diterpenoids from *Danshen* extract against experimentally induced transient cerebral ischemic damage. *Fitoterapia* 2012; 83(8): 1666-74.
24. De Caro C, Raucci F, Saviano A, Cristiano C, Casillo GM, Di Lorenzo R, et al. Pharmacological and molecular docking assessment of cryptotanshinone as natural-derived analgesic compound. *Biomed Pharmacother* 2020; 126: 110042.
25. Bai T, Yang K, Qin C, Xu T, Yu X, Zhang J. Cryptotanshinone ameliorates renal ischaemia-reperfusion injury by inhibiting apoptosis and inflammatory response. *Basic Clin Pharmacol Toxicol* 2019; 125(5): 420-9.
26. Slattery DA, Cryan JF. Using the rat forced swim test to assess antidepressant-like activity in rodents. *Nat Protoc* 2012; 7(6): 1009-14.
27. Barton CC, Bucci TJ, Lomax LG, Warbritton AG, Mehendale HM. Stimulated pulmonary cell hyperplasia underlies resistance to alpha-naphthylthiourea. *Toxicology* 2000; 143(2): 167-81.
28. Zhang J, Huang M, Guan S, Bi HC, Pan Y, Duan W, et al. A mechanistic study of the intestinal absorption of cryptotanshinone, the major active constituent of *Salvia miltiorrhiza*. *J Pharmacol Exp Ther* 2006; 317(3): 1285-94.
29. Chen L, Wang HJ, Xie W, Yao Y, Zhang YS, Wang H. Cryptotanshinone inhibits lung tumorigenesis and induces apoptosis in cancer cells in vitro and in vivo. *Mol Med Rep* 2014; 9(6): 2447-52.
30. Qi PF, Li YL, Liu XM, Jafari FA, Zhang XJ, Sung QL, et al. Cryptotanshinone suppresses non-small cell lung cancer via microRNA-146a-5p/EGFR axis. *Int J Biol Sci* 2019; 15(5): 1072-9.
31. Wang H, Zhang Y, Zhang Y, Liu W, Wang J. Cryptotanshinone inhibits lung cancer invasion via microRNA-133a/matrix metalloproteinase 14 regulation. *Oncol Lett* 2019; 18(3): 2554-9.

32. Cao L, Hong WP, Cai PH, Xu CC, Bai XP, Zhao ZX, et al. Cryptotanshinone strengthens the effect of gefitinib against non-small cell lung cancer through inhibiting transketolase. *Eur J Pharmacol* 2021; 890: 173647.
33. Li J, Zheng M, Wang C, Jiang J, Xu C, Li L, et al. Cryptotanshinone attenuates allergic airway inflammation through negative regulation of NF-kappaB and p38 MAPK. *Biosci Biotechnol Biochem* 2020; 84(2): 268-78.
34. Wang C, Zheng M, Choi Y, Jiang J, Li L, Li J, et al. Cryptotanshinone attenuates airway remodeling by inhibiting crosstalk between tumor necrosis factor-like weak inducer of apoptosis and transforming growth factor beta 1 signaling pathways in asthma. *Front Pharmacol* 2019; 10: 1338.
35. Jeon SJ, Son KH, Kim YS, Choi YH, Kim HP. Inhibition of prostaglandin and nitric oxide production in lipopolysaccharide-treated RAW 264.7 cells by tanshinones from the roots of *Salvia miltiorrhiza bunge*. *Arch Pharm Res* 2008; 31(6): 758-63.
36. Tang Y, Chen YL, Chu Z, Yan B, Xu LJ. Protective effect of cryptotanshinone on lipopolysaccharide-induced acute lung injury in mice. *Eur J Pharmacol* 2014; 723: 494-500.
37. Zhang YT, Lu WT, Zhang XL, Lu J, Xu SW, Chen SR, et al. Cryptotanshinone protects against pulmonary fibrosis through inhibiting Smad and STAT3 signaling pathways. *Pharmacol Res* 2019; 147 :104307.
38. Jiang YF, You FM, Zhu J, Zheng C, Yan R, Zeng JH. Cryptotanshinone ameliorates radiation-induced lung injury in rats. *Evid Based Complement Alternat Med* 2019; 2019: 1908416.
39. Wang XH, Wan W, Lu J, Zhang YT, Quan GL, Pan X, et al. Inhalable cryptotanshinone spray-dried swellable microparticles for pulmonary fibrosis therapy by regulating TGF-beta 1/Smad3, STAT3 and SIRT3 pathways. *Eur J Pharm Biopharm* 2022; 172: 177-92.

Comparative Toxicity Responses of Thirdhand Smoke Derived from Conventional Cigarette and Heated Tobacco Products in Human Bronchial Epithelial Cells

Rengin Reis^{1,2} , Kübra Kolci¹ 

¹Department of Pharmaceutical Toxicology, Faculty of Pharmacy, Acıbadem Mehmet Ali Aydınlar University, Istanbul, Türkiye

²Department of Toxicology, Faculty of Pharmacy, Yeditepe University, Istanbul, Türkiye

ORCID ID: K.K. 0000-0003-4228-6564; R.R. 0000-0002-3484-2201

Cite this article as: Reis R, Kolci K. Comparative toxicity responses of thirdhand smoke derived from conventional cigarette and heated tobacco products in human bronchial epithelial cells. *Experimed* 2023; 13(2): 127-132.

ABSTRACT

Objective: Thirdhand smoke (THS) is described as the accumulated chemicals left on indoor surfaces after tobacco smoking. Individuals can be exposed to THS by dermal or oral contact with THS-embedded surfaces or by breathing in the off-gasses. In the present study, the cytotoxic, oxidative, and inflammatory responses of THS extracts yielded from conventional (THS-C) and heated-tobacco products (THS-H) were examined in BEAS-2B human bronchial epithelial cell line.

Materials and Methods: The terrycloth samples were exposed to smoke in a closed polystyrene box and extracted in a complete cell culture medium for 24 hours at 37°C. Following this, the cytotoxicity of THS was assessed by MTT assay. Malondialdehyde (MDA) and intracellular glutathione (GSH) levels were determined in BEAS-2B cell lysate to assess oxidative response. The aryl hydrocarbon receptor (AhR) and interleukine-6 (IL-6) levels were determined via an ELISA kit.

Results: Both types of THS led to dose-dependent cytotoxicity in cells, which was remarkable with THS-C (50%, v/v). Moreover, GSH depletion and MDA increase were remarkable with both THS, particularly with THS-C. AhR activation was also slightly elevated with THS-C, whereas the increase in IL-6 was notable compared to THS-H.

Conclusion: THS exposure might lead to potential health risks particularly for respiratory health and the results support the need for comprehensive regulations and public health initiatives to minimize the harmful effects of THS.

Keywords: Thirdhand smoke, heated-tobacco product, oxidative stress, aryl hydrocarbon receptor, inflammation, interleukine-6.

INTRODUCTION

Smoking is one of the leading causes of preventable death worldwide. Across Organisation for Economic Co-operation and Development (OECD) countries, among smokers aged 15 and over, Türkiye is ranked second with a daily smoking rate of 28% after Indonesia, according to the latest data (1). Due to this relatively high rate of daily smoking, other risk factors may arise not only for active cigarette smokers but also for non-smokers and the environment exposed to the side stream smoke during this process (2). From this point of view, a new toxicological concept, thirdhand smoke

(THS), can be described as residual smoke that is remained after the cigarette is extinguished and might be generated from aged secondhand smoke that adheres to dust and surfaces. In addition to its cumulative hazard potential, its re-emission into the air makes the THS a public health concern, particularly for individuals who are suffering from respiratory diseases (3). Even though smoking has been prohibited in most indoor workplaces and public places in Türkiye since 2005, there are a few exceptions where ventilation is allowed for smoking such as care facilities for the elderly people, restricted areas in airports, personal accommodation places, and hotel rooms (4). Therefore,

Corresponding Author: Rengin Reis **E-mail:** rengin.reis@acibadem.edu.tr

Submitted: 25.06.2023 **Revision Requested:** 18.07.2023 **Last Revision Received:** 18.07.2023 **Accepted:** 27.07.2023 **Published Online:** 31.07.2023



Content of this journal is licensed under a Creative Commons Attribution-NonCommercial 4.0 International License.

indoor smoking might represent a current public health and environmental concern for people who do not actively smoke, despite strengthened bans.

According to the recent literature, the chemical dynamic of THS is quite different from firsthand smoke (FHS) and secondhand cigarette smoke (SHS) due to the delayed and aged exposure to smoke pollutants. In addition, the re-emitted gas phase represents a continuous environmental pollutant reservoir in terms of nicotine, nitrous acid, carcinogenic tobacco-specific nitrosamines (TSNAs), and volatile organic components (VOCs) (5). Unfortunately, physical, and chemical cleaning techniques were shown to be ineffective in removing THS residue adsorbed on surfaces and materials. Also, cleaning methods such as wiping was previously reported to cause particles to become liberated from the deposited surfaces and re-suspended in air, thus increasing the probability of exposure via the inhalation route (6). Exposure via inhalation is a common exposure route for FHS, SHS, and THS; however, due to the surface embedding potential of THS, the oral route is another exposure route for THS, which makes THS a health hazard for toddlers and children who are frequently in contact with surfaces via hand to mouth transfer with a long-lasting effect (7). In addition to the risk to children, people who are suffering from chronic respiratory diseases such as asthma, chronic obstructive pulmonary disease (COPD), and wheezing (8). According to research by Vanker and colleagues (2017), environmental cigarette smoke was suggested as an important public health concern for people, especially children, by increasing the rate of asthma, wheezing, and pulmonary infections. In addition, these health hazards were reported to be at higher rates in low and moderate-income countries in several reports (8,9).

The limited studies on THS exposure showed that it has dose-dependent cytotoxic (10) and genotoxic (11,12) potential on several cell lines and has a delaying effect on wound healing capacity in mice (13). Based on these few findings on the risk of repeated exposure to THS, a toxicological evaluation of the complex mixture of THS and its possible health effects are further needed. In recent years, in addition to the use of conventional cigarettes, "less harmful" options to smoke were started to be marketed such as heat-not-burn products or heated tobacco products (HTP). These products aim to serve a smoke containing nicotine to the consumer with a less burning product and carcinogenic intermediates since HTPs are heating the tobacco up to 300°C instead of burning as in traditional cigarettes (14,15). In our previous study, we reported the comparative cytotoxicity of the FHS extracted from HTP and conventional cigarette (3R4F) in human liver epithelial cells, and those novel products dose-dependently might be cytotoxic to the cells via inflammatory and oxidative pathways (16). However, there is no current finding on the residual potential of HTPs and their toxicity potential on the primary target organ, the lungs. Since there is no classified safety level of environmental cigarette smoke exposure, no definitive THS threshold for adverse effects has been recognized. The present study aimed to evaluate the potential cytotoxicity profile of two different types of THSs isolated from conventional

cigarette and heated tobacco products preliminarily in human bronchial epithelial cells via oxidative and inflammatory pathways *in vitro*.

MATERIAL AND METHODS

Preparation of THS Extract

THS was extracted from terrycloth fabric exposed to one 3R4F cigarette (THS-C) and heat stick heated via HTP (THS-H) device manually in a polystyrene chamber with a puff volume of 55 mL and 30 seconds of puff cycle as described in the previous smoking simulation (16). After the smoke exposure in the chamber, the terrycloth was extracted in the high glucose Dulbecco's Modified Eagle Media (DMEM, Gibco, USA) at 37°C for 24 hours. After the extraction process, the extract (100%, v/v) was filtered and stored at -80°C for further studies. The standardization of prepared extract was recorded through before and after weights of filter papers accumulates the total particulate matter (TPM) for each.

Cytotoxicity Assay

The cytotoxicity potential of the two types of THSs was assessed via 3-(4,5-dimethylthiazol-2-yl)-2,5 diphenyltetrazolium bromide (MTT) assay through mitochondrial reductase activity in human bronchial epithelial BEAS-2B cells (ATCC, CRL-9609). For this purpose, cells were cultured with Dulbecco's modified eagle medium (DMEM) supplemented with 100 IU/mL penicillin, 100 µg/mL streptomycin, and 5% (v/v) fetal bovine serum (FBS, Gibco, USA). The cells were seeded in 96-well plates before the day of exposure as 2×10^4 cells/well and incubated for 24 hours to achieve subconfluency. The following day, THS-C and THS-H were diluted with a complete cell culture medium and applied to the cells between doses at 10-100% (v/v) for 24 hours. After the incubation, the well contents were discarded and 0.5 mg/mL MTT solution was applied to the wells as previously described (17). In addition to the cytotoxicity, cell morphology was also visualized via EVOS M5000 (ThermoScientific, Singapore) at a magnification rate of 10x for 72 hours.

Oxidative Stress

For the assessment of oxidative damage induced by THS-C and THS-H, intracellular glutathione (GSH) and lipid peroxidation intermediate product malondialdehyde (MDA) levels were assessed according to our previous methods (16,17). Briefly, the cells seeded in T-25 flasks were exposed to the 10-25-50% (v/v/v) THS-C and THS-H extracts for 24 hours. The next day, cell pellets were collected and lysed with MagnaLyser (Roche, Switzerland). The collected cell lysates were used for the assessment of total protein content, GSH, and MDA level spectrophotometrically in triplicates (ThermoScientific, VarioskanLUX, Singapore).

Inflammatory Damage

Inflammation is another toxicity response against air pollutants; thus, it was evaluated in BEAS-2B cells via pro-inflammatory cytokine interleukin-6 (IL-6) and aryl hydrocarbon receptor

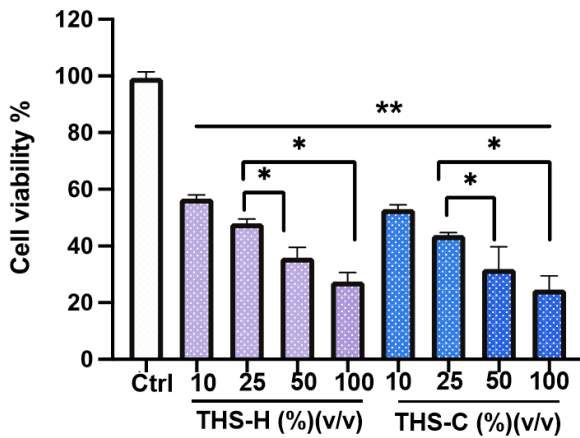


Figure 1. Cytotoxicity profiles of THS-C and THS-H in BEAS-2B cells. Ctrl: Control; THS-H: Thirdhand smoke of HTP; THS-C: Thirdhand smoke of 3R4F cigarette. Results were expressed as mean \pm SD. The significant differences between groups and Ctrl were defined as * p <0.05; ** p <0.001.

(AhR) levels via enzyme-linked Immuno sorbent assay (ELISA) kit. For this purpose, cell supernatants were assessed with a human IL-6 ELISA kit (Elabscience, E-EL-H6156, USA) and a human AhR ELISA kit (AFG Bioscience, EK700338, USA) at 450 nm spectrophotometrically in duplicates.

Statistical Analyses

Statistical analyses of data were performed with GraphPad Prism 9.0 (La Jolla, California, USA). The results of cell culture studies are presented as the mean \pm SD as triplicates. One-way analysis of variance (ANOVA) tests were used for analysis and differences were considered to be significant at p <0.05.

RESULTS

TPM of THS Extracts

The prepared extracts were standardized through collected TPM amounts on the filter papers. Based on our extractions, the TPM of THS-C was recorded as 3.7 ± 0.12 mg whereas for THS-H was 3.1 ± 0.2 mg.

Cytotoxicity

Cytotoxicity of THS-C and THS-H were shown in Figure 1. As seen in Figure 1, both extracts showed dose-dependent cytotoxicity in BEAS-2B cells, which was remarkable with the higher doses of THS-C (50-100%, v/v). Furthermore, all the tested concentrations of THS-C and THS-H were significantly cytotoxic compared to the control group (p <0.001). According to the MTT assay, the inhibiting concentration 50% (IC₅₀) values of extracts were found as $14.8 \pm 1.9\%$ for THS-C and $21.7 \pm 2.6\%$ for THS-H. The cell morphology of THS-exposed BEAS-2B cells was recorded for 72 hours and shown in Figure 2.

Oxidative Stress

Smoking is a well-known source of free radicals, reactive oxygen species (ROS), and reactive nitrogen species (RNS) formation, which play a crucial role in oxidative damage in target organs as a notable contributing factor. Hence, we assessed THS induced oxidative damage, which was yielded by a cigarette, and an HTP through intracellular GSH and MDA levels. Based on our findings, 25-50% (v/v) doses of THS-C and THS-H significantly led to a significant depletion in GSH deposits in BEAS-2B cells compared to the control (Figure 3). Moreover, the difference between the highest tested doses was remarkable with THS-C in the GSH assay (p <0.05). On the other hand, lipid peroxidation was significantly higher with THS-C (50%, v/v) compared to the same dose of THS-H (Figure 4) (p <0.001).

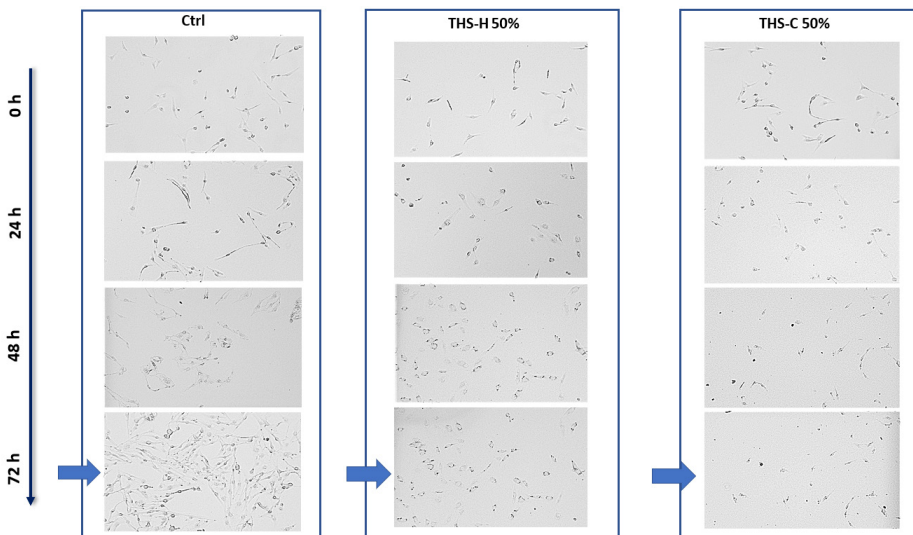


Figure 2. Morphological images of BEAS-2B cells exposed to the THS-C and THS-H for up to 72 hours.

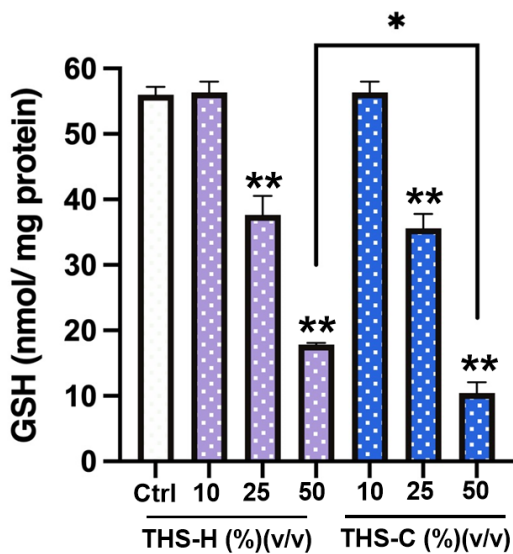


Figure 3. Intracellular GSH level in BEAS-2B cells. Ctrl: Control; THS-H: Thirdhand smoke of HTP; THS-C: Thirdhand smoke of 3R4F cigarette. Results were expressed as mean±SD. The significant differences between groups and Ctrl were defined with * p<0.05, **p<0.01

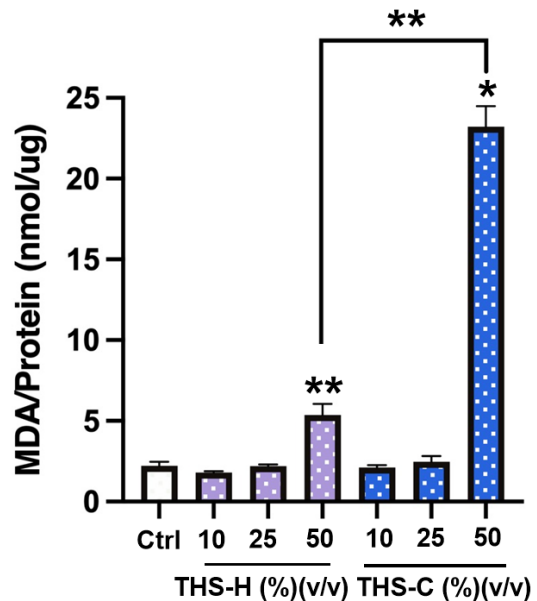


Figure 4. MDA level in BEAS-2B cells. Ctrl: Control; THS-H: Thirdhand smoke of HTP; THS-C: Thirdhand smoke of 3R4F cigarette. Results were expressed as mean±SD. The significant differences between groups and Ctrl were defined with *p<0.05; **p<0.001

Inflammatory Response

IL-6 Levels

Inflammatory response through pro-inflammatory IL-6 level was found to be elevated with THS-C and THS-H exposure

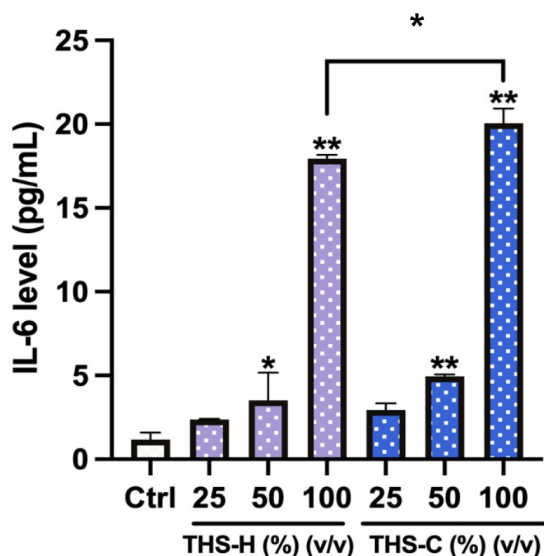


Figure 5. IL-6 level in BEAS-2B cells. Ctrl: Control; THS-H: Thirdhand smoke of HTP; THS-C: Thirdhand smoke of 3R4F cigarette. Results were expressed as mean±SD. The significant differences between groups and Ctrl were defined with *p<0.05, **p<0.001.

dose-dependently as shown in Figure 5. Based on the ELISA results, 50% and 100% (v/v) doses of the extracts exhibited a significant increase in the inflammatory response, which was the highest with THS-C. In addition, the difference in the IL-6 release was statistically significant between the highest tested doses of THSs (p<0.05).

AhR Levels

Another important inflammatory marker, AhR, which has specific ligands such as tobacco smoke cigarette smoke carcinogen benzo(a)pyrene, was evaluated in BEAS-2B cells via ELISA kit. According to the present findings, cytoplasmic AhR level was higher with THS-H (100%, v/v) exposure compared to the same dose of THS-C (Figure 6). However, the difference between the two groups was insignificant.

DISCUSSION

In the present study, we focused on the potential cytotoxicity, oxidative stress, and inflammatory response caused by THS derived from conventional cigarettes and heated tobacco products. The findings indicate that both THS-C and THS-H showed dose-dependent cytotoxicity in BEAS-2B cells, where the higher doses of THS-C exhibited more pronounced cytotoxic effects compared to THS-H based on their IC₅₀. Moreover, the cell morphology analysis further supported the cytotoxic effects of THS on the cells. Similar to our findings, Bahl and colleagues reported a dose-dependent cigarette-derived-THS cytotoxicity in human dermal fibroblasts (hDF)

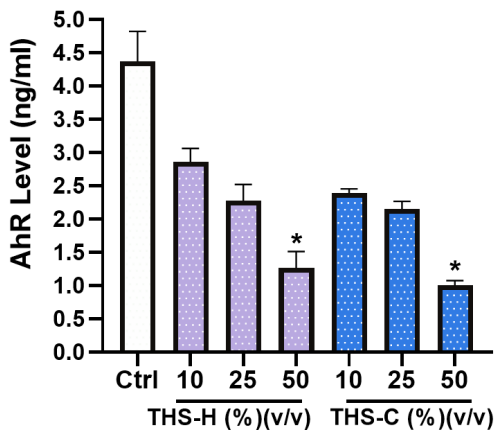


Figure 6. Cytoplasmic AhR level in BEAS-2B cells. Ctrl: Control; THS-H: Thirdhand smoke of HTP; THS-C: Thirdhand smoke of 3R4F cigarette. Results were expressed as mean±SD. The significant differences between groups and Ctrl were defined with * $p < 0.001$.

and human palatal mesenchyme cells (hPM) (10). In another study, indoor surface-derived THS was also found dose-dependently cytotoxic to mouse neural stem cells (mNSC), which represented a model for the neonatal brain (18). However, there are no records in the literature on the HTP-derived THS and potential cytotoxicity profile. Therefore, this is the first comparative report that identifies the cytotoxicity profile of HTP-derived THS *in vitro*. Oxidative stress is another important pathway involved in chronic pulmonary diseases and tobacco-induced lung deficits (19–21), and its assessment revealed that both THS-C and THS-H led to a depletion in intracellular GSH deposits in BEAS-2B cells. THS-C induced higher levels of lipid peroxidation compared to THS-H exposure, indicating its stronger potential for oxidative damage based on our findings. The other important pathway involved in respiratory diseases is inflammation, which was augmented with smoking as well, and was evaluated with pro-inflammatory IL-6 and tobacco-specific carcinogen ligand-induced-AhR level (22–25). According to the results, THS-C and THS-H exposure exhibited a dose-dependent increase in IL-6 levels, with THS-C showing a higher inflammatory response. However, there was no significant difference in cytoplasmic AhR levels between THS-C and THS-H. Previously, we reported a slight increase in HepG2 cells exposed to the FHS and SHS extracts of both conventional cigarettes and HTP, which was higher with cigarettes (16). Similarly, THS derived from a cigarette led to a higher AhR activation with a lower cytoplasmic AhR level in the current study. Based on these findings, it might be suggested that both types of THS demonstrated dose-dependent cytotoxicity, with THS-C exhibiting stronger effects. The oxidative stress assessment indicated a depletion of intracellular GSH deposits and higher lipid peroxidation with THS-C. Furthermore, THS-C induces a stronger inflammatory response through IL-6 release in BEAS-2B cells.

CONCLUSION

These findings emphasize the potential health risks associated with THS exposure, particularly in terms of respiratory health. The study contributes to the understanding of the toxicological profile of THS and highlights the importance of further research to assess the long-term effects of THS exposure on human health. The results support the need for comprehensive regulations and public health initiatives to minimize THS exposure and protect individuals, especially those with respiratory conditions, from the harmful effects of THS.

Acknowledgments: This study was presented as an oral presentation at the 11th International Turkish Society of Toxicology Congress, Antalya, Turkiye (2-5 November 2022).

Ethics Committee Approval: Ethics committee approval is not required for cell culture studies in the article.

Authors' Contributions: Conception/Design of Study- K.K., R.R.; Data Acquisition – K.K., R.R.; Data Analysis/Interpretation – K.K., R.R.; Drafting Manuscript– R.R.; Critical Revision of Manuscript- R.R.; Final Approval and Accountability– K.K., R.R.

Conflict of Interest: Authors declared no conflict of interest.

Financial Disclosure: Authors declared no financial support.

REFERENCES

1. OECD. OECD-Daily smoking rates (cited in June, 2023). Available from URL: <https://data.oecd.org/healthrisk/daily-smokers.htm>
2. Pagani LS. Environmental tobacco smoke exposure and brain development: The case of attention deficit/hyperactivity disorder. *Neurosci Biobehav Rev* 2014; 44: 195–205.
3. Matt GE, Quintana PJE, Hoh E, Dodder NG, Mahabee-Gittens EM, Padilla S, et al. Tobacco smoke is a likely source of lead and cadmium in settled house dust. *J Trace Elem Med Biol* 2021; 63: 126–36.
4. Tobacco Control Law. WHO Framework Convention on Tobacco Control-2022 (cited in June, 2023). Available from URL: <https://www.tobaccocontrollaws.org/legislation/turkey#:~:text=Smoking is prohibited in most,%2C prisons%2C and hotel rooms.>
5. Moon SY, Kim T, Kim YJ, Kim Y, Kim SY, Kang D. Public facility utility and third-hand smoking exposure without first and second-hand smoking according to urinary cotinine level. *Int J Environ Res Public Health* 2019; 16(5): 855.
6. Kuo HW, Rees VW. Third-hand smoke (THS): What is it and what should we do about it? *J Formos Med Assoc* 2019; 118: 1478–79.
7. Arguder E. Third-hand smoke exposure and results. *Eurasian J Pulmonol* 2019; 21: 81–6
8. Vanker A, Gie RP, Zar HJ. The association between environmental tobacco smoke exposure and childhood respiratory disease: a review. *Expert Rev Respir Med* 2017; 11: 661–73.
9. Zafeiridou M, Hopkinson NS, Voulvoulis N. Cigarette smoking: an assessment of tobacco's global environmental footprint across its entire supply chain. *Environ Sci Technol* 2018; 52(15): 8087–94.
10. Bahl V, Shim HJ, Jacob P, Dias K, Schick SF, Talbot P. Thirdhand smoke: chemical dynamics, cytotoxicity, and genotoxicity in outdoor and indoor environments. *Toxicol in Vitro* 2016; 32: 220–31.

11. Hang B, Wang P, Zhao Y, Chang H, Mao JH, Snijders AM. Thirdhand smoke: Genotoxicity and carcinogenic potential. *Chronic Dis Transl Med* 2020; 6(1): 27–34.
12. Hang B, Sarker AH, Havel C, Saha S, Hazra TK, Schick S, et al. Thirdhand smoke causes DNA damage in human cells. *Mutagenesis* 2013; 28(4): 381–91.
13. Martins-Green M, Adhami N, Frankos M, Valdez M, Goodwin B, Lyubovitsky J, et al. Cigarette smoke toxins deposited on surfaces: Implications for human health. *PLoS One* 2014; 9(1): 1–12.
14. Glantz S. Heated tobacco products: The example of IQOS. *Tob Control* 2018; 27: 3–6.
15. Lee CM. The impact of heated tobacco products on smoking cessation, tobacco use, and tobacco sales in South Korea. *Korean J Fam Med* 2020; 41(5): 273–81.
16. Reis R, Kolci K, Bahcivan İ, Coskun GP, Sipahi H. Alpha-lipoic acid modulates the oxidative and inflammatory responses induced by traditional and novel tobacco products in human liver epithelial cells. *Chem Biodivers* 2023; 20(3): e202200928.
17. Reis R, Orak D, Yilmaz D, Cimen H, Sipahi H. Modulation of cigarette smoke extract-induced human bronchial epithelial damage by eucalyptol and curcumin. *Hum Exp Toxicol* 2021; 40(9): 1445–62.
18. Bahl V, Weng NJH, Schick SF, Sleiman M, Whitehead J, Ibarra A, et al. Cytotoxicity of thirdhand smoke and identification of acrolein as a volatile thirdhand smoke chemical that inhibits cell proliferation. *Toxicol Sci* 2016; 150(1): 234–46.
19. Hosseini MJ, Naserzadeh P, Salimi A, Pourahmad J. Toxicity of cigarette smoke on isolated lung, heart, and brain mitochondria: induction of oxidative stress and cytochrome c release. *Toxicol Environ Chem* 2013; 95(9): 1624–37.
20. Schweitzer KS, Hatoum H, Brown MB, Gupta M, Justice MJ, Beteck B, et al. Mechanisms of lung endothelial barrier disruption induced by cigarette smoke: role of oxidative stress and ceramides. *Am J Physiol Lung Cell Mol Physiol* 2011; 301(6): 836–46.
21. Kluchová Z, Petrášová D, Joppa P, Dorková Z, Tkáčová R. The association between oxidative stress and obstructive lung impairment in patients with COPD. *Physiol Res* 2007; 56(1): 51–6.
22. Lugade AA, Bogner PN, Thatcher TH, Sime PJ, Phipps RP, Thanavala Y. Cigarette smoke exposure exacerbates lung inflammation and compromises immunity to bacterial infection. *J Immunol* 2014; 192(11): 5226–35.
23. Moghaddam SJ, Barta P, Mirabolfathinejad SG, Ammar-Aouchiche Z, Garza NT, Vo TT, et al. Curcumin inhibits COPD-like airway inflammation and lung cancer progression in mice. *Carcinogenesis* 2009; 11: 1949–56.
24. Boskabady MH, Gholami Mahtaj L. Lung inflammation changes and oxidative stress induced by cigarette smoke exposure in guinea pigs affected by *Zataria multiflora* and its constituent, carvacrol. *BMC Complement Altern Med* 2015; 15: 39.
25. Radan M, Dianat M, Badavi M, Mard SA, Bayati V, Ahmadzadeh M. The association of cigarette smoke exposure with lung cellular toxicity and oxidative stress: the protective role of crocin. *Inflammation* 2020; 43(1): 135–45.

Pressure Ulcers in Palliative Care Unit Patients

Mahmut Said Degerli¹ 

¹Department of General Surgery, Bakirkoy Dr. Sadi Konuk Training and Research Hospital, University of Health Sciences, Istanbul, Turkiye

ORCID ID: M.S.D. 0000-0002-8313-7904

Cite this article as: Degerli MS. Pressure ulcers in palliative care unit patients. *Experimed* 2023; 13(2): 133-141.

ABSTRACT

Objective: Pressure ulcers are associated with prolonged lengths of stay, increased costs, and lower discharge rates in palliative care units. This study aimed to reveal pressure ulcers' risk factors, incidence, and prevalence in a palliative care unit.

Materials and Methods: The data of 252 inpatients in a secondary-level palliative care unit were examined retrospectively. Patients were divided into groups according to pressure ulcer status, and data was comparatively analyzed. Pressure ulcer prevalence and incidence in the palliative care unit were calculated.

Results: There were 137 (54.4%) males and 115 (45.6%) females. The mean age was 67.4 ± 16.7 . Most of them were oncology patients (30.6%) and cerebrovascular patients (30.6%). Pressure ulcers' prevalence and incidence were 40.1% and 4.7%, respectively. The Braden score was a median of 13 (5-23). In patients with pressure ulcers, the Braden score and discharge home rate were significantly lower; admission from another intensive care unit, the length of stay, and the treatment costs were significantly higher.

Conclusion: Pressure ulcers negatively affect the patient's length of stay in the palliative care unit, the discharge rate to home, and the financial burden on the healthcare system. Pressure ulcer risk analysis and a standardized care plan to prevent and treat pressure ulcers should be performed for cost-effective palliative care.

Keywords: Palliative care, pressure ulcer, healthcare cost, prevalence, incidence

INTRODUCTION

With a prolonged life expectancy, increased prevalence of chronic diseases and cancer consequently increased the need for rehabilitation and palliative care. The World Health Organization defines "palliative care" as the relief of pain and other health problems in patients and families facing problems arising from a life-threatening illness (1). Palliative care does not aim to find curative treatment for diseases but to provide the management and control of symptoms and improve the comfort and life quality for the patient and his family in the last period of life (2).

A pressure ulcer is one of the most challenging problems to manage and control in palliative care units. They are lesions that occur on the skin or subcutaneous tissues due to pressure or friction and are often seen on bony prominences but can develop anywhere on the body (3, 4). Factors such as advanced age, immobilization, decreased sensorimotor sensation, a deterioration of nutritional status,

and a decreased walking ability are essential in developing pressure ulcers. In addition, the development of pressure ulcers may indicate circulatory failure that occurs in the last period of life and gradually deepens (5, 6). In this respect, all palliative care unit patients are candidates for pressure ulcer development.

Pressure ulcers are associated with prolonged hospital stays, increased costs, and lower discharge rates. So pressure ulcer frequency and risk factors, a well-known issue in intensive care units, should also be examined in palliative care units.

This study aimed to reveal the factors affecting pressure ulcer development, a critical problem in the palliative care unit, and pressure ulcer incidence and prevalence in the palliative care unit.

Corresponding Author: Mahmut Said Degerli **E-mail:** drmsdegerli@gmail.com

Submitted: 03.07.2023 **Revision Requested:** 21.07.2023 **Last Revision Received:** 21.07.2023 **Accepted:** 05.08.2023 **Published Online:** 07.08.2023



Content of this journal is licensed under a Creative Commons Attribution-NonCommercial 4.0 International License.

MATERIALS AND METHODS

The study's ethical approval was obtained by the local ethics committee of Haseki Training and Research Hospital (Approval number: 71-2022).

The data of 252 patients who received inpatient treatment in a secondary-level state palliative care unit between January 2016 and January 2022 were analyzed retrospectively.

The Braden scale was used in the risk assessment of patients for pressure ulcers (7). In the analysis, patients' admission Braden scores were considered. European Pressure Ulcer Advisory Panel (EPUAP), National Pressure Injury Advisory Panel (NPIAP), and Pan Pacific Pressure Injury Alliance (PPPIA) guidelines were used for staging pressure ulcers (3). Pressure ulcers of the patients were evaluated daily and staged. Patients with no pressure ulcers hole the palliative care period was included in group-1. Complete recovery of the existing pressure ulcer, or getting

Table 1. Demographic data of the patients

		Min-max		Median	Mean±SD	
Age (Year)		18.0	-	97.0	67.4	± 16.7
				N	%	
Sex	Male			137	54.4	
	Female			115	45.6	
Comorbidity	Diabetes mellitus			34	13.5	
	Hypertension			44	17.5	
	Heart disease			29	11.5	
	Pulmonary disease			14	5.6	
	Renal failure			1	0.4	
Admission to palliative care from	House			123	48.8	
	Other hospital			63	25.0	
	Intensive care unit			66	26.2	
Diagnosis	Oncology			77	30.6	
	Cerebrovascular disease			77	30.6	
	Alzheimer/dementia			22	8.7	
	Hypoxic brain			19	7.5	
	Traumatic brain injury			17	6.7	
	Senility			16	6.3	
	Parkinson			8	3.2	
	Other			16	6.3	
Cancer type	Colon			11	14.3	
	Gastric			11	14.3	
	Breast			8	10.4	
	Lung			8	10.4	
	Brain			8	10.4	
	Pancreas			6	7.8	
	Bladder			4	5.2	
	Endometrium			3	3.9	
	Rectum			3	3.9	
	Renal			2	2.6	
	Ovary			2	2.6	
	Cholangiocarcinoma			2	2.6	
	Cervix			2	2.6	
	Hepatocellular			1	1.3	
	Larynx			1	1.3	
	Nasopharynx			1	1.3	
	Esophagus			1	1.3	
	Prostate			1	1.3	
	Gallbladder			1	1.3	
	Salivary gland			1	1.3	

downstage, or decreasing the number of pressure ulcers were accepted as pressure ulcer healing, and these patients formed group-2. Patients whose pressure ulcers did not heal were

divided into two groups; the patients with stable pressure ulcers (group-3) and those with worsening pressure ulcers (group-4). Patients with worsening pressure ulcers (group-4) consisted of

Table 2. Pressure ulcer related patients data

		Min-max	Median	Mean ± SD
Braden score		5.0-23.0	13.0	13.0 ± 2.7
Length of stay		1.0-323.0	22.0	39.7 ± 51.6
Cost of hospitalization (dollar)		82.7-100146	3742.1	8656.6 ± 13889.4
			N	%
Pressure ulcer	Present		101	40.1
	None		151	59.9
Patients with pressure ulcer	Healed		20	19.8
	Did not healed		81	80.2
Patients whose pressure ulcers did not healed	Up staging pressure ulcers		8	9.9
	Stable pressure ulcers		61	75.3
	Added new pressure ulcers		12	14.8
Multiple pressure ulcers at admission	Present		49	48.5
	None		52	51.5
Pressure ulcer localization at admission	Sacrum		37	36.6
	Trochanter		2	2.0
	Ischium		4	4.0
	Heel		1	1.0
	Scapula		7	6.9
	Hand		1	1.0
	Multiple localization		49	48.5
Pressure ulcer localization at discharge	Sacrum		34	33.7
	Trochanter		4	4.0
	Ischium		4	4.0
	Heel		3	3.0
	Scapula		6	5.9
	Hand		1	1.0
	Multiple localization		49	48.5
Vacuum assisted closure	Present		18	7.1
	None		234	92.9
Discharge status	To home		88	34.9
	To intensive care unit		69	27.4
	Transferred		75	29.8
	Died		19	7.5
	Nursing home		1	0.4

patients whose pressure ulcers were getting up stage, or a new one was added to the existing pressure ulcer.

Groups;

group-1: patients with no pressure ulcers,

group-2: patients with healing pressure ulcers,

group-3: patients with stable pressure ulcers,

group-4: patients with worsening pressure ulcers,

Daily skincare and standard care plans were applied to all patients with pressure ulcers.

Table 3. Comparative analysis of patients with pressure ulcers and those without

		Pressure ulcer (+)		Pressure ulcer (-)		P
		Mean ± SD	Median	Mean ± SD	Median	
Age (Year)		69.6 ± 17.1	73.0	65.8 ± 16.3	67.0	0.050 ^a
Braden score		11.2 ± 1.9	11.0	14.1 ± 2.5	14.0	0.000 ^a
Length of stay		51.5 ± 57.8	29.0	31.7 ± 45.5	16.0	0.000 ^a
Cost of hospitalization (dollar)		10520 ± 13301	5155	7410 ± 14177	3014	0.000 ^a
		N	%	N	%	P
Sex	Male	53	52.5	84	55.6	0.622 ^b
	Female	48	47.5	67	44.4	
Comorbidity						
Diabetes mellitus		17	16.8	17	11.3	0.204 ^b
Hypertension		22	21.8	22	14.6	0.139 ^b
Heart disease		10	9.9	19	12.6	0.513 ^b
Pulmonary disease		4	4.0	10	6.6	0.366 ^b
Renal failure		0	0.0	1	0.7	1.000 ^b
Admission to palliative care from						
House		43	42.6	80	53.0	0.000 ^b
Other hospital		18	17.8	45	29.8	
Intensive care unit		40	39.6	26	17.2	
Vacuum assisted closure	(-)	83	82.2	151	100.0	0.000 ^b
	(+)	18	17.8	0	0.0	
Discharge status						
To home		28	27.7	60	39.7	0.049 ^b
To intensive care unit		40	39.6	29	19.2	
Transferred		27	26.7	48	31.8	
Died		5	5.0	14	9.3	
Nursing home		1	1.0	0	0.0	

^a Mann-Whitney U test / ^b Chi-square test (Fischer test)

The patients' age, gender, from where they were admitted, diagnosis on admission, comorbidities, length of hospitalization, discharge status, Braden scores in admission, oral intake insufficiency, the status of pressure ulcers, the pressure ulcer treatment method and the hospitalization costs of the patients were evaluated comparatively. In the study, prevalence means all patients who had pressure ulcers in admission and added new ones during hospitalization. Incidence means the patients who develop new pressure ulcers during the palliative care period.

Statistical Analyses

Mean, standard deviation, median, minimum, maximum, frequency, and ratio values were used for the descriptive statistics of data. The distribution of variables was calculated by the Kolmogorov-Smirnov test. Independent quantitative data were analyzed by the Mann-Whitney U test. The Chi-Square test was used to examine independent qualitative data, and the Fischer test was used when the Chi-square test conditions were not met. SPSS 28.0 program was used in the analysis.

Table 4. Comparative analysis of patients whose pressure ulcers healed and those not

		Pressure ulcer				p
		Healed		Not healed		
		Mean ± SD	Median	Mean ± SD	Median	
Age (Year)		71.7 ± 15.8	74.0	69.1 ± 17.4	72.0	0.571 ^a
Braden score		11.3 ± 1.4	11.0	11.2 ± 2.0	11.0	0.812 ^a
Length of stay		34.8 ± 39.2	23.5	55.7 ± 61.0	29.0	0.114 ^a
Cost of hospitalization (dollar)		9112.1 ± 7396.1	6285.8	10867.0 ± 14405.7	4530.2	0.506 ^a
		N	%	N	%	p
Sex	Male	11	55.0	42	51.9	0.801 ^b
	Female	9	45.0	39	48.1	
Comorbidity						
Diabetes mellitus		4	20.0	13	16.0	0.672 ^b
Hypertension		6	30.0	16	19.8	0.320 ^b
Heart disease		3	15.0	7	8.6	0.410 ^b
Pulmonary disease		1	5.0	3	3.7	1.000 ^b
Admission to palliative care from						
House		8	40.0	35	43.2	0.948 ^b
An other hospital		4	20.0	14	17.3	
Intensive care unit		8	40.0	32	39.5	
Vacuum assisted closure	(-)	17	85.0	66	81.5	0.713 ^b
	(+)	3	15.0	15	18.5	
Discharge status						
To home		4	20.0	24	29.6	0.389 ^b
To intensive care unit		11	55.0	29	35.8	
Transferred		5	25.0	22	27.2	
Died		0	0.0	5	6.2	
Nursing home		0	0.0	1	1.2	

^aMann-Whitney U test / ^bChi-square test (Fischer test)

RESULTS

The data of 252 patients who received inpatient treatment in the palliative care unit between January 2016-2022 were analyzed. There were 137 (54.4%) male and 115 (45.6%) female patients. The mean age was 67.4 ± 16.7 . The most common comorbid diseases of the patients were hypertension (17.5%) and diabetes mellitus (13.5%). Almost half, 48.8%, of the patients were admitted from home. Mainly oncology (30.6%) patients and cerebrovascular disease (30.6%) patients were admitted (Table 1).

The Braden score of the patients was found to be a median of 13 (5-23). Pressure ulcers prevalence in our palliative care unit was 40.1%. Although daily wound care was performed in 81 (80.2%) patients with pressure ulcers, healing could not be achieved. It was observed that new pressure ulcers were added in 12 of the patients whose pressure ulcers did not heal. Pressure ulcers incidence in our palliative care unit was 4.7%. There was more than one pressure ulcer at admission in 49 (48.5%) patients with pressure ulcers. Vacuum-assisted closure (VAC) was used in the treatment of 18 patients with pressure ulcers. While 34.9% of the patients were discharged home, 29.8% were transferred to a tertiary-level center, and 27.4% were transferred to the intensive care unit. Nineteen (7.5%) patients died in the palliative care unit. The mean length of stay was 39.7 ± 51.6 days, and the mean cost of hospitalization was 8656.6 ± 13889.4 dollars (Table 2).

The Braden score and the rate of discharge to home were significantly lower in patients with pressure ulcers than those without wounds ($p < 0.05$). The rate of admission from another intensive care unit, the length of hospital stay, and hospitalization cost was significantly higher in the group with pressure ulcers than in the group without pressure ulcers ($p < 0.05$) (Table 3).

In the comparative analysis of patients whose pressure ulcers healed and those who did not, no significant difference was found in terms of where they were admitted from, Braden scores, rate of vacuum assisted closure (VAC) use, the rate of discharge home, the length of hospital stay, and hospitalization cost ($p > 0.05$) (Table 4).

In the comparative analysis of patients whose pressure ulcers worsened and those were stable, it was observed that the rate of VAC use and the cost of hospitalization were significantly higher in patients with worsening pressure ulcers ($p < 0.05$) (Table 5).

DISCUSSION

The increasing elderly population, chronic diseases, and cancer have increased the need for palliative care. Palliative care aims to feel the patients and their relatives well in the last period of life, and it has been fully integrated into healthcare systems in developed countries. In modern healthcare systems, every patient has the right to palliative care (8).

With aging, there are changes such as thinning of the subcutaneous tissue, loss of collagen and elastic fibers, decrease in vascularity, and disruption of the skin's barrier function. Additional factors such as a deterioration in nutritional status, cachexia, and immunosuppression due to cytokines such as tumor necrosis factor (TNF) α , as in cancer patients, or accompanied by immobilization and loss of sensorimotor sensation, as in cerebrovascular disease, further increases pressure ulcer development risk. In addition, it should be remembered that in the last period of life, inevitable pressure ulcers may be encountered due to the inadequacy of homeostatic mechanisms. For all these reasons, palliative care patients are candidates for pressure ulcer development (9).

Pressure ulcers prevalence in palliative care is between 17% to 47% in the literature (10). In Galvin's study, pressure ulcers prevalence in the palliative care unit was 38.1%, and the incidence was 12% (11). Hendrichova et al. reported the pressure ulcers prevalence as 22.9% and the incidence as 6.7% in cancer patients in the palliative care unit (10). When we look at the data from Turkiye, Gencer et al. found the general prevalence of pressure ulcers in a university hospital was 2.49% and the incidence 1.9% (12). Studies conducted in the intensive care unit show that the rate of pressure ulcers varies between 15-29% (13). In their study, Zengin and Tasci found that the pressure ulcer frequency in the palliative care unit is as high as 36.1% (1). In our study, pressure ulcers prevalence was 40.1%, and the incidence was 4.7%. This result shows that if correct risk analysis is performed and protection is taken, the incidence of pressure ulcers could decrease even if the prevalence is very high.

In our study, the mean age, gender distribution, diagnoses in admission, and comorbid diseases of the patients were compatible with the literature.

Since the frequency of pressure ulcers varies from each other in the general population, clinical units, intensive care units, and palliative care units, all patients should be well questioned about where they are admitted from and their previous care history. The risk of pressure ulcers is higher in patients with a history of organ dysfunction that requires intensive care follow-up. Our study observed that admission from the intensive care unit was significantly higher in patients with pressure ulcers.

The Norton, Braden, and Waterlow scales are commonly used scales for pressure ulcer risk assessment of patients (14). Pressure ulcer risk analysis is performed by evaluating sensory perception, activity, mobility, humidity, nutrition, and friction/shearing with the Braden scale, and patients receive a score between 6 and 23. The risk of pressure ulcers increases as the Braden scale total score decreases (7). Our study's median Braden score was 13 (5-23). This low score shows the high risk of pressure ulcers in palliative care patients. Additionally, the Braden score was significantly lower in patients with pressure ulcers than those without wounds. This result indicates we can safely use the Braden scale in palliative care unit patients.

The rate of discharge to home in a palliative care unit is accepted as one of the indicators of success (1). Yuruyen et al. found the discharge rate to home in the tertiary level palliative care unit to be 52%. In the same study, the transfer rate to intensive care was 15.3%, and mortality in the palliative care unit was 33.4% (15). Starks et al. in their study, which used data from two different hospitals' palliative care units, found the discharge rate to home to be 13.4% and 15.3%, respectively. In the same

study, the rate of discharge to a skilled nursing facility was 15.3% and 33.0%, and the rate of discharge to a hospice was 22.1% and 3.3%. Starks et al. found 37.3% and 39.5% mortality rates in the palliative care unit in their study (16). In our study, 34.9% of the patients were discharged home, while 29.8% were transferred to a tertiary level center and 27.4% to the intensive care unit. The mortality rate was found to be 7.5%. Our study observed that the discharge rate to home was significantly

Table 5. Comparative analysis of patients whose pressure ulcers worsened and those stable

		Pressure ulcer				p
		Worsened		Stable		
		Mean ± SD	Median	Mean ± SD	Median	
Age (Year)		67.1 ± 17.3	70.0	69.8 ± 17.5	72.0	0.595 ^a
Braden score		10.7 ± 1.5		11.4 ± 2.1		0.153 ^a
Length of stay		62.8 ± 55.1		53.3 ± 63.0		0.369 ^a
Cost of hospitalization(dollar)		11638.0 ± 7927.9		10614.3 ± 16016.7		0.033 ^a
		N	%	N	%	p
Sex	Male	10	50.0	32	52.5	0.849 ^b
	Female	10	50.0	29	47.5	
Comorbidity						
Diabetes mellitus		3	15.0	10	16.3	0.224 ^b
Hypertension		3	15.0	13	21.3	0.538 ^b
Heart disease		2	10.0	5	8.2	1.000 ^b
Pulmonary disease		0	0.0	3	3.7	0.571 ^b
Admission to palliative care from						
House		5	25.0	30	49.2	0.158 ^b
An other hospital		5	25.0	9	14.8	
Intensive care unit		10	50.0	22	36.1	
Vacuum assisted closure	(-)	13	65.0	53	86.9	0.029 ^b
	(+)	7	35.0	8	13.1	
Discharge status						
To home		3	15.0	21	34.4	0.099 ^b
To intensive care unit		13	65.0	16	26.2	
Transferred		3	15.0	19	31.1	
Died		1	5.0	4	6.6	
Nursing home		0	0.0	1	1.6	

^a Mann-Whitney U test / ^b Chi-square test (Fischer test)

lower in patients with pressure ulcers than in those without. This result shows that the development of pressure ulcers directly affects the success of palliative care.

Although the rate of discharge to home was consistent with the literature in our study, transfer rates to a tertiary-level center and intensive care unit were found to be high since our unit is located in a secondary-level hospital. The 7.5% mortality rate for the palliative care unit seems relatively low. The mortality rate was low because the discharge status of the patients transferred to a tertiary-level center and intensive care unit was unknown and was not evaluated in this study.

Unfortunately, the capacity of palliative care units, which has yet to be fully integrated into healthcare systems in many countries, to afford the supply-demand balance is also limited. Therefore, how long it takes to discharge home successfully is extremely important for both patient and their relatives, and the burden on the healthcare system. Factors such as a limitation of movement, feeding tube, permanent tracheostomy, hypertension, infection, and pressure ulcers affect the duration of stay in the palliative care unit (1). Our study observed that the length of stay in the palliative care unit was longer in patients with pressure ulcers than in patients without ulcers.

Cost analyses are essential to understand the burden of palliative care units on the healthcare system and to produce appropriate solutions. Pressure ulcers increase the length of hospital stay and treatment costs and the burden on the healthcare system. Our study observed that the financial burden of patients with pressure ulcers on the healthcare system was significantly higher.

Comparative analyses of patients whose pressure ulcers healed and those who did not, revealed that no real success can be achieved even if the best care services and treatment options are offered after pressure ulcers develop in the palliative care unit. The length of stay in the palliative care unit of the patients whose wounds healed was as long as those who did not. Similarly, the discharge rate to home was found to be low, and the costs increased. This result shows the importance of pressure ulcer risk analysis and prevention of pressure ulcers before they develop.

Comparative analyses of patients with worsening pressure ulcers and patients with stable pressure ulcers showed no significant difference in the rate of discharge to home and length of hospital stay between the two groups and that the use of VAC and costs were higher in patients with worsening pressure ulcers. This result shows that despite the expensive treatment such as VAC, real success has yet to be achieved, and the costs have increased (Table 5).

The most important limitations of our study were that it is retrospective and with a limited number of patients. In addition, since our palliative care unit is in a secondary level health care

institution, the final status of the patients transferred to a tertiary-level center could not be evaluated.

In conclusion, pressure ulcers negatively affect the patient's length of stay in the palliative care unit, the rate of discharge to home, and the financial burden on the healthcare system. In order to obtain cost-effective and successful results in palliative care units, a pressure ulcer risk analysis and a standardized care plan to prevent and treat pressure ulcers should be performed.

Ethics Committee Approval: The study's ethical approval was obtained by the local ethics committee of Haseki Training and Research Hospital (Approval number: 71-2022).

Conflict of Interest: The author declare that there is no conflict of interest.

Financial Disclosure: The authors declare that this study has received no financial support.

REFERENCES

- Zengin H, Taşçı İ. Factors influencing the length of stay in the palliative care unit in patients discharged home: results from a tertiary hospital in Turkey. *Turk J Med Sci* 2021; 51(5): 2420-6.
- Dincer M, Doger C, Tas SS, Karakaya D. An analysis of patients in palliative care with pressure injuries. *Niger J Clin Pract* 2018; 21(4): 484-91.
- National Pressure Ulcer Advisory Panel, European Pressure Ulcer Advisory Panel, Pan Pacific Pressure Injury Alliance, Prevention and Treatment of Pressure Ulcers: Clinical practice guideline. Cambridge Media, 2019.
- National Pressure Injury Advisory Panel, European Pressure Ulcer Advisory Panel, Pan Pacific Pressure Injury Alliance, Prevention and Treatment of Pressure Ulcers: Clinical practice guideline. Cambridge Media, 2014.
- Edsberg LE, Black JM, Goldberg M, McNichol L, Moore L, Sieggreen M. Revised National Pressure Ulcer Advisory Panel Pressure Injury Staging System: revised pressure injury staging system. *J Wound Ostomy Continence Nurs.* 2016; 43(6): 585-97.
- Edsberg LE, Langemo D, Baharestani MM, Posthauer ME, Goldberg M. Unavoidable pressure injury: state of the science and consensus outcomes. *J Wound Ostomy Continence Nurs* 2014; 41(4): 313-34.
- Braden BJ, Bergstrom N. Predictive validity of the Braden Scale for pressure sore risk in a nursing home population. *Res Nurs Health* 1994; 17(6): 459-70.
- Kavşur Z, Sevimli E. Türkiye'deki Palyatif Bakım Hizmetlerinin Bazı Gelişmiş Ülkeler ile Karşılaştırılması. *USBAD Uluslararası Sosyal Bilimler Akademi Dergisi* 2020; 2(4): 715-30.
- B Beers EH. Palliative Wound Care: Less Is More. *Surg Clin North Am.* 2019; 99(5): 899-919.
- Hendrichova I, Castelli M, Mastroianni C, Piredda M, Mirabella F, Surdo L, et al. Pressure ulcers in cancer palliative care patients. *Palliat Med* 2010; 24(7): 669-73.
- Galvin J. An audit of pressure ulcer incidence in a palliative care setting. *Int J Palliat Nurs* 2002; 8(5): 214-21.
- Gencer Z, Özkan Ö. Pressure ulcers surveillance report. *Journal of the Turkish Society of Intensive Care-Türk Yoğun Bakım Derneği Dergisi* 2015; 13: 26-30.

13. Karayurt Ö, Akyol Ö, Kılıçaslan N, Akgün N, Sargın Ü, Kondakçı M, et al. The incidence of pressure ulcer in patients on mechanical ventilation and effects of selected risk factors on pressure ulcer development. *Turk J Med Sci* 2016; 46(5): 1314-22.
14. Šateková L, Žiaková K, Zeleníková R. Predictive validity of the Braden Scale, Norton Scale, and Waterlow Scale in the Czech Republic. *Int J Nurs Pract* 2017; 23(1).
15. Yürüyen M, Özbaş Tevetoğlu I, Tekmen Y, Polat Ö, Arslan İ, Okuturlar Y. Prognostic factors and clinical features in palliative care patients. *Konuralp Med J* 2018; 10 (1): 74-80
16. Starks H, Wang S, Farber S, Owens DA, Curtis JR. Cost savings vary by length of stay for inpatients receiving palliative care consultation services. *J Palliat Med* 2013; 16(10): 1215-20.

Investigation of the Effect of Serum IL-1 β Levels on Atherosclerosis: A Turkish Population-Based Study

Dilveen Dlawer Omer¹ , Fatma Tuba Akdeniz² , Seda Gulec Yilmaz² , Zerrin Barut³ ,
Deryanaz Billur¹ , Ayca Turer Cabbar⁴ , Turgay Isbir¹ 

¹Department of Molecular Medicine, Institute of Health Sciences, Yeditepe University, Istanbul, Turkiye.

²Department of Medical Biology, Faculty of Medicine, Yeditepe University, Istanbul, Turkiye.

³Department of Basic Medical Sciences, Faculty of Dentistry, Antalya Bilim University, Antalya, Turkiye.

⁴Department of Cardiology, Faculty of Medicine, Yeditepe University, Istanbul, Turkiye

ORCID ID: D.D.O: 0000-0001-9213-445X; F.T.A: 0000-0002-6076-0509; S.G.Y: 0000-0002-8119-2862; Z.B: 0000-0002-6289-5562;
D.B: 0000-0002-6079-8224; A.T.C: 0000-0002-3521-2666; T.I: 0000-0002-7350-6032

Cite this article as: Dlawer Omer D, Akdeniz FT, Gulec Yilmaz S, Barut Z, Billur D, Turer Cabbar A, Isbir T. Investigation of the effect of serum IL-1 β levels on atherosclerosis: A Turkish population-based study. *Experimed* 2023; 13(2): 142-147.

ABSTRACT

Objective: Atherosclerosis, as a cardiovascular disease associated with chronic inflammatory conditions and involving a large number of risk factors, harbors a lot of unknowns. Evidence has emerged that almost all stages of the disease are intertwined with inflammation. It has not been fully elucidated in which stages and how interleukin-1 beta (IL-1 β), which is associated with inflammations, plays a role in the chronic inflammatory process of the disease. Also, the effect on atherosclerosis progression and biomarker candidacy of IL-1 β in the Turkish population is unknown. The aim of this study was to investigate the serum IL-1 β expression levels and whether it is associated with changes in risk factors that develop due to the disease in the Turkish population.

Materials and Methods: ELISA method was used to analyze the serum IL-1 β levels. Statistical data was obtained utilizing the SPSS v.23 software.

Results: No linkage evidence was found between the serum IL-1 β and atherosclerosis ($p>0.05$). However, the serum IL-1 β levels were significantly associated with gender, smoking status, and diabetes history within the study population were significantly associated ($p=0.050$). According to the lipid profile result, the triglyceride value was found to be significantly decreased in atherosclerosis patients when compared to healthy individuals ($p=0.012$). Additionally, factors including, gender, smoking status, and history of diabetes were significantly associated with serum cholesterol level ($p=0.015$).

Conclusion: Although no correlation was found between the serum IL-1 β levels of the study groups, it was observed that the serum IL-1 β expression alters in patients with atherosclerosis depending on age. In addition, low triglyceride levels may be a marker of disease in atherosclerosis patients. Studies involving different ethnic groups with a large sample and identifying the stages of the disease are necessary to confirm these results.

Keywords: Atherosclerosis, inflammation, IL-1 β , triglyceride, lipid level, serum

INTRODUCTION

Atherosclerosis, which is considered to be one of the leading diseases among the causes of death worldwide, is a multi-stage disease in which many factors are involved (1). Due to the age-related development of atherosclerosis and the effect of inflammation on the formation of the

disease, it has become clear through recent studies that age and inflammation can be counted among the risk factors of atherosclerosis (2, 3). There is increasing evidence that aging has not been associated with atherosclerosis as a one-way relationship (2). The changes that occur in the vessels, especially with increased age, are similar to several characteristic pathological processes

Corresponding Author: Turgay Isbir **E-mail:** turgay.isbir@yeditepe.edu.tr

Submitted: 01.02.2023 **Revision Requested:** 13.03.2023 **Last Revision Received:** 27.03.2023 **Accepted:** 24.04.2023 **Published Online:** 10.07.2023



Content of this journal is licensed under a Creative Commons Attribution-NonCommercial 4.0 International License.

seen in atherosclerosis presentations (4). It is reported that proinflammatory changes in monocytes/macrophages in the development of atherosclerosis change with age. One of the most important factors underlying the molecular infrastructure of atherosclerosis is the alteration in the expression of cytokines. An increase in the level of free radicals was parallelly observed with the activation and increased secretion of many cytokines, including interleukin-1 beta (IL-1 β), within obtained data from patients with atherosclerosis (5).

The pathways that trigger or participate in inflammation determine the direction of atherogenesis, so risk factors linked with these pathways have long been associated with each stage of atherosclerosis and its complications. Although many molecular actors like interleukins (ILs) are detected in cardiovascular diseases, IL-1 β has emerged as a therapeutic target among these ILs (6). A substantial number of studies have demonstrated the effect of IL-1 β on atherosclerosis along with varying properties at different stages (7-9). The inflammatory response that develops in endothelial cells, which is known to occur especially in the primary stage of atherosclerosis, and the accumulation of inflammatory factors induced by this response in the vessels are promoted by IL-1 β (6). IL-1 β has a pivotal effect on atheroma growth. It is associated with a lower inflammatory response, increased IL-10 expression, and reduced plaque size when neutralized in studies on atherosclerosis disease (10). IL-1 β , a member of the IL-1 family associated with coronary diseases, is significantly elevated in both mRNA and protein levels in patients with atherosclerosis as shown in various case-control studies (11, 12). The contribution of IL-1 β in the development and progression of the disease is also related to the signals that cause its expression and the molecules involved in its synthesis. IL-1 β is a product largely produced by macrophages and monocytes as part of a multi-step process. Activation of the precursor IL-1 β is triggered by the accumulation of molecules such as cholesterol crystals and oxidized low-density lipoprotein (LDL). The maturation process is carried out by caspase-1 or various enzymes detected in human atherosclerotic plaques (6). Therefore, changes in the lipid profile are key factors in the course of the disease by contributing to the formation of a pro-inflammatory response in the development of atherosclerosis, and are important markers for understanding the molecular mechanism of this disease (6). In addition to cholesterol crystals and oxidized LDL, triglycerides are associated with the development of atherosclerosis. It has been reported that a high triglyceride level is a risk factor for coronary heart disease (13).

Since atherosclerosis is a disease that threatens public health worldwide, like other cardiovascular diseases, its exact molecular mechanism unknown, the expression level of IL-1 β as a cytokine, aging, and lipid profiles that are reported to play important roles in the course of this disease have been investigated in the Turkish population.

MATERIALS AND METHODS

Study Population and Clinical Procedures

This study was performed per tenets of the Declaration of Helsinki. Ethical approval was obtained for this study from the Yeditepe University Medical Faculty Ethics Committee (Date: 01/30/2020 and No: 1793). All participants were selected and examined by the Department of Cardiology, Yeditepe University Hospital, and signed an informed consent form prior to the investigation. A total of 69 individuals of which thirty-nine were patients (31 males / 8 females) diagnosed with atherosclerosis were utilized. The control group involved thirty healthy subjects who do not have any disease including cardiovascular diseases (26 males / 4 females). Age ranges of subjects were between 30 and 80 years. Parameters such as age, gender, smoking status, diabetes history, and serum lipid levels (high-density lipoprotein (HDL), LDL, and triglyceride) of the study population were obtained from the hospital.

IL-1 β Determination by ELISA

Following ethical procedures, the determination of serum IL-1 β levels was performed using the commercial Human IL-1 β Enzyme Linked Immunosorbent Assay (ELISA) assay kits (Biosource, Nivelles, Belgium), according to the manufacturer's instructions, and using the microplate reader with the ability to measure absorbance at 450 nm (WHYM201). The detection limit was 0.06 pg/ml for IL-1 β .

Statistical Analysis

Statistical analysis was performed using the SPSS-22 software (SPSS, Inc, Chicago, IL, USA), and the values were expressed as mean \pm standard deviation (SD). The value's significance level was $p < 0.05$. The demographic records were compared and the serum IL-1 β levels of the study population were analyzed by the student's t-test, Chi-square test, one-way ANOVA, and the Mann-Whitney U test.

RESULTS

Table 1 shows the demographic characteristics of the study participants. Of the sixty-nine total individuals, thirty-nine were patients (79.0% male, 21.0% female) with ages of 62.95 ± 10.96 years, and 30 individuals were healthy controls (87.0% male, 13.0% female) aged 59.96 ± 9.36 years. The mean age ($p=0.143$) and gender ($p=0.533$) of the study population were not significantly different. In 33.0% of patients and 17.0% of healthy individuals, a history of diabetes was present. There was no significant difference between the study groups regarding this parameter ($p=0.698$). While the frequency of smoking was 38.0% among those with atherosclerosis, it was 53.0% in the group of healthy individuals. As shown in Table 1 smoking data of both groups was not statistically significant ($p=0.470$).

When the effect of serum lipid levels on disease progression in human serum samples with atherosclerosis and healthy

Table 1. Demographic data of the study subjects.

Characteristic	Patient (n=39)	Control (n=30)	p-value
Age (Years; mean± SD)	62.9 5± 10.96	59.96 ± 9.36	0.143
Gender (Male / Female; %)	79.0 / 21.0 (n=31) / (n=8)	87.0 / 13.0 (n=26) / (n=4)	0.533
History of Diabetes (Yes / No; %)	33.0 / 67.0 (n=13) / (n=26)	17.0 / 83.0 (n=5) / (n=25)	0.698
Smoking (Yes / No; %)	38.0 / 62.0 (n=15) / (n=24)	53.0 / 47.0 (n=16) / (n=14)	0.470

n=number of the sample; SD: Standard deviation

Table 2. Comparison of total cholesterol, triglycerides, LDL, HDL parameters of the study population.

Parameter	Patient (n=39)	Control (n=30)	p-value
Cholesterol (mg/dl)	185.15 ± 7.97	174.40 ± 6.25	0.34
Triglycerides (mg/dl)	132.31 ± 6.68	142.33 ± 14.63	0.012*
LDL (mg/dl)	120.61 ± 6.72	105.23 ± 6.19	0.329
HDL (mg/dl)	36.74 ± 1.14	40.23 ± 1.55	0.685

n=number of the sample; *p<0.05

individuals were examined, no relationship was found between cholesterol (p=0.34), LDL (p=0.329), and HDL (p=0.685) concentrations and atherosclerosis, except for triglycerides. In the group of patients with atherosclerosis, it was determined that the triglyceride level was significantly decreased (p=0.012) (Table 2). Although no difference was found in cholesterol levels between the patient and control groups in our study population, it was found that gender, smoking status, and diabetes history were associated with cholesterol levels (p=0.015).

Serum IL-1β levels were measured in both patient and control groups. Although lower IL-1β levels were detected in the patient group (12.90 ± 7.538 pg/ml) as compared to the control group (13.47 ± 19.565 pg/ml), no significance was found (p>0.05). Additionally, representative histograms of serum IL-1β and triglyceride concentrations are given in Figure 1 and 2.

Further, to understand how the serum IL-1β level changes depending on age in both the patient and control groups, analyses were performed in three different age groups: less than 50 years old (<50), between 50-60 years old, and over 60 years old (60>). Out of thirty-nine patients with atherosclerosis, serum IL-1β expression levels at <50, 50-60, and 60> age groups were 17.23 ± 19.23 pg/mL, 10.93 ± 6.19 pg/mL, and 13.07 ± 6.47 pg/mL, respectively. Out of thirty healthy individuals, the IL-1β expression level results for <50, 50-60, and 60> age groups were as follows; 11.86 ± 6.28 pg/mL, 7.28 ± 5.27 pg/mL, and 19.11 ± 28.57 pg/mL. While the serum IL-1β level in

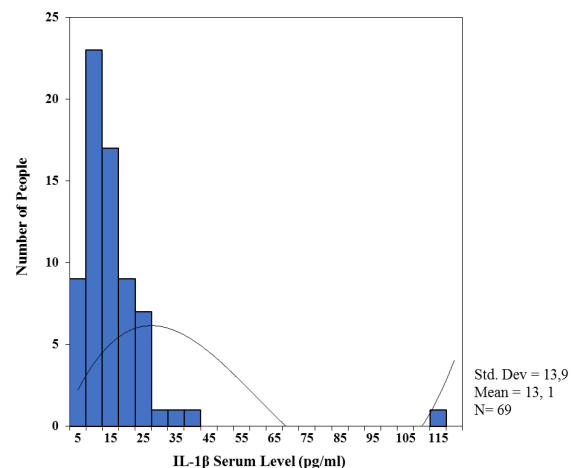


Figure 1. Representative histogram of IL-1β.

the patient group was higher in the group aged 50 years and below, the opposite result was obtained in the control group. In the control group, the highest level of IL-1β was detected in the 60 years and older group (Figure 3).

Within the scope of our research, it was also investigated whether there was any association between the demographic and clinical data of the study groups and IL-1β expression level. Smoking and history of diabetes (p=0.143) and smoking and

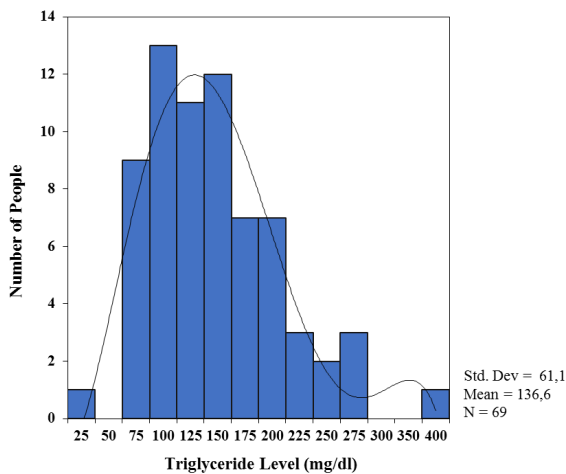


Figure 2. Representative histogram of serum triglyceride levels.

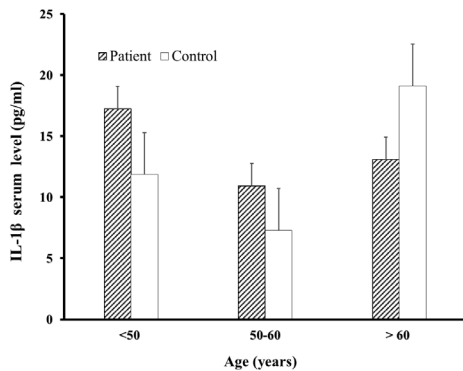


Figure 3. Distribution of serum IL-1 β level in both patients with atherosclerosis and control groups by age.

gender ($p=0.541$) did not show any significant difference for IL-1 β expression levels between the groups. Diabetes history alone was also not significantly related to serum IL-1 β between the groups ($p=0.833$). On the other hand, serum IL-1 β levels with gender, smoking, and diabetes history within the study population were significantly associated ($p=0.050$).

DISCUSSION

In literature, this is the first study to investigate the IL-1 β expression level in human serum samples, its age-related change in atherosclerosis, and the serum concentration of triglyceride value in patients with atherosclerosis in the Turkish population.

In humans, the role of the proinflammatory cytokine IL-1 β in atherosclerosis is not well-defined. By designing a case-control study in the Turkish population that included individuals with atherosclerosis and those without atherosclerosis, we examined the association of clinical data with the disease and the expression profile of the serum inflammatory cytokine IL-1 β . Extensively investigated IL-1 β levels by researchers all over the world was

not a risk factor for atherosclerosis when compared to healthy individuals in the Turkish population. In this study population it showed that IL-1 β alone does not play a role in the disease and cannot be a stand-alone biomarker for atherosclerosis.

The great majority of studies were conducted utilizing animal experiments, and very few population-based human studies have been performed. In addition, studies with the IL-1 family generally examined the consequences of their blockade of disease development and progression (14, 15). The common consensus that emerged from studies that have accumulated over the years was that inflammation has a visible link in coronary artery disease progression and each stage of the atherosclerosis process (16).

An animal study by Vromman et al. provided evidence that blocking IL-1 β mainly brought blood monocytes to a less inflammatory state during atherogenesis, reduced atheroma size, and increased plasma levels of IL-10 (10).

One of the few population-based studies in the literature, Di Iorio et al. within the scope of the InCHIANTI project, measured IL-1 β levels in 1,292 human samples collected from two different cities in Italy. As a result of the study, it showed that IL-1 β did not change depending on age and gender but was associated with clinical conditions such as angina and serum calcium level (16). A cross-sectional study was performed by Joung et al. to determine whether IL-1 β could be a marker for cardiovascular disease (15). As in our study, no significant relationship was found between the patients and study groups regarding serum IL-1 β levels. However, when its relationship with other parameters in the study was examined, it could be an independent risk factor for newly diagnosed cardiovascular disease in smoking patients (16). Though the link of IL-1 β expression with atherosclerosis development and progression has been shown in these studies, no significant relationship has been found between IL-1 β expression and atherosclerosis in this study. Such contradictory results may be because the studies were conducted on different ethnic groups, as well as the sample size, human serum samples that were used, the nutritional preferences of the individuals included in the study, and the drugs used by the individuals.

In the context of this study, we examined whether the IL-1 β expression levels change with regards to age. In patients with atherosclerosis, the IL- β serum concentration was highest in the age group of 50 and below (17.23 ± 19.23 pg/mL). IL-1 β concentration reached the highest value in the 60-year and older group within the control group (19.11 ± 28.57 pg/mL). Despite these results, there was not a significant difference within or between the groups. Studies showing that aging is an independent risk factor for atherosclerosis are growing exponentially. In addition to the changes in the aging vessels, alterations in the expression profiles of the proinflammatory molecules, IL-1 β , were observed (17). The most plausible explanation for the higher concentration of IL-1 β expression in atherosclerosis patients under 50 years of age in our study

population may be that this cytokine is activated in the early stages of inflammation (18). In the control group, the high concentration measured in individuals aged 60 and older can be considered as sign of age-related inflammatory processes.

Parallel to the increased expression of proinflammatory cytokines, there was an increase in the level of atherogenic lipoprotein. Therefore, the lipid profiles of the study groups were measured, and their association with atherosclerosis was assessed. This study reported that triglyceride levels significantly decreased in atherosclerosis patients ($p=0.012$). Although many studies were conducted regarding high triglyceride levels and increased IL-1 β activity in relation to the disease, few studies reported on the contribution of low triglyceride to the biology of atherosclerosis.

Although decreased serum triglyceride levels are predictors of cardiovascular death in patients with heart failure, the reasons for the low triglyceride levels remain unknown and require further investigation. This decline may be explained by various mechanisms. Studies that revealed these possibilities are available in the literature.

Research on chronic heart failure reported a link between low triglyceride levels and the disease. It showed that decreased triglyceride levels could be an independent marker of cardiac death (19). In addition, factors such as nutritional deficiency and increased inflammation could also be among the causes of changes in triglyceride levels. Since the triglyceride value of 150mg/dl is accepted as an indicator that does not pose a risk to human health, it is important to understand the atherosclerosis of patients in our selected population with an average of 132.31mg/dl level (20). Also, the decreased level of IL-1 β (albeit non-significant) as an outcome of this study may have contributed to the low serum triglyceride levels in atherosclerosis by preventing lipolysis. This kind of change in cytokine activity can alter the molecular response to inflammation by affecting the serum triglyceride level, leading to a change in the lipid profile.

Study Limitations

This study contained some limitations that should be discussed. The most important of these is that the sample size was not large enough to achieve substantial results. In addition, the fact that only a single population was studied could have caused the results to differ from previous studies. The varied ages of the individuals in the study groups was another factor. Different age groups may cause different outcomes, so it may be necessary to narrow the age range in future studies. In addition, there is a close relationship between cardiovascular diseases and nutrition, therefore, the dominance of the Mediterranean diet in the Turkish population may have also affected the results.

CONCLUSION

Consequently, although a significant relationship could not be demonstrated, this study exhibited data showing that

monitoring and analyzing serum IL-1 β levels according to age groups could provide information regarding the course of atherosclerosis. In addition, this study is one of the few examining the relationship between serum IL-1 β concentration and atherosclerosis amidst the Turkish population. It was found that the triglyceride level decreased in this patient group population. These results did not support the role of decreased IL-1 β level in atherosclerosis in the Turkish population, but consequently showed that triglyceride levels decreased in patients with atherosclerosis. It will be important to carry out further studies utilizing larger sample groups and different ethnic populations regarding the possible elements of the molecular mechanism that caused this result.

Ethical Approval: All procedures performed in studies involving human participants were under the ethical standards of the 1975 Declaration of Helsinki guidelines and its later amendments. The research on humans study protocol was approved by the Yeditepe University Medical Faculty Ethics Committee (Date: 01/30/2020 and No: 1793).

Authors' Contributions: Conception/Design of Study – T.I., D.D.O.; Supervision – T.I., Data Acquisition – A.T.C.; Performing experiments – D.D.O., F.T.A.; Analysis and/or Interpretation – S.G.Y., F.T.A., D.D.O., Z.B., D.B.; Drafting Manuscript – T.I., D.D.O., D.B.; Critical Revision of Manuscript – T.I., S.G.Y., F.T.A., D.D.O., Z.B., A.T.C., D.B.; Final Approval and Accountability– T.I. All authors read, revised, and approved the final article.

Conflicts of Interest: The authors declare no conflict of interest.

Financial Disclosure: The authors declare that this study has received no financial support.

REFERENCES

1. Worthley SG, Osende JI, Helft G, Badimon JJ, Fuster V. Coronary artery disease: pathogenesis and acute coronary syndromes. *Mt Sinai J Med* 2001; 68(3): 167-81.
2. Bolton E, Rajkumar C. The ageing cardiovascular system. *Rev Clinical Gerontol* 2010; 21(2): 99-109.
3. Taleb S. Inflammation in atherosclerosis. *Arch Cardiovasc Dis* 2016; 109(12): 708-15.
4. Wang JC, Bennett M. Aging and atherosclerosis: mechanisms, functional consequences, and potential therapeutics for cellular senescence. *Circ Res* 2012; 111(2): 245-59.
5. Calvert PA, Liew TV, Gorenne I, Clarke M, Costopoulos C, Obaid DR, et al. Leukocyte telomere length is associated with high-risk plaques on virtual histology intravascular ultrasound and increased proinflammatory activity. *Arterioscler Thromb Vasc Biol* 2011; 31(9): 2157-64.
6. Mai W, Liao Y. Targeting IL-1 β in the treatment of atherosclerosis. *Front Immunol* 2020; 11: 589654.
7. Libby P. Interleukin-1 Beta as a target for atherosclerosis therapy: Biological basis of CANTOS and beyond. *J Am Coll Cardiol* 2017; 70(18): 2278-89.
8. Kirii H, Niwa T, Yamada Y, Wada H, Saito K, Iwakura Y, et al. Lack of interleukin-1beta decreases the severity of atherosclerosis in ApoE-deficient mice. *Arterioscler Thromb Vasc Biol* 2003; 23(4): 656-60.

9. Abbate A, Van Tassell BW, Biondi-Zoccai GG. Blocking interleukin-1 as a novel therapeutic strategy for secondary prevention of cardiovascular events. *Biodrugs* 2012; 26(4): 217–33.
10. Vromman A, Ruvkun V, Shvartz E, Wojtkiewicz G, Santos Masson G, Tesmenitsky Y, et al. Stage-dependent differential effects of interleukin-1 isoforms on experimental atherosclerosis. *Eur Heart J* 2019; 40(30): 2482–91.
11. Galea J, Armstrong J, Gadsdon P, Holden H, Francis SE, Holt CM. Interleukin-1 beta in coronary arteries of patients with ischemic heart disease. *Arterioscler Thromb Vasc Biol* 1996; 16(8): 1000–6.
12. Dewberry R, Holden H, Crossman D, Francis S. Interleukin-1 receptor antagonist expression in human endothelial cells and atherosclerosis. *Arterioscler Thromb Vasc Biol* 2000; 20(11): 2394–400.
13. Nakamura K, Miyoshi T, Yunoki K, Ito H. Postprandial hyperlipidemia as a potential residual risk factor. *J Cardiol* 2016; 67(4): 335–9.
14. Di Iorio A, Ferrucci L, Sparvieri E, Cherubini A, Volpato S, Corsi A, et al. Serum IL-1 β levels in health and disease: a population-based study. The InCHIANTI study. *Cytokine* 2003; 22(6): 198–205.
15. Joung KH, Kim JM, Choung S, Lee JH, Kim HJ, Ku BJ. Association between IL-1beta and cardiovascular disease risk in patients with newly diagnosed, drug-naïve type 2 diabetes mellitus: a cross-sectional study. *Ann Transl Med* 2020; 8(5): 225.
16. Hansson GK. Inflammation, atherosclerosis, and coronary artery disease. *N Engl J Med* 2005; 352(16): 1685–95.
17. Wang M, Zhang J, Jiang LQ, Spinetti G, Pintus G, Monticone R, et al. Proinflammatory profile within the grossly normal aged human aortic wall. *Hypertension* 2007; 50(1): 219–27.
18. Starr ME, Saito M, Evers BM, Saito H. Age-associated increase in cytokine production during systemic inflammation-II: The role of IL-1 β in age-dependent IL-6 upregulation in adipose tissue. *J Gerontol A Biol Sci Med Sci* 2015; 70(12): 1508–15.
19. Rauchhaus M, Koloczek V, Volk H, Kemp M, Niebauer J, Francis DP, et al. Inflammatory cytokines and the possible immunological role for lipoproteins in chronic heart failure. *Int J Cardiol* 2000; 76(2–3): 125–33.
20. Kozdag G, Ertas G, Emre E, Akay Y, Celikyurt U, Sahin T, et al. Low serum triglyceride levels as predictors of cardiac death in heart failure patients. *Tex Heart Inst J* 2013; 40(5): 521–8.

The Potential Role of Hematological and Biochemical Parameters in Pregnant Women with Viral Infection

Nadire Elif Ergun¹ , Saime Surmen² , Saide Erturk^{3,4} , Derya Buyukkayhan⁵ ,
Mustafa Gani Surmen² 

¹Department of Medical Microbiology, Hamidiye Institute of Health Sciences, University of Health Sciences, Istanbul, Turkiye

²Department of Molecular Medicine, Hamidiye Institute of Health Sciences, University of Health Sciences, Istanbul, Turkiye

³Esenler Maternity and Children's Hospital, Istanbul, Turkiye

⁴Pediatric Hematology and Oncology Clinic, Basaksehir Cam and Sakura City Hospital, University of Health Sciences Istanbul, Turkiye

⁵Division of Neonatology, Clinic of Pediatrics, Haseki Training and Research Hospital, University of Health Sciences, Istanbul, Turkiye

ORCID ID: N.E.E. 0009-0004-5962-9556; S.S. 0000-0002-7748-0757; S.E. 0000-0002-6731-9337; D.K. 0000-0001-7172-0812;
M.G.S. 0000-0001-9084-7528

Cite this article as: Ergun NE, Surmen S, Erturk S, Buyukkayhan D, Surmen MG. The potential role of hematological and biochemical parameters in pregnant women with viral infection. *Experimed* 2023; 13(2): 148-155.

ABSTRACT

Objective: Pregnancy is a process in which not only physical changes occur, but also immune responses are modulated. Therefore, pregnant women are more susceptible to viral infections due to these changes during the pregnancy. The present study aimed to evaluate the hematological and biochemical parameters of pregnant women diagnosed with viral infection.

Materials and Methods: The study groups consisted of pregnant women diagnosed with cytomegalovirus (CMV), hepatitis B virus (HBV), influenza, Covid-19 and healthy pregnant women as control group. The data of a total of 522 pregnant women were analyzed retrospectively. SPSS 22.0 statistics package program was used for data analysis.

Results: Significant differences were found in aspartate aminotransferase (AST) and alanine aminotransferase (ALT) levels, and neutrophil counts between CMV and control groups. There were also significant differences in AST, ALT, red blood cell distribution width (RDW), neutrophil lymphocyte ratio (NLR), white blood cell (WBC), platelet (PLT), neutrophil and lymphocyte values between hepatitis B surface antigen (HBsAg) positive and HBsAg negative pregnant groups. NLR and basophil (BASO) % of pregnant women with influenza infection were significantly higher than the control group. In Covid-19 positive pregnant women, AST, ALT, WBC, BASO values and BASO% were found to be significantly different from the control group. In addition, WBC and NLR values in Covid-19 positive pregnant women were found to be significantly lower than the influenza group.

Conclusion: All these results suggest that especially the NLR value may have diagnostic and prognostic significance for viral infections in pregnant women. However, studies with larger samples and prospective analyses are needed for stronger evidence.

Keywords: Viral infection, neutrophil lymphocyte ratio, pregnancy, retrospective

INTRODUCTION

Pregnant women are at high risk for viral infections and related complications due to the physiological and immunological changes during pregnancy. The adaptation of the immune system to tolerate the allogeneic fetus in this process is among the main reasons for these changes (1).

Cytomegalovirus (CMV) is one of the common congenital contagious infections. Serological screening test is performed during pregnancy for the diagnosis of primary infection of CMV. However, detection of DNA for CMV by amniocentesis is considered as the gold standard for diagnosis in the estimation of primary infection. CMV infection can cause serious sequelae such as neurological

Corresponding Author: Mustafa Gani Sürmen **E-mail:** mustafagani.surmen@sbu.edu.tr

Submitted: 01.06.2023 **Revision Requested:** 11.07.2023 **Last Revision Received:** 19.07.2023 **Accepted:** 29.07.2023 **Published Online:** 04.08.2023



Content of this journal is licensed under a Creative Commons Attribution-NonCommercial 4.0 International License.

disability, hearing loss and vision loss in new-borns. Although the primary infection during pregnancy is asymptomatic in most of the mothers, care should be taken because of the sequelae that may occur later in the newborn (2).

Another issue that may pose a serious risk for both mother and fetus during pregnancy is hepatitis B virus (HBV) infection. HBV infection carries serious risks for the mother, especially in the second trimester and during delivery. In addition, pregnant women with high viremia are at risk of mother-to-child transmission of HBV (3). For this reason, follow-up during pregnancy and postpartum against pregnancy-associated hepatitis B reactivation is of great importance.

On the other hand, the literature contains various information regarding the influenza virus infection, which caused pandemics in the past due to its rapid spread potential, affecting both maternal health and pregnancy outcome. The study results implied that disease severity was associated with preterm birth and stillbirth. The fact that pregnant women are more susceptible to flu-related complications has been attributed to immunological (changes in T and B cell counts) and physiological adaptations (increased respiratory rate and intra-abdominal pressure) during pregnancy (4).

Nowadays, the Covid-19 pandemic, which affected millions of people, was experienced. The main symptoms of Covid-19 such as fever, cough and shortness of breath have clinical manifestations similar to influenza (5). Some hematological parameters have been reported and can serve as diagnostic and prognostic markers depending on Covid-19 severity (6).

In the fight against viral infections, including influenza and Covid-19, anti-viral treatments and vaccinations can help to prevent negative pregnancy outcomes. However, information on the adverse effects of vaccines and antiviral treatments on mother and baby is limited. In this context, it is critical to detect viral infections before they pose a threat to maternal and infant health.

This study aimed to evaluate the relationship between viral infections during pregnancy and pregnant women's hematological and biochemical parameters.

MATERIALS AND METHODS

Istanbul Medeniyet University Goztepe Training and Research Hospital, Clinical Research Ethics Committee approval was obtained for this study (Date: 10.02.2021, Decision No: 2021/0140).

Data Collection

The present retrospective study aimed to evaluate the hematological and biochemical parameters of pregnant patients diagnosed with viral infection. Data were collected from 555 pregnant patients and 141 healthy pregnant women who attended to the Istanbul Esenler Obstetrics and Pediatrics Hospital and Istanbul Haseki Sultangazi Training and Research

Hospital, Gynecology outpatient clinic, between the years 2018 and 2020. Among these, 140 pregnant women with HBV infection, 4 pregnant women with Covid-19 infection and 30 pregnant women with CMV infection were subsequently excluded due to missing data. Pregnant women with gestational diabetes mellitus (GDM), preeclampsia, hypothyroidism, hyperthyroidism, pregnancy-related autoimmune diseases, and different concomitant viral infections were also excluded.

Patients' symptoms at presentation, white blood cell (WBC, $10^3/\mu\text{L}$) count, red blood cell (RBC, $10^{12}/\text{L}$) count, platelet (PLT, $10^3/\mu\text{L}$) count, mean platelet volume (MPV, fL), platelet distribution width (PDW, %), neutrophil (NEU, $10^3/\mu\text{L}$) count and percent, basophil (BASO, $10^3/\mu\text{L}$) count and percent, eosinophil (EOS, $10^3/\mu\text{L}$) count and percent, monocyte (MONO, $10^3/\mu\text{L}$) count and percent, lymphocyte (LYM, $10^3/\mu\text{L}$) count, red blood cell distribution width (RDW, %), alanine aminotransferase (ALT, U/L), aspartate aminotransferase (AST, U/L) and neutrophil lymphocyte ratio (NLR) were evaluated. Routine blood tests were performed using the fluorescence flow cytometry (FFC) method and an automated hematology analyzer (Sysmex XN-1000). Using an automated biochemical analyser, AST and ALT parameters were measured by the enzymatic colorimetric method, and vitamin D (ng/mL) was determined by paramagnetic particle chemiluminescent immunoassay (Beckman Coulter AU680). Anti-CMV IgG and HBsAg were analyzed by chemiluminescent microparticle immunoassay (CMIA) (Architect i2000SR and Architect i1000, Abbott).

Statistical Analyses

The IBM SPSS Statistics 22 program was used for statistical analysis of this study. The distribution of variables was evaluated with Kolmogorov-Smirnov and Shapiro Wilks tests. Student's t test was used to compare normally distributed variables, and the Mann-Whitney U test was used to compare non-normally distributed continuous variables. The correlation between the NLR value and gestational week were determined by the Spearman's correlation test. The Pearson's correlation analysis was also used to evaluate the relationship between vitamin D and ALT levels. Statistical significance was taken as p-values less than 0.05.

RESULTS

CMV Infection

The first group consisted of 53 CMV positive and 141 CMV negative pregnant women. The mean age of the CMV and control groups was 28.6 ± 5.2 and 29.2 ± 4.3 , respectively ($p > 0.05$). In this study group, WBC, NEU, LYM, AST and ALT values, which are routine blood parameters of pregnant women, were evaluated retrospectively. AST and ALT values of the pregnant group with CMV infection were found to be statistically significantly higher than the CMV negative control group. While no significant difference was observed in WBC and LYM values, the NEU value was found to be significantly lower than the control group. The other parameters are presented Table 1.

Table 1. Comparison of CMV and control groups.

	CMV (n=53)	Control (n=141)	p-value
AST	29.68 ± 24.92	18.36 ± 32.9	² 0.001*
ALT	14.16 ± 3.75	12.22 ± 18.56	² 0.000*
WBC	10.16 ± 4.04	10.14 ± 3.09	² 0.744
NEU	67.06 ± 8.51	70.16 ± 13.59	² 0.019*
LYM	21.68 ± 8.37	20.45 ± 7.13	¹ 0.463

Cytomegalovirus (CMV), aminotransferase (AST), alanine aminotransferase (ALT), white blood cell (WBC), neutrophil (NEU), lymphocyte (LYM), ¹Student t Test, ²Mann Whitney U Test, all values are shown as mean ± SD, SD: Standard deviation, *p<0.05

Table 2. Comparison of HBsAg positive and HBsAg negative groups.

	HBsAg (+) (n=135)	HBsAg (-) (n=66)	p-value
MPV	9.72 ± 0.86	9.78 ± 1.41	¹ 0.715
AST	24.25 ± 7.27	16.21 ± 4.95	¹ 0.000*
ALT	15.6 ± 9.89	13.46 ± 8.2	² 0.007*
RDW	13.6 ± 3.98	14.17 ± 1.42	² 0.000*
PDW	10.69 ± 1.56	16.14 ± 1.57	¹ 0.000*
NLR	1.59 ± 1.39	3.55 ± 1.42	¹ 0.000*
Vitamin D	16.49 ± 6.56	19.44 ± 9.14	¹ 0.194
WBC	8.48 ± 2.13	9.51 ± 2.43	² 0.003*
PLT	306.63 ± 75.59	246.34 ± 83.38	¹ 0.000*
NEU	4.67 ± 4.18	6.70 ± 2.34	² 0.000*
LYM	3.19 ± 1.02	2.03 ± 0.57	² 0.000*

Mean platelet volume (MPV), aminotransferase (AST), alanine aminotransferase (ALT), red blood cell distribution width (RDW), platelet distribution width (PDW), neutrophil lymphocyte ratio (NLR), white blood cell (WBC), platelet (PLT), neutrophil (NEU), lymphocyte (LYM), ¹Student t Test, ²Mann Whitney U Test, all values are shown as mean± SD, SD: Standard deviation, *p<0.05

Hepatitis B Surface Antigen (HBsAg) Infection

Group 2 consisted of 135 HBsAg positive and 66 HBsAg negative pregnant women. The mean age of the influenza and control groups was 27.2 ± 4.7 and 26.3 ± 4.9, respectively (p>0.05). The NLR was calculated from these parameters. While the WBC and NEU values of the HBsAg positive pregnant group were statistically significantly lower than the healthy control group, the LYM value was found to be higher, and accordingly, the NLR value was significantly lower (Table 2). In addition, RDW, PLT and PDW values were found to be significantly different in HbsAg positive pregnant women (p<0.001). AST and ALT values in the patient group were also higher than the control group (p<0.01). However, no statistically significant difference was observed between the HBsAg positive and negative control groups in terms of vitamin D values (Table 2). No correlation was also found between the vitamin D and ALT in both groups (r=-0.316; p=0.153 in control, r=0.173; p=0.344 in HbsAg positive).

Influenza Infection

The third group consisted of 63 influenza positive and 67 healthy pregnant women. The mean age of the influenza and control groups was 28.4 ± 6.0 and 28.8 ± 5.5, respectively (p>0.05). WBC, RBC, PLT, NEU, LYM, EOS, BASO, NEU%, LYM%, EOS%, BASO% values of this group were evaluated retrospectively. In addition, LYM x PLT and NLR values were calculated. BASO% values (p<0.001) and NLR values (p<0.01) of the pregnant group with influenza infection were found to be statistically significantly higher than the control group. A more detailed description of the data is given in Table 3. In influenza-infected pregnant women, a weak correlation was also observed for the NLR value and gestational week (r=0.279; p<0.05).

Covid-19 Infection

In the last group, there were 130 Covid-19 positive and 67 negative pregnant women. The mean age of the influenza and control groups was 26.3 ± 4.2 and 28.8±5.5, respectively

Table 3. Comparison of influenza and control groups.

	Influenza (n=63)	Control (n=67)	p-value
Age	28.43 ± 6.06	28.88 ± 5.54	¹ 0.666
WBC	9.85 ± 3.06	9.96 ± 3.25	² 0.608
RBC	4.19 ± 0.42	4.19 ± 0.49	¹ 0.945
PLT	237.64 ± 55.77	237.34 ± 82.2	² 0.483
NEU	7.4 ± 2.5	7.21 ± 3.35	² 0.422
LYM	2.1 ± 0.92	1.97 ± 0.62	² 0.837
EOS	0.19 ± 0.16	0.12 ± 0.09	² 0.328
BASO	0.02 ± 0.02	0.04 ± 0.13	² 0.858
NEU%	71.69 ± 9.93	71.11 ± 10	² 0.610
LYM%	19.31 ± 8.84	21.76 ± 8.59	² 0.060
EOS%	2.13 ± 2.18	1.39 ± 1.3	² 0.494
BASO%	0.48 ± 0.32	0.23 ± 0.14	² 0.000*
LYMxPLT	512.07 ± 314.32	481.15 ± 242.09	² 0.973

White blood cell (WBC), red blood cell (RBC), platelet (PLT), neutrophil (NEU), lymphocyte (LYM), eosinophil (EOS), basophil (BASO), ¹Student t Test, ²Mann Whitney U Test, all values are shown as mean± SD, SD: Standard deviation, *p<0.05

(p<0.05). AST, ALT, WBC, PLT, NEU, LYM, EOS, BASO, NEU%, LYM%, EOS%, BASO% parameters of the pregnant women were evaluated retrospectively. AST (p<0.001) and ALT (p<0.01) values of pregnant women with Covid-19 infection were found to be statistically significantly higher than the healthy control group (Table 4). In addition, BASO (p<0.001), BASO% (p<0.05) values were found to be statistically significant higher and WBC values (p<0.01) were lower in pregnant women with Covid-19 infection. The detailed information is shown in Table 4. The Covid-19 infection group was also compared with the influenza group (Table 5). Finally, Table 6 summarizes the parameters with significant differences and related groups.

DISCUSSION

This study aimed to examine the hematological and biochemical parameters of pregnant women who had viral infections during pregnancy such as CMV, HBV, Influenza and Covid-19. The first group consisted of CMV, one of the most common congenital infections. While no difference was found in WBC counts in this group, significant differences were found in ALT, AST and NEU values. CMV-associated infection in fibroblast and macrophage cells causes activation of the nuclear factor κB (NF-κB) (7). NF-κB, is responsible for the activation of various cytokines, and may also be associated with the increase in ALT and AST levels in CMV infection (8).

In the study by Nigro et al., ALT, AST and LYM% were found to be higher in pregnant women with primary and recurrent CMV infection compared to the control group. Accordingly,

an increase in AST and at least 40% LYM may indicate the presence of primary CMV infection (9). Interestingly, although a significant increase in ALT and AST values was detected in this study, the increase in LYM% was not significant.

The effects of pregnancy on chronic HBV infection (CHB) or the effects of HBV infection on pregnancy are not clearly known. However, it is possible that changes in the immune system during pregnancy allow for greater viral replication in individuals with chronic HBV. Detection of HBsAg is one of the main serological markers of acute and chronic hepatitis B (10). However, some values in routine blood parameters may also give clues about infection. In this study, AST and ALT values of the HBsAg positive pregnant group were found to be statistically significantly higher than the healthy control group, and these values are consistent with the literature. In addition, several studies have reported high RDW levels in CHB patients (11-13). It has been noted that viral load can have a significant effect on RDW when ALT levels are more than 2 times higher than in the normal group (14). High RDW is positively associated with the severity of CHB disease and may be a determining factor in the follow-up of patients with liver cirrhosis (11-13). Although the increase in ALT levels in this study altered significantly, there was no two-fold difference compared to the control group. Interestingly, the RDW values of the HBsAg positive pregnant group were significantly lower than the control group. Conflicting results regarding the RDW value may be due to different cohorts. On the other hand, anemia and, nutrition, folate and B12 deficiencies in pregnancy may also be the reason for these differences.

Table 4. Comparison of Covid-19 positive and control groups.

	Covid-19 (n=130)	Control (n=67)	p-value
Age	26.36 ± 4.17	28.88 ± 5.54	¹ 0.003*
AST	28.55 ± 33.3	16.76 ± 5.21	² 0.000*
ALT	25.08 ± 52.69	13.97 ± 9.46	² 0.002*
WBC	8.64 ± 3.39	9.96 ± 3.25	² 0.001*
PLT	237.78 ± 85.49	237.34 ± 82.2	² 0.977
NEU	10.59 ± 16.59	7.21 ± 3.35	² 0.067
LYM	3.1 ± 5.25	1.97 ± 0.62	² 0.091
EOS	0.19 ± 0.36	0.12 ± 0.09	² 0.119
BASO	0.038 ± 0.15	0.037 ± 0.13	² 0.000*
NEU%	65.71 ± 18.06	71.11 ± 10	² 0.087
LYM%	21.44 ± 10.18	21.76 ± 8.59	² 0.858
BASO%	0.31 ± 1.03	0.23 ± 0.14	² 0.026*

Aspartate aminotransferase (AST), alanine aminotransferase (ALT), white blood cell (WBC), platelet (PLT), neutrophil (NEU), lymphocyte (LYM), eosinophil (EOS), basophil (BASO), ¹Student t Test, ²Mann Whitney U Test, all values are shown as mean± SD, and median values are presented in brackets, SD: Standard deviation, *p<0.05.

Table 5. Comparison of Covid-19 positive and influenza groups.

	Covid-19 (n=130)	Influenza (n=63)	p-value
PLT	237.78 ± 85.49	237.64 ± 55.77	² 0.459
MPV	10.15 ± 1.14	9.51 ± 1.87	¹ 0.371
PDW	14.35 ± 2.43	15.08 ± 1.77	² 0.599
NEU	10.59 ± 16.59	7.4 ± 2.5	² 0.330
EOS	0.19 ± 0.36	0.19 ± 0.16	² 0.258
NEU%	65.71 ± 18.06	71.69 ± 9.93	² 0.041*
EOS%	1.27 ± 1.49	2.13 ± 2.18	² 0.251
WBC	8.64 ± 3.39	9.85 ± 3.06	² 0.002*
RBC	3.98 ± 0.55	4.19 ± 0.42	¹ 0.008*
LYM	3.1 ± 5.25	2.1 ± 0.92	² 0.480
MONO	0.96 ± 1.74	6.55 ± 3.03	² 0.000*
BASO	0.04 ± 0.15	0.02 ± 0.02	² 0.238
LYM%	21.44 ± 10.18	19.31 ± 8.84	² 0.111
BASO%	0.31 ± 1.03	0.48 ± 0.32	² 0.000*
MONO%	6.16 ± 2.54	5.83 ± 2.41	² 0.746

Platelet (PLT), mean platelet volume (MPV), platelet distribution width (PDW), neutrophil (NEU), eosinophil (EOS), white blood cell (WBC), red blood cell (RBC), lymphocyte (LYM), monocyte (MONO), basophil (BASO), ¹Student t Test, ²Mann Whitney U Test, all values are shown as mean± SD, and median values are presented in brackets, SD: Standard deviation, *p<0.05

Table 6. Representation of the parameters with significant differences in study groups.

	Group I			Group II	Group III
	CMV	Influenza	Covid-19	Hepatitis B	Covid-19
AST	+	NC	+	+	NC
ALT	+	NC	+	+	NC
WBC	-	-	+	+	+
RBC	NC	-	NC	NC	+
NEU	+	-	-	+	-
NEU%	NC	-	-	NC	+
BASO	NC	-	+	NC	-
BASO%	NC	+	+	NC	+
RDW	NC	NC	NC	+	NC
PDW	NC	NC	NC	+	-
NLR	NC	NC	NC	+	NC
PLT	NC	-	-	+	-
LYM	-	-	-	+	-

Significant ones are indicated with plus, non-significant ones are indicated with minus. NC: not-compared. Group I: CMV vs Control, Influenza vs Control and Covid-19 (+) vs Control; Group II: HBsAg (+) vs HBsAg (-); Group III: Covid-19 (+) vs Influenza. Aspartate aminotransferase (AST), alanine aminotransferase (ALT), white blood cell (WBC), red blood cell (RBC), neutrophil (NEU), basophil (BASO), red blood cell distribution width (RDW), platelet distribution width (PDW), neutrophil lymphocyte ratio (NLR), lymphocyte (LYM), CMV (Cytomegalovirus)

Moreover, the PLT value was found to be significantly higher and the NLR value to be lower in pregnant women with HBV in this study. Recently, the NLR value, which can be easily detected from peripheral blood, has attracted attention as a marker of systemic inflammation. Atay et al. found an increase in NLR rates in the CHB group compared to the controls and in the advanced fibrosis group compared to the mild fibrosis group (15). However, in some recent studies, PLT values were found to be higher in CHBs without cirrhosis and liver failure, and lower NLR values compared to controls (13,16-18). Although it is thought that the increase in the NLR value may be associated with poor prognosis and survival, according to studies conducted with various diseases, the results have not been sufficiently clarified.

The detection of NLR may also play an important role in the fight against Covid-19 and influenza-related infections. Neutrophils show potent antimicrobial effects as important components of the leukocyte population. In addition to triggering the release of multiple cytokines to fight infections, they increase the production of reactive oxygen species (ROS) that can result in tissue damage. Although the antiviral responses of neutrophils are not well known, they are immune effector cells that play a primary role in viral infection sites (19). Routine laboratory findings of pregnant women and other adult patients in the early period of Covid-19 infection are contradictory. However,

most of them have normal or decreased WBC, high NLR value and lymphocytopenia (6, 20, 21). The NLR value can be a prognostic biomarker and was reported in various studies including patients with non-severe, mild and severe Covid-19 infections (22, 23). In addition, a meta-analysis showed that individuals with severe Covid-19 have a higher NLR than non-severe ones (24). In various studies conducted in our country, high NLR values have been reported in individuals with severe Covid-19. NLR has attracted attention as a predictive factor for Covid 19 diagnosis, prognosis, and survival (25-27). Yilmaz et al. reported that WBC, NEU and LEU values were significantly lower in Covid 19 positive pregnant women compared to negative ones, but they did not find a significant difference in NLR values (28). However, the NLR value showed significant differences when evaluated according to disease severity (28, 29). On the other hand, a retrospective analysis of a large cohort revealed that the NLR values in the first, second and third trimesters of pregnancy may vary (30). In this context, it is important to know in which trimester the pregnant woman is during the measurement of NLR values. In this study, the WBC count was found to be significantly lower between Covid-19 and control groups, while the increase in NLR and LYM values and the decrease in LYM and NEU percentages were not significant. The reason for this may be asymptomatic or mild symptoms of the disease, or the study group may be composed of pregnant

women in different trimesters. Mild thrombocytopenia, liver enzymes (i.e. ALT and AST), lactate dehydrogenase and C-reactive protein (CRP) are also likely to increase in the early period of Covid-19 infection (31). Less common symptoms, according to the laboratory findings of Guan et al., include elevated ALT, AST, and creatine kinase levels (21). In this study, high AST and ALT values were observed in the pregnant group with Covid-19 infection compared to controls.

On the other hand, the clinical symptoms of Covid-19 and influenza are quite similar. In this context, the data of pregnant patients with Covid-19 and flu were also analyzed to determine the distinguishing parameters in the study. The results obtained from various studies have shown that the NLR and WBC values are remarkably lower in Covid-19 individuals than in the influenza group (5, 26, 32). Consistent with other studies, NLR and WBC values were significantly decreased in pregnant women with infection due to the presence of Covid-19 in this study.

There are 5 subtypes of white blood cells, the number of which increases significantly during infection, consisting of neutrophils, lymphocytes, monocytes, eosinophils, and basophils. Unlike the study by Kazancıoğlu et al., a significant increase in BASO and BASO% values were observed in Covid-19 pregnant women in this study (26). Basophils are relatively rare leukocytes that contribute to allergic inflammations due to their ability to migrate from the blood to various other tissues. In addition, there are studies showing that basophils have the capacity to produce Th2-type cytokines and the ability to initiate Th2 immunity (33). In other studies, it has been reported that basophils were decreased during acute disease but were returned to normal after a few days. It has been suggested that basophil counts, which decrease at the beginning of the disease and change afterward, may be an important prognostic marker (34).

CONCLUSION

Immunomodulation, which mediates tolerance of the allogeneic fetus during pregnancy, may render the pregnant woman more susceptible to viruses. According to this study, WBC values were decreased in Covid-19 positive pregnant women, and BASO% and BASO were increased. However, data on the variation of the basophil values due to viral infections are limited. In addition, the WBC, RBC, NEU%, MONO and BASO values of pregnant women with Covid-19 were lower than those with influenza infection. Finally, in line with the literature, high AST and ALT values in the CMV infected group and increased AST, ALT, PLT and RDW values in HBsAg positive patients may help the prediction of infections. Although these changes in blood parameters give clues about the presence of infection, they are not sufficient to be a distinctive pattern of disease. To understand the hematological and biochemical data relation, the study needs to be improved with various larger patient groups.

LIMITATIONS

Since this study was evaluated retrospectively, demographic data of pregnant women such as body mass index, weight averages and pregnancy complications could not be obtained. Chronic or acute infection information of pregnant women with HBV infection could not be obtained either.

Acknowledgments: We would like to thank Professor Sebahat Aksaray and Professor Nesrin Emekli for their support and critical comments on this study.

Ethics Committee Approval: The study protocol was approved from the ethical committee of the Istanbul Medeniyet University Goztepe Training and Research Hospital, Clinical Research Ethics Committee (Decision No: 2021/0140).

Authors' Contributions: Conception/Design of Study – M.G.S., D.B., N.E.E.; Data Acquisition – D.B., S.E., M.G.S., N.E.E.; Data Analysis/ Interpretation – N.E.E., S.S., M.G.S.; Drafting Manuscript– N.E.E., M.G.S., S.S.; Critical Revision of Manuscript- M.G.S., S.S., D.B., S.E.; Final Approval and Accountability– M.G.S., D.B., S.E., S.S., N.E.E.

Conflict of Interest: Authors declared no conflict of interest.

Financial Disclosure: Authors declared no financial support.

REFERENCES

1. Vojtek I, Dieussaert I, Doherty TM, Franck V, Hanssens L, Miller J, et al. Maternal immunization: where are we now and how to move forward? *Ann Med* 2018; 50(3): 193-208.
2. Davis NL, King CC, Kourtis AP. Cytomegalovirus infection in pregnancy. *Birth Defects Res* 2017; 109(5): 336-46.
3. Borgia G, Carleo MA, Gaeta GB, Gentile I. Hepatitis B in pregnancy. *World J Gastroenterol* 2012; 18(34): 4677-83.
4. Memoli MJ, Harvey H, Morens DM, Taubenberger JK. Influenza in pregnancy. *Influenza Other Respir Viruses* 2013; 7(6): 1033-9.
5. Osman M, Klopfenstein T, Belfeki N, Gendrin V, Zayet S. A comparative systematic review of COVID-19 and influenza. *Viruses* 2021; 13(3): 452.
6. Üstündağ Y, Kazancı EG, Sevçican E, Erdem C, Huysal K. Hematological parameters in pregnant women with COVID-19: a systematic review. *J Clin Chem Lab Med* 2021; 4(2): 1000163.
7. Benedict CA, Angulo A, Patterson G, Ha S, Huang H, Messerle M, et al. Neutrality of the canonical NF-kappa B-dependent pathway for human and murine cytomegalovirus transcription and replication in vitro. *J Virol* 2004; 78(2): 741-50.
8. Ye B, Zhao H. Early abnormal liver enzyme levels may increase the prevalence of human cytomegalovirus antigenaemia after hematopoietic stem cell transplantation. *J Int Med Res* 2017; 45(2): 673-9.
9. Nigro G, Anceschi MM, Cosmi EV. Congenital cytomegalic disease collaborating group. Clinical manifestations and abnormal laboratory findings in pregnant women with primary cytomegalovirus infection. *BJOG* 2003; 110(6): 572-7.
10. Chang JJ, Lewin SR. Immunopathogenesis of hepatitis B virus infection. *Immunol Cell Biol* 2007; 85(1): 16-23.
11. Wang J, Huang R, Yan X, Li M, Chen Y, Xia J, et al. Red blood cell distribution width: A promising index for evaluating the severity and long-term prognosis of hepatitis B virus-related diseases. *Dig Liver Dis* 2020; 52(4): 440-6.

12. Huang R, Yang C, Wu K, Cao S, Liu Y, Su R, et al. Red cell distribution width as a potential index to assess the severity of hepatitis B virus-related liver diseases. *Hepatol Res* 2014; 44(14): E464-70.
13. Zhang X, Wang D, Chen Z, Guo N, Wang W, Xiong C, et al. Red cell distribution width-to-lymphocyte ratio: A novel predictor for HBV-related liver cirrhosis. *Medicine (Baltimore)* 2020; 99(23): e20638.
14. Gao P, Xiao P, Yang YL, Chen QF, Mao XR, Zhao ZB, et al. Effects and clinical significance of virus load on red blood cell parameters in different stage of hepatitis B. *Beijing Da Xue Bao Yi Xue Ban* 2014; 46(6): 941-4.
15. Atay K. Relationship between neutrophil-to-lymphocyte ratio, mean platelet volume, and fibrosis level in patients with chronic hepatitis B. *Turkish J Academic Gastroenterol* 2019; 18(1): 7-11.
16. Ahmad AE, Bakari AG, Musa BOP, Mustapha SK, Nasir AI, Tahir MI, et al. Haematological and immunological parameters in patients with chronic hepatitis b infection in Zaria, Nigeria. *Sokoto J Med Lab Sci* 2018; 3(4): 84-88.
17. Cai J, Wang K, Han T, Jiang H. Evaluation of prognostic values of inflammation-based makers in patients with HBV-related acute-on-chronic liver failure. *Medicine (Baltimore)* 2018; 97(46): e13324.
18. Chen L, Lou Y, Chen Y, Yang J. Prognostic value of the neutrophil-to-lymphocyte ratio in patients with acute-on-chronic liver failure. *Int J Clin Pract* 2014; 68(8): 1034-40.
19. Burn GL, Foti A, Marsman G, Patel DF, Zychlinsky A. The neutrophil. *Immunity* 2021; 54(7): 1377-91.
20. Vakili S, Savardashtaki A, Jamalnia S, Tabrizi R, Nematollahi MH, Jafarinia M, et al. Laboratory findings of COVID-19 infection are conflicting in different age groups and pregnant women: A literature review. *Arch Med Res* 2020; 51(7): 603-7.
21. Guan WJ, Ni ZY, Hu Y, Liang WH, Ou CQ, He JX, et al. Clinical characteristics of Coronavirus Disease 2019 in China. *N Engl J Med* 2020; 382(18): 1708-20.
22. Yang AP, Liu JP, Tao WQ, Li HM. The diagnostic and predictive role of NLR, d-NLR and PLR in COVID-19 patients. *Int Immunopharmacol* 2020; 84: 106504.
23. Kong M, Zhang H, Cao X, Mao X, Lu Z. Higher level of neutrophil-to-lymphocyte is associated with severe COVID-19. *Epidemiol Infect* 2020; 148: e139.
24. Chan AS, Rout A. Use of neutrophil-to-lymphocyte and platelet-to-lymphocyte ratios in COVID-19. *J Clin Med Res* 2020; 12(7): 448-53.
25. Erdogan A, Can FE, Gönüllü H. Evaluation of the prognostic role of NLR, LMR, PLR, and LCR ratio in COVID-19 patients. *J Med Virol* 2021; 93(9): 5555-9.
26. Kazancioglu S, Bastug A, Ozbay BO, Kemirtlek N, Bodur H. The role of haematological parameters in patients with COVID-19 and influenza virus infection. *Epidemiol Infect* 2020; 148: e272.
27. Nalbant A, Kaya T, Varim C, Yaylaci S, Tamer A, Cinemre H. Can the neutrophil/lymphocyte ratio (NLR) have a role in the diagnosis of coronavirus 2019 disease (COVID-19)? *Rev Assoc Med Bras (1992)* 2020; 66: 746-51.
28. Yılmaz Z, Güvey H, Çelik S, Çalışkan CS. Effect of complete blood count parameters on the clinical course of COVID-19 in pregnant women. *Exp Clin Med* 2022; 39(2): 409-13.
29. Arslan B, Bicer IG, Sahin T, Vay M, Dilek O, Destegul E. Clinical characteristics and hematological parameters associated with disease severity in COVID-19 positive pregnant women undergoing cesarean section: A single-center experience. *J Obstet Gynaecol Res* 2022; 48(2): 402-10.
30. Hershko Klement A, Hadi E, Asali A, Shavit T, Wisner A, Haikin E, et al. Neutrophils to lymphocytes ratio and platelets to lymphocytes ratio in pregnancy: A population study. *PLoS One* 2018; 13(5): e0196706.
31. Deniz M, Tezer H, Tapisiz A. Yenidoğan ve gebelerde yeni koronavirüs hastalığı 2019 (Covid 19). *Turkish J Pediatr Dis* 2020; 14(3): 274-8.
32. Prozan L, Shusterman E, Ablin J, Mitelpunkt A, Weiss-Meilik A, Adler A, et al. Prognostic value of neutrophil-to-lymphocyte ratio in COVID-19 compared with Influenza and respiratory syncytial virus infection. *Sci Rep* 2021; 11(1): 21519.
33. Gibbs BF, Streatfield C, Falcone FH. Basophils as critical orchestrators of Th2-type immune responses. *Expert Rev Clin Immunol* 2009; 5(6): 725-34.
34. Murdaca G, Di Gioacchino M, Greco M, Borro M, Paladin F, Petrarca C, et al. Basophils and mast cells in COVID-19 pathogenesis. *Cells* 2021; 10(10): 2754.

The Effect of Otitis Media with Effusion on Language and Cognitive Skills in School Age Children

Merve Savas¹ 

¹Faculty of Health Sciences, Istanbul Atlas University, Istanbul, Turkiye

ORCID ID: M.S. 0000-0002-7138-2603

Cite this article as: Savas M. The effect of otitis media with effusion on language and cognitive skills in school age children. *Experimed* 2023; 13(2): 156-162.

ABSTRACT

Objective: Otitis media with effusion (OME) is a common condition in childhood and can interfere with cognitive development. The fact that it can be easily overlooked causes it to become chronic and has negative consequences in the long term (1). The negative consequences of OME in terms of speech and language disorders include speech sound disorders and developmental language disorders. For this purpose, cases admitted to the speech and language therapy clinic were screened for OME consecutively, and its relationship with language disorders was analyzed.

Materials and Methods: 50 children aged 8 to 10 years without mental retardation and hearing impairment were evaluated with audiology, language, repetition (non-word and sentence), and visual perceptual tests. In addition to standard language assessment, narrative samples were obtained and analyzed which is considered a descriptive approach.

Results: 26 children were positive for OME. Children with OME scored lower on language and repetition tests. There was no significant difference between the groups with and without OME in terms of syntactic complexity, narrative skills and visual perceptual performance. The Mann-Whitney U test was used for the comparison of parameters between groups ($p < 0.05$).

Conclusion: The presence of OME negatively affected language development. However, the structural complexity dimension of storytelling, complex sentence production performance, and visual perceptual skills were not affected negatively by OME. Although OME positivity is not accompanied by mental retardation and developmental delay, language development and verbal working memory may be negatively affected. OME should be routinely screened in childhood and should be addressed more closely in children with speech and language disorders.

Keywords: Otitis media with effusion, language development, speech sound disorder

INTRODUCTION

Otitis media with effusion (OME) or serous is an inflammation of the middle ear mucosa characterized by fluid accumulation in a preserved tympanic membrane and cavum tympani without signs and symptoms of acute infection (1). OME is extremely common in early childhood due to an immature immune system, frequent upper respiratory tract infections, and a shorter and more horizontal Eustachian tube than in adults (2). When OME becomes chronic, it can lead to hearing loss, cognitive dysfunction, behavioral problems, and academic failure,

resulting in a reduced quality of life (3). When children with a history of chronic OME were compared with their healthy peers in terms of language development and auditory processing performance, articulation and phonemic discrimination skills were found to be negatively affected (4). Similarly, it was found that the longer the duration of the presence of OME in the cavum tympani, the more negatively expressive language skills were affected (5). The impairment of the acoustic-phonetic properties of auditory signals due to OME can lead to an incomplete and inaccurate encoding of speech sounds into phonological working memory and to the misconstruction of mental

Corresponding Author: Merve Savas **E-mail:** merve.savas@atlas.edu.tr

Submitted: 20.06.2023 **Revision Requested:** 26.07.2023 **Last Revision Received:** 28.07.2023 **Accepted:** 08.08.2023 **Published Online:** 09.08.2023



Content of this journal is licensed under a Creative Commons Attribution-NonCommercial 4.0 International License.

representations of words. Children with OME may not hear or could mis-hear short-duration and low-intensity morphemes (6). Since OME may lead to language-cognitive developmental delays, its presence in children with speech and language disorders should be investigated and its relationship with affected language areas should be demonstrated (7). For this purpose, school-age children admitted to a speech and language therapy clinic were screened consecutively for OME, and the effect of middle ear inflammation with effusion on the components of language was analyzed.

Language, as a basic expression of the human mind, is a code system that enables the emergence and transmission of thoughts and the continuity of communication between people (8). Semantic knowledge of concepts, actual use of words, and connotative/symbolic transfer of words constitute the semantic component of language (9). The syntactic/morphosyntactic side is the arrangement of words to form meaningful and regular sentences (10). Pragmatics refers to the full range of skills required for communicative purposes in the social context of language (11). Linguistic processing is closely related to executive functions such as planning, reasoning, abstraction, working memory, and inhibition (12). Turkish is a suffixal and morphologically rich language (13). Morphemes have critical importance in language comprehension and speech, and morphological processing is closely related to cognitive processes (14). The multilayered nature of language makes linguistic assessment difficult in clinical settings. Therefore, in addition to standardized tests, repetition tests (sentence and nonword repetition tests) and narrative tools that address the pragmatic dimension should be used.

The aim of this study was to draw attention to the importance of audiological evaluation and linguistic cognitive examination in school-age children to identify possible risks such as cognitive dysfunction, academic failure and social communication difficulties due to OME.

MATERIALS AND METHODS

Participants

50 monolingual Turkish-speaking children aged 8 to 10 years (23 girls, 27 boys; mean age 8.78 ± 0.73 years) were included in the study. Ethics committee approval and voluntary consent were obtained from Istanbul Atlas University Ethic Committee (14.03.2023-24890) and in compliance with the Declaration of Helsinki. Inclusion criterias were an absence of developmental delay and primary neurological psychiatric diagnosis, a score of 100 or above on the Wechsler Intelligence Scale for Children-Revised (WISC-R), absence of symptoms of acute otitis media, and right and left ear pure tone hearing averages within the normal range (0-15 dB).

Acute otitis media includes otorrhea of middle ear origin, otalgia, middle ear fluid or effusion, and symptoms of acute local or systemic disease (15). Acute otitis media may also present with a type B tympanogram and is not defined as OME if

Table 1. Demographical and Clinical Information of Participants

	EOM	Age	Frequency	Percentage	
Age	OME-	8	10	41.7	
		9	9	37.5	
		10	5	20.8	
		Total	24	100	
	OME+	8	10	38.5	
		9	12	46.2	
10		4	15.4		
	Total	26	100		
SSD	OME-	SSD	Frequency	Percentage	
		SSD+	13	54.2	
		SSD-	11	45.8	
		Total	24	100	
	OME+	SSD+	17	65.4	
		SSD-	9	34.6	
Total		26	100		
LD	OME-	OME	LD	Frequency	Percentage
		LD+	1	4.2	
		LD-	23	95.8	
		Total	24	100	
	OME+	LD+	10	38.5	
		LD-	16	61.5	
Total		26	100		
Gender	OME-	OME	Gender	Frequency	Percentage
		Female	11	45.8	
		Male	13	54.2	
		Total	24	100	
	OME+	Female	12	46.2	
		Male	14	53.8	
Total		26	100		

OME: otitis media with effusion; OME+: Presence of otitis media with effusion; OME-: Absence of otitis media with effusion; SSD: Speech sound disorder; SSD+: Presence of speech sound disorder; SSD-: absence of speech sound disorder; LD+: Presence of language disorder; LD-: Absence of language disorder.

clinical signs of infection are present (16). Type B tympanogram with a flat curve and normal canal volume is considered diagnostic criteria of OME (17). The otolaryngologist diagnosed OME by considering the clinical examination and bilateral type B values together. Children with bilateral type B results were grouped as otitis media with effusion positive (OME+); children with bilateral type A were grouped as otitis media with effusion negative (OME-).

Participants whose equivalent test score according to the Turkish Articulation and Phonology Test (SST) was below their chronological age were diagnosed as speech sound disorder (SSD). The verbal language composite score (VLSC), obtained from the Test of Language Development-Primary-Fourth Edition Turkish Version (TOLDP-4:T) was used to determine language development. Children with very poor, weak, and below-average VLSC scores were classified as language disorder (LD+), and children with average, above-average, advanced, and very advanced VLSC scores as an absence of language disorder (LD-).

Table 1 shows the distribution of clinical and demographic data.

Instruments

Audiological Assessment

Tympanometry is a technique to determine whether the ventilation and ossicles in the middle ear are normal. Abnormal tympanometry values indicate that the patient has a problem with the middle ear. In tympanometry, the response of the eardrum to different pressures and the pressure in the middle ear are evaluated. The results of tympanometry are categorized into three categories: harmonious movement of the eardrum against different pressure values (Type A); presence of fluid in the middle ear/perforation of the membrane (Type B); and cases of negative pressure in the middle ear due to a problem in the Eustachian tube/end stage of ear infection/allergy-related obstruction (Type C) (18).

Pure tone audiometry is used to determine the degree of hearing loss by recording the thresholds at which acoustic stimuli of different intensities are heard at frequencies of 125, 250, 500, 750, 1000, 1500, 2000, 3000, 4000, 6000 and 8000 hertz. According to pure tone average results, hearing loss grades are classified as normal hearing (-10 to 15 dB), very mild (16 to 25 dB), mild (26 to 40 dB), moderate (41 to 55 dB), moderate to severe (56 to 70 dB), severe (71 to 90 dB), very severe (> 90 dB) (19).

Language Assessment

TOLDP-4:T is a norm-referenced and standardized test that measures receptive and expressive language skills in children aged 4 to 8 years. It consists of 9 subtests: picture vocabulary, relational vocabulary, oral vocabulary, syntactic understanding, sentence repetition, morphological

completion, word discrimination, word analysis and word articulation. By converting the raw scores of certain subtests into standard scores, the VLSC which consists of the composite score of listening, speaking, organizing, semantics, grammar, and the sum of all of them, is obtained. According to the VLSC, language development is classified as very poor (<70), poor (70-79), below average (80-89), average (90-110), above average (111-120), advanced (121-130) and very advanced (>130) (20). The reliability and validity scores of the TOLD-P:4:T has been conducted up to the age of 8 years and 11 months, and there is not yet a standardized test to assess the language development of Turkish-speaking individuals over the age of 8 years and 11 months in Turkey. 8 years and 11 months normative values were used for elder children. Since there were participants over the age of 8 years and 11 months in the study, both the VLSC score and whether there was a language disorder according to the VLSC score were categorized and a comparison was made between the groups.

Turkish Nonword Repetition Test (TNRT) performance is indexed to phonological working memory capacity and auditory attention skills. The TNRT is a practical tool used to distinguish children with developmental language disorder/risk from normally developing children. The test items are played to the participant once and then asked to repeat them. The correctly produced item is scored as 1 and the total number of correctly produced items is used as the score obtained from the test (21). In Turkey, there is no standardized test developed to determine phonological working memory capacity. Validity and reliability studies of the TNRT in Turkish-speaking school-age children are ongoing. However, there are studies comparing various disease groups and healthy subjects using TNRT in Turkish-speaking school-age children (22-23).

The Turkish Multilingual Sentence Repetition Test (LITMUS-TR) includes sentences in 5 different categories: subject-object-predicate sequences, what-whom questions, noun phrases, relative clauses, clausal adjuncts, conditional structures, and assesses morphosyntactic skills. Consisting of 30 sentences, LITMUS-TR is administered by repeating the sentence heard once. When the sentence is repeated completely correctly, it is scored as 1; otherwise, it is scored as 1 (24-25). Several studies have shown that sentence repetition tests can distinguish between children with language impairment and typical language development (26). Sentence repetition tests are therefore part of a group of language tests commonly used by clinicians to assess children's language skills. The TOLD-P:4:T includes a sentence repetition subtest, but compared to the LITMUS-TR, the sentences are longer, more complex, and contain more items. The sentences in LITMUS-TR are structured to contain a minimum of 11 and a maximum of 14 syllables and a minimum of 4 and a maximum of 6 words. In this way, the load on verbal working memory was balanced and the determinants of morphosyntactic structures on correct repetition performance were emphasized. LITMUS-TR normative studies in Turkish-speaking school-age children are ongoing.

Assessment of Speech Sound Disorder

The SST is a test that is used for screening and differential diagnosis of children with articulation and phonological problems and for which validity, reliability and standardization studies have been conducted. The Articulation Subtest measures the production of 24 phonemes in various positions in the word and the seven most common consonant phrases in Turkish in the context of picture naming. The auditory discrimination test measures the auditory-visual discrimination of 21 consonant phonemes in the smallest monosyllabic word pairs according to their phoneme position, form, and voicing/nonvoicing features. For example, the sounds /k/ and /t/ are different in terms of phoneme position and form, but they share the same in articulatory features (27).

Assessment of Narrative Skills

The Turkish version of Multilingual Assessment Instrument for Narratives-TR (MAIN) is one of the effective tools for analyzing the micro- and macrostructural features of narrative in children. By analyzing the narrative sample, it makes it possible to evaluate the semantic, morphosyntactic and pragmatic components of language. In this study, the number of complex sentences (main clause with a subordinate clause formed with a verb or inflected verb) productions interpreted in favor of syntactic maturation (28). The number of completed episodes (goal, attempt, outcome [GAO]), is considered the most effective indicator of story complexity (29).

Assessment of Visual Perceptual Motor Skills

The Bender-Gestalt Visual Motor Perception Test (BG), developed by Bender in 1938, measures the perception of visual stimuli and the ability to integrate visually perceived information into motor systems. In this test consisting of 9 drawings, each figure is placed on a separate page and it is asked to draw the pictures shown one by one in order. There is no time limit for the drawings, which are drawn sequentially using a single A4 size paper. A pencil and eraser are used for drawing. Preliminary Turkish validity and reliability studies were conducted by Ozer (30). The total score was obtained by calculating the participants' error scores. The child's drawings are scored according to the number of errors (30).

Statistical Analysis

The distribution of variables was calculated by Shapiro Wilk test. Likewise, two group comparisons were performed with Student t or Mann-Whitney U tests. All data are presented as mean \pm standard deviation (SD), and p-values. Statistical analyzes were performed with SPSS IBM 25.0 and p-values <0.05 were considered significant.

RESULTS

Table 2 shows the cognitive and linguistic parameters of the participants. There was no significant difference between

Table 2. Comparison of cognitive and linguistic parameters of the participants

	OME	N	Mean	SD	Z	p
Age	OME+	26	8.77	0.71	-0.042	0.967
	OME-	24	8.79	0.779		
VLSC	OME+	26	92.46	13.189	-4.002	0.001*
	OME-	24	108.83	10.218		
SSD	OME+	26	0.65	0.48	-0.08	0.423
	OME-	24	0.54	0.5		
LD	OME+	26	0.38	0.49	-2.895	0.004*
	OME-	24	0.41	0.2		
TNRT	OME+	26	8.5	2.486	-3.911	0.005*
	OME-	24	11.79	2.449		
LITMUS-TR	OME+	26	16.46	4.658	-4.523	0.002*
	OME-	24	23.75	4.089		
BG	OME+	26	9.27	4.618	-1.141	0.254
	OME-	24	10.58	4.211		
Complex Sentence	OME+	26	4.08	1.129	-0.425	0.671
	OME-	24	3.92	0.929		
GAO	OME+	26	0.5	0.51	-1.147	0.251
	OME-	24	0.71	0.624		

OME: otitis media with effusion; OME+: Presence of otitis media with effusion; OME-: Absence of otitis media with effusion; SSD: Speech sound disorder; VLSC: The verbal language composite score; TNRT: Turkish Nonword Repetition Test; LITMUS-TR: The Turkish Multilingual Sentence Repetition Test; BG: The Bender-Gestalt Visual Motor Perception Test; GAO: Goal, attempt, outcome.

OME+ and OME- groups according to age ($p > 0.05$). TNRT value of OME- group was significantly higher than OME+ group ($p < 0.05$). The LITMUS-TR value of the OME- group was significantly higher than the OME+ group ($p < 0.05$). There was no significant difference between OME+ and OME- groups according to BG, SSD, complex sentence, and GAO ($p > 0.05$).

The VLSC value of the OME- group was significantly higher than the OME+ group ($p < 0.05$). The LD frequency of the OME+ group was significantly higher than the OME- group ($p < 0.05$).

DISCUSSION

Various studies have shown that unilateral hearing loss negatively affects language and cognitive functions in children. (31). Similarly, the presence of middle ear cavity effusion without hearing loss may impair the perception of

phonetic and phonological features of speech sounds (32). In our study, the presence of isolated OME without hearing loss negatively affected language skills. There is a lot of evidence that OME is comorbidity with the SSD (33). Similarly, SSD was seen with a higher frequency in OME+ cases included in this study. Since SSD is the clinical counterpart of articulation disorder and auditory discrimination problems, it can cause social communication difficulties by negatively affecting the intelligibility of the individual (34). This situation can be considered as a finding that supports the need for OME screening in cases with SSD.

In this study, school-age children with and without OME were compared in terms of language skills and visuospatial functions. BG is sensitive to measuring the level of maturation necessary for the integration of the visual perceptual process into motor skills (35). BG performance is not affected by the presence of OME. The incidence of language disorders was found to be higher in the OME+ group. However, since children older than TOLD-P:4:T normative data were included, a comparison was made according to VLSC scores. VLSC scores were found to be lower in the OME+ group. Therefore OME+ can be considered a risk factor for language disorder. Descriptive analyzes are needed due to the fact that standard language assessments are norm dependent, do not provide clues for the use of language in social contexts, and are insufficient to reveal the strong and weak language skills of children who are unfamiliar with the test or who come from different cultural/ethnic backgrounds (36). For this reason, we used MAIN-TR to assess the children's storytelling and narrative skills in terms of complex syntactic production and story complexity.

Syntax, the structural basis of language, is defined as the organization/sequencing of words in sentences to express thoughts, feelings, preferences, and observations in a clear, precise, and efficient way. Syntax emerges in early childhood and continues to develop throughout childhood, adolescence, and early adulthood. With development, sentence lengths increase and sentences contain more dependent clauses (37). This increase in the number of clauses embedded in the main clause (complex sentence production) and their addition to independent clauses is considered a consequence of language maturation (38). The data obtained in this study show that the presence of OME does not lead to morphosyntactic involvement in expressive language.

MAIN-TR consists of stories with pictures in which the actions of the protagonists are clearly described. The narrator has to infer the character's motivation and triggering situations by interpreting the actions in the pictures. The inclusion of statements about the purpose of the protagonist's actions (Goal), the realization of the intended action (Attempt), and the outcome of the action (Outcome) within a story section (GAO sequences) is considered a structural complexity parameter. GAO is the highest level indicator of coherent storytelling ability (39). OME has no direct effect on the ability to produce plots based on temporal and causal relationships.

Clinical Significance of Repetition Tests

Sentence comprehension tasks in standard language assessment tools require the visual-spatial perception of pictures, storing the entire sentence in working memory to reach its final meaning, and directing attentional resources to the target in order to select the picture most relevant to the meaning. In sentence repetition tests, it is accepted that the cognitive load is relatively less because there is no visual processing and semantic judgment for the repetition of the heard sentence. Therefore, sentence repetition tests are preferred in children with language impairment in order to control the reflection of cognitive dysfunctions on language as much as possible. Repetition of short sentences may not require the use of working memory and implicit grammatical acquisition. However, long sentences may exceed memory capacity. The inability to repeat the sentence exactly may not be due to morphosyntactic difficulties but to the length of the target structure (40). For this reason, the sentences in LITMUS-TR were controlled in terms of sentence length, number of phrases, number of words/ suffixes and number of syllables in each sentence (41). In our study, it was observed that the LITMUS-TR sentence repetition scores of OME+ subjects were lower. It seems that OME has a negative effect on the morphosyntactic processing needed in sentence repetition.

Nonword repetition tests can measure the capacity of phonological processing and phonological working memory, which are considered critical skills in new word acquisition. In order to repeat a meaningless word without error, acoustic representations must be formed. Similarly, when a new word is heard for the first time, acoustic signals must be stored in auditory working memory until a connection is made between the real-world referent of the word and its phonological representation (42). In the case of OME, nonword performance is becoming poor. It leads to the conclusion that OME causes difficulties in the construction and storage of phonotactic and phonological representations of auditory verbal signals. In various studies, it has been revealed that EOM negatively affects verbal working memory performance (43-44). There are no studies directly addressing the relationship between EOM and repetition tests. The low scores of the EOM+ group in the LITMUS-TR and TNRT tests may be related to the determinant role of working memory on repetition performance.

In conclusion, OME causes language impairment despite normal hearing thresholds and negatively affects morphosyntactic and phonological processing. It has no effect on storytelling skills and visual-spatial copying performance. Although OME is one of the most common clinical pictures encountered by physicians providing outpatient clinic services for children, (32) easily overlooked and negatively affects the course of development in childhood (16). Therefore, OME should be routinely screened and treatment indications should be evaluated in childhood.

Limitations

One of the key limitations was the insufficient number of participants, which might have affected the statistical power and generalizability of the findings. Additionally, due to the inability to access the previous infectious otitis media history of the OME+ group, the formation of chronic and acute OME+ subgroups was not feasible. Furthermore, although the study included participants with type B tympanometry, a recognized indicator of OME, the lack of information regarding the frequency of previous infectious otitis media in the sample remains a constraint that needs to be addressed in future research. These limitations emphasize the importance of a cautious interpretation of the results and underscore the need for larger sample sizes and comprehensive data collection in future investigations on this subject.

Ethical Approval: Ethical approval of the study was obtained from Istanbul Atlas University Local Ethics Committee (14.03.2023-24890).

Ethical Committee Approval: N/A.

Conflicts of Interest: The author declare no conflict of interest.

Financial Disclosure: The author declare that this study has received no financial support.

REFERENCES

1. Mills R, Hathorn I. Aetiology and pathology of otitis media with effusion in adult life. *J Laryngol Otol* 2016; 130(5): 418-24.
2. Marchisio P, Nazzari E, Torretta S, Esposito S, Principi N. Medical prevention of recurrent acute otitis media: an updated overview. *Expert Rev Anti Infect Ther* 2014; 12(5): 611-20.
3. Vanneste P, Page C. Otitis media with effusion in children: Pathophysiology, diagnosis, and treatment. A review. *J Otol* 2019; 14(2): 33-39.
4. Klausen O, Møller P, Holmefjord A, Reisaeter S, Asbjørnsen A. Lasting effects of otitis media with effusion on language skills and listening performance. *Acta Otolaryngol Suppl* 2000; 543: 73-6.
5. Rach GH, Zielhuis GA, van den Broek P. The influence of chronic persistent otitis media with effusion on language development of 2- to 4-year-olds. *Int J Pediatr Otorhinolaryngol* 1988; 15(3): 253-61.
6. Roberts J, Hunter L. Otitis media and children's language and learning. *The ASHA Leader*. 2002; 7(18): 6-19.
7. Sezgin Z. Efüzyonlu otitis media: tanı ve tedavi yaklaşımlarına genel bakış [Otitis media with effusion: overview of diagnosis and treatment approaches]. *Pediatr Pract Res* 2016; 4(1): 1-11.
8. Petinou KC, Schwartz RG, Gravel JS, Raphael LJ. A preliminary account of phonological and morphophonological perception in young children with and without otitis media. *Int J Lang Commun Disord* 2001; 36(1): 21-42.
9. Coates WA. The description of language use. *Word* 1966; 22(1-3): 243-258.
10. Georgakopoulos T, Polis S. The semantic map model: State of the art and future avenues for linguistic research. *Lang Linguist Compass* 2018; 12(2): e12270.
11. Martin I, McDonald S. Weak coherence, no theory of mind, or executive dysfunction? Solving the puzzle of pragmatic language disorders. *Brain Lang* 2003; 85(3): 451-66.
12. Kaushanskaya M, Park JS, Gangopadhyay I, Davidson MM, Weismer SE. The relationship between executive functions and language abilities in children: A latent variables approach. *J Speech Lang Hear Res* 2017; 60(4): 912-23.
13. Güven S, Friedmann N. Developmental letter position dyslexia in Turkish, a morphologically rich and orthographically transparent language. *Front Psychol* 2019; 10: 2401.
14. Finley S. Cognitive and linguistic biases in morphology learning. *Wiley Interdiscip Rev Cogn Sci* 2018; 9(5): e1467.
15. Dowell SF, Marcy SM, Phillips WR, Gerber MA, Schwartz B. Otitis media—principles of judicious use of antimicrobial agents. *Pediatrics* 1998; 101(suppl): 165-71.
16. Hacimustafaoğlu MK. Çocuklarda akut otitis media. *Güncel Pediatri* 2003; 1(1): 29-34.
17. Anwar K, Khan S, Rehman HU, Javaid M, Shahabi I. Otitis media with effusion: Accuracy of tympanometry in detecting fluid in the middle ears of children at myringotomies. *Pak J Med Sci* 2016; 32(2): 466-70.
18. Kırkım G. Immitansmetric evaluation methods. In: *Basic Audiology*. Ankara: Güneş Tıp Kitabevleri; 2015. pp. 105-12.
19. American Speech-Language-Hearing Association. Degree of hearing loss. [Accessed on April 1, 2023]. Available from: <https://www.asha.org/public/hearing/Degree-of-Hearing-Loss/>
20. Topbaş S, Güven OS. Turkish School Age Language Development Test-TODİL, Test Battery. Detay Publishing; 2013.
21. Topbaş S, Kaçar-Kütükcü D, Kopkalli-Yavuz H. Performance of children on the Turkish Nonword Repetition Test: Effect of word similarity, word length, and scoring. *Clin Linguist Phon* 2014; 28(7-8): 602-16.
22. Savaş M, Tunçer AM, Çokar AÖ, Demirbilek AV, Tüzün E. Impact of epilepsy on language and discourse: Two self-limited focal epileptic syndromes of childhood. *Epilepsy Behav* 2020; 102: 106671.
23. Savaş M, Tunçer AM, Çelik İ, Yaşgüçlükal MA, Demirbilek AV, Çokar AÖ. Does electrical status epilepticus in sleep adversely affect language in self-limiting focal epilepsies of childhood? *Noro Psikiyatr Ars* 2023; 60(1): 62-7.
24. Taha J, Stojanovic V, Pagnamenta E. Sentence repetition as a clinical marker of developmental language disorder: Evidence from Arabic. *J Speech Lang Hear Res* 2021; 64(12): 4876-99.
25. Topbaş SS. Litmus Türkçe cümle tekrarı testinin geçerlik güvenilirlik çalışması [dissertation]. [Order No. 29071890]. [Place of Publication]: ProQuest Dissertations & Theses Global; 2021. (2665129516)
26. Stokes SF, Wong AM, Fletcher P, Leonard LB. Nonword repetition and sentence repetition as clinical markers of specific language impairment: the case of Cantonese. *J Speech Lang Hear Res* 2006; 49(2): 219-36.
27. Topbas S. Turkish Pronunciation-Phonology Test: Validity-reliability and standardisation study. *Turk J Psychol* 2006; 21(58): 39-56.
28. Nippold MA. School-age children talk about chess: does knowledge drive syntactic complexity? *J Speech Lang Hear Res* 2009; 52(4): 856-71.
29. Bohnacker UTE. Tell me a story in English or Swedish: Narrative production and comprehension in bilingual preschoolers and first graders. *Appl Psycholinguist* 2016; 37(1): 19-48.
30. Ozer S. Turkish children's Bender-Gestalt Test performance: a pilot study and preliminary norms. *Percept Mot Skills* 2007; 105(3 Pt 1): 872-82.

31. José MR, Mondelli MF, Feniman MR, Lopes-Herrera SA. Language disorders in children with unilateral hearing loss: a systematic review. *Int Arch Otorhinolaryngol* 2014; 18(2): 198-203.
32. Uclés P, Alonso MF, Aznar E, Lapresta C. The importance of right otitis media in childhood language disorders. *Int J Otolaryngol* 2012; 2012: 818927.
33. Shriberg LD, Kent RD, Karlsson HB, McSweeney JL, Nadler CJ, Brown RL. A diagnostic marker for speech delay associated with otitis media with effusion: backing of obstruents. *Clin Linguist Phon* 2003; 17(7): 529-47.
34. Hitchcock ER, Harel D, Byun TM. Social, emotional, and academic impact of residual speech errors in school-aged children: A survey study. *Semin Speech Lang*. 2015; 36(4): 283-94.
35. Keppeke Lde F, Cintra Ide P, Schoen TH. Bender Visual-Motor Gestalt Test in adolescents: relationship between visual-motor development and the Tanner Stages. *Percept Mot Skills* 2013; 117(1): 1299-317.
36. Acarlar F. Türkçe ediniminde gelişimsel özelliklerin dil örneği ölçümleri açısından incelenmesi. *Türk Psikoloji Dergisi* 2005; 20(56), 61.
37. Nippold MA, Mansfield TC, Billow JL. Peer conflict explanations in children, adolescents, and adults: Examining the development of complex syntax. *Am J Speech Lang Pathol* 2007; 16: 179-188.
38. Nippold MA. School-age children talk about chess: does knowledge drive syntactic complexity? *J Speech Lang Hear Res* 2009; 52(4): 856-71.
39. Gagarina N, Bohnacker U, Lindgren J. Macrostructural organisation of adults' oral narrative texts. *ZAS Papers in Linguistics* 2019; 62: 190-208.
40. Marinis T. On the nature and cause of specific language impairment: A view from sentence processing and infant research. *Lingua* 2011; 121(3): 463-75.
41. Topbaş SS. Litmus Türkçe cümle tekrarı testinin geçerlik güvenilirlik çalışması [dissertation]. [Order No. 29071890]. [Place of Publication]: ProQuest Dissertations & Theses Global; 2021. (2665129516)
42. Coady JA, Evans JL. Uses and interpretations of non-word repetition tasks in children with and without specific language impairments (SLI). *Int J Lang Commun Disord* 2008; 43(1): 1-40.
43. Machado MS, Teixeira AR, da Costa SS. Correlation between cognitive functions and central auditory processing in adolescents with non-cholesteatomatous chronic otitis media. *Dement Neuropsychol* 2018; 12(3): 314-20.
44. Mody M, Schwartz RG, Gravel JS, Ruben RJ. Speech perception and verbal memory in children with and without histories of otitis media. *J Speech Lang Hear Res* 1999; 42(5): 1069-79.

EXPERIMED

AIMS AND SCOPE

Experimed is an international, scientific, open access periodical published in accordance with independent, unbiased, and double-blinded peer-review principles. The journal is the official online-only publication of Istanbul University Aziz Sancar Institute of Experimental Medicine and it is published triannually on April, August, and December. As of 2022 the publication language of the journal is only English. The manuscripts submitted for publication in the journal must be scientific work in English.

Experimed aims to contribute to the literature by publishing manuscripts at the highest scientific level on all fields of basic and clinical medical sciences. The journal publishes original articles, case reports, reviews, and letters to the editor that are prepared in accordance with ethical guidelines.

The scope of the journal includes but not limited to; experimental studies in all fields of medical sciences.

The target audience of the journal includes specialists and professionals working and interested in all disciplines of basic and clinical medical sciences.

The editorial and publication processes of the journal are shaped in accordance with the guidelines of the International Committee of Medical Journal Editors (ICMJE), World Association of Medical Editors (WAME), Council of Science Editors (CSE), Committee on Publication Ethics (COPE), European Association of Science Editors (EASE), and National Information Standards Organization (NISO). The journal is in conformity with the Principles of Transparency and Best Practice in Scholarly Publishing (doaj.org/bestpractice).

Processing and publication are free of charge with the journal. No fees are requested from the authors at any point throughout the evaluation and publication process. All manuscripts must be submitted via the online submission system, which is available at <http://experimed.istanbul.edu.tr/en/>. The journal guidelines, technical information, and the required forms are available on the journal's web page.

All expenses of the journal are covered by the Istanbul University.

Statements or opinions expressed in the manuscripts published in the journal reflect the views of the author(s) and not the opinions of the Istanbul University Aziz Sancar Institute of Experimental Medicine, editors, editorial board, and/or publisher; the editors, editorial board, and publisher disclaim any responsibility or liability for such materials.

Experimed is an open access publication and the journal's publication model is based on Budapest Open Access Initiative (BOAI) declaration. Journal's archive is available online, free of charge at <http://experimed.istanbul.edu.tr/en/>. Experimed's content is licensed under a Creative Commons Attribution-NonCommercial 4.0 International License.

Editor in Chief: Prof. Bedia Çakmakođlu

Address: Istanbul University, Aziz Sancar Institute of Experimental Medicine, Vakıf Gureba Avenue, 34093, Çapa, Fatih, Istanbul, Türkiye

Phone: +90 212 414 2000-33305

Fax: +90 212 532 4171

E-mail: bedia@istanbul.edu.tr

Publisher: Istanbul University Press

Address: Istanbul University Central Campus, 34452 Beyazit, Fatih / Istanbul - Türkiye

Phone: +90 212 440 0000

EXPERIMED

INSTRUCTIONS TO AUTHORS

Context

Experimed is an international, scientific, open access periodical published in accordance with independent, unbiased, and double-blinded peer-review principles. The journal is the official on-line-only publication of Istanbul University Aziz Sancar Institute of Experimental Medicine and it is published triannually on April, August, and December. The publication language of the journal is English.

Experimed aims to contribute to the literature by publishing manuscripts at the highest scientific level on all fields of basic and clinical medical sciences. The journal publishes original articles, case reports, reviews, and letters to the editor that are prepared in accordance with ethical guidelines.

Editorial Policy

The editorial and publication processes of the journal are shaped in accordance with the guidelines of the International Council of Medical Journal Editors (ICMJE), the World Association of Medical Editors (WAME), the Council of Science Editors (CSE), the Committee on Publication Ethics (COPE), the European Association of Science Editors (EASE), and National Information Standards Organization (NISO). The journal conforms to the Principles of Transparency and Best Practice in Scholarly Publishing (doaj.org/bestpractice).

Originality, high scientific quality, and citation potential are the most important criteria for a manuscript to be accepted for publication. Manuscripts submitted for evaluation should not have been previously presented or already published in an electronic or printed medium. The journal should be informed of manuscripts that have been submitted to another journal for evaluation and rejected for publication. The submission of previous reviewer reports will expedite the evaluation process. Manuscripts that have been presented in a meeting should be submitted with detailed information on the organization, including the name, date, and location of the organization.

Peer-Review Policy

Manuscripts submitted to Experimed will go through a double-blind peer-review process. Each submission will be reviewed by at least two external, independent peer reviewers who are experts in their fields in order to ensure an unbiased evaluation process. The editorial board will invite an external and independent editor to manage the evaluation processes of manuscripts submitted by editors or by the editorial board members of the journal. The Editor in Chief is the final authority in the decision-making process for all submissions.

Ethical Principles

An approval of research protocols by the Ethics Committee in accordance with international agreements (World Medical Association Declaration of Helsinki "Ethical Principles for Medical Research Involving Human Subjects," amended in October 2013, www.wma.net) is required for experimental, clinical, and drug studies and for some case reports. If required, ethics committee reports or an equivalent official document will be requested from the authors. For manuscripts concerning experimental research on humans, a

statement should be included that shows that written informed consent of patients and volunteers was obtained following a detailed explanation of the procedures that they may undergo. For studies carried out on animals, the measures taken to prevent pain and suffering of the animals should be stated clearly. Information on patient consent, the name of the ethics committee, and the ethics committee approval number should also be stated in the Materials and Methods section of the manuscript. It is the authors' responsibility to carefully protect the patients' anonymity. For photographs that may reveal the identity of the patients, signed releases of the patient or of their legal representative should be enclosed.

Plagiarism

Experimed is extremely sensitive about plagiarism. All submissions are screened by a similarity detection software (iThenticate by CrossCheck) at any point during the peer-review or production process. Even if you are the author of the phrases or sentences, the text should not have unacceptable similarity with the previously published data.

When you are discussing others' (or your own) previous work, please make sure that you cite the material correctly in every instance.

In the event of alleged or suspected research misconduct, e.g., plagiarism, citation manipulation, and data falsification/fabrication, the Editorial Board will follow and act in accordance with COPE guidelines.

Authorship

Each individual listed as an author should fulfill the authorship criteria recommended by the International Committee of Medical Journal Editors

(ICMJE - www.icmje.org). The ICMJE recommends that authorship be based on the following 4 criteria:

1. Substantial contributions to the conception or design of the work; or the acquisition, analysis, or interpretation of data for the work; AND
2. Drafting the work or revising it critically for important intellectual content; AND
3. Final approval of the version to be published; AND
4. Agreement to be accountable for all aspects of the work in ensuring that questions related to the accuracy or integrity of any part of the work are appropriately investigated and resolved.

In addition to being accountable for the parts of the work he/she has done, an author should be able to identify which co-authors are responsible for specific other parts of the work. In addition, authors should have confidence in the integrity of the contributions of their co-authors.

All those designated as authors should meet all four criteria for authorship, and all who meet the four criteria should be identified as authors. Those who do not meet all four criteria should be acknowledged in the title page of the manuscript.

EXPERIMED

Experimed requires corresponding authors to submit a signed and scanned version of the authorship contribution form (available for download through <http://experimed.istanbul.edu.tr/en/>) during the initial submission process in order to act appropriately on authorship rights and to prevent ghost or honorary authorship. If the editorial board suspects a case of "gift authorship," the submission will be rejected without further review. As part of the submission of the manuscript, the corresponding author should also send a short statement declaring that he/she accepts to undertake all the responsibility for authorship during the submission and review stages of the manuscript.

Conflict of Interest

The journal requires the authors and all individuals taking part in the evaluation process to disclose any existing or potential conflict of interest (such as financial ties, academic commitments, personal relationships, institutional affiliations) that could unduly influence one's responsibilities. To disclose potential conflicts of interest, the ICMJE Potential Conflict of Interest Disclosure Form should be filled in and submitted by authors as explained in the Author Form of the journal. Cases of a potential conflict of interest are resolved within the scope of COPE Conflict of Interest Flowcharts and ICMJE Conflict of Interest guidelines.

Besides conflict of interest, all financial support received to carry out research must be declared while submitting the paper.

The Editorial Board of the journal handles all appeal and complaint cases within the scope of COPE guidelines. In such cases, authors should get in direct contact with the editorial office regarding their appeals and complaints. When needed, an ombudsperson may be assigned to resolve cases that cannot be resolved internally. The Editor in Chief is the final authority in the decision-making process for all appeals and complaints.

Copyright and Licensing

Authors publishing with the journal retain the copyright to their work licensed under the Creative Commons Attribution-NonCommercial 4.0 International license ("<https://creativecommons.org/licenses/by-nc/4.0/>" CC BY-NC 4.0) which permits unrestricted, non-commercial use, distribution, and reproduction in any medium, provided the original work is properly cited.

Open Access Statement

The journal is an open access journal and all content is freely available without charge to the user or his/her institution. Except for commercial purposes, users are allowed to read, download, copy, print, search, or link to the full texts of the articles in this journal without asking prior permission from the publisher or the author. This is in accordance with the HYPERLINK "<https://www.budapestopenaccessinitiative.org/read>" BOAI definition of open access.

The open access articles in the journal are licensed under the terms of the Creative Commons Attribution-NonCommercial 4.0 International ("<https://creativecommons.org/licenses/by-nc/4.0/deed.en>" CC BY-NC 4.0) license.

Disclaimer

Statements or opinions expressed in the manuscripts published in Experimed reflect the views of the author(s) and not the opinions

of the editors, the editorial board, or the publisher; the editors, the editorial board, and the publisher disclaim any responsibility or liability for such materials. The final responsibility in regard to the published content rests with the authors.

MANUSCRIPT PREPARATION

The manuscripts should be prepared in accordance with ICMJE-Recommendations for the Conduct, Reporting, Editing, and Publication of Scholarly Work in Medical Journals (updated in December 2015 - <http://www.icmje.org/icmje-recommendations.pdf>). Authors are required to prepare manuscripts in accordance with the CONSORT guidelines for randomized research studies, STROBE guidelines for observational original research studies, STARD guidelines for studies on diagnostic accuracy, PRISMA guidelines for systematic reviews and meta-analysis, ARRIVE guidelines for experimental animal studies, and TREND guidelines for non-randomized public behavior.

Manuscripts can only be submitted through the journal's online manuscript submission and evaluation system, available at <http://experimed.istanbul.edu.tr/en/>. Manuscripts submitted via any other medium will not be evaluated.

Manuscripts submitted to the journal will first go through a technical evaluation process where the editorial office staff will ensure that the manuscript has been prepared and submitted in accordance with the journal's guidelines. Submissions that do not conform to the journal's guidelines will be returned to the submitting author with technical correction requests.

Authors are required to submit the following:

- Copyright Agreement Form,
- ICMJE Potential Conflict of Interest Disclosure Form (should be filled in by all contributing authors)

during the initial submission. These forms are available for download at <http://experimed.istanbul.edu.tr/en/>.

Preparation of the Manuscript

Title page: A separate title page should be submitted with all submissions and this page should include:

- The full title of the manuscript as well as a short title (running head) of no more than 50 characters,
- Name(s), affiliations, ORCID IDs and highest academic degree(s) of the author(s),
- Grant information and detailed information on the other sources of support,
- Name, address, telephone (including the mobile phone number) and fax numbers, and email address of the corresponding author,
- Acknowledgment of the individuals who contributed to the preparation of the manuscript but who do not fulfill the authorship criteria.

Abstract: A English abstract should be submitted with all submissions except for Letters to the Editor. The abstract of Original Articles should be structured with subheadings (Objective, Material and Method, Results, and Conclusion). Please check Table 1 below for word count specifications.

EXPERIMED

Keywords: Each submission must be accompanied by a minimum of three to a maximum of six keywords for subject indexing at the end of the abstract. The keywords should be listed in full without abbreviations. The keywords should be selected from the National Library of Medicine, Medical Subject Headings database (<https://www.nlm.nih.gov/mesh/MBrowser.html>).

Manuscript Types

Original Articles: This is the most important type of article since it provides new information based on original research. The main text of original articles should be structured with Introduction, Material and Method, Results, and Discussion subheadings. Please check Table 1 for the limitations for Original Articles.

Statistical analysis to support conclusions is usually necessary. Statistical analyses must be conducted in accordance with international statistical reporting standards (Altman DG, Gore SM, Gardner MJ, Pocock SJ. Statistical guidelines for contributors to medical journals. *Br Med J* 1983; 7; 1489-93). Information on statistical analyses should be provided with a separate subheading under the Materials and Methods section and the statistical software that was used during the process must be specified.

Units should be prepared in accordance with the International System of Units (SI).

Editorial Comments: Editorial comments aim to provide a brief critical commentary by reviewers with expertise or with high reputation in the topic of the research article published in the journal. Authors are selected and invited by the journal to provide such comments. Abstract, Keywords, and Tables, Figures, Images, and other media are not included.

Review Articles: Reviews prepared by authors who have extensive knowledge on a particular field and whose scientific background has been translated into a high volume of publications with a high citation potential are welcomed. These authors may even be invited by the journal. Reviews should describe, discuss, and evaluate the current level of knowledge of a topic in clinical practice and should guide future studies. The main text should contain Introduction, Clinical and Research Consequences, and Conclusion sections. Please check Table 1 for the limitations for Review Articles.

Case Reports: There is limited space for case reports in the journal and reports on rare cases or conditions that constitute challeng-

es in diagnosis and treatment, those offering new therapies or revealing knowledge not included in the literature, and interesting and educative case reports are accepted for publication. The text should include Introduction, Case Presentation, Discussion, and Conclusion subheadings. Please check Table 1 for the limitations for Case Reports.

Letters to the Editor: This type of manuscript discusses important parts, overlooked aspects, or lacking parts of a previously published article. Articles on subjects within the scope of the journal that might attract the readers' attention, particularly educative cases, may also be submitted in the form of a "Letter to the Editor." Readers can also present their comments on the published manuscripts in the form of a "Letter to the Editor." Abstract, Keywords, and Tables, Figures, Images, and other media should not be included. The text should be unstructured. The manuscript that is being commented on must be properly cited within this manuscript.

Tables

Tables should be included in the main document, presented after the reference list, and they should be numbered consecutively in the order they are referred to within the main text. A descriptive title must be placed above the tables. Abbreviations used in the tables should be defined below the tables by footnotes (even if they are defined within the main text). Tables should be created using the "insert table" command of the word processing software and they should be arranged clearly to provide easy reading. Data presented in the tables should not be a repetition of the data presented within the main text but should be supporting the main text.

Figures and Figure Legends

Figures, graphics, and photographs should be submitted as separate files (in TIFF or JPEG format) through the submission system. The files should not be embedded in a Word document or the main document. When there are figure subunits, the subunits should not be merged to form a single image. Each subunit should be submitted separately through the submission system. Images should not be labeled (a, b, c, etc.) to indicate figure subunits. Thick and thin arrows, arrowheads, stars, asterisks, and similar marks can be used on the images to support figure legends. Like the rest of the submission, the figures too should be blind. Any information within the images that may indicate an individual or institution should be blinded. The minimum resolution of each submitted figure should be 300 DPI. To prevent delays in the evaluation process, all submitted figures should be clear in resolution and large in size (minimum

Table 1. Limitations for each manuscript type

Type of manuscript	Word limit	Abstract word limit	Reference limit	Table limit	Figure limit
Original Article	3500	200 (Structured)	30	6	7 or total of 15 images
Review Article	5000	200	50	6	10 or total of 20 images
Case Report	1000	200	15	No tables	10 or total of 20 images
Letter to the Editor	500	No abstract	5	No tables	No media

EXPERIMED

dimensions: 100 × 100 mm). Figure legends should be listed at the end of the main document.

All acronyms and abbreviations used in the manuscript should be defined at first use, both in the abstract and in the main text. The abbreviation should be provided in parentheses following the definition.

When a drug, product, hardware, or software program is mentioned within the main text, product information, including the name of the product, the producer of the product, and city and the country of the company (including the state if in USA), should be provided in parentheses in the following format: "Discovery St PET/CT scanner (General Electric, Milwaukee, WI, USA)"

All references, tables, and figures should be referred to within the main text, and they should be numbered consecutively in the order they are referred to within the main text.

Limitations, drawbacks, and the shortcomings of original articles should be mentioned in the Discussion section before the conclusion paragraph.

References

While citing publications, preference should be given to the latest, most up-to-date publications. Authors are responsible for the accuracy of references. References should be prepared according to Vancouver reference style. If an ahead-of-print publication is cited, the DOI number should be provided. Journal titles should be abbreviated in accordance with the journal abbreviations in Index Medicus/ MEDLINE/PubMed. When there are six or fewer authors, all authors should be listed. If there are seven or more authors, the first six authors should be listed followed by "et al." In the main text of the manuscript, references should be cited using Arabic numbers in parentheses. The reference styles for different types of publications are presented in the following examples.

Journal Article: Rankovic A, Rancic N, Jovanovic M, Ivanović M, Gajović O, Lazić Z, et al. Impact of imaging diagnostics on the budget – Are we spending too much? *Vojnosanit Pregl* 2013; 70: 709-11.

Book Section: Suh KN, Keystone JS. Malaria and babesiosis. Gorbach SL, Barlett JG, Blacklow NR, editors. *Infectious Diseases*. Philadelphia: Lippincott Williams; 2004.p.2290-308.

Books with a Single Author: Sweetman SC. *Martindale the Complete Drug Reference*. 34th ed. London: Pharmaceutical Press; 2005.

Editor(s) as Author: Huizing EH, de Groot JAM, editors. *Functional reconstructive nasal surgery*. Stuttgart-New York: Thieme; 2003.

Conference Proceedings: Bengjsson S, Sothemin BG. Enforcement of data protection, privacy and security in medical informatics. In: Lun KC, Degoulet P, Piemme TE, Rienhoff O, editors. *MEDINFO 92. Proceedings of the 7th World Congress on Medical Informatics; 1992 Sept 6-10; Geneva, Switzerland*. Amsterdam: North-Holland; 1992. pp.1561-5.

Scientific or Technical Report: Cusick M, Chew EY, Hoogwerf B, Agrón E, Wu L, Lindley A, et al. Early Treatment Diabetic Retinopathy Study Research Group. Risk factors for renal replacement therapy in the Early Treatment Diabetic Retinopathy Study (ETDRS), Early Treatment Diabetic Retinopathy Study Kidney Int: 2004. Report No: 26.

Thesis: Yılmaz B. *Ankara Üniversitesindeki Öğrencilerin Beslenme Durumları, Fiziksel Aktiviteleri ve Beden Kitle İndeksleri Kan Lipidleri Arasındaki İlişkiler*. H.Ü. Sağlık Bilimleri Enstitüsü, Doktora Tezi. 2007.

Manuscripts Accepted for Publication, Not Published Yet: Slots J. The microflora of black stain on human primary teeth. *Scand J Dent Res*. 1974.

Epub Ahead of Print Articles: Cai L, Yeh BM, Westphalen AC, Roberts JP, Wang ZJ. Adult living donor liver imaging. *Diagn Interv Radiol*. 2016 Feb 24. doi: 10.5152/dir.2016.15323. [Epub ahead of print].

Manuscripts Published in Electronic Format: Morse SS. Factors in the emergence of infectious diseases. *Emerg Infect Dis* (serial online) 1995 Jan-Mar (cited 1996 June 5): 1(1): (24 screens). Available from: URL: <http://www.cdc.gov/ncidod/EID/cid.htm>.

REVISIONS

When submitting a revised version of a paper, the author must submit a detailed "Response to the reviewers" that states point by point how each issue raised by the reviewers has been covered and where it can be found (each reviewer's comment, followed by the author's reply and line numbers where the changes have been made) as well as an annotated copy of the main document. Revised manuscripts must be submitted within 30 days from the date of the decision letter. If the revised version of the manuscript is not submitted within the allocated time, the revision option may be canceled. If the submitting author(s) believe that additional time is required, they should request this extension before the initial 30-day period is over.

Accepted manuscripts are copy-edited for grammar, punctuation, and format. Once the publication process of a manuscript is completed, it is published online on the journal's webpage as an ahead-of-print publication before it is included in its scheduled issue. A PDF proof of the accepted manuscript is sent to the corresponding author and their publication approval is requested within 2 days of their receipt of the proof.

Editor in Chief: Prof. Bedia Çakmakoğlu
Address: Istanbul University, Aziz Sancar Institute of Experimental Medicine, Vakıf Gureba Avenue, 34093, Çapa, Fatih, Istanbul, Türkiye
Phone: +90 212 414 2000-33305
Fax: +90 212 532 4171
E-mail: bedia@istanbul.edu.tr

Publisher: Istanbul University Press
Address: Istanbul University Central Campus, 34452 Beyazıt, Fatih / Istanbul - Türkiye
Phone: +90 212 440 0000